YU ISSN 0042-8450

ВОЈНОСАНИТЕТСКИ ПРЕГЛЕД

Часопис лекара и фармацеута Војске Србије

Military Medical and Pharmaceutical Journal of Serbia

Vojnosanitetski pregled

Vojnosanit Pregl 2015; October Vol. 72 (No. 10): p. 855–946.

YU ISSN 0042-8450 vol. 72, br. 10, 2015.

VOJNOSANITETSKI PREGLED

Prvi broj *Vojnosanitetskog pregleda* izašao je septembra meseca 1944. godine

Časopis nastavlja tradiciju *Vojno-sanitetskog glasnika*, koji je izlazio od 1930. do 1941. godine

IZDAVAČ
Uprava za vojno zdravstvo MO Srbije

Adresa redakcije: Vojnomedicinska akademija, Institut za naučne informacije, Crnotravska 17, poštanski fah 33–55, 11040 Beograd, Srbija. Telefoni: glavni i odgovorni urednik 3609 311, glavni menadžer časopisa 3609 479, pretplata 3608 997. Faks 2669 689. E-mail (redakcija): **vsp@vma.mod.gov.rs**

Radove objavljene u „Vojnosanitetskom pregledu“ indeksiraju: Science Citation Index Expanded (SCIE), Journal Citation Reports/Science Edition, Index Medicus (Medline), Excerpta Medica (EMBASE), EBSCO, Biomedicina Serbica. Sadržaje objavljuju Giornale di Medicine Militare i Revista de Medicina Militara. Prikaze originalnih radova i izvoda iz sadržaja objavljuje International Review of the Armed Forces Medical Services.

Časopis izlazi dvanaest puta godišnje. Pretplate: Žiro račun br. 840-314849-70 MO – Sredstva objedinjene naplate – VMA (za Vojnosanitetski pregled), poziv na broj 1227423129552141 5. Za pretplatu iz inostranstva obratiti se službi pretplate na tel. 3608 997. Godišnja pretplata: 5 000 dinara za građane Srbije, 10 000 dinara za ustanove iz Srbije i 150 € (u dinarskoj protivvrednosti na dan uplate) za pretplatnike iz inostranstva. Kopiju uplatnice dostaviti na gornju adresu.

Štampa Vojna štamparija, Beograd, Resavska 40 b.

YU ISSN 0042-8450 vol. 72 No. 10, 2015

VOJNOSANITETSKI PREGLED

The first issue of *Vojnosanitetski pregled* was published in September 1944
The Journal continues the tradition of *Vojno-sanitetski glasnik* which was published between 1930 and 1941

PUBLISHER
Military Health Department, Ministry of Defence, Serbia

Editorial Office: Military Medical Academy, INI; Crnotravska 17, PO Box 33–55, 11040 Belgrade, Serbia. Phone: Editor-in-chief +381 11 3609 311; Main Journal Manager +381 11 3609 479; Fax: +381 11 2669 689; E-mail: **vsp@vma.mod.gov.rs**

Papers published in the Vojnosanitetski pregled are indexed in: Science Citation Index Expanded (SCIE), Journal Citation Reports/Science Edition, Index Medicus (Medline), Excerpta Medica (EMBASE), EBSCO, Biomedicina Serbica. Contents are published in Giornale di Medicine Militare and Revista de Medicina Militara. Reviews of original papers and abstracts of contents are published in International Review of the Armed Forces Medical Services.

The Journal is published monthly. Subscription: Giro Account No. 840-314849-70 Ministry of Defence – Total means of payment – VMA (for the Vojnosanitetski pregled), refer to number 12274231295521415. To subscribe from abroad phone to +381 11 3608 997. Subscription prices per year: individuals 5,000.00 RSD, institutions 10,000.00 RSD, and foreign subscribers 150 €.

Printed by: Vojna štamparija, Beograd, Resavska 40 b.

CONTENTS / SADRŽAJ

ORIGINAL ARTICLES / ORIGINALNI RADOVI

World Osteoporosis Day takes place every year on October 20, raising global awareness of the need for better prevention, diagnosis and treatment of osteoporosis and metabolic bone disease.
On this occasion, Editorial board of the "Vojnosanitetskog pregleda" invites all authors, readers and collaborators of the Journal to take an active part in promoting activities aimed to maintain and improve bone health (change lifestyles to a healthier alternative by regular exercises, reducing smoking and alcohol intake and eating a balanced and nutritious diet).

Svetski dan protiv osteoporoze obeležava se svake godine 20. oktobra sa ciljem podizanja svesti o potrebi za boljom prevencijom, dijagnozom i lečenjem osteoporoze i metaboličkih bolesti kostiju.
Tim povodom, Uređivački odbor Vojnosanitetskog pregleda poziva sve autore, čitaoce i saradnike časopisa da aktivno učestvuju u promovisanju aktivnosti koje imaju cilj da održe i unaprede zdravlje kostiju (promena životnih navika u smeru „zdravijih alternativa" kao što su redovno bavljenje sportom, smanjenje pušenja i unosa alkohola i balansirana i zdrava ishrana).

ORIGINAL ARTICLE

UDC: 575:61]:[616.8:616.74-007.23
DOI: 10.2298/VSP140328072Z

Association between the SMN2 gene copy number and clinical characteristics of patients with spinal muscular atrophy with homozygous deletion of exon 7 of the SMN1 gene

Povezanost broja kopija SMN2 gena i kliničkih karakteristika bolesnika sa spinalnom mišićnom atrofijom sa homozigotnom delecijom egzona 7 gena SMN1

Marija Žarkov*, Aleksandra Stojadinović†, Slobodan Sekulić*, Iva Barjaktarović‡, Olivera Stojiljković§, Stojan Perić‖, Goran Keković¶, Biljana Drašković†, Zorica Stević‖

***Neurology Clinic, Clinical Center of Vojvodina, Faculty of Medicine, University of Novi Sad, Novi Sad, Serbia; †Child and Youth Health Care Institute of Vojvodina, Faculty of Medicine, University of Novi Sad, Novi Sad, Serbia; ‡Center for Forensic Medicine, Toxicology and Molecular Genetics, Clinical Center of Vojvodina, Novi Sad, Serbia; §Department of Neurology, General Hospital, Subotica, Serbia; ‖Neurology Clinic, Clinical Center of Serbia, Faculty of Medicine, University of Belgrade, Belgrade, Serbia; ¶Institute for Biological Research "Siniša Stanković", University of Belgrade, Belgrade, Serbia**

Abstract

Background/Aim. Spinal muscular atrophy (SMA) is an autosomal recessive disease characterized by degeneration of alpha motor neurons in the spinal cord and the medulla oblongata, causing progressive muscle weakness and atrophy. The aim of this study was to determine association between the SMN2 gene copy number and disease phenotype in Serbian patients with SMA with homozygous deletion of exon 7 of the SMN1 gene. **Methods.** The patients were identified using regional Serbian hospital databases. Investigated clinical characteristics of the disease were: patients' gender, age at disease onset, achieved and current developmental milestones, disease duration, current age, and the presence of the spinal deformities and joint contractures. The number of SMN1 and SMN2 gene copies was determined using real-time polymerase chain reaction (PCR). **Results.** Among 43 identified patients, 37 (86.0%) showed homozygous deletion of SMN1 exon 7. One (2.7%) of 37 patients had SMA type I with 3 SMN2 copies, 11 (29.7%) patients had SMA type II with 3.1 ± 0.7 copies, 17 (45.9%) patients had SMA type III with 3.7 ± 0.9 copies, while 8 (21.6%) patients had SMA type IV with 4.2 ± 0.9 copies. There was a progressive increase in the SMN2 gene copy number from type II towards type IV ($p < 0.05$). A higher SMN2 gene copy number was associated with better current motor performance ($p < 0.05$). **Conclusion.** In the Serbian patients with SMA, a higher SMN2 gene copy number correlated with less severe disease phenotype. A possible effect of other phenotype modifiers should not be neglected.

Key words:
muscular atrophy, spinal; genetic diseases, inborn; chromosome aberations; serbia.

Apstrakt

Uvod/Cilj. Spinalna mišićna atrofija (SMA) je autosomno recesivno oboljenje koje se karakteriše degeneracijom alfa motornih neurona kičmene moždine i produžene moždine, što uzrokuje progresivnu mišićnu slabost i atrofiju. Cilj rada bio je da se utvrdi povezanost broja kopija gena SMN2 i fenotipa kod srpske populacije bolesnika sa SMA sa homozigotnom delecijom egzona 7 gena SMN1. **Metode.** Podaci o bolesnicima sa SMA preuzeti su iz registara regionalnih bolnica u Srbiji. Ispitivane su sledeće kliničke karakteristike: pol bolesnika, uzrast pri pojavi bolesti, postignuti stepen motornog razvoja na početku bolesti i trenutno stanje, trajanje bolesti, sadašnji uzrast i prisustvo deformiteta kičme i kontrakture zglobova. Broj kopija gena SMN1 i SMN2 utvrđivan je pomoću lančane reakcije polimeraze (*polymerase chain reaction* – PCR) u realnom vremenu. **Rezultati.** Od 43 identifikovana bolesnika, 37 (86.0%) je imalo homozigotnu deleciju egzona 7 gena SMN1. Jedan (2.7%) od 37 bolesnika imao je SMA tipa I sa 3 kopije SMN2, 11 (29.7%) je imalo

Correspondence to: Marija Žarkov, Neurology Clinic, Clinical Center of Vojvodina, Hajduk Veljkova 1–9, 21 000 Novi Sad, Serbia.
E-mail: zarkovns@gmail.com

SMA tipa II sa 3.1 ± 0.7 kopija, 17 (45.9%) imalo je SMA tipa III sa 3.7 ± 0.9 kopija, dok je 8 (21.6%) bolesnika imalo SMA tipa IV sa 4.2 ± 0.9 kopija. Zabeležen je progresivan porast broja kopija gena SMN2 od tipa II ka tipu IV ($p < 0.05$). Veći broj kopija gena SMN2 bio je povezan sa boljim trenutnim motornim sposobnostima ($p < 0.05$). **Zaključak.** U srpskoj populaciji bolesnika sa SMA, veći broj kopija gena SMN2 koreliše sa blažim fenotipom bolesti. Pored toga, ne treba isključiti ni mogući uticaj drugih faktora koji mogu modifikovati fenotip.

Ključne reči:
mišići, atrofija, spinalna; genetičke bolesti, urođene; hromosomi, aberacije; srbija.

Introduction

Spinal muscular atrophy (SMA) is an autosomal recessive disease characterized by degeneration of alpha motor neurons in the spinal cord and the medulla oblongata, causing progressive muscle weakness and atrophy. The incidence of the disease is 1 per 10,000 live births, with a carrier frequency of approximately 1 in 50 [1, 2]. In 95% of cases, the cause is deletion of both copies of exon 7 on the SMN1 gene in chromosome 5, whereas point mutations are present in the rest of the cases [3].

The SMN1 gene normally provides production of fully functional survival of the motor neuron protein (SMN), unlike the SMN2 gene transcript, which results in 80–90% of the cases with dysfunctional protein chains [4]. Insufficient production of SMN1 results in apoptosis of alpha motor neurons [5]. Several studies have demonstrated a correlation between the number of SMN2 gene copies and the type of SMA. The lowest number of SMN2 gene copies is seen in SMA type 1, while in other types this number is higher [6–8]. However, the correlation between symptom severity and SMN2 copy number is not linear and there seem to exist other factors impacting on the disease phenotype, such as gender, other genes, epigenetics and variant point mutations [9].

The aim of this study was to determine the association between SMN2 gene copy number and disease phenotype of Serbian SMA patients with homozygous deletion of exon 7 of the SMN1 gene.

Methods

The study included 43 patients with SMA identified through hospital databases of the Neurology Clinics in Novi Sad and Belgrade in 2011. It was approved by the Ethical Committee of the Clinical Center of Vojvodina, Novi Sad. All the patients or the adult guardians of the children gave written informed consent to take part in the study.

SMA was uniformly classified according to the International SMA Consortium Meeting Report recommendations [10]. Disease onset before 6 months of age, i.e. before the ability to sit independently, was classified as SMA type I. Disease onset between 6 and 15 months of age, with the absence of the ability to walk independently, was classified as SMA type II. Disease onset after the patient developed the ability to walk, between 15 months of age and 20 years, was classified as SMA type III. Disease onset after the age of 20 years was classified as SMA type IV.

Medical documentation and clinical examination were used to collect the following data: patients' gender, age at disease onset, achieved and current developmental milestones (graded as follows: not able to sit, sitting with support, sitting independently, walking with support, walking independently), disease duration, current age, and the presence of the spinal deformities and joint contractures.

Molecular diagnosis

The genomic DNA isolation from single samples was performed by the silica membrane-based DNA extraction using the QIAamp DNA Micro Kit (Qiagen, Hilden, Germany) and followed by the spectrophotometric measurement of DNA concentration in each isolate. Isolated nuclear DNAs were amplified using the Taqman Universal PCR Master Mix. For SMN1 and SMN2 exon 7 amplification, we used the sequences of primers and probes described by Passon et al. [11]. The same authors described the conditions for performance of PCR reactions. PCR conditions were 2 min 50°C, 10 min 95°C, 40 cycles consisting of 15 s 95°C, and 1 min 60°C. Serum albumin was employed as a reference gene. The PCR reaction of amplification of SMN1, SMN2 and the reference gene was performed using the ABI Prism 7000 Sequence Detection System (Applied Biosystems, Foster City, CA, USA). The DNA sample of the patient with a known SMN1 copy number and the DNA sample of the patient with a known SMN2 copy number were used as calibrators in all SMN1 and SMN2 exon 7 amplification reactions. DNA of each sample, including calibrators, was used for amplification of SMN1, SMN2 and the reference gene. SMN1 and SMN2 copy number was determined using $\Delta\Delta C_t$ method.

Statistical tests were performed using the commercial software SPSS (IBM, USA), with the level of statistical significance of $p < 0.05$ and the high statistical significance of $p < 0.01$. The following methods of descriptive statistics were used: proportion, mean and standard deviation. For comparisons between non-continuous variables, χ^2 test was used. For continuous non-normal distributions, we used Mann-Whitney *U*-test for analysis between the two groups, and Kruskal-Wallis test for analysis of more than two groups. For normal distributions, data were analyzed using Student *t*-test for comparison between the two groups and ANOVA one way breakdown test for comparison between three or more groups. We also calculated the odds ratio (OR) with 95% confidence interval (CI) describing the risk of patients with 4 or 5 copy numbers of SMN2 gene compared to patients with 3 copies to develop mild form SMA (type 3 or 4 SMA *vs* type 2). Comparison of survival in patients with different SMN2 gene copy numbers was analyzed by the Kaplan–

Meier log-rank test, with SMA onset as zero time and inability to walk as the end-point event.

Results

A total of 43 patients with SMA were identified. Among them, 37 (86.0%) patients showed homozygous deletion of SMN1 exon 7. The additional four (9.3%) cases showed deletion of the exon 7 of only one allele of SMN1 gene, while two (4.7%) patients had both copies of the SMN1 exon 7. Only the homozygous cases were further analyzed in the study.

Only one of 37 (2.7%) patients with homozygous deletion had SMA type I. SMA type II was registered in 11 (29.7%) cases, SMA type III in 17 (45.9%) and SMA IV in 8 (21.6%) patients.

Sociodemographic and clinical features of investigated patients with different SMA types are presented in Table 1. There was no association between disease type and gender ($p > 0.05$). Significant association between better current motor performance and less severe SMA types was observed ($p < 0.01$). Also, the increased incidence of cases with spine and extremity deformities was observed in more severe SMA types ($p < 0.05$).

Regarding all SMA types, mean number of SMN2 copies was 3.6 ± 0.9; 2 copies were present in 1 (2.8%) patient, 3 in 20 (55.6%), 4 in 7 (19.4%), 5 in 7 (19.4%) patients and 6 in 1 (2.8%) patient. A significant increase in SMN2 copy number was observed from SMA type II towards types IV (3.1 ± 0.7 copies in SMA II, 3.7 ± 0.9 in SMA III, and 4.2 ± 0.9 in SMA IV, $p < 0.05$) (Figure 1). The patients with 4 copies of SMN2 gene had 1.6 times higher risk to develop mild form of SMA (OR 1.6, 95% CI 1.1–2.4; $p < 0.05$), while patients with 5 copies had 4.9 times higher risk but this was not

Table 1

Sociodemographic and clinical features of the investigated patients with spinal muscular atrophy (SMA) types II, III and IV (n = 36)

Features	SMA type II	SMA type III	SMA type IV
Number of patients	11	17	8
Gender (males), %	36.4	47.1	25.0
Age at disease onset (years), mean ± SD**	1.00 ± 0.00	5.24 ± 6.02	33.62 ± 16.69
Achieved milestones, % **			
not able to sit	0	0	0
sitting with support	27.3	0	0
sitting independently	27.3	0	0
walking with support	45.4	0	0
walking independently	0	100	100
Disease duration (years), mean ± SD	11.81 ± 6.64	22.05 ± 16.38	12.37 ± 11.24
Current age (years), mean ± SD**	12.36 ± 6.74	27.29 ± 17.02	46.00 ± 15.38
Current motor performance, % **			
not able to sit	0	0	0
sitting with support	36.4	5.9	0
sitting independently	36.4	17.7	0
walking with support	27.2	11.8	37.5
walking independently	0	64.6	62.5
Spinal deformities and joint contractures, % **	72.7	41.2	37.5

**$p < 0.01$

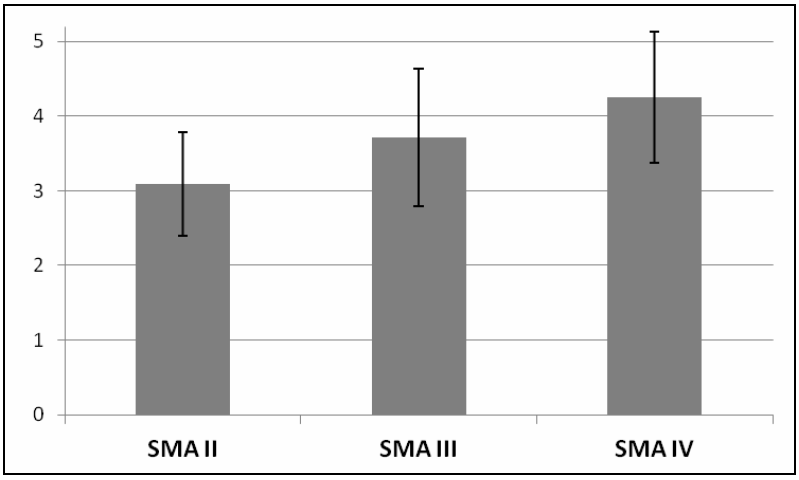

$p < 0.05$

Fig. 1 – SMN2 gene copy number in the patients with different types of spinal muscularatrophy(SMA) with homozygous deletion of exon 7 in SMN1 gene (n = 36).
SMA II – disease onset between 6 and 15 years of age with the absence of the ability to walk independantly; SMA III – disease onset developed the ability to walk, between 15 months of age and 20 years; SMA IV – disease onset after 20 years.

of statistical significance due to the small number of observed cases (OR 4.9; 95% CI 0.5–48.6; $p > 0.05$).

The SMN2 gene copy number did not depend on gender ($p > 0.05$). Also, it did not show any correlation with achieved motor milestones ($p > 0.05$) and with the presence of the spine deformities and limb contractures ($p > 0.05$). A higher SMN2 gene copy number was associated with a better current motor performance ($p < 0.05$) (Table 2). Log-rank test showed similar survival until inability to walk in patients with 4 and 5 SMN2 gene copy numbers, thus we finally compared survival in the patients with 3 *vs* 4 or 5 copies (Figure 2). In the patients with 3 copies inability to walk developed after 23.7 (95% CI 12.2–35.2) years, and in those with 4 or 5 copies after 37.4 (95% CI 31.5–43.2) years ($p < 0.05$).

Table 2

Association between SMN2 gene copy number and current motor performance in the patients with spinal muscular atrophy (SMA) (n = 36)

Achieved milestones	SMN2 gene copy number
Not able to sit	2.8 ± 0.5
Sitting with support	3.0 ± 0.0
Sitting independently	3.5 ± 0.8
Walking with support	3.6 ± 0.9
Walking independently	3.8 ± 1.0

***p* < 0.05**

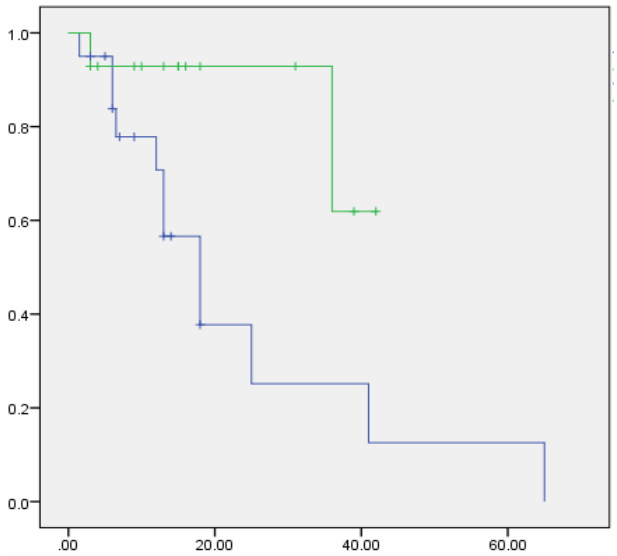

Fig. 2 – Survival analysis until inability to walk in the patients with 3 *vs* 4 or 5 SMN2 gene copy numbers.
x-axis – duration of disease until inability to walk; y-axis – percentage of patients who are able to walk; $p < 0.05$ when compare the patients with 3 SMN2 gene copies (in blue) with 4 or 5 SMN2 gene copies (in green).

Discussion

The proportion of our SMA patients with homozygous deletion of exon 7 of the SMN1 gene was 86% which is similar to the findings of other authors, i.e. 94–95% [12]. Deletion of the exon 7 of only one allele of SMN1 gene was found in 9% of our cases and it was probably in association with the point mutation on the other allele which we were not able to test. It is also possible that 5% of patients with both copies of the SMN1 exon 7 had two point mutations, one in each SMN1 copy. However, one should not rule out the possibility that disease in these patients might be caused by mutations in some other gene.

Almost half of our patients had SMA type III, while SMA type I was registered in only one patient. Short survival of patients with SMA type I, and a cross-sectional design of the study resulted in an almost complete lack of patients with the most severe form of SMA.

Less severe SMA types were in association with later age at onset and better milestones achievement, which was expected by SMA classification [10]. Also, patients with less severe SMA types were elder and had better current motor performance which is in line with previous findings that patients with later onset of SMA have normal or almost normal life expectancy [13]. Furthermore, later disease onset is accompanied by a milder disease course and longer independent ambulation [14]. We also observed the increased incidence of cases with spine and extremity deformities in more severe SMA types. It is well-known that muscle weakness in SMA patients leads to the limited joint motion and consequent contractures [15]. Muscle weakness is considered the main factor in the etiology of these changes [16, 17].

In the present study, the number of SMN2 gene copies was statistically significantly higher in the patients with less severe SMA types which correspond with the published data. Patients with SMA type I usually have 1–3 SMN2 gene copies, most frequently 2 [8, 18, 19], patients with type II have 2–4 copies, usually 3 [8, 18, 20]. In type III, more than 90% of cases have 3–4 copies [8, 17, 19]. In type IV, 4–6 SMN2 gene copies have been found [21]. Furthermore, in our patients with the SMA number of SMN2 gene copies correlated with better current motor performance. Survival until inability to walk was almost 14 years longer in SMA patients with 4 or 5 copies of SMN2 gene compared to patients with only 2 copies.

According to our and previous findings, it is generally possible to predict SMA severity on the basis of the SMN2 gene copy number [6–8]. However, the absence of the direct correlation of the SMN2 gene copy number with achieved motor milestones and the presence of the spine deformities and limb contractures, suggest that clear prognosis of SMA phenotype cannot be based only on SMN2 copies. This is in line with previous data [18]. The prognosis might be more precise with determination of the status of another gene responsible for synthesis of the neuronal apoptosis inhibitory protein (NAIP). In SMA patients, homozygous deletion of the NAIP gene is present in 44.8% of patients, and the highest number of patients with homozygous deletions of the NAIP gene and the SMN1 gene belongs to the SMA type I [8, 9]. Other disease modifiers are suggested in the literature, such as genes for plastin 3, chondrolectin, NAIP, p44, H4F5, occludin etc. [22–24]. Also, a larger deletion of the SMN1 gene might be in association with more severe phenotype since neighbor genes (SERF1A, GTF2H2, RAD17) may also be affected. Studies are contradictory in regard to differences in the severity of SMA between males and females. While one study found a greater decline in female pulmonary function [25], another one showed that feminine gender has a mitigating effect on disease severity [17]. In our study patients gender

was not associated with SMA type, the presence of spine and joint contracture, and current motor status. Furthermore, the number of SMN2 gene copies does not differ between sexes. This finding is in accordance with previous studies [9, 25].

Conclusion

In Serbian patients with spinal muscular atrophy, a higher SMN2 gene copy number correlated with the less severe disease phenotype. A possible effect of other phenotype modifiers should not be neglected.

Acknowledgements

This work was funded by the Hungary-Serbia IPA Cross-Border Co-Operation Program: Research Cooperation to Improve Symptoms in Neurological Disorders, and Quality of Life of Patients. 2010-2012, Project ID: HU-SRB/0901/214/052.

REFERENCES

1. *Sugarman EA, Nagan N, Zhu H, Akmaev VR, Zhou Z, Rohlfs EM,* et al. Pan-ethnic carrier screening and prenatal diagnosis for spinal muscular atrophy: clinical laboratory analysis of >72,400 specimens. Eur J Hum Genet 2012; 20(1): 27−32.
2. *Stipoljev F, Sertić J, Latin V, Rukavina-Stavljenić A, Kurjak A.* Prenatal diagnosis of spinal muscular atrophy type I (Werdnig-hoffmann) by DNA deletion analysis of cultivated amniocytes. Croat Med J 1999; 40(3): 433−7.
3. *Brzustowicz LM, Lehner T, Castilla LH, Penchaszadeh GK, Wilhelmsen KC, Daniels R,* et al. Genetic mapping of chronic childhood-onset spinal muscular atrophy to chromosome 5q11.2−13. 3. Nature 1990; 344(6266): 540−1.
4. *Lefebvre S, Burlet P, Liu Q, Bertrandy S, Clermont O, Munnich A,* et al. Correlation between severity and SMN protein level in spinal muscular atrophy. Nat Genet 1997; 16(3): 265−9.
5. *Kerr DA, Nery JP, Traystman RJ, Chau BN, Hardwick JM.* Survival motor neuron protein modulates neuron-specific apoptosis. Proc Natl Acad Sci USA 2000; 97(24): 13312−7.
6. *McAndrew PE, Parsons DW, Simard LR, Rochette C, Ray PN, Mendell JR,* et al. Identification of proximal spinal muscular atrophy carriers and patients by analysis of SMNT and SMNC gene copy number. Am J Hum Genet 1997; 60(6): 1411−22.
7. *Mailman MD, Heinz JW, Papp AC, Snyder PJ, Sedra MS, Wirth B,* et al. Molecular analysis of spinal muscular atrophy and modification of the phenotype by SMN2. Genet Med 2002; 4(1): 20−6.
8. *Taylor JE, Thomas NH, Lewis CM, Abbs SJ, Rodrigues NR, Davies KE,* et al. Correlation of SMNt and SMNc gene copy number with age of onset and survival in spinal muscular atrophy. Eur J Hum Genet 1988; 6(5): 467−74.
9. *Jedrzejowska M, Milewski M, Zimowski J, Borkowska J, Kostera-Pruszczyk A, Sielska D,* et al. Phenotype modifiers of spinal muscular atrophy: the number of SMN2 gene copies, deletion in the NAIP gene and probably gender influence the course of the disease. Acta Biochim Pol 2009; 56(1): 103−8.
10. *Munsat TL, Davies KE.* International SMA consortium meeting. (1992 June 26−28, Bonn, Germany). Neuromuscul Disord 1992; 2(5−6): 423−8.
11. *Passon N, Pozzo F, Molinis C, Bregant E, Gellera C, Damante G,* et al. A simple multiplex real-time PCR methodology for the SMN1 gene copy number quantification. Genet Test Mol Biomarkers 2009; 13(1): 37−42.
12. *Wirth B.* An update of the mutation spectrum of the survival motor neuron gene (SMN1) in autosomal recessive spinal muscular atrophy (SMA). Hum Mutat 2000; 15(3): 228−37.
13. *D'Amico A, Mercuri E, Tiziano FD, Bertini E.* Spinal muscular atrophy. Orphanet J Rare Dis 2011; 6: 71.
14. *Mercuri E, Bertini E, Iannaccone ST.* Childhood spinal muscular atrophy: controversies and challenges. Lancet Neurol 2012; 11(5): 443−52.
15. *Wang HY, Ju YH, Chen SM, Lo SK, Jong YJ.* Joint range of motion limitations in children and young adults with spinal muscular atrophy. Arch Phys Med Rehabil 2004; 85(10): 1689−93.
16. *Rodillo E, Marini ML, Heckmatt JZ, Dubowitz V.* Scoliosis in spinal muscular atrophy: review of 63 cases. J Child Neurol 1989; 4(2): 118−23.
17. *Mesfin A, Sponseller PD, Leet AI.* Spinal muscular atrophy: manifestations and management. J Am Acad Orthop Surg 2012; 20(6): 393−401.
18. *Feldkötter M, Schwarzer V, Wirth R, Wienker TF, Wirth B.* Quantitative analyses of SMN1 and SMN2 based on real-time lightCycler PCR: fast and highly reliable carrier testing and prediction of severity of spinal muscular atrophy. Am J Hum Genet 2002; 70(2): 358−68.
19. *Harada Y, Sutomo R, Sadewa AH, Akutsu T, Takeshima Y, Wada H,* et al. Correlation between SMN2 copy number and clinical phenotype of spinal muscular atrophy: three SMN2 copies fail to rescue some patients from the disease severity. J Neurol 2002; 249(9): 1211−9.
20. *Zheleznyakova GY, Kiselev AV, Vakharlovsky VG, Rask-Andersen M, Chavan R, Egorova AA,* et al. Genetic and expression studies of SMN2 gene in Russian patients with spinal muscular atrophy type II and III. BMC Med Genet 2011; 12: 96.
21. *Wirth B, Brichta L, Schrank B, Lochmüller H, Blick S, Baasner A,* et al. Mildly affected patients with spinal muscular atrophy are partially protected by an increased SMN2 copy number. Hum Genet 2006; 119(4): 422−8.
22. *Prior TW, Krainer AR, Hua Y, Swoboda KJ, Snyder PC, Bridgeman SJ,* et al. A positive modifier of spinal muscular atrophy in the SMN2 gene. Am J Hum Genet 2009; 85(3): 408−13.
23. *Sleigh JN, Barreiro-Iglesias A, Oliver PL, Biba A, Becker T, Davies KE,* et al. Chondrolectin affects cell survival and neuronal outgrowth in in vitro and in vivo models of spinal muscular atrophy. Hum Mol Genet 2014; 23(4): 855−69.
24. *Amara A, Adala L, Ben-Charfeddine I, Mamaï O, Mili A, Lazreg TB,* et al. Correlation of SMN2, NAIP, p44, H4F5 and Occludin genes copy number with spinal muscular atrophy phenotype in Tunisian patients. Eur J Paediatr Neurol 2012; 16(2): 167−74.
25. *Kaufmann P, McDermott MP, Darras BT, Finkel R, Kang P, Oskoui M,* et al. Observational study of spinal muscular atrophy type 2 and 3: functional outcomes over 1 year. Arch Neurol 2011; 68(6): 779−86.

Received on March 28, 2014.
Revised on August 8 , 2014.
Accepted on August 13, 2014.
Online First August, 2015.

ORIGINAL ARTICLE

UDC: 616.314
DOI: 10.2298/VSP140310071M

Analysis of the mineral composition of hypomineralized first permanent molars

Analiza mineralnog sastava hipomineralizovanih prvih stalnih molara

Brankica Martinović*, Mirjana Ivanović†, Zoraida Milojković*, Raša Mladenović*

***Department of Dentistry, Faculty of Medicine, University of Priština, Kosovska Mitrovica, Serbia; †Department of Preventive Dentistry and Pedodontics, Faculty of Dental Medicine, University of Belgrade, Belgrade, Serbia**

Abstract

Background/Aim. Hypomineralization of molars and incisors (molar-incisor hypomineralization – MIH) is defined as enamel hypomineralization of systemic origin of one or more of the four first permanent molars, which may be associated with changes in the maxillary, and less frequently in the permanent mandibular incisors. The aim of this study was to investigate the mineral content in hypomineralized teeth as a contribution to under-standing the origin of these changes, which will be important for effective restorative approach. **Methods.** A total of 10 extracted first permanent molars diagnosed with MIH were used in the study as the experimental group, and intact first premolars extracted for orthodontic reasons were used as the control group. A certain surface of hypomineralized and healthy enamel and dentin was analyzed using a scanning electron microscope equipped with an energy-dispersive spectrometer (SEM/EDS). **Results.** By conducting quantitative chemical analysis of the distribution of the basic chemical elements, it was found that the concentration of calcium (Ca) and phosphorus (P) was significantly higher in healthy enamel (Ca = 28.80 wt%, and P = 15.05 wt%) compared to hypomineralized enamel (Ca = 27.60 wt% and P = 14.32 wt%). Carbon (C) concentration was statistically significantly higher in hypomineralized enamel (C = 11.70 wt%) compared to healthy enamel (C = 10.94 wt%). Hypomineralized and healthy enamel did not differ significantly regarding the ratio of calcium and phosphorus concentrations whereas the ratio of calcium and carbon concentrations was statistically significantly higher in healthy enamel compared to hypomineralized enamel. **Conclusion.** Concentration of the main chemical elements, primarily calcium and phosphorus, is significantly reduced in hypomineralized enamel whereas carbon concentration is increased compared to healthy enamel.

Key words:
tooth demineralization; molar; dental enamel; dentin; elements; microscopy, electron, scanning.

Apstrakt

Uvod/Cilj. Hipomineralizacija molara i sekutića (*molar-incisor hipomineralisation* – MIH) definiše se kao hipomineralizacija sistemskog porekla jednog ili više od četri prva stalna molara, koja može biti udružena sa promenama na maksilarnim, a nešto ređe na mandibularnim sekutićima. Cilj ovog rada bio je da se istraži mineralni sadržaj hipomineralizovanih zuba kao doprinos razumevanju nastanka ovih promena, što će biti od značaja za efikasniji restaurativni pristup. **Metode.** U istraživanju je korišćeno 10 izvađenih prvih stalnih molara sa dijagnozom MIH, kao eksperimentalna grupa, a kao kontrolna grupa zuba korišćeni su prvi intaktni premolari izvađeni iz ortodonskih razloga. Određena površina hipomineralizovane i zdrave gleđi i dentina analizirana je pomoću elektronskog mikroskopa opremljenog energetskim disperzionim spektrometrom (SEM/EDS). **Rezultati.** Kvantitativnom hemijskom analizom raspodele osnovnih hemijskih elemenata, utvrđeno je da je koncentracija kalcijuma (Ca) i fosfora (P) bila statistički značajno veća u zdravoj gleđi (Ca = 28,80% tež. i P = 15,05% tež) u odnosu na hipomineralzovanu gleđ (Ca = 27,60% tež. i P = 14.32% tež). Koncentracija ugljenika (C) bila je statistički značajno veća u hipomineralizovanoj gleđi (C = 11,70% tež) u odnosu na zdravu gleđ (C = 10,94% tež). Zdrava i hipomineralizovana gleđ nisu se statistički značajno razlikovale u odnosu koncentracija kalcijuma i fosfora, dok je odnos koncentracija kalcijuma i ugljenika statistički bio značajno veći u zdravoj gleđi u odnosu na hipomineralizovanu gleđ. **Zaključak.** Koncentracija osnovnih hemijskih elemenata, pre svega kalcijuma i fosfora, značajno je snižena u hipomineralizovanoj gleđi, a koncentracija ugljenika povišena u poređenju sa zdravom gleđi.

Ključne reči:
zub, demineralizacija; molari; zub, gleđ; dentin; elementi; mikroskopija, elektronska, skenirajuća.

Correspondence to: Brankica Martinović, Department of Dentistry, Faculty of Medicine, University of Priština, Kosovska Mitrovica, Serbia. E-mail: brankicamartinovic@gmail.com

Introduction

Hypomineralization of molars and incisors (molar-incisor hypomineralization – MIH) [1] is defined as enamel hypomineralization of systemic origin of one or more of the four first permanent molars, which may be associated with changes in the maxillary, and less frequently in the mandibular permanent incisors [1].

This condition has been found in children throughout Europe and is considered to be a significant problem in terms of dental health in many countries [2].

Former studies indicate that hypomineralization changes in the first permanent molars and incisors are the result of the interruption of the enamel formation process from about 37 weeks to 3 years of age. Obstacles during the formation process of enamel matrix will manifest as quantitative or morphological defects (hypoplasia or hypoplastic changes) [3], while interruptions in the process of mineralization or maturation can produce morphologically normal, but structurally or qualitatively defective hypomineralized enamel [4].

Hypomineralized teeth which are not part of some other structural anomaly have been noticed in everyday dental practice since a long time ago. Hypomineralization is clinically manifested as a disturbance in translucency of enamel (enamel opacities). Defective opaque enamel is of normal thickness, with smooth surface and can be whitish, white-yellow or yellow-brown and the defect typically has a clear line between affected and healthy enamel. These changes are usually localized to the vestibular surface of incisors and cusps of molars [5, 6].

Hypomineralized molars, depending on their degree of hypomineralization, are brittle, fragile and, as such, liable to posteruptive chipping of enamel caused by chewing forces. Teeth affected by MIH are sensitive to thermal, mechanical and chemical stimuli [7–9].

It has been discovered that mechanical characteristics in MIH teeth such as hardness and modulus of elasticity are significantly lower than in healthy enamel [10, 11].

Hypomineralized enamel surface is substantially disorganized, its content of inorganic compounds, primarily Ca/P ratio, is reduced by 5–20%, and increased content of carbon and carbonates can be noted if compared to normal enamel. Enamel in the cervical area of a tooth usually retains normal structure [12–14].

While biological and physicochemical factors or the ones of environmental origin that lead to these disorders still remain unclear, the effects of the changes in mechanical properties of hypomineralized enamel, as well as reduced concentration of basic inorganic compounds are quite clear. The microstructure of hypomineralized enamel in permanent teeth has been described in several studies to have less organized prismatic structure with wide interprismatic zones [15–17].

Numerous studies, using different methods for studying morphological, chemical and mechanical properties of hypomineralized enamel compared to normal enamel of permanent teeth, show that there is a significant difference between the two [13, 14, 16, 18].

The fact that some basic analyses of the enamel in the first permanent molars with the diagnosis of MIH in some researches show changes in chemical and mineral composition of the enamel, the aim of this study was to examine the mineral composition of hypomineralized teeth as the contribution to understanding the causes of these changes, which will be of significant importance to some more efficient and restorative approach.

Methods

The study was approved by the Ethics Committee of the Faculty of Medicine, University of Pristina, with the headquarters in Kosovska Mitrovica.

A total of 10 extracted first permanent molars diagnosed with severe MIH were used in the study as the teeth of the experimental group. The increased risk of posteruptive enamel loss and failure of restoration, rapid development of caries, unpredictable behavior of the remaining enamel, the failure to achieve an adequate level of analgesia, dental fear and anxiety of children, were all the justifying reasons for extraction of first permanent molars diagnosed with severe MIH and in combination with orthodontic treatment applied upon the extraction.The optimal time for extraction is the beginning of calcification and bifurcation of the root of the mandibular second molar at the age of 8.5–9.5 years. If extraction is performed after that time, a problem of space and ill-positioning of the second permanent molar may incur.

Intact first premolars extracted for orthodontic reasons were used as the teeth of the control group, since healthy first permanent molars were not indicated for extraction and thus difficult to collect for evaluation. According to the literature, there is no evidence that the enamel structure of premolars is different from the enamel structure of molars [16].

We used the teeth of children aged 8.5–10 years for whom we received written parental consent to participate in the study, and who had previously been fully informed, orally and in writing, about the aims of the study.

The extracted teeth were fixed in 4% formalin and kept until preparations and measurements in test tubes without identification, so that none of the teeth could point to a specific patient.

The analysis of the chemical properties of the enamel was performed in the Laboratory for Scanning Electron Microscopy with Energy-Dispersive Spectrometry (SEM-EDS) at the Faculty of Mining and Geology, University of Belgrade.

Specific surface was examined by means of a scanning electron microscope (SEM) type JEOL JSM-6610LV at 20 kV. Relative amounts of the measured chemical elements were calculated using Energy-Dispersive System-EDS, model X-Max Large Area Analytical Silicon Drift connected with INCA Energy 350 Microanalysis System, with the detection limit of 0.1 mas. % and resolution of 126 eV.

For the initial preparation of samples, the coronal part of the selected teeth was separated from the roots using a diamond disc, and then the crown was cut into a buccal and oral part in the mesial-distal direction, with constant cooling

at the speed of 6000 rev/min. The resultant of the tooth crown was put into epoxy resin, so that the longitudinal section of enamel and dentin was visible. The obtained portion was polished on the surface on one side with the fine silicon carbide paper, and finally with 9 and 1 μm diamond paste. Polishing was needed to obtain highly polished surfaces for a quantitative chemical analysis. Then the samples were sprayed and coated with the carbon layer of 15–25 nm thickness, so that the surface could be electron transparent for the penetrating electron beam. The device SCD005 LEICA model was used for carbon vapor deposition of the samples. The samples for the SEM analysis had to be previously cleaned by plunging into ethanol and keeping in an ultrasonic bath for a few minutes, and then dried under an ordinary lamp. The sample was then fixed on the holder and placed on the table in the scanning electron microscope chamber. The signals from the sample, *via* the detectors placed in the sample chamber, were transferred electronically to a computer, which is a part of an energy-dispersive system, for EDS analyses. The image of back-scattered electrons (BSE) and secondary electrons (SE) can also be transferred to a computer for EDS analysis, making it possible to choose points for analysis directly on the image, and the analysis can be at a single point or along a selected line.

Quantitative analysis of the distribution of chemical elements in enamel and dentine was done by applying "dotted" analysis at various distances of previously determined line of analysis. For analysis, 31 points were selected on each examined section both in the enamel and the dentine as follows: the first examined point was randomly selected in dentine and the following 30 points from the enamel-dentine border in occlusal direction through the enamel section surface (Figures 1 and 2). The following methods of statistical processing were used to test the results: Mann-Whitney *U*-test, Student's *t*-test and χ^2 test.

Results

Basic chemical elements of both healthy and hypomineralized enamel and dentin were distributed by conducting quantitative chemical analysis. Basic chemical elements plus oxygen whose content had been calculated by stoichiometric calculations were detected. The results of the analysis are displayed in Table 1.

Basic chemical elements analysis of healthy enamel showed that the mean value of Ca concentration was 28.80 wt% whereas the mean value of calcium concentration in hypomineralized enamel was 27.60 wt%. It is observed that the concentration of calcium was significantly higher in healthy enamel compared to hypomineralized enamel ($F = 7.24$; $p = 0.014$). Analysis of the distribution of calcium concentration indicated the values in enamel layers, going from the enamel-dentine border occlusally, to be as follows: the first 12 of the analyzed spectra were of no statistical significance compared to hypomineralized enamel. The spectra was used to label the relative mass distribution *per* element within the examined point, the same way as operated and defined by EDS spectrometer. The values of calcium concentration in healthy enamel in other spectra compared to hypomineralized enamel were statistically significantly higher ($p < 0.05$).

The mean value of phosphorus concentration in healthy enamel was 15.05 wt% and in hypomineralized enamel 14.32 wt%. Phosphorus concentration was statistically significantly higher in healthy enamel compared to hypomineralized enamel ($F = 6.09$; $p = 0.024$). Analysis of the results confirmed that the distribution of phosphorus concentration in enamel layers, going from the enamel-dentine border occlusally, at the first 14 analyzed spectra, was of no statistical significance, whereas at the following 16 analyzed spectra these values were significantly higher in healthy enamel compared to hypomineralized enamel ($p < 0.05$).

The mean value of carbon concentration in healthy enamel was 10.94 wt% and in hypomineralized enamel 11.70 wt%. Carbon concentration was statistically significantly higher in hypomineralized enamel compared to healthy enamel ($F = 6.22$; $p = 0.023$). Analysis of the results of carbon concentration distribution indicated that, go-

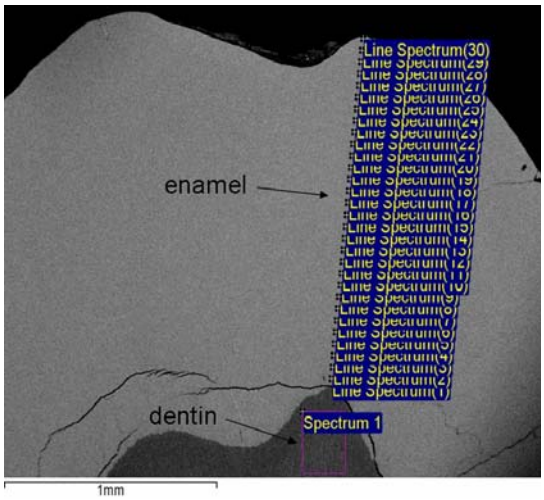

Fig. 1 – Selected area for energy dispersive spectrometry (EDS) analysis – hypomineralization of first permanent molars (molar incisor hipomineralization group).

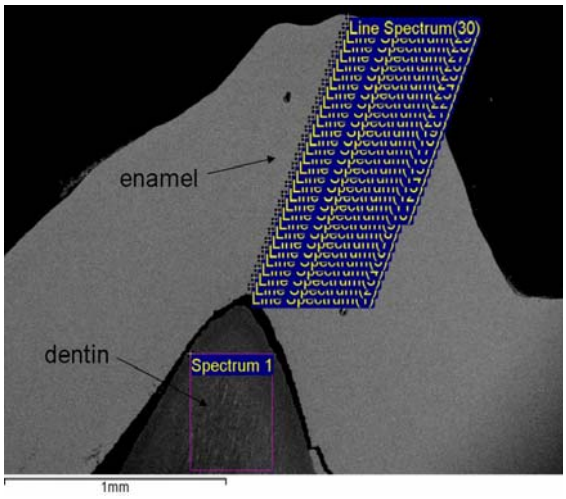

Fig. 2 – Selected area for energy dispersive spectrometry (EDS) analysis – first permanent premolars (healthy enamel group).

Table 1

The concentration profile of chemical elements of hypomineralized and healthy tooth enamel and dentin expressed in weight percentage

Spectrum	Calcium (%)		Phorporus (%)		Carbon (%)		Oxygen (%)	
	MIH	HE	MIH	HE	MIH	HE	MIH	HE
Spectrum 1	14.21	14.35	8.30	8.41	9.62	9.03	44.53	44.72
Line Spectrum (1)	27.69	28.07	14.51	14.37	11.71	12.51	44.56	43.68
Line Spectrum (2)	27.80	27.97	14.68	14.95	10.78	10.86	44.34	43.98
Line Spectrum (3)	28.15	28.76	14.97	15.02	10.98	10.97	44.74	44.04
Line Spectrum (4)	27.66	28.53	14.56	14.83	11.52	11.20	44.72	43.15
Line Spectrum (5)	27.61	28.42	14.46	14.84	11.78	11.26	44.67	44.42
Line Spectrum (6)	28.00	28.17	14.94	15.19	10.89	10.53	44.86	44.32
Line Spectrum (7)	27.55	27.98	14.85	15.00	11.01	10.98	44.74	43.90
Line Spectrum (8)	28.15	28.31	14.52	15.11	11.72	11.07	44.79	44.29
Line Spectrum (9)	28.16	28.14	14.44	14.72	10.56	10.47	45.07	44.08
Line Spectrum (10)	27.92	28.08	14.34	14.79	11.01	11.22	44.86	44.12
Line Spectrum (11)	28.09	28.15	14.90	15.08	11.84	11.26	45.13	44.21
Line Spectrum (12)	27.18	27.63	14.23	14.74	12.08	11.02*	45.19	43.98
Line Spectrum (13)	27.14	28.61*	14.98	15.02	12.12	11.10*	45.00	43.97
Line Spectrum (14)	27.24	28.61*	14.13	14.64	11.96	11.08*	44.98	44.13
Line Spectrum (15)	27.19	28.39*	13.36	14.80*	11.63	11.24	44.02	44.00
Line Spectrum (16)	27.17	28.53*	13.83	14.93*	11.66	11.11	45.02	43.90
Line Spectrum (17)	26.53	28.65*	14.08	15.01*	11.94	10.76*	45.00	43.86
Line Spectrum (18)	26.73	28.63*	13.71	14.78*	11.92	10.95*	44.98	43.60
Line Spectrum (19)	27.23	28.94*	13.97	15.19*	11.94	10.75*	44.97	43.86
Line Spectrum (20)	26.36	28.70*	13.89	15.04*	11.90	10.97*	45.08	43.60
Line Spectrum (21)	26.52	27.91*	14.16	15.18*	11.99	10.76*	44.67	43.64
Line Spectrum (22)	27.06	28.82*	13.84	15.24*	11.62	10.75*	44.73	43.21
Line Spectrum (23)	27.03	27.70*	14.59	15.40*	11.68	10.45*	44.85	43.29
Line Spectrum (24)	26.71	28.26*	13.73	15.42*	11.82	10.46*	44.35	43.30
Line Spectrum (25)	26.98	28.32*	14.86	15.39*	11.33	10.48*	44.49	43.04
Line Spectrum (26)	26.87	28.58*	13.74	15.55*	11.45	10.26*	44.21	43.31
Line Spectrum (27)	26.40	28.22*	13.79	15.53*	11.33	10.27*	44.11	43.06
Line Spectrum (28)	26.88	28.56*	14.82	15.51*	11.61	10.30*	43.97	42.71
Line Spectrum (29)	26.73	28.93*	13.82	15.78*	10.99	9.96*	44.10	42.84
Line Spectrum (30)	26.95	28.75*	13.60	15.74*	11.11	10.04*	44.72	43.77
Mean	27.06	28.80*	14.32	15.05*	11.70	10.94*	44.62	43.17
Std. deviation	1.47	1.03	0.78	0.06	1.06	0.95	1.25	0.09
Max.	28.16	28.94	14.97	15.78	12.12	12.51	45.19	44.42
Min.	26.36	27.63	13.36	14.37	10.56	9.96	43.97	42.71

***Statistically significant ($p < 0.05$); MIH – molar incisor hipomineralization group; HE – healthy teeth group.**

ing from the enamel-dentine border occlusally, at the first 12 analyzed spectra, these values were of no statistical significance, as well as in the 15th and 16th analyzed spectrum, whereas at the following examined points these values were significantly lower in healthy enamel compared to hypomineralized enamel ($p < 0.05$).

The experimental and control groups of teeth did not differ significantly when the concentration of calcium and phosphorus was considered, as well as the carbon in dentin ($F = 3.30$; $p = 0.087$).

Analysis of the ratio of calcium and phosphorus concentration in healthy enamel was 1.91, whereas the ratio of calcium and phosphorus concentration in hypomineralized enamel was 1.90. Analysis of the ratio of calcium and carbon concentration in healthy enamel was 2.65, and the ratio of calcium and carbon concentration in hypomineralized enamel was 2.39. Healthy and hypomineralized enamel did not differ significantly in terms of statistics considering the ratio of calcium and phosphorus concentration ($F = 3.30$; $p = 0.087$), whereas the ratio of calcium and carbon concentration was statistically significantly higher in healthy enamel compared to hypomineralized enamel ($F = 6.14$; $p = 0.023$) (Table 2).

Table 2

The ratio of calcium/phosphorus and calcium/carbon concentrations of healthy and hypomineralized tooth enamel of the examined teeth

Parameter	Ca-P		Ca-C	
	MIH	HE	MIH	HE
number of teeth	10	10	10	10
mean	1.90	1.91	2.39	2.65
SD	0.05	0.04	0.36	0.28
p	< 0.000		< 0.000	

MIH – molar incisor hipomineralization group; HE – healthy teeth group; SD – standard deviation.

Discussion

In previous studies a number of different methods have been used for studying chemical and mineral properties of hypomineralized enamel in teeth with MIH [12, 16, 18–21].

A number of studies analyzing the enamel in permanent first molars diagnosed with MIH have shown changes in chemical composition, as well as reduction in mineral composition [9, 12, 13]. A reduction in the volume of mineral content by 20% indicates the presence of higher concentration of organic compounds in the area of hypomineralized enamel [14]. It is assumed that in hypomineralized teeth the removal of the remaining proteins (amelogenin, enamelin, etc.) may be incomplete [22–24].

In this study, analysis of basic chemical elements in enamel shows that in terms of statistics the concentration of calcium and phosphorus is significantly higher in healthy enamel compared to hypomineralized enamel. The finding of lower levels of calcium and phosphorus in hypomineralized enamel compared to healthy one is in line with the research conducted by Fagrell et al. [20]. Similar results have been shown in other studies, too [12, 18, 19].

Analysis of the results of carbon concentration shows that the values are significantly higher in hypomineralized enamel compared to healthy enamel.

Jälevik et al. [13] assumed in their study that increased carbon content, determined by means of radiographic microanalysis, may be the result of increased carbonate concentration, or an increase in organic components of the enamel.

Increased carbon content in hypomineralized enamel compared to normal enamel has been proved in other studies, too [12, 17, 19, 20].

Analysis of healthy and hypomineralized enamel shows that there is no significant difference regarding calcium and phosphorus concentration.

Fagrell et al. [20] also found in their study in 2010 that calcium / phosphorus ratio was not significantly different between normal and hypomineralized enamel.

This was in contrast to the previous study conducted by Jälevik et al. [18]. However, other studies have also found a stable calcium/phosphorus ratio (Ca/P), despite some differences in the level of mineralization.

Different results in the literature have been discussed by Mahoney et al. [10, 17], leaving some room for further discussion. The explanation for the stable calcium/phosphorus ratio (Ca/P) is in what it actually represents. It is assumed that in hypomineralized enamel with a higher content of organic matter, phosphorus analyzed by means of radiographyc microanalysis, possibly derives not only from hydroxyl apatites, but also from organic matter.

In this study, the ratio of calcium and carbon concentration is statistically significantly higher in healthy enamel compared to hypomineralized enamel.

As well as in ours, the research conducted by Fagrell et al. [20] indicated that the average value of carbon was significantly higher in hypomineralized enamel compared to normal one, whereas calcium/carbon ratio had significantly lower values in hypomineralized enamel compared to normal.

This study confirms the findings of other researchers – hypomineralized first permanent molars do not only have morphological changes but also reduced concentration of basic chemical elements in the basis of their defects.

A reduced concentration of basic chemical elements of hypomineralized enamel in first permanent molars explains the reduced resistance of the affected enamel to pressure during mastication and inadequate retention of the material during restoration.

Further studies of mineral content, ultrastructure and mechanical properties of hypomineralized teeth would be useful for understanding the origin of these phenomena and would help with the selection of restorative materials.

Conclusion

This study confirms the findings of other researchers – hypomineralized first permanent molars do not only have morphological changes but also a reduced concentration of basic chemical elements in the basis of their defects. By conducting quantitative chemical analysis of the distribution of the basic chemical elements, it was found that, in terms of statistics, the concentration of calcium and phosphorus was significantly higher in healthy enamel when compared to hypomineralized enamel. Carbon concentration was significantly higher in hypomineralized enamel compared to healthy enamel. Healthy and hypomineralized enamel do not differ significantly regarding the ratio of calcium and phosphorus concentration whereas the ratio of calcium and carbon concentration is significantly higher in healthy enamel compared to hypomineralized enamel.

Further studies of the mineral composition of hypomineralized teeth would contribute to obtaining a clearer etiology of the changes on MIH affected teeth as well as the influence on mechanical resistance during the mastication process. Furthermore, clearer knowledge on irregularities of structural integrity of hypomineralized tooth enamel would lead to better diagnostics, prevention and treatment of this malformation on the first permanent molars and incisors.

REFERENCES

1. *Weerheijm KL.* Molar incisor hypomineralisation (MIH). Eur J Paediatr Dent 2003; 4(3): 114−20.
2. *Weerheijm KL, Mejare I.* Molar incisor hypomineralization: A questionnaire inventory of its occurrence in member countries of the European Academy of Paediatric Dentistry (EAPD). Int J Paediatr Dent 2003; 13(6): 411−6.
3. *Sabel N, Klingberg G, Dietz W, Nietzsche S, Norén JG.* Polarized light and scanning electron microscopic investigation of enamel hypoplasia in primary teeth. Int J Paediatr Dent 2010; 20(1): 31−6.
4. *Weerheijm KL1, Jälevik B, Alaluusua S.* Molar–incisor hypomineralisation. Caries Res 2001; 35(5): 390−1.

5. *Jalevik B, Noren JG.* Enamel hypomineralization of permanent first molars: A morphological study and survey of possible aetiological factors. Int J Paediatr Dent 2000; 10(4): 278−89.
6. *Ivanović M, Živojinović V, Šindolić M, Marković D.* Molar incisor hypomineralisation Srp Arh Celok Lek 2006; 135(7−8): 472−7. (Serbian)
7. *Willmott NS, Bryan RA, Duggal MS.* Molar-incisor-hypomineralisation: a literature review. Eur Arch Paediatr Dent 2008; 9(4): 172−9.
8. *Kotsanos N, Kaklamanos EG, Arapostathis K.* Treatment management of first permanent molars in children with Molar Incisor Hypomineralisation. Eur J Paediatr Dent 2005; 6(4): 179−84.
9. *Rodd HD, Boissonade FM, Day PF.* Pulpal status of hypomineralized permanent molars. Pediatr Dent 2007; 29(6): 514−20.
10. *Mahoney EK, Rohanizadeh R, Ismail FS, Kilpatrick NM, Swain MV.* Mechanical properties and microstructure of hypomineralised enamel of permanent teeth. Biomaterials 2004; 25(20): 5091−100.
11. *Xie ZH, Mahoney EK, Kilpatrick NM, Swain MV, Hoffman M.* On the structure-property relationship of sound and hypomineralized enamel. Acta Biomater 2007; 3(6): 865−72.
12. *Farah RA, Swain MV, Drummond BK, Cook R, Atieh M.* Mineral density of hypomineralised enamel. J Dent 2010; 38(1): 50−8.
13. *Jälevik B, Odelius H, Dietz W, Norén J.* Secondary ion mass spectrometry and X-ray microanalysis of Hypomineralized enamel in human permanent first molars. Arch Oral Biol 2001; 46(3): 239−47.
14. *Fearne J, Anderson P, Davis GR.* 3D X-ray microscopic study of the extent of variations in enamel density in first permanent molars with idiopathic enamel hypomineralisation. Br Dent J 2004; 196(10): 634−8.
15. *Braly A, Darnell LA, Mann AB, Teaford MF, Weihs TP.* The effect of prism orientation on the indentation testing of human molar enamel. Arch Oral Biol 2007; 52(9): 856−60.
16. *Xie Z, Kilpatrick NM, Swain MV, Munroe PR, Hoffman M.* Transmission electron microscope characterisation of molar-incisor-hypomineralisation. J Mater Sci Mater Med 2008; 19(10): 3187−92.
17. *Mahoney E, Ismail FM, Kilpatrick N, Swain M.* Mechanical properties across hypomineralized/hypoplastic enamel of first permanent molar teeth. Eur J Oral Sci 2004; 112(6): 497−502.
18. *Jälevik B.* Enamel Jälevik B. Enamel hypomineralization in permanent first molars. A clinical, histo-morphological and biochemical study. Swed Dent J Suppl 2001; (149): 1−86.
19. *Fagrell TG.* Molar incisor hypomineralization. Morphological and chemical aspects, onset and possible etiological factors. Swed Dent J Suppl 2011; 216(5): 11−83.
20. *Fagrell TG, Dietz W, Jälevik B, Norén JG.* Chemical, mechanical and morphological properties of hypomineralized enamel of permanent first molars. Acta Odontol Scand 2010; 68(4): 215−22.
21. *Baroni C, Marchionni S.* MIH supplementation strategies: prospective clinical and laboratory trial. J Dent Res 2011; 90(3): 371−6.
22. *Paine ML, Zhu D, Luo W, Snead ML.* Overexpression of TRAP in the enamel matrix does not alter the enamel structural hierarchy. Cells Tissues Organs 2004; 176(1−3): 7−16.
23. *Farah RA, Monk BC, Swain MV, Drummond BK.* Protein content of molar-incisor hypomineralisation enamel. J Dent 2010; 38(7): 591−6.
24. *Mangum JE, Crombie FA, Kilpatrick N, Manton DJ, Hubbard MJ.* Surface integrity governs the proteome of hypomineralized enamel. J Dent Res 2010; 89(10): 1160−5.

Received on March 10, 2014.
Revised on August 14, 2014.
Accepted on September 5, 2014.
Online First August, 2015.

ORIGINAL ARTICLE

UDC: 616.831-006-07:616-073.75
DOI: 10.2298/VSP140229073I

Apparent diffusion coefficient in the evaluation of cerebral gliomas malignancy

Difuzioni koeficijent u proceni stepena maligniteta cerebralnih glioma

Jelena Ignjatović*, Dragan Stojanov*, Vladimir Živković†, Srdjan Ljubisavljević*, Nebojša Stojanović*, Ivan Stefanović*, Daniela Benedeto-Stojanov*, Nebojša Ignjatović*, Sladjana Petrović*, Aleksandra Aracki-Trenkić‡, Zoran Radovanović*, Lazar Lazović‡

***Faculty of Medicine, University of Niš, Niš, Serbia; †Ministry of Defence, Belgrade, Serbia; ‡Center of Radiology, Clinical Center of Niš, Niš, Serbia**

Abstract

Background/Aim. Magnetic resonance imaging (MRI) is a key modality not only for lesion diagnosis, but also to evaluate the extension, type and grade of the tumor. Advanced MRI techniques provide physiologic information that complements the anatomic information available from conventional MRI. The aim of this study was to determine whether there is a correlation between apparent diffusion coefficient (ADC) maps of intracranial glial tumors and histopathologic findings and whether ADCs can reliably distinguish low-grade from high-grade gliomas. **Methods.** This retrospective study included 25 patients with MRI examination up to seven days before surgery, according to the standard protocol with the following sequences: T1WI, T2WI, FLAIR, DWI and post contrast T1WI. Data obtained from DW MRI were presented by measuring the value of ADC. The ADC map was determined by utilizing Diffusion-Perfusion (DP) Tools software. All the patients underwent surgical resection of the tumor. Histological diagnosis of tumors was determined according to the World Health Organization (WHO) classification. The ADC values were compared with the histopathologic findings according to the WHO criteria. **Results.** The ADC values of astrocytomas grades I (0.000614 ± 0.000032 mm^2/s) were significantly higher (< 0.001) than the ADC values of anaplastic astrocytomas (0.000436 ± 0.000016 mm^2/s) and the ADC values of glioblastomas multiforme (0.000070 ± 0.000008 mm^2/s). The ADC values of astrocytomas grades II (0.000530 ± 0.000114 mm^2/s) were significantly higher (< 0.001) than the ADC values of anaplastic astrocytomas (0.000436 ± 0.000016 mm^2/s) and glioblastomas multiforme (0.000070 ± 0.000008 mm^2/s). The ADC values of anaplastic astrocytomas (0.000436 ± 0.000016 mm^2/s) were significantly higher (< 0.001) than the ADC values of glioblastomas multiforme (0.000070 ± 0.000008 mm^2/s). The ADC values in the cystic part of the tumor for astrocytomas grades I (0.000775 ± 0.000023 mm^2/s) were significantly higher (< 0.001) than the ADC values of anaplastic astrocytomas (0.000119 ± 0.000246 mm^2/s) and glioblastomas multiforme (0.000076 ± 0.000004 mm^2/s). The ADC values astrocytomas grades II (0.000511 ± 0.000421 mm^2/s) were significantly higher (< 0.001) than the ADC values of glioblastomas multiforme (0.000076 ± 0.000004 mm^2/s). **Concluson.** DWI with calculation of ADC maps can be regarded as a reliable useful diagnostic tool, which indirectly reflects the proliferation and malignancy of gliomas. The ADCs maps can both predict the results of histopathological tumor and distinguish between low- and high-grade gliomas, and provide significant information for presurgical planning, treatment and prognosis for patients with high-grade astrocytomas.

Key words:
glioma; diffusion magnetic resonance imaging; diagnosis; neoplasm staging.

Apstrakt

Uvod/Cilj. Magnetna rezonanca (MRI) je ključni modalitet ne samo za dijagnostiku lezija, već i za procenu tipa i gradusa tumora i stepena širenja u okolno tkivo. Savremene MRI tehnike, kao što je *diffusion-weighted imaging* (DWI), obezbeđuje fiziološke informacije o tumoru, dopunjujući anatomske informacije dobijene na konvencionalnom MRI. Cilj naše studije bio je da se utvrdi da li postoji korelacija mape prividnog difuzionog koeficijenta (ADC) i patohistološkog nalaza, i da li ADC koeficijent može napraviti razliku između niskogradusnih i visokogradusnih glioma. **Metode.** Ovom retrospektivnom studijom bilo je obuhvaćeno 25 bolesnika, kod kojih je urađen MRI pregled do sedam dana pre operacije, prema standaradnom protokolu sa sledećim sekvencama: T1WI, T2WI, FLAIR, DWI i postkontrastna T1WI. Podaci dobijeni od DW MRI predstavljeni su merenjem vrednosti ADC koeficijenta. ADC mapa je određivana korišćenjem *Diffusion-Perfusion* (DP) *Tools* softvera. Svi bo-

Correspondence to: Dragan Stojanov, Faculty of Medicine, University of Niš, 11800 Niš, Serbia. Phone +381 18 20 20 40, +381 63 109 4197. E-mail: drstojanov@gmail.com

lesnici bili su podvrgnuti hirurškoj resekciji tumora. Histološka klasifikacija tumora izvršena je prema kriterijumima Svetske zdravstvene organizacije. Dobijene ADC vrednosti upoređivane su sa patohistološkim nalazom tumora. **Rezultati.** Vrednost ADC koeficijenta astrocitoma gradus I (0,000614 ± 0,000032 mm^2/s) bila je statistički značajno viša (< 0,001) od vrednosti ADC koeficijenta anaplastičnog astrocitoma (0,000436 ± 0,000016 mm^2/s) i glioblastoma multiforme (0,000070 ± 0,000008 mm^2/s). Vrednosti ADC koeficijenta astrocitoma gradusa II (0,000530 ± 0,000114 mm^2/s) bila je statistički značajno viša (< 0,001) od vrednosti ADC koeficijenta anaplastičnog astrocitoma (0,000436 ± 0,000016 mm^2/s) i glioblastoma multiforme (0,000070 ± 0,000008 mm^2/s). Vrednosti ADC koeficijenta anaplastičnog astrocitoma (0,000436 ± 0,000016 mm^2/s) bila je statistički značajno viša (< 0,001) od vrednosti ADC koeficijenta glioblastoma multiforme (0,000070 ± 0,000008 mm^2/s). Astrocitom gradusa I (0,000775 ± 0,000023 mm^2/s) imao je vrednost ADC koeficijenta cisticnog dela tumorskog tkiva statistički značajno višu (< 0,001) od vrednosti ADC anaplastičnog astrocitoma (0,000119 ± 0,000246 mm^2/s) i glioblastoma multiforme (0,000076 ± 0,000004 mm^2/s). Vrednost ADC koeficijenta astrocitoma gradusa II (0,000511 ± 0,000421 mm^2/s) je bila statistički značajno viša (< 0,001) od vrednosti ADC koeficijenta glioblastoma multiforme (0,000076 ± 0,000004 mm^2/s). **Zaključak.** DWI sa određivanjem ADC mape može se smatrati pouzdanim dijagnostičkim sredstvom koje posredno odražava proliferaciju i malignitet glioma. Vrednost ADC mape može predvideti histopatološke rezultate tumora, razlikovati niskogradusne od visokogradusnih glioma, ali i pružiti značajne informacije za prehirurško planiranje, lečenje i prognozu bolesnika sa visokogradusnim astrocitomima.

Ključne reči:
gliom; magnetna rezonanca, difuziona; dijagnoza; neoplazme, određivanje stadijuma.

Introduction

'The first application of magnetic resonance imaging (MRI) in the early 1980s radically changed the radiographic diagnosis of primary and secondary brain tumors. MRI is a key modality not only for lesion diagnosis, but also to evaluate the extension, type and grade of the tumor. Advanced MRI techniques such is diffusion weighted imaging (DWI) provide physiologic information that complements the anatomic information available with conventional MRI [1]. In recent years the increasing number of the world's researches has been focused on proving the fundamental and practical importance of DWI and apparent diffusion coefficient (ADC) and the possibility of using the results in tumor grading, determination of tumor cellularity, to differentiate tumor and perifocal edema and especially emphasizes the possible ability to predict response to applied treatment of tumor [2]. There appears to be a correlation between the apparent diffusion coefficient values on the one hand and tumor cellularity and tumor grade on the other [3]. Research data on intracranial tumors indicate that high ADC values were attributable to low cellularity, necrosis or cysts, and lower values to dense, highly cellular tumor [4].

The aim of this study was to determine whether there is a correlation between ADC maps of intracranial glial tumors and histopathologic findings and whether ADC values can reliably distinguish low- grade from high-grade gliomas.

We have hypothesized that the ADC value can make the difference between low and high grades gliomas, and ADC value ratio can predict the histoapthological results of tumros.

Methods

A retrospective study involved a group of 25 patients with histologically proven intracranial gliomas. MRI examination was performed on the Siemens Avanto MR device (Erlangen, Germany) with magnetic field of 1.5 Tesla (T). The examinations were performed in all the patients, up to seven days before surgery, according to the standard protocol with the following sequence: T1WI, T2WI, FLAIR, DWI and post contrast T1WI. All the patients underwent surgical resection of the tumor. Histological diagnosis of tumors was determined according to the World Health Organization (WHO) classification.

Data obtained from DWI MRI were presented by measuring the value of ADC coefficients. The ADC map was determined by utilizing DP Tools software (Figure1). Based on the typical MR output, data in terms of localization, size and morphological characteristics of the tumor were determined; based on the quantity of DWI MRI values and its degree of malignancy (biological potential) was established. The ADC values were compared with the histopathologic findings according to the WHO criteria.

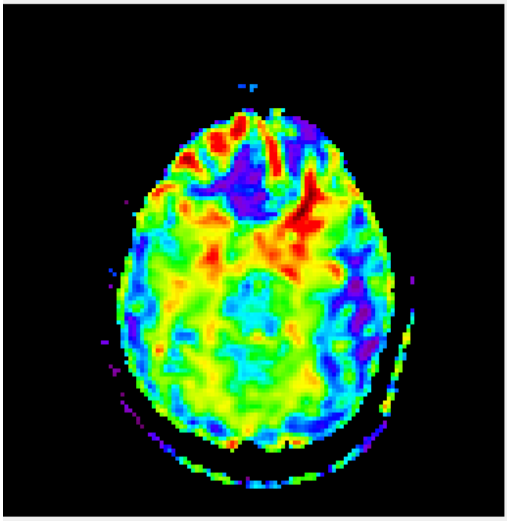

Fig. 1 – Apparent diffusion coefficients (ADC) map of patients with glioblastoma multiforme.

For registration, grading, grouping, graphical and tabular representation of the data, Microsoft Excel 2003 software was utilized. The results were analysed by SPSS software, version 10.0. Within this analysis the statistical boundary of an error was within 0.05 (5%). The following statistical pa-

rameters were shown: arithmetic mean ($\bar{x}$), standard deviation (SD), median, minimal value, maximum value and index of structure (%). By comparing the values of DWI and ADC among different patients that were researched with pathological diagnostics, analysis of variance (ANOVA) and Dunnett *post hoc* test were performed. The correlation was carried out by quantitative comparison of the vales of ADCs with the degree of malignancy, and the DWI MR diagnosis with definite histopathological diagnosis of brain tumors.

Results

Out of 25 patients with gliomas included in the study 15 (60%) were men and 10 (40%) women. Malignancy of the tumor was graded by WHO I–IV. The diagnosis of the tumor was astrocytoma grade I (2 patients), astrocytoma grade II (5 patients), anaplastic astrocytoma (5 patients), glioblastoma multiforme (13 patients) (Table 1).

The average age of all the patients was 50.40 ± 12.53 years. The youngest patient had 19 and the oldest ones 77 years. The patients with glioblastoma multiforme (54.08 ± 2.83 years) and anaplastic astrocytomas (52.00 ± 9.59 years) were older those with the astrocytoma grade I (49.00 ± 2.83 years) and astrocytoma grade II (39.80 ± 9.63 years) (Table 2).

The ADC values of astrocytomas grade I (0.000614 ± 0.000032 mm^2/s) were significantly higher (< 0.001) than the ADC values of anaplastic astrocytomas (0.000436 ± 0.000016 mm^2/s) and ADC values of glioblastomas multiforme (0.000070 ± 0.000008 mm^2/s) (Tables 3 and 4). The ADC values of astrocytomas grade II (0.000530 ± 0.000114 mm^2/s) were significantly higher (< 0.001) than the ADC values of anaplastic astrocytomas (0.000436 ± 0.000016 mm^2/s) and glioblastomas multiform (0.000070 ± 0.000008 mm^2/s). The ADC values of anaplastic astrocytomas (0.000436 ± 0.000016 mm^2/s) were significantly higher (< 0.001) than ADC values of glioblastomas multiform (0.000070 ± 0.000008 mm^2/s).

Table 1

Distribution of patients compared to histopathological diagnosis and sex

Histopathological diagnosis	Sex, n (%)		Total
	men	woman	
Astrocitomas grades I	2 (8)	–	2 (8)
Astrocytomas grades II	3 (12)	2 (8)	5 (20)
Anaplastic astrocytomas	4 (16)	1 (4)	5 (20)
Glioblastoma multiforme	6 (24)	7 (28)	13 (52)
Gliomas total	15 (53.6)	10 (31.3)	25 (100)

Table 2

Distribution of the patients compared to histopathological diagnosis and age

Histopathological diagnosis	Age (years)				
	$\bar{x}$	SD	med	min	max
Astrocitomas grades I	49.00	2.83	49.00	47.00	51.00
Astrocytomas grades II	39.80	9.63	43.00	29.00	52.00
Anaplastic astrocytomas	52.00	19.56	61.00	24.00	72.00
Glioblastoma multiforme	54.08	9.59	55.00	38.00	77.00
Gliomas total	50.40	12.53	51.00	24.00	77.00

$\bar{x}$ – arithmetic mean; SD – standard deviation; min – minimal value; max – maximal value; med – mediana.

Table 3

The value of apparent diffusion coefficients (ADC) of the solid part of the tumor in comparison with histopathological diagnosis

Histopathological diagnosis	ADC (mm^2/s)				
	$\bar{x}$	SD	med	min	max
Astrocitomas grades I	0.000614	0.000032	0.000636	0.000565	0.000645
Astrocytomas grades II	0.000530	0.000114	0.000510	0.000222	0.000671
Anaplastic astrocytomas	0.000436	0.000016	0.000432	0.000412	0.000462
Glioblastoma multiforme	0.000070	0.000008	0.000069	0.000059	0.000082
Gliomas total	0.000491	0.000160	0.000495	0.000059	0.000671

$\bar{x}$ – arithmetic mean; SD – standard deviation; min – minimal value; max – maximal value; med – mediana.

Table 4

Comparison of the apparent diffusion coefficients (ADC) values of the solid part of the tumor between the different histologic diagnosis (ANOVA and Bonferroni post-hoc test - *p*)

Histopathological diagnosis	Astrocitomas grades II	Astrocitomas grades III	GBM
Astrocitomas grades I	0.0018	< 0.001	< 0.001
Astrocitomas grades II		0.001	< 0.001
Astrocitomas grades III			< 0.001

GBM – glioblastoma multiforme.

The ADC values in the cystic part of tumor for astrocytomas grade I (0.000775 ± 0.000023 mm^2/s) were significantly higher (< 0.001) than the ADC values of anaplastic astrocytomas (0.000119 ± 0.000246 mm^2/s) and glioblastomas multiforme (0.000076 ± 0.000004 mm^2/s) (Tables 5 and 6). The ADC values of astrocytomas grade II (0.000511 ± 0.000421 mm^2/s) were significantly higher (< 0.001) than the ADC values of glioblastomas multiforme (0.000076 ± 0.000004 mm^2/s).

Discussion

Astrocytomas are the most common primary brain neoplasms in adults and account for more than 70% of all gliomas. The WHO Grades III and IV malignant astrocytomas include anaplastic astrocytoma and glioblastoma multiforme and are the most prevalent astrocytomas, with the annual incidence of 3–4 per 100.000. At least 80% of malignant gliomas are glioblastoma [5]. Anaplastic astrocytoma and glioblastoma tend to invasion of the surrounding brain. Histopathological studies found malignant cells in macroscopically unsuspicious brain parenchyma remote from the primary tumor, even affecting the contralateral hemisphere. In early stages, diffuse interneural infiltration with changes of the ADC occurs. Only about 2% of patients with high-grade brain tumors survive the first 5 years after diagnosis. One of the main factors for the poor prognosis of glioblastomas is the invasiveness of malignant cells. These infiltrating glioma cells can hardly be imaged by standard techniques [6].

Conventional MRI can display the anatomical appearance of brain tumor, but fails to provide physiologic and functional information that is crucial for tumor grading, predicting clinical outcome and response to therapy [7]. Advanced MRI technics such as quantitative DWI, which utilizes the Brownian motion of water molecules, has been shown to be able to provide information [8] at the cellular or physiologic level [9] about cellular density and properties of the extracellular matrix. Because extracellular water molecules move more freely than those in the intracellular spaces, the ADC value calculated from DWI can serve as a marker of cellularity [8]. ADC is a direct reflection of tumor cell density [10]. This potential biomarker can be obtained without any radiation hazard or contrast media in only few minutes, and has been proven to be effective in predicting and monitoring the treatment of various cancers [8].

It is believed that ADC can be an important diagnostic and prognostic biomarker as it is thought to be inversely proportional and correlated with cellularity and tumor malignancy [8, 9]. So it indicates that the most aggressive and most cellularity places within heterogeneous tumors, which are prognostic essential, correspond to the minimum ADC value [9]. For now, have also been spotted some limitations of the DW such as: poor spatial resolution, the inability to eliminate certain artefacts (eg. skull base bone, the air in the sinus cavities) and there are some changes in ADC values in the presence of hemorrhagic, necrotic and cystic fields. Strength matches and mismatches with the ADC map also affect the furthest outcome measurements and results [9].

ADC values of some tumors are inversely related to cellularity and the ratio of nuclear area to total cytoplasm, and thus decreased ADCs may be found in some aggressive tumors. Differences in ADCs likely reflect differences in cellularity and density, nuclear-to-cytoplasmic ratio, extracellular matrix, and edema. For instance, a low ADC value is the result of reduced extracellular water motion within the crowded interstitium of a hypercellular area, or from impeded intracellular water motion within cells of a high nuclear-to-cytoplasmic ratio. Gliomas have been found to have ADC values inversely correlated to cell density and the ratio of nuclear area to total cytoplasm, with lower values correlating with more aggressive tumor. ADC can accurately predict tumor behavior and monitor treatment responses with standardized protocols [11]. A functional diffusion map, made by mapping the changes in ADC values potentially reflects cellularity, as a predictive biomarker for the anti-angiogenic treatment of malignant gliomas. Hypercellular regions defined by the functional diffusion map

Table 5

Apparent diffusion coefficients (ADC) value of the cystic part of the tumor in comparison with histopathological diagnosis

Histopathological diagnosis	ADC (mm^2/s)				
	$\bar{x}$	SD	med	min	max
Astrocitomas grades I	0.000755	0.000023	0.000761	0.000701	0.000789
Astrocytomas grades II	0.000511	0.000421	0.000640	0.000000	0.000992
Anaplastic astrocytomas	0.000119	0.000246	0.000000	0.000000	0.000604
Glioblastoma multiforme	0.000076	0.000004	0.000075	0.000071	0.000081
Gliomas total	0.000446	0.000396	0.000598	0.000000	0.000992

$\bar{x}$ – arithmetic mean; SD – standard deviation; min – minimal value; max – maximal value; med – mediana.

Table 6

Comparison of the apparent diffusion coefficients (ADC) values of the cystic part of the tumor between the different histologic diagnosis (ANOVA and Bonferroni *post-hoc* test – *p*)

Histopathological diagnosis	Astrocitomas grades II	Astrocitomas grades III	GBM
Astrocitomas grades I	0.106	< 0.001	< 0.001
Astrocitomas grades II		0.017	< 0.001
Astrocitomas grades III			0.999

GMB – glioblastoma multiforme.

were shown to be predictive of tumor progression. Patients with persistent diffusion restriction demonstrated better survival, which was explained by atypical necrosis [8].

A lower value of ADC indicates highly malignant gliomas, and high ADC value corresponds to low grades astrocytomas, as evidenced in the results of previous studies [12]. Our findings are in accordance with the previously reported. Barajas et al. [13] suggest that while ADC measurements correlate with tumor cell density, DWI is a more accurate predictor of clinical outcome, given the capacity of this technique to summate additional unidentified prognostic biologic features of tumor aggressiveness beyond cell density. Several other studies have demonstrated change in post-therapeutic ADC values following radiation and chemotherapy in primary glial brain tumors [13].

The ADC has been found to have an inverse relation with the grade of astrocytomas. Lower ADC values suggest a malignant high-grade astrocytoma, whereas higher ADCs suggest low-grade astrocytoma. On the basis of specific histologic features of the tumor, such as cellularity, nuclear atypia, mitosis, pleomorphism, vascular hyperplasia, and necrosis, the revised WHO classification subdivides gliomas into four grades. Among mean ADC, minimum ADC, and maximum ADC values, minimum ADC value was the strongest prognostic factor in glioblastoma multiforme (GBM) patients for overall survival [14]. Brasil Caseiras et al. [15] distinguished low-grade gliomas (grade II astrocytomas) as having no effect on prognosis with respect to ADC values. None of the ADC parameters proved to be a useful predictor of malignant transformation in low-grade gliomas. Low ADC values, independent of tumor grade, correlate with poor survival in malignant astrocytomas. Pretreatment DWI with calculation of ADC values may be helpful for planning therapy and in prognostication for patients with high-grade astrocyotomas [14].

A study conducted by Yin et al. [16] showed that the ADC values were inversely correlated to the degree of malignancy of gliomas, namely that high grade gliomas had significantly lower ADC and relative ADC (rADC) values in relation to gliomas categorized as low grade. Also, Ristić-Baloš et al. [17] reported that DWI can be useful in differentiating benign and malignant tumors from normal parenchyma and in grading gliomas. The results of our research correspond with previous findings from the literature that glial tumors grade II and grade III showed a statistical significance. In the patients with anaplastic astrocytoma, values of ADC were between glioblastom (GBM) and astrocytoma grade II. Our findings are in accordance with the previously reported [18–20].

In a series of 20 patients with histologically proven gliomas, the ADC value of high grade gliomas was significantly lower than the value of low- grade gliomas [21], which coincides with our results. The lower ADC value of GBM compared to low-grade astrocytomas was observed in a series of 56 patients with intracranial tumors [22]. In our study, the ADC value of the GBM was significantly lower than the ADC value of astrocytoma grade I. Qualitative assessment of the ADC map shows low signal in the contrast discolorated area compared to the no-discolorated peritumoral and edema in high- grade gliomas [23]. However, some researchers argue that the ADC map helps in differentiating tumors from the normal brain tissue and grading of malignant neoplasms, but it is impossible to distinguish between malignant and benign tumors [24].

Some researchers argue that there is a considerable overlap of ADC values of the normal brain tissue and those of high- and low- grade neoplasms raising the question of their utility in individual patients [22, 25]. However, Lam et al. [26], based on their research, found that there was no significant difference between the grade of the tumor based on ADC values. DWI can be used for assessment of glioma invasion and detection of necrotic tumor. There is also a correlation between ADC values after surgery with postoperabtive radiotherapy and survival time in patients with glioblastoma. A significant shorter median survival time has been shown for patients with low ADC values within residual T2 hyperintense zone [24].

Conclusion

ADC values of tumor parenchyma can indirectly reflect the proliferation and malignancy of gliomas. ADC maps can distinguish low- and high-grade gliomas, and ADC values can predict the results of histopathological findings.

Therefore, DWI with calculation of ADC maps can be regarded as reliable useful diagnostic tools which provide useful information not only for the diagnosis and grading of gliomas, but also for presurgical planning, treatment and prognosis for patients with high-grade astrocytomas.

REFERENCES

1. *Rollin N, Guyotat J, Streichenberger N, Honnorat J, Tran MV, Cotton F.* Clinical relevance of diffusion and perfusion magnetic resonance imaging in assessing intra-axial brain tumors. Neuroradiology 2006; 48(3): 150−9.
2. *Baehring JM, Bi WL, Bannykh S, Piepmeier JM, Fulbright RK.* Diffusion MRI in the early diagnosis of malignant glioma. J Neurooncology 2007; 82(2): 221−5.
3. *Yamasaki F, Kurisu K, Satoh K, Arita K, Sugiyama K, Ohtaki M,* et al. Apparent diffusion coefficient of human brain tumors at MR imaging. Radiology 2005; 235(3): 985−91.
4. *Yang D, Korogi Y, Sugahara T, Kitajima M, Shigematsu Y, Liang L,* et al. Cerebral gliomas: prospective comparison of multivoxel 2D chemical-shift imaging proton MR spectroscopy, echoplanar perfusion and diffusion-weighted MRI. Neuroradiology 2002; 44(8): 656−66.
5. *Zulfiqar M, Yousem DM, Lai H.* ADC Values and Prognosis of Malignant Astrocytomas: Does Lower ADC Predict a Worse Prognosis Independent of grade of Tumor. Am J Radilology 2013; 200(3): 624−9.
6. *Kallenberg K, Goldmann T, Menke J, Strik H, Bock HC, Stockhammer F,* et al. Glioma infiltration of the corpus callosum: early signs detected by DTI. J Neurooncology 2013; 112(2): 217−22.
7. *Wang S, Kim S, Melhem ER.* Diffusion Tensor Imaging: Introduction and Applications to Brain Tumor Characterization. In: Pillai JJ, editor. Functional Brain Tumor Imaging. New York, USA: Springer Science Business Media; 2014. p. 27−38.

8. *Hwang EJ, Cha Y, Lee EL, Yun TJ, Kim TM, Park CK*, et al. Early response evaluation for recurrent high grade gliomas treated with bevacizumab: a volumetric analysis using diffusion-weighted imaging. J Neurooncology 2013; 112(3): 427−35.
9. *Nakamura H, Murakami R, Hirai T, Kitajima M, Yamashita Y*. Can MRI-derived factors predict the survival in glioblastoma patients. Acta Radiology 2013; 54(2): 214−20.
10. *Ellingson BE, Timothy F, Cloughesy TF, Lai A, Nghiemphu PL, Pope WB*. Cell invasion, motility, and proliferation level estimate (CIMPLE) maps derived from serial diffusion MR images in recurrent glioblastoma treated with bevacizumab. J Neurooncology 2011; 105(1): 91−101.
11. *Yeom KW, Lober RM, Andre JB, Fisher PG, Barnes PD, Edwards MS*, et al. Prognostic role for diffusion-weighted imaging of pediatric optic pathway glioma. J Neurooncology 2013; 113(3): 479−83.
12. *Noguchi K, Watanabe N, Nagayoshi T, Kanazawa T, Toyoshima S, Shimizu M,* et al. Role of diffusion-weighted echo-planar MRI in distinguishing between brain brain abscess and tumour: a preliminary report. Neuroradiology 1999; 41(3): 171−4.
13. *Barajas RF, Rubenstein JJ, Chang JS, Hwang J, Cha S*. Diffusion-Weighted MR Imaging Derived Apparent Diffusion Coefficient Is Predictive of Clinical Outcome in Primary Central Nervous System Lymphoma. Am J Neuroradiology 2010; 31(1): 60−6.
14. *Zulfiqar M, Yousem DM, Lai H*. ADC values and prognosis of malignant astrocytomas: does lower ADC predict a worse prognosis independent of grade of tumor?-a meta-analysis. AJR 2013; 200(3): 624−9.
15. *Brasil Caseiras G, Ciccarelli O, Altmann DR, Benton CE, Tozer DJ, Tofts PS,* et al. Low-grade gliomas: six-month tumor growth predicts patient outcome better than admission tumor volume, relative cerebral blood volume, and apparent diffusion coefficient. Radiology 2009; 253(2): 505−12.
16. *Yin Y, Tong D, Liu X, Yuan T, Yan Y, Ma Y*, et al. Correlation of apparent diffusion coefficient with Ki-67 in the diagnosis of gliomas. Zhongguo Yi Xue Ke Xue Yuan Xue Bao 2012; 34(5): 503−8.
17. *Ristić-Balos D, Gavrilović S, Lavrnić S, Vasić B, Macvanski M, Damjanović D,* et al. Proton magnetic resonance spectroscopy and apparent diffusion coefficient in evaluation of solid brain lesions. Vojnosanit Pregl 2013; 70(7): 637−44.
18. *Bergui M, Zhong J, Bradac GB, Sales S*. Diffusion-weighted images of intracranial cyst-like lesions. Neuroradiology 2001; 43(10): 824−9.
19. *Castillo M, Smith JK, Kwock L, Wilber K*. Apparent diffusion coefficients in the evaluation of high-grade cerebral gliomas. Am J Neuroradiology 2001; 22(1): 60−4.
20. *Sinha S, Bastin ME, Whittle IR, Wardlaw JM*. Diffusion tensor MR imaging of high grade cerebral gliomas. Am J Neuroradiology 2002; 23(4): 520−7.
21. *Sugahara T, Korogi Y, Kochi M, Ikushima I, Shigematu Y, Hirai T,* et al. Usefulness of diffusion-weighted MRI with echo-planar technique in the evaluation of cellularity in gliomas. J Magn Reson Imaging 1999; 9(1): 53−60.
22. *Kono K, Inoue Y, Nakayama K, Shakudo M, Morino M, Ohata K*, et al. The role of diffusion-weighted imaging in patients with brain tumors. Am J Neuroradiology 2001; 22(6): 1081-1088.
23. *Tien RD, Felsberg GJ, Friedman H, Brown M, Mac Fall J*. MR imaging of high-grade cerebral gliomas: value of diffusion-weighted echoplanar pulse sequences. Am J Roentgenology 1994; 162(3): 671−7.
24. *Bulakbasi N, Kocaoglu M, Ors F, Tayfun C, Ucoz T*. Combination of single-voxel proton MR spectroscopy and common brain tumors. Am J Neuroradiology 2003; 24(2): 225−33.
25. *Guo AC, Cummings TJ, Dash RC, Provenzale JM*. Lymphomas and high-grade astrocytomas: comparison of water diffusibility and histologic characteristics. Radiology 2002; 224(1): 177−83.
26. *Lam WW, Poon WS, Metreweli C*. Diffusion MR imaging in glioma: does it have any role in the pre-operation determination of grading of glioma? Clin Radiol 2002; 57(3): 219−25.

Received on February 29, 2014.
Revised on March 27, 2014.
Accepted on April 4, 2014.
Online First August, 2015.

ORIGINAL ARTICLE

UDC: 616.379-008.64-06::617.7-08
DOI: 10.2298/VSP140402074J

Intravitreal bevacizumab injection alone or combined with macular photocoagulation compared to macular photocoagulation as primary treatment of diabetic macular edema

Intravitrealna primena bevacizumaba sa ili bez laser-tretmana u poređenju sa laser-tretmanom kao primarnim načinom lečenja dijabetesnog edema makule

Sandra Jovanović*, Vladimir Čanadanović*, Ana Sabo†, Zorka Grgić*, Milena Mitrović‡, Dušan Rakić§

***Clinic for Eye Diseases, ‡Endocrinology, Diabetes and Metabolic Disorders Clinic, Clinical Center of Vojvodina, Faculty of Medicine, University of Novi Sad, Novi Sad, Serbia; †Department of Pharmacology, Toxicology and Clinical Pharmacology, Faculty of Medicine, University of Novi Sad, Novi Sad, Serbia;§Department of Mathematics, Faculty of Technology, University of Novi Sad, Novi Sad, Serbia**

Abstract

Background/Aim. Within diabetic retinopathy (DR), diabetic macular edema (DME) is one of the leading causes of the loss of visual acuity. The aim of this study was to determine the efficacy of the intravitreal vascular endothelial growth factor (VEGF) inhibitor application alone or combined with macular focal/grid lasephotocoagulation compared with laser treatment alone. **Methods.** This prospective randomized clinical trial included 72 patients (120 treated eyes) with varying degrees of DR and DME. The DME treatment included intravitreal VEGF inhibitor bevacizumab (Avastin®) application, with and without laser treatment. Bevacizumab (1.25 mg/0.05 mL) was administered intravitreally in 4–6-week intervals. Laser is applied 4–6 weeks after last dose of the drug as a part of combined treatment, or as the primary treatment. **Results.** The mean reduction in central macular thickness (CMT) for the eyes (n = 31) treated with bevacizumab alone was 162.23 μm, for the eyes (n = 53) treated with combined treatment the mean reduction in CMT was 124.24 μm, both statistically significant at $p < 0.001$. Laser macular photocolagulation as a part of combined treatment (in 53 eyes) significantly contributed to the CMT reduction, based on the paired *t*-test results (366.28 *vs* 323.0 μm at $p < 0.05$). In our study, the mean visual acuity improvement of 0.161 logMAR was achieved in the group of eyes treated with bevacizumab alone, and 0.093 logMAR in the group with combined treatment, both statistically significant at $p < 0.05$. The effect of laser photocolagulation alone on visual acuity and CMT was not statistically significant. **Conclusion.** Treatment with bevacizumab alone or within combined treatment is more effective in treating DME than conventional macular laser treatment alone, both anatomically and functionally.

Key words:
diabetic retinopathy; macular edema; ophthalmologic surgical procedures; vascular endothelial growth factors; light coagulation; treatment outcome.

Apstrakt

Uvod/Cilj. U sklopu dijabetesne retinopatije (DR) jedan od najranijih razloga koji dovodi do pada oštrine vida je dijabetesni makularni edem (DME). Cilj rada bio je utvrđivanje efikasnosti lečenja DME intravitrealnom primenom inhibitora vaskularnog endotelnog faktora rasta (VEGF) samostalno ili u sklopu kombinovanog lečenja laserfotokoagulacijom makule tipa fokal/*grid* i poređenje sa konvencionalnim lečenjem makule laserom. **Metode.** Istraživanje je sprovedeno kao prospektivna, randomizirana klinička studija na 72 bolesnika (120 lečena oka) sa različitim stepenom DR i DME. Lečenje DME podrazumevalo je intavitrealnu primenu inhibitora VEGF bevacizumaba (Avastin®) sa ili bez primene lasera. Lek je primenjivan u dozi 1,25 mg u 0,05 mL u razmacima od 4 do 6 nedelja. Laserfotokoagulacija vršena je u kontrolnoj grupi kao primarni vid terapije ili kao dopuna prethodnog lečenja makule aplikacijom bevacizumaba nakon 4–6 nedelja od poslednje doze ukoliko nije došlo do poboljšanja centralne debljine makule (CMT). **Rezultati.** Prosečna vrednost smanjenja CMT za oči (n = 31) lečene samo bevacizumabom iznosila je 162,23 μm, za oči lečene kombinovanom metodom (n = 53) redukcija CMT iznosila je 124,24 μm; statistički značajno u obe grupe $p < 0,05$. Laserfotokoagulacija makule kod bolesnika/očiju sa kombinovanim lečenjem statistički značajno je doprinosila dodatnom redukovanju CMT na osnovu uporednog *t*-testa (366,28 prema 323,0 μm; $p < 0,05$). U našoj studiji postignuto

Correspondence to: Sandra Jovanović, Clinic for Eye Diseases, Clinical Center of Vojvodina, Hajduk Veljkova 1–3, 21 000 Novi Sad, Serbia. E-mail: drjovanovicsns@gmail.com

prosečno poboljšanje oštrine vida u grupi očiju lečenih intravitrealnom primenom bevacizumaba iznosilo je 0,161 logMAR, kod očiju sa kombinovanim lečenjem, 0,093 logMAR, statistički značajno u obe grupe $p < 0,05$. Uticaj laserfotokoagulacije, samostalno, na oštrinu vida i CMT bio je bez statističke značajnosti. **Zaključak.** Lečenje DME intravitrealnim aplikacijama bevacizumaba samostalno ili u sklopu kombinovanog lečenja je efikasnije nego konvencionalno lečenje makule laserom, kako anatomski tako i funkcionalno.

Ključne reči:
dijabetesna retinopatija; žuta mrlja, edem; hirurgija, oftalmološka, procedure; faktori rasta endotela krvnih sudova; fotokoagulacija; lečenje, ishod.

Introduction

Diabetic retinopathy (DR), a microangiopathic complication of diabetes mellitus (DM), is among the leading causes of acquired blindness in developed countries (in patients aged 65 or older), as well as developing countries (in working-age population, aged 45 to 65) [1]. Thus, DR is not only medical, but also socioeconomic issue. DR is one of the most frequent DM complications, occurring in 40% of affected individuals above the age of 40 [2].

Within DR, diabetic macular edema (DME) is one of the earliest causes of the loss of visual acuity. The development of DME is typically noted in older patients diagnosed with Type II DM [3]. DME prevalence of approximately 14% has been reported in DM affected individuals [4]. While DME onset can occur at any stage of DR development, it is more frequent in more severe DR forms, and its prevalence increases with the illness duration. The type of DM, as well as therapy (insulin, orally administered hypoglycemic agents, or diet), is also noteworthy. In addition to the aforementioned factors, further contributors to DR and DME onset and progression are metabolic glycemic control, arterial hypertension, dyslipidemia and proteinuria [5].

In the DME pathophysiology, chronic hyperglycemia plays the key role, causing oxidative stress and retinal capillary endothelial cell damage accompanied by inflammatory response, the consequence of the breakdown of hematoretinal (H-R) barrier [6]. The disruption of the flow control mechanisms leads to hypoxia, causing the release of vascular endothelial growth factor (VEGF).

VEGF plays an important role in the early phases of DR development, as the decomposition of the "tight junctions" leads to the breakdown of the inner H-R barrier, which results in increased permeability and development of DME [7]. On the other hand, in the hypoxia conditions, VEGF represents the most potent mitogen for the vascular endothelial cells, as it induces the angiogenesis process. VEGF-A is most frequently encountered in ocular pathology, and is the target of most anti-VEGF agents [8, 9]. Application of anti-VEGF agents has led to significant improvements in the treatment of vascular-ischemic ophthalmic diseases.

Bevacizumab **(**Avastin®; Genentech, San Francisco, USA**)** provides recombined humanized monoclonal IgG1 antibodies in their entirety, aimed against all VEGF-A isoforms. In 2004 bevacizumab was approved by the Food and Drug Administration for intravenous infusion application, as a part of chemotherapy in the treatment of metastatic carcinoma of the colon and the rectum. Off-label bevacizumab application in ophthalmology in the form of intravitreal injections was first introduced as a part of the treatment of age-related macular degeneration – the wet form. The application scope subsequently widened to include DME, following the favorable results reported in the DR clinical research network studies [10].

In treating DME, in addition to the necessary management of the primary condition and other risk factors, thus far, laser photocoagulation used to be a gold standard. However, numerous studies have demonstrated that laser treatment can only stabilize the current state [11]. Recently, new promising treatment forms have emerged, including the aforementioned medications in the VEGF inhibitor group.

The aim of this study was to evaluate the efficacy of DME treatment consisting of intravitreal VEGF inhibitor application alone or as a part of combined treatment (intravitreal VEGF inhibitor plus laserphotocoagulation) compared with laser treatment alone.

Methods

The research was conducted as a prospective randomized clinical study at the Clinic for Eye Diseases, Clinical Center of Vojvodina, in Novi Sad during a 2012–2013 period. The study was approved by the Clinical Center of Vojvodina Ethics Committee. The participating patients provided their informed consent, after being provided written and verbal information on the application of off-label medications and their potential side-effects. The study included 72 patients (120 treated eyes) with varying degrees of DR and DME. DR and DME were defined according to the International Clinical Diabetic Retinopathy and Diabetic Macular Edema Disease Severity Scale, published by the International Council of Ophthalmology (ICO) in 2002 [12].

The treatment consisted of intravitreal VEGF inhibitor bevacizumab (Avastin®) application, with and without laser treatment. In the control group the patients were treated with lasephotocoagulation only. The patients that met the following criteria were included in the study: severe DME that affects the fovea, reduction in visual acuity and/or metamorphopsia, diffuse edema with or without cystic edema [confirmed by fluorescein angiography (FA) and by optical coherence tomography (OCT)], central macular thickness (CMT) $\geq$ 300 μm, the absence of hard lipid exudates in the form of plaque in the subfoveal region, no prior laser treatment, no prior VEGF inhibitor treatment, and no previous intravitreal or subtenonian corticosteroid administration. The exclusion criteria were: high risk and advanced proliferative DR (PDR), the presence of other eye diseases that could affect visual acuity, prior eye surgeries, recent myocardial in-

farction, insult, and unregulated DM (Hb1c higher than 11%) and hypertension.

All the participating patients were given full ophthalmological examination, which included determining the best corrected visual acuity (BCVA), intraocular pressure (IOP) measurement, examination of the anterior eye segment, examination of the posterior segment in medical mydriasis *via* contactless ophthalmoscopy using the 90 D magnifying glass (by Volk). The auxiliary diagnostic procedures performed included FA and OCT. FA was initially performed with the aim of diagnosing the edema type, and was repeated upon the treatment completion (both pharmacological and laser components). OCT was instrumental in assessing the patients for inclusion in the study, as well as in the monitoring of treatment efficacy. It was performed on the apparatus manufactured by Carl Zeiss Meditec, Dublin, CA, "Stratus" model, using the "fast macula" or "fast macula thickness map" program.

Intravitreal application of 1.25 mg bevacizumab (0.05 mL of Avastin®) was performed under surgical microscope at 4 mm distance from limbus, in the *pars plana* region of the ciliary body, using a 27 G diameter syringe. Avastin® was administered in the operating theatre in strict sterile conditions.

Control follow-ups were performed four weeks after the treatment, and included BCVA determination, fundus examination in mydriasis, and OCT. Visual acuity was converted into the logarithm of the Minimal Angle of Resolution (logMAR). If required, the treatment was repeated 4 to 6 weeks after the initial application, and at two further occasions at the same intervals. Once the pharmacological treatment was completed, due to satisfying results or no further improvement, next step of treatment, laserphotocoagulation using the focal/grid method, was performed after 4 to 6 weeks. The effect of combined therapy was evaluated after 6 weeks. The aim was to achieve the CMT below 250 μm, *ie*, as close to normal values as feasible.

All statistical analyses were performed using the software package Statistica (version 10). The mean values of the obtained results were analyzed *via* paired *t*-test at 95% confidence interval. This approach was most suitable for this study, as the values obtained for each patient were compared individually, at different treatment stages.

Results

The study included 72 patients (120 treated eyes), all of whom had complete data and were followed-up for a minimum of six months. The average age of patients diagnosed with DR and DME was 62.5, ranging from 25 to 78 years.

The mean duration of DM and insulin therapy was 14.7 and 7.2 years, respectively. Among the participating patients, the greatest number (61%) suffered from Type II DM, all of whom were secondarily insulin dependent. The mean glycemia level among the participating patients was 8.85 mmol/L, for adult with DM, the target level is between 4 and 7 mmol/L while HbA1c was 7.7% (it is recommended to be as close to normal as possible < 6%).

Among the 72 study participants, 3% of patients were diagnosed with mild non proliferative DR (NPDR), 46% with moderate NPDR form, 44% had severe NPDR form and 7% low risk PDR. The patients with both high risk and advanced PDR were excluded from the study, as the six-month follow-up was not feasible due to the need to perform laser intervention (panretinal laser photocoagulation), which is known to affect the DME.

One injection of bevacizumab application was required to achieve adequate CMT in 12 eyes (14%), two doses were required in 28 eyes (34%), while in most cases (37, or 44%), three doses were required. Finally, in 7 eyes (8%), four Avastin® doses were necessary before satisfactory CMT values were obtained and better conditions for subsequent laserphotocoagulation treatment achieved.

Figure 1 shows macular optical coherence tomography in the patient with DME, before and after the treatment with a single dose of Avastin®.

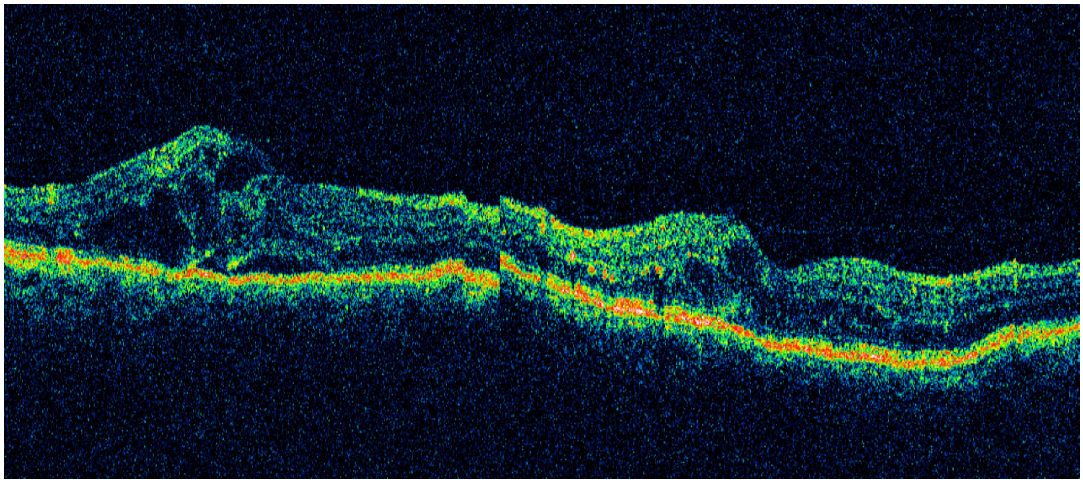

CMT 495 +/- 43 μm BCVA = 0.4 logMAR	CMT 296 +/- 20 μm, BCVA = 0.2 logMAR

Fig. 1 – Macular optical coherence tomography of an eye before the treatment with a single anti-vascular endothelial growth factor therapy, bevacizumab (Avastin®), and four weeks after the treatment.
CMT – central macula thickness; BCVA – best corrected visual activity; MAR – minimum angle of resolution.

The data presented in Table 1 indicates the manner in which the patients (n = 51 patients, 84 eyes) were grouped according to the number of doses received. It is evident that the number of administered doses is directly proportional to the increasing CMT values, indicating that progressively more severe forms of edema required longer treatment and a greater number of doses. In the first group of eyes requiring a single dose, edema was least pronounced, and the initial and the final mean CMT values were 348 μm and 220.5 μm, respectively, corresponding to 127.5 μm, or 36.6%, reduction. In 9 of 12 eyes, the CMT declined below the 250 μm threshold (representing the normal value). In the group of eyes that required two Avastin® doses, the initial and the final mean CMT values were 411.6 μm and 255.6 μm, respectively, corresponding to the 156 μm, or 37.9%, reduction. In addition, in 17 of the 28 eyes, the CMT declined below the 250 μm threshold. In the group requiring thee Avastin® doses, at 508.4 μm, the initial mean CMT value was greater than in the previous two groups, declining to 381.6 μm post-treatment, thus achieving the CMT reduction of 126.8 μm, *ie*, 29.4%. A reduction to the thickness below 250 μm was achieved in 7 of 37 eyes. In the fourth group of eyes that required four applications of medication, the initial mean CMT was the highest, 525.5 μm, and declined to 379.1 μm upon treatment completion. The achieved CMT reduction of 146.4 μm corresponded to 27.8%, with only one case reaching the normal thickness of 250 μm. The data presented in Table 2 indicate that each post-treatment CMT value is statistically significantly different from the initial one ($p < 0.05$).

Once the pharmacological treatment was completed, due to satisfying results or no further improvement, the next step of treatment, laser photocoagulation using the focal/grid method on 53 eyes, was performed after 4 to 6 weeks. The effect of combined therapy was evaluated after 6 weeks.

The mean reduction in CMT for the eyes (n = 31) treated with bevacizumab alone was 162.23 μm, for the eyes (n = 53) treated with combined treatment the mean reduction in CMT was 124.24 μm which was achieved with 2.4 doses on the average in the bevacizumab group and 2.5 doses in the bevacizumab plus laser group. The difference between the initial and the final mean CMT values in both patient groups are statistically significant at $p < 0.001$ (Table 3). The difference between the final values of achieved CMT comparing the groups bevcizumab *vs* bevacizumab plus macular laser is not significant ($p = 0.52$). In the control group, the eyes treated with laserphotocoagulation alone (n = 36) reduction in CMT was 6.88 μm, which was not statistically significant.

The mean visual acuity improvement of 0.161 logMAR was achieved in the group of eyes treated with bevacizumab alone, 0.093 logMAR in the eyes treated with combined treatment. The difference between the initial and the final mean logMAR values in both patient groups was statistically significant at $p < 0.05$. On the other hand, there was no statistical difference between final visual acuity comparing groups bevacizumab *vs* bevacizumab plus macular laser $p = 0.81$ (Table 3).

Table 1

Initial and final central macula thickness (CMT) values by patient group (classification based on the number of administered doses)

Doses (n)	CMT (μm)		Improvement		Treated eyes	Below	Below
	Initial	Final	Absolute (μm)	Relative (%)	(n)	250 μm (n)	300 μm (n)
1	347.92	220.58	127.33	36.60	12	9	11
2	411.68	255.64	156.03	37.90	28	17	23
3	508.38	381.57	126.81	24.94	37	7	8
4	525.57	379.14	146.43	27.86	7	1	2

Table 2

Paired *t*-test of initial and final central macula thickness (CMT) values by the groups (based on the number of administered doses)

CMT vs OCT	x̄ ± SD	*t*-test	*t*	df	Final value
CMT 0	347.9167 ± 90.86499	CMT *vs* CMT 1	5.743785	11	2.2281388
CMT 1	220.5833 ± 52.80575				
CMT 0	411.6786 ± 89.51807	CMT *vs* CMT 2	7.278081	27	2.0555294
CMT 2	255.6429 ± 76.98254				
CMT 0	508.3784 ± 159.2392	CMT *vs* CMT 3	4.757189	36	2.0301079
CMT 3	381.5676 ± 122.7714				
CMT 0	525.5714 ± 77.0127	CMT *vs* CMT 4	2.391307	6	2.5705818
CMT 4	379.1429 ± 138.9561				

OCT – optical coherence tomography; x̄ – mean value; SD – standard deviation; df – degrees of freedom.

Table 3

Paired *t*-test of visual acuity (VA) and central macula thickness (CMT) before (1) and after (2) the treatment with bevacizumab (– b) *vs* bevacizumab plus macular laserphotocoagulation (b+lfc) and laser group only (lfc)

Treatment	n	VA, mean ± SD (LogMAR)	*p*	CMT, mean ± SD (μm)	*p*
b+lfc 1	53	0.484 ± 0.322	0.0019	447.245 ± 121.059	< 0.0001
b+lfc 2		0.388 ± 0.393		323.000 ± 134.114	
b 1	31	0.572 ± 0.432	< 0.0001	467.323 ± 164.934	< 0.0001
b 2		0.409 ± 0.398		305.097 ± 100.963	
lfc 1	36	0.429 ± 0.349	0.0114	347.177 ± 101.428	0.4604
lfc 2		0.474 ± 0.360		340.294 ± 101.966	

SD – standard deviation.

Following the macular laser photocoagulation as the first treatment, visual acuity worsened, 0.046 logMAR, with statistical significance ($p < 0.05$).

The results presented in Table 4 indicate that the additional CMT reduction achieved through macular laser photocoagulation, as a part of the combined treatment, was statistically significant, as confirmed by the paired *t*-test (366.28 μm *vs* 323.0 μm) at $p < 0.05$. There is no improvement in visual acuity in the group with combined treatment after additional laserphotocogulation ($p > 0.05$).

In order to determine if the degree of DR had influence on severity of DME and treatment response, the patients (treated eyes) were grouped into groups – mild to moderate NPDR and severe NPDR with low risk PDR, as presented in Table 5. CMT was improved by 117.25 μm in the group of eyes with mild to moderate NPDR (34 eyes treated with bevacizumab), and the group with severe NPDR to low risk PDR average improvement was 152.54 μm. In both groups this difference was statistically significant ($p < 0.001$). The difference between the two final mean values of achieved CMT comparing the two groups was not statistically significant (326.059 ± 50.618 μm *vs* 309.820 ± 37.420 μm; $p = 0.55$).

Visual acuity improved 0.168 logMAR in the first group compared to 0.089 logMAR in the second. This improvement was also significant in the first and the second group ($p < 0.0001$, and $p < 0.005$, respectively) (Table 5). The difference between this two mean values of final visual acuity comparing the two groups was not significant (0.318 ± 0.290 logMAR *vs* 0.448 ± 0.444 logMAR, $p = 0.14$). In the group of eyes (n = 36) treated with laser there was no statistically significant improvement, nor in the mild to moderate, neither in the severe and low risk PDR group.

A low value ($r = 0.036$) of Pearson's correlation coefficient between Hba1c and the difference of OCT value before and after anti-VEGF treatment indicates no significant relation between them.

Discussion

Our study was prospective, randomized, clinical study, designed to evaluate and compare effectiveness of pharmacological treatment with anti-VEGF therapy (bevacizumab – Avastin®) alone and combined treatment with anti-VEGF (bevacizumab – Avastin®) plus macular laserphotocoagulation in relation to macular laserphotocoagulation like conventional therapy only. A total of 72 patients were examined, 120 eyes treated, and the minimum follow-up period was 6 months. Some of the previous studies had similar design. For example, in a study of Iranian authors [13], the follow-up was at 6 months; 40 patients – 80 eyes were examined, each patient underwent intravitreal bevacizumab treatment in one eye and in the second one intravitreal bevacizumab at the same time as macular laser treatment. In that way the systemic conditions are the same in the experimental and the control group, which is preferable but we did not have this possibility during our research. The BOLT study had a much

Table 4

Paired *t*-test of visual acuity (VA) and central macula thickness (CMT) values of eyes treated by bevacizumab before (1) and after (2) additional laser treatment (focal/grid)

Treatment	n	VA, mean ± SD (LogMAR)	*p*	CMT, mean ± SD (μm)	*p*
b+lfc 1	53	0.376 ± 0.346	0.631200	366.28 ± 117.2	0.006
b+lfc 2		0.388 ± 0.393		323.00 ± 134.114	

b + lfc – bevacizumab + laserphotocoagulation; SD – standard deviation; OCT – optical coherence tomography.

Table 5

Paired *t*-test of visual acuity (VA) and central macula thickness (CMT) before (1) and after (2) the treatmen in the group of mild to moderate nonproliferative diabetic retinopathy (NPDR) compared to the severe NPDR-low risk proliferative diabetic retinopathy [treated with bevacizumab only and in combined therapy (b) *vs* macular laserphotocoagulation (lfc)]

Treatment	n	VA, mean ± SD (logMAR)	*p*	CMT, mean ± SD (μm)	*p*
b1 mod	34	0.486 ± 0.292	< 0.0001	443.323 ± 49.500	< 0.0001
b2 mod		0.318 ± 0.290		326.059 ± 50.618	
b1 sev	50	0.537 ± 0.411	0.0033	462.360 ± 36.020	< 0.0001
b2 sev		0.448 ± 0.444		309.820 ± 37.420	
lfc1 mod	18	0.396 ± 0.360	0.1213	362.250 ± 107.086	0.1604
lfc2 mod		0.447 ± 0.396		340.250 ± 111.550	
lfc 1 sev	18	0.462 ± 0.345	0.0033	333.778 ± 97.201	0.5486
lfc 2 sev		0.501 ± 0.330		340.333 ± 95.933	

SD – standard deviation; mod – moderate; sev - severe.

longer follow-up period – up to two years [14]. A total of 80 patients were examined with center involving CSME. One group of eyes underwent injections of bevacizumab at baseline, at 6, and at 12 weeks. The patients were examined every 6 weeks and the treatment was stopped if CMT was stabile (3 consecutive visits and CMT within 20 μm of the thinnest recorded CMT), while we considered that the treatment was finalized when there was no change in OCT at the two latest visits. A Diabetic Retinopathy Clinical Research Network (DRCR) study was also designed to compare the effect of two different doses of bevacizumab alone and in combined treatment [10]. Haritoglou et al [15], Kook et al. [16], and Mehta et al. [17], in their studies, assessed patients with resistant DME who were previously unsuccessfully treated by macular focal laser, panretinal laserphotocoagulation, pars plana vitrectomy with internal limiting membrane peeling, and intravitreal triamcinolone. These authors reported that bevacizumab therapy could yield greater improvements in refractory edema in comparison to other therapy modes. This model is different to our study model, because we included new cases without any treatment before.

The data presented in Table 1 indicate that the first and the second group included patients with quantitatively less severe edema; thus, the treatment could be achieved through fewer Avastin® doses, but was also more effective. The third and the fourth group in particular, included cases of more severe edema, which required greater number of Avastin® doses, yet failed to achieve efficacy noted in the first two groups. The mean CMT reduction in all the treated eyes was 139.15 μm (31.81%), which was achieved with 2.46 doses, on the average. In 34 of the 84 (40.47%) eyes subjected to treatment, edema reduction ≤ 250 μm was achieved. It is evident that the number of administered doses is directly proportional to the increasing CMT values, indicating that progressively more severe forms of edema required longer treatment and a greater number of doses.

Intravitreal injections of bevacizumab administration was at 4–6 weeks interval, until satisfying results were obtained. If there was no further improvement, the next step of treatment was performed – focal/grid laserphotocoagulation mostly at 4–6 weeks after the last intravitreal application. In the study conducted by Roh et al. [18], the author investigated the duration of the period after which edema reoccured unless anti-VEGF therapy was repeated. In 24 patients (31 eyes) from that study, edema reoccurred 12 weeks after the initial treatment, unless a new dose was administered. A conclusion was that next doses should be administrated until edema reoccured. In a Pan-American study on 16 eyes (20.5%) second injection was administrated, on the average 13.8 weeks apart (4–28 weeks); 6 eyes (7.7%) received third injection on the average interval 11.5 weeks (5–20 weeks). This type of administration at the time when edema reoccurs is not recommended [19]. Most of the authors like Scott et al. [10], Haritoglou et al. [15], Kook et al. [16], Mehta et al. [17] and Kumar and Sinha [20] choose administration with 6 weeks apart.

The mean reduction in CMT in our study for the eyes (n = 31) treated with bevacizumab alone was 162.23 μm, for the eyes (n = 53) treated with combined treatment it was 124.24 μm which was achieved with 2.4 doses on the average in the bevacizumab group and 2.5 doses in the bevacizumab plus laser group. The difference between the initial and the final mean CMT values in each patient group was statistically significant at $p < 0.001$. In the control group, eyes treated with laserphotocoagulation alone (n = 36), a reduction in CMT was 6.88 μm, which was not statistically significant. In the Iranian study a reduction in CMT in the first group of eyes intravitreal bevacizuma (IVB) was 40 +/- 38 μm and in the second one [IVB+ macular photocongulation (MPC)] 43 +/- 13 μm, the results were achieved with 2.23 injections in first group (IVB) and 2.49 injections in the second group (IVB+MPC). Edemas in the Iranian study were very mild compared to our study, the CMT at baseline for the IVB group was 261 ± 115 μm and for the IVB plus MPC group 270 ± 93 μm [13]. In our study baseline CMT was much higher – 467.323 μm in the group of eyes treated with bevacizumab only, 447.245 μm in the group of eyes treated with combined therapy, which could explain a better response to the treatment.

The mean reduction in CMT in the bevacizumab group was 146 μm and 118 μm in the macular laserphotocoagulation (MLC) group in the BOLT study [14], achieved with 13 injections (9 in the first and 4 in the second year), and 4 macular laser treatment (3 in the first and 1 in the second year). In the Kumar and Sinha [20] study the treatment efficacy of 120 μm achieved through two doses 6 weeks apart at 6 months analyses; Haritoglou et al. [15], Kook et al. [16] and Mehta et al. [17] reported the improvement in CMT from 106–124 μm, and Arevalo et al. [19] in the Pan-American study 111 μm. We obtained similar results concerning CMT reduction (13915 μm) using 2.46 doses on the average.

In our study, the mean visual acuity improvement of 0.161 logMAR was achieved in the group of eyes treated with bevacizumab alone, 0.093 logMAR in the eyes treated with combined treatment. The difference between the initial and the final mean logMAR values in each patient group was statistically significant at $p < 0.05$ Following the macular laser photocoagulation as a first treatment, visual acuity worsened 0.046 logMAR with a statistical significance ($p < 0.05$). In the Iranian study [13] BCVA was improved in the first group (0.138 logMAR), and 0.179 logMAR in the second, which is very similar to our results. Haritoglou et al. [15], Kook et al. [16] and Mehta et al. [17] in their studies which analyzed treatment of edema have results from 0.05 to 0.11 logMAR. Their results are slightly lower than ours, probably because they included patients with persistent, chronic edema.

In our study, the mean CMT improved more in the group of eyes treated with bevacizumab only compared to the eyes with combined treatment. Focusing on the group of eyes with combined therapy, laser has been done 6 weeks apart of the last injection, and CMT significantly improved due to laser treatment (363.3 *vs* 323.0 μm) $p < 0.05$. Many studies showed that there is no difference between bevacizumab group only an bevacizumab plus macular laser therapy. In the Iranian study [13], the authors conclude at the end of treatment that there are no differences between the group of eyes treated with bevacizumab and the group of eyes treated with bevacizumab plus macular laser. They consider application of laser 2–3 weeks after the anti-

VEGF treatment in order to have better consolidative effect. In our study, laser is applied 4–6 weeks apart from the last injection, with a significant improvement of CMT and no improvement in visual acuity. Korean authors [21] applied laser 4 weeks after the last injection. Combined therapy in DRCR did not achieve a significantly greater improvement compared to the treatments based on bevacizumab alone [9].

In order to determine if the degree of DR has influence on severity of DME and treatment response, patients (treated eyes) were grouped into groups – mild to moderate NPDR and severe NPDR with low risk PDR, as presented in Table 5. In both groups improvement of CMT was on statistical level of 99%, in visual acuity improvement was on the statistical level of 99% on moderate, 95% significance for severe NPDR and low risk PDR. In the laser group there was no improvement, visual acuity was worsened in the group with severe NPDR-low risk PDR. In the Pan-American study [19], ANOVA analysis could not find a statistically significant difference in the reduction of edema in eyes with NPDR and PDR (panretinal laserphotocoagulation is performed at least 6 months before).

A low value ($r = 0.036$) of Pearson's correlation coefficient between Hba1c and the difference of OCT value before and after anti-VEGF treatment indicate no significant relation between them.

In a study of Korean authors [21], they tried to make a correlation between the reduction of macular edema and the type of edema (diffuse, cystoid, edema with serous retinal detachment and mixed edema). This could be a very good approach for the next phase of our research.

Conclusion

The treatment with bevacizumab alone or combined treatment (consisting of bevacizumab administration and macular laserphotocolagulation) are more effective in treating diabetic macular edema than conventional macular laser treatment alone, both anatomically and functionally.

R E F E R E N C E S

1. *Klein R.* Retinopathy in a population-based study. Trans Am Ophthalmol Soc 1992; 90: 561−94.
2. *Kempen JH, O'Colmain BJ, Leske MC, Haffner SM, Klein R, Moss SE,* et al. The prevalence of diabeticretinopathy among adults in the United States. Arch Ophthalmol. 2004; 122(4): 552−63.
3. *Orchard TJ, Dorman JS, Maser RE, Becker DJ, Drash AL, Ellis D,* et al. Prevalence of complications in IDDM by sex and duration. Pittsburgh Epidemiology of Diabetes Complications Study II. Diabetes 1990; 39(9): 1116−24.
4. *Girach A, Lund-Andersen H.* Diabetic macular oedema: a clinical overview. Int J Clin Pract 2007; 61(1): 88−97.
5. *Williams R, Airey M, Baxter H, Forrester J, Kennedy-Martin T, Girach A.* Epidemiology of diabetic retinopathy and macular oedema: a systematic review. Eye 2004; 18(10): 963−83.
6. *Gardner TW, Antonetti DA, Barber AJ, LaNoue KF, Levison SW.* Diabetic retinopathy: more than meets the eye. Surv Ophthalmol 2002; 47(Suppl 2): S253−62.
7. *Cai J, Boulton M.* The pathogenesis of diabetic retinopathy: old concepts and new questions. Eye (Lond) 2002; 16(3): 242−60.
8. *Ferrara N.* Role of vascular endothelial growth factor in physiologic and pathologic angiogenesis: therapeutic implications. Semin Oncol 2002; 29(6 Suppl 16): 10−4.
9. *Takahashi H, Shibuya M.* The vascular endothelial growth factor (VEGF)/VEGF receptor system and its role under physiological and pathological conditions. Clin Sci 2005; 109(3): 227−41.
10. *Scott IU, Edwards AR, Beck RW, Bressler NM, Chan CK, Elman MJ,* et al. A phase II randomized clinical trial of intravitreal bevacizumab for diabetic macular edema. Ophthalmology 2007; 114(10): 1860−7.
11. *Fong DS, Strauber SF, Aiello LP, Beck RW, Callanan DG, Danis RP,* et al. Writing Committee for the Diabetic Retinopathy Clinical Research Network. Comparison of the modified Early Treatment Diabetic Retinopathy Study and mild macular grid laser photocoagulation strategies for diabetic macular edema. Arch Ophthalmol 2007; 125(4): 469−80.
12. *Wilkinson CP, Ferris FL, Klein RE, Lee PP, Agardh CD, Davis M,* et al. Proposed international clinical diabetic retinopathy and diabetic macular edema disease severity scales. Ophthalmology 2003; 110(9): 1677−82.
13. *Faghihi H, Esfahani MR, Harandi ZA, Madani SH.* Intravitreal bevacizumab vs. combination of intravitreal bevacizumab plus macular photocoagulation in clinically significant diabetic macular edema: 6 months results of a randomized clinical trial. Iranian J Ophthalmol 2010; 22(1): 21−6.
14. *Rajendram R, Fraser-Bell S, Kaines A, Michaelides M, Hamilton RD, Esposti SD,* et al. A 2-year prospective randomized controlled trial of intravitreal bevacizumab or laser therapy (BOLT) in the management of diabetic macular edema: 24-month data: report 3. Arch Ophthalmol 2012; 130(8): 972−9.
15. *Haritoglou C, Kook D, Neubauer A, Wolf A, Priglinger S, Strauss R,* et al. Intravitreal bevacizumab (Avastin) therapy for persistent diffuse diabetic macular edema. Retina 2006; 26(9): 999−1005.
16. *Kook D, Wolf A, Kreutzer T, Neubauer A, Strauss R, Ulbig M,* et al. Long-term effect of intravitreal bevacizumab (avastin) in patients with chronic diffuse diabetic macular edema. Retina 2008; 28(8): 1053−60.
17. *Mehta S, Blinder KJ, Shah GK, Kymes SM, Schlief SL, Grand MG.* Intravitreal bevacizumab for the treatment of refractory diabetic macular edema. Ophthalmic Surg Lasers Imaging 2010; 41(3): 323−9.
18. *Roh MI, Byeon SH, Kwon OW.* Repeated intravitreal injection of bevacizumab for clinically significant diabetic macular edema. Retina 2008; 28(9): 1314−8.
19. *Arevalo J, Fromow-Guerra J, Quiroz-Mercado H, Sanchez JG, Wu L, Maia M,* et al. Primary intravitreal bevacizumab (Avastin) for diabetic macular edema: results from the Pan-American Collaborative Retina Study Group at 6-month follow-up. Ophthalmology 2007; 114(4): 743−50.
20. *Kumar A, Sinha S.* Intravitreal bevacizumab (Avastin) treatment of diffuse diabetic macular edema in an Indian population. Indian J Ophthalmol 2007; 55(6): 451−5.
21. *Lee SJ, Kim ET, Moon SY.* Intravitreal bevacizumab alone versus combined with macular photocoagulation in diabetic macular edema. Korean J Ophthalmol 2011; 25(5): 299−304.

Received on April 2, 2014.
Revised on September 5, 2014.
Accepted on September 15, 2014.
Online First August, 2015.

ORIGINAL ARTICLE

UDC: 617-089.168:[616.6-0221:615.472.5
DOI: 10.2298/VSP140624078M

Catheter-associated urinary tract infection in a surgical intensive care unit

Infekcije urinarnog trakta kod bolesnika sa urinarnim kateterom u hirurškoj jedinici intenzivne nege

Jovan Mladenović*†, Milić Veljović†‡, Ivo Udovičić‡, Srdjan Lazić*†, Željko Jadranin*, Zoran Šegrt†§, Petar Ristić‖, Vesna Šuljagić†¶

***Institute of Epidemiology, ‡Clinic for Anesthesiology and Intensive Care, §Sector for Treatment, ‖Clinic for Endocrinology, ¶Department of Hospital Infections Control, Military Medical Academy, Belgrade, Serbia; †Faculty of Medicine of the Military Medical Academy, University of Defence, Belgrade, Serbia**

Abstract

Background/Aim. Because patients in intensive care units usully have an urinary catheter, the risk of urinary tract infection for these patients is higher than in other patients. The aim of this study was to identify risk factors and causative microrganisms in patients with catheter-associated urinary tract infection (CAUTI) in the Surgical Intensive Care Unit (SICU) during a 6-year period. **Methods.** All data were collected during prospective surveillance conducted from 2006 to 2011 in the SICU, Military Medical Academy, Belgrade, Serbia. This case control study was performed in patients with nosocomial infections recorded during surveillance. The cases with CAUTIs were identified using the definition of the Center for Disease Control and Prevention. The control group consisted of patients with other nosocomial infections who did not fulfill criteria for CAUTIs according to case definition. **Results.** We surveyed 1,369 patients representing 13,761 patient days. There were a total of 226 patients with nosocomial infections in the SICU. Of these patients, 64 had CAUTIs as defined in this study, and 162 met the criteria for the control group. Multivariate logistic regression analysis identified two risk factors independently associated to CAUTIs: the duration of having an indwelling catheter (OR = 1.014; 95% CI 1.005–1.024; $p = 0.003$) and female gender (OR = 2.377; 95%CI 1.278–4.421; $p = 0.006$). Overall 71 pathogens were isolated from the urine culture of 64 patients with CAUTIs. *Candida* spp. (28.2%), *Pseudomonas aeruginosa* (18.3%) and *Klebsiella* spp. (15.5%) were the most frequently isolated microorganisms. **Conclusions.** The risk factors and causative microrganisms considering CAUTIs in the SICU must be considered in of planning CAUTIs prevention in this setting.

Key words:
urinary tract infections; cross infection; intensive care units; surgery department, hospital; risk factors; urinary catheterization.

Apstrakt

Uvod/Cilj. Rizik od infekcije urinarnog trakta je viši kod bolesnika u jedinicama intenzivne nege nego kod ostalih bolesnika zbog toga što oni obično imaju urinarni kateter. Cilj rada bio je da se ispitaju bolesnici sa infekcijom urinarnog trakta povezanom sa kateterom [*catheter-associated urinary tract infection* (CAUTI)] tokom 6 godina u Hirurškoj jedinici intenzivne nege (HJIN) da bi se utvrdili značajni faktori rizika i uzročnici oboljenja. **Metode.** Podaci su prikupljeni tokom prospektivnog epidemiološkog nadzora u periodu od 2006. do 2011. godine u HJIN Vojnomedicinske akademije, Beograd, Srbija. Studija slučaja i kontrola je obuhvatila bolesnike sa bolničkim infekcijama zabeleženim tokom epidemiološkog nadzora. Bolesnici sa CAUTI identifikovani su na osnovu definicije Centra za kontrolu i prevenciju bolesti. Kontrolna grupa je obuhvatila bolesnike sa drugim bolničkim infekcijama koji nisu ispunjavali definiciju CAUTI. **Rezultati.** Epidemiološkim nadzorom obuhvaćeno je 1 369 bolesnika i 13 761 bolničkih dana. Ukupno je zabeleženo 226 bolesnika u HJIN sa bolničkim infekcijama u posmatranom periodu. Među njima, 64 bolesnika imala su CAUTI i 162 su ispunjavala kriterijume za kontrolnu grupu. Multivarijantna logistička regresiona analiza identifikovala je dva faktora rizika nezavisno povezana sa CAUTI: dužina nošenja urinarnog katetera (OR = 1,014; 95% CI 1,005–1,024; $p = 0,003$) i ženski pol (OR = 2,377; 95% CI 1,278– 4,421; $p = 0,006$). Izolovan je ukupno 71 patogen iz urinokultura 64 bolesnika sa CAUTI. *Candida* spp. (28,2%), *Pseudomonas aeruginosa* (18,3%) i *Klebsiella* spp. (15,5%) bili su najčešće izolovani mikroorganizmi. **Zaključak.** Faktori rizika i uzročnici koji su povezani sa nastankom CAUTI u HJIN moraju biti uzeti u obzir pri planiranju mera prevencije CAUTI u ovom okruženju.

Ključne reči:
urinarni trakt, infekcije; infekcija, intrahospitalna; intenzivna nega, odeljenja; bolnice, hirurško odeljenje; faktori rizika; kateterizacija urinarnog trakta.

Correspondence to: Jovan Mladenović, Institute of Epidemiology, Military Medical Academy, Crnotravska 17, 11 000 Belgrade, Serbia. Phone: +381 11 3609 332; 064 128 6959. Email: jovan.mladenovic@gmail.com

Introduction

Nosocomial infections (NIs) affect about 30% of patients in intensive-care units (ICU) [1]. It has been reported that ICUs account for 25% of NIs even though they occupy only approximately 10% capacity of a hospital [2]. The risk of NIs in ICU is 5–10 times greater than those acquired in general and surgical wards [3].

Urinary tract infections (UTIs) comprise 30% to 40% of all NIs, and 8% to 21% of all NIs are UTIs occurring in ICUs [4, 5]. Richards et al. [6, 7] found that UTI was responsible for 20–30% of NIs in medical/surgical ICUs. According to a large surveillance program in Europe UTIs were the third most common type of infection in ICUs after pneumonia and lower respiratory tract infections [3]. UTI is the most common NI in North America and among the most frequent NIs in critically ill patients [6, 8, 9].

The presence of a urinary catheter is associated with increased risk of nosocomial UTI and the incidence of UTIs among patients with urinary catheters is about 15% [10]. Because patients in ICUs usually have a urinary catheter, the risk of UTI for these patients is higher than in other patients.

Catheter-associated UTI (CAUTI) has been associated with increased morbidity, mortality, hospital cost, and length of stay [11, 12].

CAUTI is recognized as a leading cause of secondary nosocomial bloodstream infections and approximately 17% of nosocomial bacteremias are from a urinary source [13].

There has only been a limited number of studies on CAUTIs in ICUs. This case control study investigated patients with CAUTI over a 6-year period at the surgical ICU to identify significant risk factors and causative microorganisms.

Methods

All data was collected during prospective surveillance conducted from February 1, 2006 to December 30, 2011 at the 30 bedded Surgical Intensive Care Unit (SICU), Military Medical Academy (MMA), Belgrade, Serbia. All the patients admitted in SICU for more than 48 h were included and followed up. These critical patients were referred for monitoring, observation, and management from different surgical departments, *eg* general surgery, neurosurgery, urology, traumatology, etc.

The active prospective surveillance was performed by the hospital epidemiologist and infection control nurses following the recommendations of the Hospital in Europe Link for Infection Control through Surveillance (HELICS) and USA National Healthcare Safety Network (NHSN) [14, 15]. They visited the ICU daily, gathered information from medical records, microbiologic and X-ray reports, and interviews with nurses and physicians in charge. NIs were defined according to the diagnostic criteria of the Center for Disease Control and Prevention (CDC) [16, 17]. Collected variables included all NIs, demographic characteristics, admission diagnoses, exposure to invasive devices.

Microbiological testing was performed at the MMA's Institute of Medical Microbiology and all microbiological methods used were consistent with the current National Commitee for Clinical Laboratory Standards recommendations.

Retrograde analysis was performed in patients with NIs recorded during surveillance between February 1, 2006 and December 30, 2011 in SICU of MMA.

The patients with CAUTIs were, identified using definition of the CDC [18]. The control group consisted of ICU patients with other NIs who did not fulfill criteria for UTI according to the case definition.

According to CDC definition,[18] CAUTI is: "A UTI where an indwelling urinary catheter was in place for > 2 calendar days on the date of event, with the day of device placement being day 1, and an indwelling urinary catheter was in place on the date of event or the day before. If an indwelling urinary catheter was in place for > 2 calendar days and then removed, the UTI criteria must be fully met on the day of discontinuation or the next day".

Indications for placement of urinary catheters were [19–21]: acute urinary retention, acute bladder outlet obstruction, need for accurate measurements of urinary output in the critically ill, to assist in healing of open sacral or perineal wounds in incontinent patients, patient requires strict prolonged immobilization and selected perioperative needs [22, 23] [urologic surgery or other surgery on contiguous (adjacent) structures of the genitourinary tract, anticipated prolonged duration of surgery, large volume infusions or diuretics anticipated during surgery and need for intraoperative monitoring of urinary output].

Statistical analyses

Infection rate (IR) was expressed as the total number of UTI *per* 1,000 patient days. Also, we calculated device utilization rates for the period 2008–2011 by dividing the total number of devices days by the total number of ICU patient days [24]. Statistical analysis was performed by using the IBM SPSS ver. 20.0 (IBM Co., Armonk, NY, USA). The χ^2 test and Student's *t*-test were used for data analyses. Any *p*-values less than 0.05 were considered significant. Multivariate logistic regression analysis included only variables that showed a statistically significant association.

Results

We surveyed 1,369 patients representing 13,761 patient days (Table 1). During the period from 2006 to 2011, IR of UTI ranged from 1.1 in 2007 to 8.6 in 2010 with the average value of 4.7.

The device utilization rates from 2008 to 2011 are presented in Table 2. Catheter-associated IR was in range from 7.23 to 15.57 for period from 2008 to 2011 with the average value of 10.38. Urinary catheter days/ patient days ranged from 0.5 to 0.7.

Patient population

There were a total of 226 patients with NIS in our hospital's SICU between February 2006 and December 2011. Of these patients, 64 had CAUTI as defined in this study, and 162 met the criteria for the control group. The mean age of infected patient was 58.3 ± 20.4 (range, 15–92) years. Of 226

Table 1

Distribution of patients with surgical intensive care units, nosocomial infections and infection rate (IR) by year

Years of follow-up	Patients (n)	Patients-days (n)	UTI (IR*1000)
2006	201	1,900	3 (1.6)
2007	143	1,819	2 (1.1)
2008	255	2,263	12 (5.3)
2009	227	2,251	9 (4.0)
2010	234	2,905	25 (8.6)
2011	309	2,623	13 (5.0)
	Total: 1,369	Total: 13,761	Avarage: 64 (4.7)

UTI – urinary tract infection.

Table 2

Device utilization rates for urinary catheter (UC) from 2008 to 2011

Years of follow-up	UC-days	Patient-days	UC utilization	UTI	UC associated IR
2008	1,228	2,263	0.5	12	9.77
2009	1,054	2,251	0.5	9	8.54
2010	1,606	2,905	0.5	25	15.57
2011	1,797	2,623	0.7	13	7.23
	Total : 5,685	Total : 10,042	0.6	Total : 59	Average: 10.38

UTI – urinary tract infection; IR – infection rate.

patients, 141 (62.4%) were males and 85 (37.6%) were females. A total of 185 (81.9%) patients had surgery before their ICU admission and 41 (18.1%) did not; 30 (13.3%) patients had diabetes and 196 (86.7%) did not, and 38 (16.8%) patients had cancer. The mean duration of having an inserted catheter was 29.87 ± 35.11 days, and the mean duration of ICU stay was 20.94 ± 20.29 days.

Clinical factors

The results of χ^2 test and *t*-test to observe differences between the patients with CAUTI and the control group are shown in Table 3. The difference in the duration of having an indwelling catheter was statistically significant between the two groups ($p = 0.002$). The duration of having an indwelling catheter was longer in CAUTI patients (43.53 ± 45.26 days) than in the control group (24.47 ± 28.59 days). Female sex was also a significant risk factor for CAUTI (OR = 2.06; 95%CI 1.09–3.87; $p = 0.016$). Age also appear to be a significant risk factor ($p = 0.039$) in univariate analysis. Other factors were not significantly different between the groups ($p > 0.05$).

Multivariate logistic regression analysis (Homer-Lemeshow Goodness of Fit test) identified two risk factors independently associated with CAUTI: the duration of having an indwelling catheter (OR = 1.014; 95% CI 1.005–1.024; $p = 0.003$) and female gender (OR = 2.377; 95%CI 1.278– 4.421; $p = 0.006$). Age did not appear to have a significant effect.

Table 3

Results of univariate analysis of factors contributing to catheter-associated urinary tract infection (CAUTI) occurrence

Clinical factors	CAUTI (n = 64)	Controls (n = 162)	*p* value
Sex, n (%)			0.016
male	32 (50)	109 (67.28)	
female	32 (50)	53 (32.72)	$\chi^2 = 5.84$; OR = 2.06 (1.09–3.87)
Age (years), mean ± SD (SE)	53.84 ± 21.08 (2.635)	60.06 ± 19.94 (1.567)	0.039
Diabetes mellitus, n (%)			
diabetic patient	9 (14.4)	21 (13.0)	0.826
nondiabetic patient	55 (85.9)	141 (87.0)	
Cancer, n (%)			
cancer patient	13 (20.3)	25 (15.4)	0.377
noncancer patient	51 (79.7)	137 (84.6)	
Recent surgery, n (%)			
yes	54 (84.4)	131 (80.9)	0.537
no	10 (15.6)	31 (19.1)	
Duration of ICU stay (days), mean ± SD (SE)	25.28 ± 25.20 (3.151)	19.22 ± 17.79 (1.398)	0.082
Duration of catheterization (days), mean ± SD (SE)	43.53 ± 45.26 (5.658)	24.47 ± 28.59 (2.247)	0.002

The values are presented as number (%) or mean ± standard deviation (SD); SE – standard error; ICU – intensive Care Unit.

Microbiological factors

Overall 71 pathogens were isolated from the urine culture of 64 patients with CAUTI. *Candida* spp. was the most frequently isolated microorganisms (20 patients, 28.2%) (Table 4). Of the *Pseudomonas aeruginosa* isolates, second most frequently causative agent (13 patients, 18.3%), 69.2 % (9/13) and 46.1% (6/13) were resistant to ciprofloxacin, and imipenem, respectively. Other found species were *Klebsiella* spp. (11 patients, 15.5%), out of which 81.8% (9/11) were the third generation of cephalosporin resistant, and *Eneterococcus* spp (9 patients, 12.7%). Among the enterococcal isolates, vancomycin resistance was found in 11.1% (1/9). Carbapenem-resistant *Klebsiella* spp. was first reported in urine culture in 2011 (1 patient, 9.0%).

Table 4

Etiology of catheter-associated urinary tract infections in the Surgical Intensive Care Unit of the Military Medical Academy, Belgrade, Serbia

Pathogen	No. of isolates (%)
Gram-negative bacteria	41 (57.7)
Pseudomonas aeruginosa	13 (18.3)
Klebsiella spp.	11 (15.5)
Escherichia coli	8 (11.3)
Acinetobacter spp.	5 (7.0)
Proteus spp.	3 (4.2)
Pseudomonas spp.	1 (1.4)
Gram-positive bacteria	10(14.1)
Enterococcus spp.	9 (12.7)
Staphylococcus aureus	1 (1.4)
Fungi	20 (28.2)
Candida spp.	20 (28.2)
Total	71 (100)

Discussion

The catheter-associated IR was in the range from 7.23 to 15.57 (10.38) infections *per* 1000 catheter days for the period from 2008 to 2011. Summary of device-associated infections data collected and reported by hospitals participating in the NHSN from January through December 2006 showed that pooled mean CAUTI rates ranged 3.1–7.5 infections *per* 1,000 catheter days [25]. Finklestein et al [26] found the incidence of 10–14 UTI *per* 1,000 catheter days among 337 patients in a single Israeli ICU.

Urinary catheter days/patient days ranged from 0.5 to 0.7 in our study. Between 15% and 25% of hospitalized patients may receive indwelling urinary catheters [27, 28]. In many cases, catheters are placed for inappropriate indications or there is a prolonged, unnecessary use of catheters [29–31]. In a NHSN report in 2006, pooled mean urinary catheter utilization ratios in ICU was in the range from 0.29 to 0.91 urinary catheter-days/patient-days [25].

The urinary catheter provides a route for bacterial entry along both its external and internal surfaces (extraluminal and intraluminal route of microorganism migration) [32]. Contamination of urine in the drainage bag can allow organisms to access the bladder through the drainage tube and the catheter lumen.

The formation of biofilms on the surface of the catheter and drainage system is associated with prolonged durations of catheterization [33]. Microorganisms that colonize the periurethral skin can migrate into the bladder through a biofilm that forms between the epithelial surface of the urethra and the catheter. Also, the presence of the catheter itself impairs many of the normal defense mechanisms of the urinary tract.

In this study, two risk factors (duration of catheterization and female gender) were found to be independently associated with infection. Female gender was a significant factor associated with UTI in several other studies also [34–37]. Increased duration of catheterization was identified as independently associated with CAUTI in this study and in some other [38–40]. Rosser et al. [41] found that the length of catheterization was one of the independent factors associated with the development of nosocomial UTI. The daily risk of bacteriuria with catheterization is 3% to 10% [42, 43], approaching 100% after 30 days [44].

The most common microorganisms responsible for ICU-acquired UTIs in this study were *Candida* spp., *Pseudomonas aeruginosa*, and *Klebsiella* spp.

The most frequent pathogens associated with CAUTI according to summary of data that hospitals reported to NHSN from January 2006 through October 2007 were *Escherichia coli* (21.4%) and *Candida* spp. (21.0%), followed by *Enterococcus* spp. (14.9%), *Pseudomonas aeruginosa* (10.0%), and *Enterobacter spp.* (4.1%) [45].

Similarly to data in our study, the most common causative microorganism of ICU-acquired UTI was *Candida* spp. in study of intensive care unit-acquired UTIS in Singapore [46].

Laupland et al. [47] found that the most frequent microorganisms in ICU-acquired UTIs were *Escherichia coli* (23%), *Candida albicans* (20%), *Enterococcus* spp. (15%) and *Pseudomonas aeruginosa* (10%).

Antimicrobial resistance among nosocomial pathogens is the increasing problem in our hospital, especially in SICU [48, 49]. Resistance of gram-negative pathogens to third-generation cephalosporin and ciprofloxacin was few times higher than in NHNS reported during the three periods, 1992–2004, 2006–2007 and 2008–2009 [15, 45, 50]. In our SICU carbapenem-resistant *Klebsiella* spp. was first reported in urine culture in 2011. Prevention is a top priority for reducing person-to-person transmission of carbapenem-resistant *Klebsiella* spp. and will be a challenge for all healthcare workers in our hospital in future. This is especially true because there are very limited treatment options to use after the development of carbapenem-resistance.

Candida spp. is unusual cause of UTI in healthy individuals, but common causes of UTI in the hospital setting. Most of the patients in our study received broad-spectrum antibiotics in the ICU. This could have resulted in decolonization of normal bacterial flora, allowing *Candida* spp. to grow and become the dominant microorganism.

Conclusion

The results of the case-control study confirm that a critical illness is commonly complicated by the development of nosocomial CAUTI. The length of urinary catheterization and female gender are significant risk factors of

CAUTI. The most frequently isolated microorganisms responsible for SICU acquired CAUTI in this study were *Candida* spp., *Pseudomonas aeruginosa*, and *Klebsiella* spp.

Risk factors and causative microorganisms associated with CAUTI in SICU patients must be considered in planning of preventive measures against urinary tract infections in this setting.

REFERENCES

1. *Vincent J.* Nosocomial infections in adult intensive-care units. Lancet 2003; 361(9374): 2068−77.
2. *Fridkin SK, Welbel SF, Weinstein RA.* Magnitude and prevention of nosocomial infections in the intensive care unit. Infect Dis Clin North Am 1997; 11(2): 479−96.
3. *Vincent JL, Bihari DJ, Suter PM, Bruining HA, White J, Nicolas-Chanoin MH,* et al. The prevalence of nosocomial infection in intensive care units in Europe. Results of the European Prevalence of Infection in Intensive Care (EPIC) Study. EPIC International Advisory Committee. JAMA 1995; 274(8): 639−44.
4. *Eriksen HM, Iversen BG, Aavitsland P.* Prevalence of nosocomial infections in hospitals in Norway, 2002 and 2003. J Hosp Infect 2005; 60(1): 40−5.
5. *Lizioli A, Privitera G, Alliata E, Antonietta BE, Boselli L, Panceri ML,* et al. Prevalence of nosocomial infections in Italy: result from the Lombardy survey in 2000. J Hosp Infect 2003; 54(2): 141−8.
6. *Richards MJ, Edwards JR, Culver DH, Gaynes RP.* Nosocomial infections in combined medical-surgical intensive care units in the United States. Infect Control Hosp Epidemiol 2000; 21(8): 510−5.
7. *Richards MJ, Edwards JR, Culver DH, Gaynes RP.* Nosocomial infections in medical intensive care units in the United States. National Nosocomial Infections Surveillance System. Crit Care Med 1999; 27(5): 887−92.
8. *Laupland KB, Zygun DA, Davies H, Church DL, Louie TJ, Doig CJ.* Incidence and risk factors for acquiring nosocomial urinary tract infection in the critically ill. J Crit Care 2002; 17(1): 50−7.
9. *Haley RW, Culver DH, White JW, Morgan WM, Emori TG.* The nationwide nosocomial infection rate. A new need for vital statistics. Am J Epidemiol 1985; 121(2): 159−67.
10. *Stamm WE.* Catheter-associated urinary tract infections: epidemiology, pathogenesis, and prevention. Am J Med 1991; 91(3B): 65S−71S.
11. *Saint S.* Clinical and economic consequences of nosocomial catheter-related bacteriuria. Am J Infect Control 2000; 28(1): 68−75.
12. *Tambyah PA, Knasinski V, Maki DG.* The direct costs of nosocomial catheter-associated urinary tract infection in the era of managed care. Infect Control Hosp Epidemiol 2002; 23(1): 27−31.
13. *Weinstein MP, Towns ML, Quartey SM, Mirrett S, Reimer LG, Parmigiani G,* et al. The clinical significance of positive blood cultures in the 1990s: a prospective comprehensive evaluation of the microbiology, epidemiology, and outcome of bacteremia and fungemia in adults. Clin Infect Dis 1997; 24(4): 584−602.
14. HELICS. Surveillance of Nosocomial Infections in Intesive Care Units. Protocol. Version 6.1. 2004. [cited 2014 Jun 19]. Available from: http://www.sicsag.scot.nhs.uk/HAI/helics_protocol.pdf
15. *National Nosocomial Infections Surveillance System.* National Nosocomial Infections Surveillance (NNIS) System Report, data summary from January 1992 through June 2004, issued October 2004. Am J Infect Control 2004; 32(8): 470−85.
16. *Garner JS, Jarvis WR, Emori TG, Horan TC, Hughes JM.* CDC definitions for nosocomial infections, 1988. Am J Infect Control 1988; 16(3): 128−40.
17. *Horan TC, Andrus M, Dudeck MA.* CDC/NHSN surveillance definition of health care-associated infection and criteria for specific types of infections in the acute care setting. Am J Infect Control 2008; 36(5): 309−32.
18. CDC. NHSN. Catheter-Associated Urinary Tract Infection (CAUTI) Event. [cited 2014 January] Available from: http://www.cdc.gov/nhsn/PDFs/pscManual/7pscCAUTIcurrent.pdf
19. *Gokula R, Smith M, Hickner J.* Emergency room staff education and use of a urinary catheter indication sheet improves appropriate use of foley catheters. Am J Infect Control 2007; 35(9): 589−93.
20. *Gould CV, Umscheid GA, Agarwal RK, Kuntz G, Pegues DA,* - Healthcare Infection Control Practices Advisory Committee . . Guideline for prevention of catheter-associatedurinary tract infections 2009. 2010. [cited 2010 Mar 19]. Available from: http://www.cdc.gov.login.ezproxy.library.ualberta.ca/hicpac/cauti/001_cauti.html
21. *Hooton TM, Bradley SF, Cardenas DD, Colgan R, Geerlings SE, Rice JC,* et al. Diagnosis, prevention, and treatment of catheter-associated urinary tract infection in adults: 2009 International Clinical Practice Guidelines from the Infectious Diseases Society of America. Clin Inf Dis 2010; 50(5): 625−63.
22. *Dolin SJ, Cashman JN.* Tolerability of acute postoperative pain management: nausea, vomiting, sedation, pruritus, and urinary retention. Evidence from published data. Br J Anaesth 2005; 95(5): 584−91.
23. *Wald HL, Ma A, Bratzler DW, Kramer AM.* Indwelling urinary catheter use in the postoperative period: analysis of the national surgical infection prevention project data. Arch Surg 2008; 143(6): 551−7.
24. *Emori TG, Culver DH, Horan TC, Jarvis WR, White JW, Olson DR,* et al. National nosocomial infections surveillance system (NNIS): description of surveillance methods. Am J Infect Control 1991; 19(1): 19−35.
25. *Edwards JR, Peterson KD, Andrus ML, Tolson JS, Goulding JS, Dudeck MA,* et al. National Healthcare Safety Network (NHSN) Report, data summary for 2006, issued June 2007. Am J Infect Control 2007; 35(5): 290−301.
26. *Finkelstein R, Rabino G, Kassis I, Mahamid I.* Device-associated, device-day infection rates in an Israeli adult general intensive care unit. J Hosp Infect 2000; 44(3): 200−5.
27. *Warren JW.* Catheter-associated urinary tract infections. Int J Antimicrob Agents 2001; 17(4): 299−303.
28. *Weinstein JW, Mazon D, Pantelick E, Reagan-Cirincione P, Dembry LM, Hierholzer WJ.* A decade of prevalence surveys in a tertiary-care center: trends in nosocomial infection rates, device utilization, and patient acuity. Infect Control Hosp Epidemiol 1999; 20(8): 543−8.
29. *Munasinghe RL, Yazdani H, Siddique M, Hafeez W.* Appropriateness of use of indwelling urinary catheters in patients admitted to the medical service. Infect Control Hosp Epidemiol 2001; 22(10): 647−9.
30. *Jain P, Parada JP, David A, Smith LG.* Overuse of the indwelling urinary tract catheter in hospitalized medical patients. Arch Intern Med 1995; 155(13): 1425−9.
31. *Saint S, Wiese J, Amory JK, Bernstein ML, Patel UD, Zemencuk JK,* et al. Are physicians aware of which of their patients have indwelling urinary catheters. Am J Med 2000; 109(6): 476−80.
32. *Nickel JC, Costerton JW, Mclean RJ, Olson M.* Bacterial biofilms: influence on the pathogenesis, diagnosis and treatment of urinary tract infections. J Antimicrob Chemother 1994; 33 Suppl A: 31−41.
33. *Saint S, Chenoweth CE.* Biofilms and catheter-associated urinary tract infections. Infect Dis Clin North Am 2003; 17(2): 411−32.

34. *van der Kooi TII, de Boer AS, Manniën J, Wille JC, Beaumont MT, Mooi BW,* et al. Incidence and risk factors of device-associated infections and associated mortality at the intensive care in the Dutch surveillance system. Intensive Care Med 2007; 33(2): 271−8.
35. *Bochicchio GV, Joshi M, Shih D, Bochicchio K, Tracy K, Scalea TM.* Reclassification of urinary tract infections in critically III trauma patients: A time-dependent analysis. Surg Infect 2003; 4(4): 379−85.
36. *Leone M, Albanèse J, Garnier F, Sapin C, Barrau K, Bimar M,* et al. Risk factors of nosocomial catheter-associated urinary tract infection in a polyvalent intensive care unit. Intensive Care Med 2003; 29(7): 1077−80.
37. *Tissot E, Limat S, Cornette C, Capellier G.* Risk factors for catheter-associated bacteriuria in a medical intensive care unit. Eur J Clin Microbiol Infect Dis 2001; 20(4): 260−2.
38. *Foxman B.* Epidemiology of urinary tract infections: Incidence, morbidity, and economic costs. Am J Med 2002; 113(Suppl 1A): 5−13.
39. *Platt R, Polk BF, Murdock B, Rosner B.* Risk factors for nosocomial urinary tract infection. Am J Epidemiol 1986; 124(6): 977−85.
40. *Medina M, Martínez-Gallego G, Sillero-Arenas M, Delgado-Rodríguez M.* Risk factors and length of stay attributable to hospital infections of the urinary tract in general surgery patients. Enferm Infecc Microbiol Clin 1997; 15(6): 310−4.
41. *Rosser CJ, Bare RL, Meredith JW.* Urinary tract infections in the critically ill patient with a urinary catheter. Am J Surg 1999; 177(4): 287−90.
42. *Garibaldi RA, Mooney BR, Epstein BJ, Britt MR.* An evaluation of daily bacteriologic monitoring to identify preventable episodes of catheter-associated urinary tract infection. Infect Control 1982; 3(6): 466−70.
43. *Saint S, Lipsky BA, Goold SD.* Indwelling urinary catheters: A one-point restraint. Ann Intern Med 2002; 137(2): 125−7.
44. *Warren JW, Tenney JH, Hoopes JM, Muncie HL, Anthony WC.* A prospective microbiologic study of bacteriuria in patients with chronic indwelling urethral catheters. J Infect Dis 1982; 146(6): 719−23.
45. *Hidron AI, Edwards JR, Patel J, Horan TC, Sievert DM, Pollock DA,* et al. NHSN annual update: antimicrobial-resistant pathogens associated with healthcare-associated infections: annual summary of data reported to the National Healthcare Safety Network at the Centers for Disease Control and Prevention, 2006-2007. Infect Control Hosp Epidemiol 2008; 29(11): 996−1011.
46. *Tay MK, Lee JY, Wee IY, Oh HM.* Evaluation of intensive care unit-acquired urinary tract infections in Singapore. Ann Acad Med Singap 2010; 39(6): 460−5.
47. *Laupland KB, Bagshaw SM, Gregson DB, Kirkpatrick AW, Ross T, Church DL.* Intensive care unit-acquired urinary tract infections in a regional critical care system. Crit Care 2005; 9(2): R60−5.
48. *Šuljagić V, Cobeljić M, Janković S, Mirović V, Marković-Denić L, Romić P*, et al. Nosocomial bloodstream infections in ICU and non-ICU patients. Am J Infect Control 2005; 33(6): 333−40.
49. *Šuljagić V, Jevtic M, Djordjevic B, Jovelic A.* Surgical site infections in a tertiary health care center: prospective cohort study. Surg Today 2010; 40(8): 763−71.
50. *Sievert DM, Ricks P, Edwards JR, Schneider A, Patel J, Srinivasan A,* et al. Antimicrobial-resistant pathogens associated with healthcare-associated infections: summary of data reported to the National Healthcare Safety Network at the Centers for Disease Control and Prevention, 2009-2010. Infect Control Hosp Epidemiol 2013; 34(1): 1−14.

Received on June 24, 2014.
Revised on September 4, 2014.
Accepted on September 4, 2014.
Online First August, 2015.

ORIGINAL ARTICLE

UDC: 616.34-089-06-07
DOI: 10.2298/VSP140723011K

Diagnostic value of serial measurement of C-reactive protein in serum and matrix metalloproteinase-9 in drainage fluid in the detection of infectious complications and anastomotic leakage in patients with colorectal resection

Dijagnostička vrednost serijskog merenja C-reaktivnog proteina u serumu i matriksne metaloproteinaze-9 u drenažnoj tečnosti za detekciju infektivnih komplikacija i dehiscencije anastomoze kod bolesnika sa kolorektalnom resekcijom

Zoran Kostić*†, Marina Panišić*, Boško Milev*, Zoran Mijušković†‡, Damjan Slavković*, Mile Ignjatović*

***Clinic for General Surgery, ‡Institute of Medical Biochemistry, Military Medical Academy, Belgrade, Serbia; †Faculty of Medicine of the Military Medical Academy, University of Defence, Belgrade, Serbia**

Abstract

Background/Aim. Postoperative infectious complications are one of the most important problems in surgical treatment of colorectal cancer (CRC), being present in up to 40% of patients. The aim of this paper was to establish the significance of serial measurement of C-reactive protein (CRP) in serum and matrix metalloproteinase-9 (MMP-9) in drainage fluid for the detection of infectious complications and anastomotic leakage (AL) in patients with colorectal resection. **Methods.** CRP and MMP-9 values in serum and drainage fluid, respectively, were measured on the first, third, fifth, and seventh postoperative day (POD) in 150 patients with colorectal resection and primary anastomosis. The values obtained were compared between the patients without complicatons and those with surgical site and remote infections and AL. **Results.** Surgical site infections (SSIs) were observed in 41 (27.3%), and remote infections in 10 (6.7%) patients. Clinically evident AL was observed in 15 (10%) patients. In 82% of the patients with SSIs, serum CRP value on POD 5 exceeded 82 mg/L, with 81% specificity. AL was reported in 85% and 92% of the patients on PODs 5 and 7, respectively, with CRP values of 77 mg/L and 90 mg/L, respectively. The specificity was 77% for POD 5 and 88% for POD 7. All the patients with CRP values exceeding 139 mg/L on POD 5 had some of SSIs and/or AL. The mean values of MMP-9 were not statistically different between the group without complications (n = 99) and the group with AL (n = 15). **Conclusion.** Serial measurement of CRP is recommended for screening of infectious complications of colorectal resection. Patients with CRP values above 139 mg/L on POD 5 cannot be discharged from hospital, and require an intensive search for infectious complications, particularly AL. MMP-9 measurement in drainage fluid is not relevant in the detection of AL in patients with colorectal resection.

Key words:
c-reactive protein; matrix metalloproteinases; anastomosis surgical; postoperative complications; digestive system surgical procedures.

Apstrakt

Uvod/Cilj. Postoperativne infektivne komplikacije spadaju u najveće probleme hirurškog lečenja kolorektalnog karcinoma [*colorectal cancer* (CRC)] i nastaju kod 40% bolesnika. Cilj rada bio je utvrđivanje značaja serijskog merenja vrednosti C-reaktivnog proteina (CRP) u serumu i matriks metaloproteinaze-9 (MMP-9) u drenažnoj tečnosti za detekciju infektivnih komplikacija i dehiscencije anastomoze kod bolesnika sa resekcijom kolona i rektuma. **Metode.** Prvog, trećeg, petog i sedmog postoperativnog dana određivane su vrednosti CRP u serumu i MMP-9 u drenažnoj tečnosti kod 150 bolesnika sa kolorektalnom resekcijom i primarnom anastomozom. Dobijene vrednosti su upoređivane između grupa bolesnika bez komplikacija i onih sa specifičnim i udaljenim infektivnim komplikacijama i dehiscencijom anastomoze. **Rezultati.** Specifične infektivne komplikacije operativnog lečenja registrovane su kod 41 (27,3%), a udaljene kod 10 (6,7%) obolelih. Klinički manifestnu dehiscenciju anastomoze imalo je 15 (10%) bolesnika. Kod 82% bolesnika sa specifičnim komplikacijama vrednost CRP petog postoperativnog dana bila je veća od 82 mg/L, uz specifič-

Correspondence to: Zoran Kostić, Clinic for General Surgery, Military Medical Academy, Crnotravska 17, 11 000 Belgrade, Serbia. Phone: +381 11 3609 273. E-mail: sara_kostic@yahoo.com

nost od 81%. Dehiscencija anastomoze registrovana je kod 85% bolesnika petog i kod 92% sedmog postoperativnog dana pri vrednostima CRP od 77 mg/L i 90 mg/L, respektivno. Specifičnost je bila 77% petog dana i 88% sedmog postoperativnog dana. Svi bolesnici sa vrednošću CRP preko 139 mg/L petog postoperativnog dana imali su neku od specifičnih infektivnih komplikacija i/ili dehiscenciju anastomoze. Srednja vrednost MMP-9 bila je bez statistički značajne razlike između grupe bolesnika bez komplikacija (n = 99) i grupe sa dehiscencijom anastomoze (n = 15). **Zaključak.** Serijsko merenje vrednosti CRP u serumu može da se preporuči za otkrivanje infektivnih komplikacija. Operisani bolesnici sa vrednostima CRP iznad 139 mg/L petog postoperativnog dana ne mogu se otpustiti iz bolnice i kod njih se mora tragati za infektivnim komplikacijama operativnog lečenja, prvenstveno dehiscencijom anastomoze. Određivanje MMP-9 u drenažnoj tečnosti nema značaj za detekciju dehiscencije anastomoze kod bolesnika sa kolorektalnom resekcijom.

Ključne reči:
c-reaktivni protein; matriks metaloproteinaze; anastomoza, hirurška; postoperativne komplikacije; hirurgija digestivnog sistema, procedure.

Introduction

Postoperative infectious complications are one of the most important problems in surgical treatment of colorectal cancer (CRC), being present in up to 40% of patients [1]. Leakage of anastomosis created during surgical treatment is the most severe treatment complication, posing dilemmas for surgeons as to the prevention, early detection, and appropriate further treatment. Not only that it significantly impacts postoperative morbidity and mortality [2, 3], quality of life [4], prolongs length of hospital stay and increases treatment costs [2, 5], but is largely correlated with local recurrence rates and reduced tumor-specific survival of patients [6]. The reported leak rate varies, between 3% to 19%, depending on the definition [2, 3, 7–9]. It is more common after rectal surgery, between 8% and 14% [3, 8, 10, 11], compared to the colon, ranging from 3% to 7% [12, 13]. Early detection of this, potentially most dangerous complication, in the absence of clear clinical manifestations, would make possible early introduction of appropriate therapeutic measures intended to alleviate or eliminate adverse effects. The possibility of anticipating a postoperative course without complications in the era of adoption of the Enhanced Recovery After Surgery (ERAS) [14] protocol, is of significance with regard to earlier patient discharge and shorter length of hospital stay.

C-reactive protein (CRP) is the most popular and most widely available marker of the acute inflammatory response. In recent years, the significance of association of elevated systemic inflammatory response and worse cancer specific survival of the patients with colorectal cancer has been emphasized, regardless of the tumor disease stage [15]. CRP is synthesized in the hepatocytes, being released during the acute phase of inflammatory response, after the stimulation with interleukin 6 (IL-6), tumor necrosis factor α (TNF-α), and interleukin 1 β (IL-1 β), originating in the infection site [16]. CRP values in serum rise even before the clinical signs of infection become apparent [17]. These properties make CRP an ideal predictor of postoperative infectious complications, and combined with the clinical presentation, can be a marker of postoperative course, including both surgical and non-surgical treatment complications [18]. Since it is a non-selective marker of the inflammatory process, before searching for more specific ones, it is necessary to exclude remote infectious complications [17].

Matrix metalloproteinases (MMPs) are the most important factor in the preservation of extracellular matrix homeostasis in numerous tissues, being involved in numerous processes such as reproduction, morphogenesis, embryonal development, bone remodeling, angiogenesis, and tissue healing [19]. These are endopeptidases by nature, and 23 members of the family have been described in humans. At the transcriptional level, their synthesis is induced by proinflammatory cytokines, growth factors, hormones, ultraviolet radiation, physical stress, cell-cell and cell-matrix interactions [19, 20]. They are secreted into the environment in their inactive form as zymogens or promatrix metalloproteinases, with the exception of neutrophils, macrophages, and Paneth cells, where they are stored in the granules [19]. They have a complex function, which depends on the relationship of numerous activators and inhibitors of tissue matrix metalloproteinases (TIMMPs) [20]. Increased MMPs activity in the immediate vicinity of an anastomosis in experimental studies, has given rise to the idea that increased MMP activity in the immediate postoperative course could be responsible for anastomotic leakage (AL) [21, 22]. According to our knowledge there have been only two clinical papers elaborating a possible association of MMPs and AL in patients with colorectal resection [23, 24].

The aim of this paper was to establish the significance of serial measurement of CRP in serum and MMP-9 in drainage fluid for the detection of infectious complications and AL in patients with colorectal resection.

Methods

This prospective analysis enrolled 150 patients with cancer of the left colon and rectum surgically treated at the Clinic for General Surgery, Military Medical Academy, Belgrade, in the period from April 2011 to November 2012.

Preoperatively, appropriate investigations were performed in all the patients in order to establish the diagnosis and degree of disease spread [clinical examinations, endoscopic examination with biopsy and histopathology, abdominal ultrasound (US), chest x-ray]. Additional investigations, such as multislice computerized tomography (MSCT) of the abdomen and/or chest in patients with colon cancer, were done only in those cases in which the baseline tests (US, chest x-ray) had aroused suspicion of disease dissemination. In those with cancer of the distal and middle third of rectum, MSCT of the small pelvis was performed in order to establish local cancer spread and the need for preoperative adjuvant therapy.

The parameters relevant for the outcome of surgical treatment were registered for all the patients: age, anemia, comorbid conditions (diabetes mellitus, chronic obstructive pulmonary disease, arterial hypertension), and body mass index (BMI).

The patients with clinical signs of infection or some other inflammatory condition present preoperatively, were excluded from the study.

All the operations were done at the Clinic for General Surgery, Military Medical Academy, by the surgeons with at least 30 similar surgical interventions performed *per* year.

Mechanical preoperative large bowel preparation was done only in those with rectal cancers.

The analysis involved only the patients in whom conventional elective, radical, or palliative surgical intervention was done, with colo-colonic or colorectal anasomosis, handsawn or stapled. The patients operated for tumor recurrence were excluded from the study. The creation of diverting ileostomy or transversocolostomy depended on the individual assessment of surgeons. Before the closure of laparotomy incision, abdominal cavity of the patients was routinely drained with at least one drain placed in the area of the pouch of Douglas or in the presacral area, in the region of colorectal anastomosis.

In the immediate postoperative course, within a month of surgery, all remote (pneumonia, urinary infection, infections caused by the central venous line) and surgical site (wound infection, anastomotic leakage, intra-abdominal abscess collections) infectious complications were registered. Redness, edema, and purulent secretion at the site of laparotomy wound were the clinical criteria establishing the presence of infection in the surgical incision site [18]. Clinical parameters of AL were defined by the presence of purulent or fecal content at the drain site, pelvic abscess, peritonitis, rectovaginal fistula, or the appearance of purulent content from the rectum (*per recti*) [25]. Routine, contrast-enhanced x-ray control of the anastomosis was not implemented, since the patients with asymptomatic leakage, were not relevant for the study. In patients with low colorectal anastomosis, digital rectal examination was an integral part of the examination to detect possible AL. Intraabdominal abscesses were detected by way of the presence of purulent secretion after surgical or percutaneous ultrasound-guided drainage of these collections [18]. Appropriate clinical presentation with a positive x-ray finding in pneumonia, urinary sediment and urine culture in urinary infection, and positive blood culture in infections caused by central venous line, defined the presence of individual remote infections.

On the first, third, fifth, and seventh postoperative day (POD), serum CRP values were measured, utilizing the method immunonephelometry on a SIEMENS autoanalyzer (Dade Behring BN II), and MMP-9 activity was measured in intraperitoneal drainage fluid utilizing the enzyme-linked immunosorbent assay (ELISA) method. These laboratory parameters were measured at the Institute of Medical Biochemistry, Military Medical Academy, Belgrade.

The usual descriptive statistic parameters were used in statistical analysis of the obtained results (mean value, standard deviation, range, 95% confidence interval, frequency of individual characteristics). Depending on the normality of distribution of the observed parameters and the number of groups among which statistical significance was sought for, out of parametric tests the Students *t*-test was used for independent characteristics, and out of non-parametric tests the Mann-Whitney *U*-test. The existance of a statistically significant difference between the frequency distributions of individual groups was validated using the χ^2-test. The sensitivity and specificity of relevant biochemical markers were analyzed using the receiver operating characteristic curve (ROC).

Commercially available statistical software package SPSS version 17 (USA) was used for statistical analysis.

Results

We analyzed 150 patients in total, 94 (66.7%) men and 56 (33.3%) women (male-to-female ratio, 1.7:1). The youngest operated patient was 33, and the oldest one 87 years of age. The average age of the patients was 65 ± 11 years. Table 1 presents some of the characteristics of our surgically treated patients.

Table1

Characteristics of the surgically treated patients

Patients characteristics	Values
Gender, n (%)	
male	94 (66.7)
female	56 (33.3)
Age (years)	
$\bar{x}$ ± SD	65 ± 11
range	33–87
median	65
Body mass index (kg/m^2)	
$\bar{x}$ ± SD	25.80 ± 4.14
median	25.18
Comorbidities, n (%)	
yes	85 (56.7)
no	65 (43.3)
Tumor site, n (%)	
splenic flexure	12 (8)
descendent colon	2 (1.3)
sygmoid colon	33 (22)
rectosigmoid junction	38 (25.3)
rectum – upper (10–15 cm)	9 (6)
rectum – middle (5–10 cm)	36 (24)
rectum – lower (< 5 cm)	20 (13.3)
Disease stage, n (%)	
T1	11 (7.3)
T2	14 (9.3)
T3	122 (81.3)
T4	3 (2)
N0	91 (60.7)
N1 (1–3)	41 (27.3)
N2 (4–6)	16 (10.7)
N3 (> 6)	2 (1.3)
M0	136 (90.7)
M1	14 (9.3)
Astler-Coller, n (%)	
A	10 (6.7)
B1	12 (8)
B2	66 (44)
C1	2 (1.3)
C2	46 (30.7)
D	14 (9.3)
Anastomosis, n (%)	
colo-colo	47 (31.3)
colo-recto	103 (68.7)
handsawn	63 (42)
stapled	87 (58)
Preoperative radiation, n (%)	
yes	28 (18.7)
no	122 (81.3)
Diverting stoma, n (%)	
transverse colostomy	45 (30)
ileostomy	4 (2.7)
no	101 (67.3)
Morbidity, n (%)	
total complications	51/150 (34)
surgical site infections	41/150 (27.3)
remote infections	10/150 (6.7)
Mortality	6/150 (4)

Comorbidities were present in 85 (56.7%) of the patients. Cancer of the left colon was present in 85 (56.7%), and rectal cancer in 65 (43.3%) of the patients. There were 122 (81.3%) of the patients with T3 tumors; metastatic lymph node involvement was present in 59 (39.3%) of the patients, and distant metastatic disease in 14 (9.3%) of the patients. There were 20 (13.3%) colo-colonic, and 130 (86.7%) colo-rectal anastomoses performed. In four patients, atypical segment resection of the liver with metastatic foci was performed, in two cases typical liver resection, and in eight metastatic deposits were only biopsied. There were 63 (42%) handsewn anastomoses, and 87 (58%) were created using staplers. Preoperative radiation therapy was administered in 28 patients, i.e. in 50% of those with cancers of the middle and distal portion of the rectum.

The overall morbidity rate associated with surgical treatment was 34%, and mortality rate 4%. Surgical site infections (SSIs) were observed in 41 (27.3%) and remote infections in 10 (6.7%) of the patients. In 99 surgically treated patients postoperative course was without any complications.

Clinically evident AL was observed in 15 of the patients – in two patients (4.2%) with left colonic surgery, and in 13 (12.6%) patients with colo-rectal anastomosis. Postoperative mortality rate associated with AL was 13%, and out of six fatal outcomes, leakage was the immediate cause of death in two. Table 2 shows the results of univariate and multivariate analysis of risk factors for the occurrence of AL.

Male patients with tumors of the middle and distal third of the rectum (≤ 10 cm), those undergoing preoperative radiation therapy, and those with created diverting stomas were at the highest risk of developing AL.

In Table 3 the mean CRP values in serum for the observed postoperative days in the group of patients without sur-

Table 2

Characteristics of patients with anastomotic leakage (AL) – univariate and multivariate analysis

Variable	Patients with AL (n = 15)	All patients (n = 150)	Univariate analysis	Multivariate analysis 95% CI			
				RR	lower	upper	*p*
Age (years), $\bar{x} \pm SD$	68 ± 14	65 ± 11	$t = 0.953$ $p = 0.342$	1.02	0.98	1.08	0.32
≤ 65, n (%) > 65, n (%)	5/77 (65) 10/73 (13.7)		$\chi^2 = 1.435$ $p = 0.231$	2.29	0.74	7.04	0.15
Gander, n (%) male	14/94 (14.9)		$\chi^2 = 5.322$	9.26	1.23	75.34	0.03
female	1/56 (1.6)		$p = 0.02$				
Body mass index (kg/m^2), $\bar{x} \pm SD$	25.35 ± 3.85	25.8 ± 4.14	$t = 0.404$ $p = 0.687$	0.97	0.84	1.11	0.65
Tumor site, n (%) left colon	2/47 (4.2)		$\chi^2 = 3.525$	7.72	0.99	60.55	0.052
rectum	13/103 (12.6)		$p = 0.060$				
Anastomosis (cm), n (%) > 10	2/85 (2.3)		$\chi^2 = 0.86$	10.37	2.25	47.84	0.003
≤ 10	13/65 /20)		$p < 0.001$				
Comorbidities, n (%) yes	10/85 (11.7)		$\chi^2 = 0.302$	1.17	0.39	3.48	0.78
no	5/56 (7.7)		$p = 0.583$				
Disease stage, n (%) T_1, T_2	3/25 (12)		$\chi^2 = 0.000$	1.28	0.33	4.93	0.71
T_3, T_4	12/125 (9.6)		$p = 1.000$				
N0	8/91 (8.8)		$\chi^2 = 0.112$	1.40	0.48	4.08	0.54
N+	7/59 (11.9)		$p = 0.738$				
Anastomosis, n (%) handsaw	3/63 (4.8)		$\chi^2 = 2.384$	3.20	0.86	11.86	0.08
stapled	12/87 (13.8)		$p = 0.123$				
Preoperative radiation, n (%) yes	8/29 (28.6)		$\chi^2 = 10.778$	153.14	16.74	1400.74	0.001
no	7/122 (5.7)		$p = 0.001$				
Divert stoma, n (%) yes	10/49 (20.4)		$\chi^2 = 7.126$	268.00	28.50	2520.20	0.001
no	5/101 (5)		$p = 0.008$				

***RR – relative risk; CI – confidence interval; χ^2 – chi square test; *t* – Student's *t*-test.**

Table 3

Correlation of serial serum C-reactive protein (CRP) (mg/L) measurement with infectious surgical treatment complications, by postoperative days (POD)

POD	No complications (n = 99)	SSIs (n = 41)		Remote infections (n = 10)		AL (n = 15)	
	$\bar{x} \pm SD$	$\bar{x} \pm SD$	*p*	$\bar{x} \pm SD$	*p*	$\bar{x} \pm SD$	*p*
1	95.15 ± 37.97	109.39 ± 47.81	0.151	121.63 ± 27.78	0.014	102.11 ± 39.65	0.595
3	113.47 ±40.72	200.58 ± 69.46	< 0.001	145.20 ± 52.90	0.059	197.25 ± 75.76	0.001
5	57.10 ± 28.15	154.84 ± 69.96	< 0.001	103.91 ± 52.70	0.001	175.93 ± 72.51	< 0.001
7	49.71 ± 29.95	119.86 ± 72.59	< 0.001	102.17 ± 71.66	0.003	155.61 ± 77.49	< 0.001

***Mann-Whitney U-test, comparison with patients with no complications; SSIs – surgical site infections; AL – anastomotic leakage.**

gical treatment complications (n = 99) and those with SSIs (n = 41) and remote (n = 10) infectious complications, and those with AL (n = 15) are given. On POD 1, there were no statistically significant differences in CRP values between the group of patient without and those with surgical treatment complications.

Figure 1 illustrates the mean CRP values by the group of patients for the observed PODs.

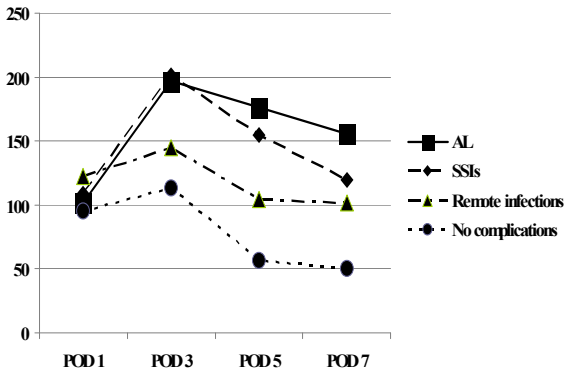

Fig. 1 – Serum C-reactive protein (CRP) values (mg/L) in the patients without, and those with surgical site infections (SSIs) remote infections, and anastomotic leakage (AL), by postoperative days (POD).

In all the patients there was the increase of CRP, with maximum values reported for POD 3. In those without complications, there was a descending tendency, significantly more evident compared to descending CRP values in those with SSIs and AL. While serum CRP values in patients with SSIs and AL remained high on PODs 5 and 7, in those with remote infections CRP values returned to the baseline on POD 7.

Sensitivity and specificity of serum CRP measurement in the detection of SSIs and AL were analyzed using the ROC curve and are shown in Table 4 and Figures 2 and 3. CRP values on POD 5 are most important in the detection of SSIs, and on PODs 5 and 7 in the detection of AL. The area under the ROC curve on POD 5 in the patients with SSIs was 0.926, and in those with AL 0.920 on POD 5, and 0.960 on POD 7. In 82% of the patients with SSIs, CRP values on POD 5 exceeded 82 mg/L, with 81% specificity. All the patients with CRP values above 139 mg/L on POD 5 had some of SSIs. AL was observed in 85% of the patients on POD 5 and in 92% on POD 7, with CRP values of 77 mg/L and 90 mg/L. The method specificity was 77% for POD 5, and 88% for POD 7. All the patients with AL had CRP values above 139 mg/L on POD 5.

Table 5 illustrates the results of cutoff CRP values in postoperative infectious complications in different authors' papers, including ours.

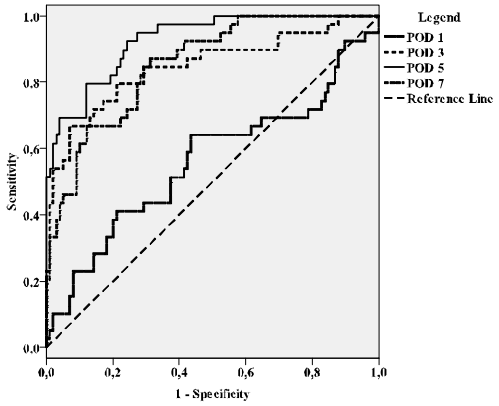

Fig. 2 – Diagnostic accuracy of serum C-reactive protein (CRP) in the detection of surgical site infections (SSIs) expressed as a receiver operating characteristic (ROC) curve. POD – postoperative day.

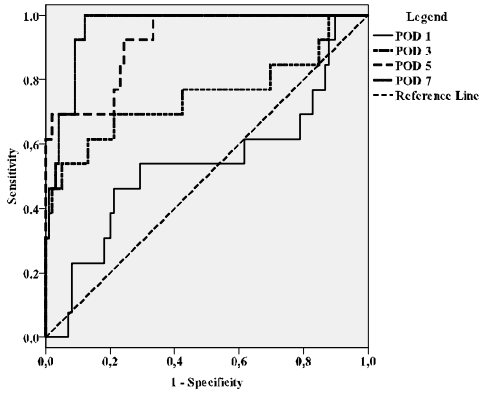

Fig. 3 – Diagnostic accuracy of serum C-reactive protein (CRP) in the detection of anastomotic leakage (AL), expressed as a receiver operating characteristic (ROC) curve. POD – postoperative day.

Table 4

Sensitivity and specificity of serum C-reactive protein (CRP) in the patients with surgical site infections and anastomotic leakage by postoperative days (POD), espressed as an area under the receiver operating chracteristic (ROC) curve (AUC)

POD	Cutoff value CRP (mg/L)	Sensitivity (%)	Specificity (%)	AUC (95% CI)	*p*
Surgical site infections (n = 41)					
1	100	51	63	0.567 (0.454 – 0.681)	0.28
3	150	73	84	0.847 (0.766 – 0.928)	< 0.001
5	82	82	81	0.926 (0.882 – 0.970)	< 0.001
7	82	67	88	0.854 (0.789 – 0.920)	< 0.001
Anastomotic leakage (n = 15)					
1	111	54	71	0.538 (0.348 – 0.729)	0.65
3	140	69	79	0.748 (0.567 – 0.929)	0.004
5	77	85	77	0.920 (0.849 – 0.991)	< 0.001
7	90	92	89	0.960 (0.925 – 0.994)	< 0.001

CI – confidence interval.

Table 5

Cutoff values of serum C-reactive protein (CRP) in postoperative infectious complications

Study	CRP (mg/L)
POD 1	
MacKay et al. [31]	82
Korner et al. [34]	89
Scepanovic et al. [36]	187
Warschkow et al. [38]	123
Kostic et al. (this study)	112
POD 2	
Welsch et al. [17]	140
MacKay et al. [31]	164
Scepanovic et al. [36]	164
Warschkow et al. [38]	173
POD 3	
Welsch et al. [17]	140
MacKay et al. [31]	195
Korner et al. [34]	190
Scepanovic et al. [36]	135
Warschkow et al. [38]	185
Kostic et al. (this study)	150
POD 4	
Welsch et al. [17]	140
MacKay et al. [31]	145
Ortega-Deballon et al. [32]	125
Scepanovic et al. [36]	116
Warschkow et al. [38]	123
POD 5	
MacKay et al. [31]	135
Korner et al. [34]	154
Scepanovic et al. [36]	114
Warschkow et al. [38]	83
Kostic et al. (this study)	82
POD 7	
Korner et al. [34]	215
Scepanovic et al. [36]	85
Kostic et al. (this study)	82

POD – postoperative day.

Table 6 shows the relationship of the mean MMP-9 values in drainage fluid for the observed PODs between the group of patients without surgical complications (n = 99) and the group of those with AL (n = 15). There were no statistically significant differences in MMP-9 values between the analyzed groups.

patients with AL in our study was 13%, and out of six deaths, leakage was the immediate cause of death in two. Rickert et al. [12], analyzing the treatment results in 1,731 patients with colon resection, have reported the AL rate of 3.5% and the mortality rate of 25% in those with complications. In 807 patients with colorectal resection, Buchs et al. [2] have reported the AL rate of 3.6% and the mortality rate of 13% in the affected. A half of the patients were surgically treated for CRC, and AL rate after rectal resection was 13%. Reporting the results of treatment of 739 patients with colorectal resection in a ten years' period (1997–2007), in a tertiary care institution in Netherlands, Komen et al. [8] stated that AL occurred in 64 (8.7%) patients, out of which nine (14%) died. The incidence of AL in patients with left hemicolectomy was 12%, with resection of sygmoid colon 8%, rectosygmoid colon 17%, and with low anterior resection and with total mesorectal excision 13%.

Numerous risk factors could be considered significant for the occurrence of AL, such as age [27, 28], gender [3, 7, 13], smoking [10], obesity [2, 8, 27], malnutrition [27, 29], American Society of Anesthesiologists (ASA) score [2, 7], laparoscopic access [13], duration of surgery [2, 8, 30], intraoperative blood transfusions [13], level of anastomosis [3, 7, 10], site of rectal cancer [2], preoperative steroid [30] and radiation therapy [7], diverting stoma [7, 9, 11], and prophylactic intraoperative abdominal drainage [8, 10]. Univariate and multivariate analysis of our patients demonstrated male gender, anastomosis created below 10 cm from the anal verge, preoperative radiation therapy, and diverting stoma to be significant risk factors for AL. Years of age, body mass index, comorbidities, tumor size, lymphonodal status, and type of anastomosis (handsewn or stapled) did not have an impact on the incidence of AL. Tumor site (colon *vs* rectum) could probably be a significant risk factor if the study included patients with cancer of the right colon, in view of a lower incidence of AL after resection of the right compared to the left colon [13]. In contrast to other authors' papers, where the incidence of AL was lower in those with intraoperatively created diverting stoma [9, 11, 25],

Table 6

Matrix metalloproteinase-9 (MMP-9) values in the drainage fluid in patients without complications compared to those with anastomotic leakage (AL)

POD	No complications (n = 99) $\bar{x} \pm SD$	AL (n = 15) $\bar{x} \pm SD$	Z adjusted	*p*
1	1239.09 ± 618.22	1296.10 ± 687.71	0.112136	0.91
3	1151.31 ± 975.58	1114.79 ± 715.96	0.479493	0.61
5	1147.17 ± 559.64	1166.43 ± 599.55	0.799385	0.42
7	1086.55 ± 466.47	948.16 ± 393.48	0.608981	0.54

***Mann-Whitney *U*-test; POD – postoperative day.**

Discussion

Anastomotic leakage (AL) is potentially the most serious surgical treatment complication in patients with CRC. It is the leading cause of postoperative mortality of patients with CRC, and an immediate cause of the one third of deaths after surgery [10, 12]. In the analysis of our patients, we used exclusively the clinical criteria to establish AL [26], and it was reported in 15 patients. The postoperative mortality rate of in our study AL was significantly more common in the patients with stoma. The explanation for this could be found in our patient selection criteria. In other authors' papers, stoma was most commonly created depending on the level of anastomosis, and patients with surgical treatment complications were excluded from the analysis. Diverting stoma did not prevent anastomotic leakage, but it reduced adverse septic consequences of leakage instead [7, 9]. In our patients, the creation of diverting transversocolostomy or ileostomy depended

exclusively on the surgeon's decision, and it was most commonly performed in patients with surgery-related problems, such as long lasting surgical procedure, intraoperative hypotension, bleeding and the need for blood transfusion, difficulties in the creation of anastomosis, incomplete rings in the anastomosis created with mechanical staplers, and similar, and these are the factors significantly contributing to the incidence of the complication [7].

The closer an anastomosis is to the anocutaneous junction, the higher is the risk of leakage. Trencheva et al. [3], in their prospective analysis of 616 patients with colorectal resection, with leakage incidence of 5.7%, have emphasized that anastomoses created below 10 cm from the anal verge were the most important prognostic risk factor, which was in accordance with our own results. Shiomi et al. [11] have recommended mandatory fecal diversion for the anastomoses below 5 cm from the anal verge, taking into consideration a significant difference in the incidence of clinically evident AL in this group of patients with and without defunctioning stoma (3.8% *vs* 12.7%). Similarly, Mathiessen et al. [9] have found a statistically significant difference in the incidence of AL in patients with anastomosis up to 7 cm from the anal verge, without and with diverting stoma (28% *vs* 10.3%).

Complications are an inevitable companion of any surgical treatment, and their prevention and/or earlier detection and timely therapeutic management are the prerequisite of improved overall treatment results. In the immediate postoperative course, often septic condition cannot be reliably distinguished from normal systemic inflammatory response to surgical trauma. Since clinical examination most often cannot be the sole approach in making the diagnosis, the need for selective and specific markers of infectious complications is essential, enabling their early detection and implementation of appropriate measures to improve treatment outcomes [17, 31]. The ability to predict a complication-free postoperative course in the era of adoption of the Enhanced Recovery After Surgery (ERAS) [14] protocol, is essential regarding earlier discharge and shorter length of hospital stay [32].

C-rective protein (CRP) is the protein of acute inflammatory phase and most commonly measured non-specific marker of systemic inflammatory response. Serum half-life of CRP is constant, being 19 hours, and its elevated concentrations are the consequence of increased synthesis in response to stimulus intensity, being the measure of acute inflammatory response [33]. What is even more important, serum CRP values increase even before the clinical signs of infection become evident, such as increased body temperature, rapid heartbeat, and pain [17]. These properties make CRP an ideal predictor of postoperative infectious complications. Since it is a non-selective marker of the inflammation process, before searching for specific ones it is necessary to exclude other infectious complications [17]. That is why we analyzed serum CRP values in the patient groups without, with surgical site, and remote infections, and especially in those with AL. In all the patient groups there was an increase of CRP after surgery, with maximum values observed on POD 3. After that, in those without complications there was a gradual decline, while high CRP values were maintained on PODs 5 and 7 in those with SSIs and AL (Figure 1 and Table 3).

Similar results can be found in papers of other authors [17, 34, 35]. Welsch et al. [17] have recorded infectious complications in 383 patients with cancer of the rectum in whom resection and primary anastomosis were performed. Serum CRP values, number of leukocytes, thrombocytes, and body temperature were recorded every day during twelve PODs. Two groups were compared – 48 patients with complications and 48 with normal postoperative course. The authors found that in patients without complications, after an initial rise of CRP values (with maximum mean value of 140 mg/L) on POD 2, there was a gradual decline of CRP values on days to follow. In those with complications, high CRP values persisted after POD 2. Korner et al. [34] analyzed the results of serum CRP values on PODs 1, 3, 5, and 7 in 231 patients with colorectal resection divided into three groups: those without complications, with intraabdominal complications, and with extra-abdominal infectious complications. On POD 1, CRP was elevated in all the patients. The authors found that the mean value of CRP was highest in patients with intra-abdominal complications, and that high CRP values persisted in this group on PODs 5 and 7. In those without complications, a decrease of CRP was observed after POD 3, while in the group of patients with extra-abdominal complications a small rise and more modest decline of mean values were observed. This finding is similar to our own results, since CRP values on POD 7 correspond to the values observed on POD 1 in the group of patients with remote infections.

The results of a prospective study in France on 133 patients with colorectal resection point out the significance of CRP measurement on PODs 2 and 4 in early identification of patients with AL. The incidence of AL was 15.5% in this patient series [32]. The relationship of AL and CRP values in 342 patients with colorectal resection was analyzed by Woeste et al. [35]. In contrast to the patients without complications, in 26 (7.6%) patients with AL there was not any decline of CRP values after the maximum reached on POD 3. What was most important was that these high values were measured before clinical evidence of AL. MacKay et al. [31] studied all postoperative infectious complications altogether, regardless of the type of complication. They concluded that there was a statistically significant difference in CRP values between the patients with and without infections starting from POD 2, and that CRP measurement was most relevant on POD 4 in view of the observed difference. Most authors today regard CRP measurement between PODs 3 and 5 as most important for the detection of infectious complications [17, 31, 32, 34, 36].

Serum CRP values significantly vary during postoperative course in both the patients with and without complications [17]. It is therefore necessary to monitor changes of CRP values in the immediate postoperative course utilizing serial measurements. Diagnostic accuracy of CRP values monitored as a constant variable depends significantly on the cutoff value. For this purpose, the statistical analysis with ROC curve is believed to be the most appropriate [37]. For any clinical assumptions to be drawn based on CRP values, one has to know that sensitivity and specificity are inversely related to the chosen cutoff value.

Considering the statistically assessed cutoff value of 123 mg/L on POD 4, Warschkow et al. [38] have reported sensitivity and specificity of 66% and 77%, respectively, in

the prediction of infectious complications. In view of the fact that it could not be used as a completely reliable diagnostic indicator of infection, the authors concluded that CRP values could be taken into consideration only within the clinical presentation context. According to Welsch et al. [17], the serum CRP value of 140 mg/L on PODs 3 and 4 was the cutoff value for the patients with infectious complications, with sensitivity of 80% and 54.3%, and specificity of 81% and 92.3%, respectively. For this CRP value on PODs 3 and 4, a positive predictive value for a postoperative course with complications was 80.7% and 90.5%, respectively. Korner et al. [34] found that the CRP value of 190 mg/L on POD 3 was a cutoff value indicating intra-abdominal infectious complications with sensitivity and specificity of 82% and 73%, respectively. The area under the ROC curve was 0.82. An identical diagnostic accuracy was established for CRP values measured on PODs 5 and 7. According to Ortega-Deballon et al. [32], measurement of CRP had the highest diagnostic accuracy out of all clinical and laboratory data. The values on PODs 2 and 4 had the highest predictive value in early detection of AL (the area under the ROC curve being 0.715 and 0.845, respectively), as well as other postoperative septic complications (the area under the ROC curve being 0.804 and 0.787, respectively). They concluded that the patients with CRP values above 125 mg/L on POD 4 could not be discharged from the hospital. MacKay et al. [31] found the positive and negative predictive value of 61% and 96% in the detection of infectious complications, with high sensitivity and specificity, for CRP values exceeding 125 mg/L on POD 4. Patients with CRP values below 135 mg/L on POD 3, according to Šćepanović et al. [36], were considered to be without infectious complications and could be safely discharged from the hospital.

Analysis of our results using the ROC curve for serum CRP values demonstrated that the values on POD 5 were most significant in the detection of SSIs, and on PODs 5 and 7 in the detection of AL. Area under the ROC curve on POD 5 for those with SSIs and AL was 0.926 and 0.920, respectively. In 82% of patients with SSIs, CRP values on POD 5 exceeded 82 mg/L, with 81% specificity. All the patients with CRP values above 139 mg/L on POD 5, had some of SSIs. Those with CRP values of 150 mg/L and 82 mg/L on PODs 3 and 7, had the highest risk of developing SSIs, with sensitivity and specificity of 73% and 84% for POD 3, and 67% and 88% for POD 7. AL was detected in 85% of the patients on POD 5 and 92% on POD 7, with CRP values of 77 mg/L and 90 mg/L, and specificity of 77% and 89%, respectively. AL was present in all the patients with serum CRP values above 139 mg/L on POD 5, and 150 mg/L on POD 7.

Increased serum CRP values can indicate the presence of infectious complications of surgical treatment, but the type of complication can not be established using this method, which is of utmost importance in further therapeutic management. We therefore tried to establish whether MMP-9 measurement in the peritoneal drainage fluid could be of use in early identification of the patients with AL as the most serious complication of surgical treatment. Biomechanical strength of an anastomosis depends primarily on the integrity of collagen-rich submucosal layer [39]. Experimental models have shown that in the immediate postoperative course, collagen decomposition prevails collagen synthesis, making an anastomosis most vulnerable in the first three to five days [40]. Studies on experimental animals have associated increased collagen decomposition with increased activity of MMPs [21, 22]. In general, healing represents a complex process of balancing of extracellular matrix components, involved in its synthesis and breakdown. Stumpf et al. [41] have compared in their prospective study a group of 15 patients with, and 104 patients without AL. Type I to type III collagen relationship was significantly lower in patients with AL. In these, tissue levels of MMPs 1, 2 and 9 were significantly higher, so that the analysis of biopsy samples of normal colonic wall in this group showed increased tissue expression of MMPs 1 and 2 in the mucosa, and MMPs 2 and 9 in the submucosa.

Drainage fluid is a complex mixture of different biological substances, involving different MMPs, both latent and active enzyme forms, and tissue inhibitors of metalloproteinase (TIMP) and their complexes. Preservation of extracellular matrix structure depends on the activity of MMPs and their endogenous inhibitors, and increased activity of MMP-8 and MMP-9 in the immediate vicinity of anastomosis has prompted the idea in experimental studies that increased MMP activity in the immediate postoperative course could be responsible for AL [21, 22]. Both active form and total (active and latent) MMP concentrations can be measured in the drainage fluid [42].

According to our knowledge, only two clinical papers have been published referring to the association of MMP with AL in patients with colorectal resection [23, 24]. Pasternak et al. [23] have analyzed the drainage fluid samples in 29 out of 30 patients in whom low anterior resection of the rectum was performed for cancer. The total morbidity was 41%, and symptomatic AL was detected in 10 (34%) patients. Such a high rate of AL was explained by a small patient sample. Drainage fluid was sampled only once, immediately following the surgery (after 2–6 hours), and the MMP levels were determined using multiplex flow cytometry. The levels of MMP-8 and MMP-9 were statistically significantly higher in the group with AL. The mean value of the difference was 259 ng/mL for MMP-8 ($p = 0.02$) and 1,180 ng/mL for MMP-9 ($p = 0.03$). The observed values for other MMPs (1, 2, 3, 7, and 13) were without any significant difference between the groups. As the shortcomings of the study, the authors reported small number of the patients, the absence of multiple testing and multivariate analysis of the results. In view of the strong observed association of MMP-8 and MMP-9 levels with AL, they suggested further studies in the area that would certainly contribute to earlier detection of AL and timely therapeutic intervention. However, one should not forget that while MMP-8 measurement is a routine, bedside procedure [43], it is not the case with MMP-9, and flow-cytometry, although highly sensitive, is a costly method requiring highly trained personnel.

The paper of Baker et al. [24] describes the measurement of MMP and TIMP levels in 58 patients undergoing various

surgical procedures, from right hemicolectomy to low anterior rectal resection. Samples of peritoneal drainage fluid were taken daily during the postoperative course, and MMP and TIMP measurements were done using the ELISA method. The result analysis showed a significant positive correlation of MMP-2 levels (POD 3), total MMP-2 (POD 6), and total MMP-9 (PODs 6 and 7) with surgical complications, while there was a negative correlation with TIMP-1 (POD 7) and TIMP-2 (PODs 2 and 3). The highest values of active and total MMP-9 were observed on POD 1, and gradually decline till POD 7. High MMP-9 values immediately after the surgery are the consequence of its increased release from neutrophils and monocyte cells, leading to an increased breakdown of stromal and basal membrane components, facilitating the infiltration of these cells in the area of the wound. The shortcomings of the study were heterogeneous groups of patients and the lack of data about the type of postoperative complications.

In our patients, MMP-9 values were determined using the ELISA method in the samples of drainage fluid taken on PODs 1, 3, 5, and 7. In contrast to Pasternak et al. [23], we did not find any statistically significant difference between the average, mean values of MMP-9 levels in the group of patients without surgical complications and those with AL for the studied days. A declining tendency in the average MMP-9 levels was observed in both groups of our patients, which was in agreement with the results of Baker et al. [24]. A possible explanation of the differences in the results in our study compared to the cited papers could be possibly found in the manner and time of analysis. MMP-9 tests used by us were adjusted by the manufacturer to test a larger number of samples, so that analysis was not done immediately; the collected samples were stored at -70ºC until the sufficient number of samples was collected. Such a procedure of keeping the samples for a period of time could have an impact on the composition and relationships of various biological materials in a complex mixture such as drainage fluid.

Conclusion

Serial measurement of C-reactive protein in serum in the immediate postoperative course makes possible an early detection of patients with surgical site infectious and anastomotic leakage and those with normal postoperative course. Patients with C-reactive protein values above 139 mg/L on postoperative day 5 can not be discharged from the hospital and require an intensive search for infectious complications, particularly anastomotic leakage. Early detection of this, potentially most dangerous complication, in the absence of clear clinical manifestations, would make possible an early introduction of appropriate therapeutic measures intended to alleviate or eliminate adverse effects. Patients without complications can be early released from the hospital afer a shortened length of hospital stay and with lower costs of treatment. Matrix metalloproteinase-9 measurement in drainage fluid is not relevant in the detection of anastomotic leakage in patients with colorectal resection.

R E F E R E N C E S

1. *Ugolini G, Rosati G, Montroni I, Zanotti S, Manaresi A, Giampaolo L*, et al. Can elderly patients with colorectal cancer tolerate planned surgical treatment? A practical approach to a common dilemma. Colorectal Dis 2009;11(7): 750−5.
2. *Buchs NC, Gervaz P, Secic M, Bucher P, Mugnier-Konrad B, Morel P.* Incidence, consequences, and risk factors for anastomotic dehiscence after colorectal surgery: a prospective monocentric study. Int J Colorectal Dis 2008; 23(3): 265−70.
3. *Trencheva K, Morrissey KP, Wells M, Mancuso CA, Lee SW, Sonoda T,* et al. Identifying important predictors for anastomotic leak after colon and rectal resection: prospective study on 616 patients. Ann Surg 2013; 257(1): 108−13.
4. *Nesbakken A, Nygaard K, Lunde OC.* Outcome and late functional results after anastomotic leakage following mesorectal excision for rectal cancer. Br J Surg 2001; 88(3): 404−8.
5. *Koperna T.* Cost-effectiveness of defunctioning stomas in low anterior resections for rectal cancer: a call for benchmarking. Arch Surg 2003; 138: 1334−8.
6. *Mirnezami A, Mirnezami R, Chandrakumaran K, Sasapu K, Sagar P, Finan P.* Increased local recurrence and reduced survival from colorectal cancer following anastomotic leak: systematic review and meta-analysis. Ann Surg 2011; 253(5): 890−9.
7. *Jestin P, Påhlman L, Gunnarsson U.* Risk factors for anastomotic leakage after rectal cancer surgery: a case-control study. Colorectal Dis 2008; 10(7): 715−21.
8. *Komen N, Dijk J, Lalmahomed Z, Klop K, Hop W, Kleinrensink G,* et al. After-hours colorectal surgery: a risk factor for anastomotic leakage. Int J Colorectal Dis 2009; 24(7): 789−95.
9. *Matthiessen P, Hallböök O, Rutegård J, Simert G, Sjödahl R.* Defunctioning stoma reduces symptomatic anastomotic leakage after low anterior resection of the rectum for cancer: a randomized multicenter trial. Ann Surg 2007; 246(2): 207−14.
10. *Alberts JC, Parvaiz A, Moran BJ.* Predicting risk and diminishing the consequences of anastomotic dehiscence following rectal resection. Colorectal Dis 2003; 5(5): 478−82.
11. *Shiomi A, Ito M, Saito N, Hirai T, Ohue M, Kubo Y,* et al. The indications for a diverting stoma in low anterior resection for rectal cancer: a prospective multicentre study of 222 patients from Japanese cancer centers. Colorectal Dis 2011; 13(12): 1384−9.
12. *Rickert A, Willeke F, Kienle P, Post S.* Management and outcome of anastomotic leakage after colonic surgery. Colorectal Dis 2010; 12(10 Online): e216−23.
13. *Krarup PM, Jorgensen LN, Andreasen AH, Harling H.* A nationwide study on anastomotic leakage after colonic cancer surgery. Colorectal Dis 2012; 14(10): e661−7.
14. *Gianotti L, Nespoli L, Torselli L, Panelli M, Nespoli A.* Safety, feasibility, and tolerance of early oral feeding after colorectal resection outside an enhanced recovery after surgery (ERAS) program. Int J Colorectal Dis 2011; 26(6): 747-−53.
15. *Leitch EF, Chakrabarti M, Crozier JE, Mckee RF, Anderson JH, Horgan PG,* et al. Comparison of the prognostic value of selected markers of the systemic inflammatory response in patients with colorectal cancer. Br J Cancer 2007; 97(9): 1266−70.
16. *Gabay C, Kushner I.* Acute-phase proteins and other systemic responses to inflammation. N Engl J Med 1999; 340(6): 448−54.

17. *Welsch T, Müller SA, Ulrich A, Kischlat A, Hinz U, Kienle P,* et al. C-reactive protein as early predictor for infectious postoperative complications in rectal surgery. Int J Colorectal Dis 2007; 22(12): 1499−507.
18. *Moyes LH, Leitch EF, McKee RF, Anderson JH, Horgan PG, McMillan DC.* Preoperative systemic inflammation predicts postoperative infectious complications in patients undergoing curative resection for colorectal cancer. Br J Cancer 2009; 100(8): 1236−9.
19. *Agren MS, Jorgensen LN, Delaissé J.* Matrix metalloproteinases and colon anastomosis repair: a new indication for pharmacological inhibition. Mini Rev Med Chem 2004; 4(7): 769−78.
20. *Bedirli A, Kerem M, Karahacioglu E, Ofluoglu E, Yilmaz UT, Pasaoglu H,* et al. Effects of two conventional preoperative radiation schedules on anastomotic healing in the rat colon. Eur Surg Res 2007; 39(3): 141−7.
21. *de Hingh IH, Lomme RM, van Goor H, Bleichrodt RP, Hendriks T.* Changes in gelatinase activity in the gastrointestinal tract after anastomotic construction in the ileum or colon. Dis Colon Rectum 2005; 48(11): 2133−41.
22. *Ågren MS, Andersen TL, Mirastschijski U, Syk IM, Schiødt CB, Surve V*, et al. Action of matrix metalloproteinases at restricted sites in colon anastomosis repair: an immunohistochemical and biochemical study. Surgery 2006; 140(1): 72−82.
23. *Pasternak B, Matthiessen P, Jansson K, Andersson M, Aspenberg P.* Elevated intraperitoneal matrix metalloproteinase - 8 and - 9 in patients who develop anastomotic leakage after rectal cancer surgery: a pilot study. Colorectal Dis 2010; 12(7 Online): e93−8.
24. *Baker EA, Leaper D.* Profiles of matrix metalloproteinases and their tissue inhibitors in intraperitoneal drainage fluid: relationship to wound healing. Wound Rep Reg 2003; 11(4): 268−74.
25. *Cong Z, Fu C, Wang H, Liu L, Zhang W, Wang H.* Influencing factors of symptomatic anastomotic leakage after anterior resection of the rectum for cancer. World J Surg 2009; 33(6): 1292−7.
26. *Kingham TP, Pachter PL.* Colonic anastomotic leak. J Am Coll Surg 2009; 208(2): 268−78.
27. *Asteria CR, Gagliardi G, Pucciarelli S, Romano G, Infantino A, La Torre F*, et al. Anastomotic leaks after anterior resection for mid and low rectal cancer: survey of the Italian Society of Colorectal Surgery. Tech Coloproctol 2008; 12(2): 103−10.
28. *Daams F, Luyer M, Lange JF.* Colorectal anastomotic leakage: aspects of prevention, detection and treatment. World J Gastroenterol 2013; 19(15): 2293−7.
29. *Schwegler I, von Holzen A, Gutzwiller JP, Schlumpf R, Mühlebach S, Stanga Z.* Nutritional risk is a clinical predictor of postoperative mortality and morbidity in surgery for colorectal cancer. Br J Surg 2010; 97(1): 92−7.
30. *Suding P, Jensen E, Abramson MA, Itani K, Wilson SE.* Definitive risk factors for anastomotic leaks in elective open colorectal resection. Arch Surg 2008; 143(9): 907−12.
31. *MacKay GJ, Molloy RG, O'Dwyer PJ.* C-reactive protein as a predictor of postoperative infective complications following elective colorectal resection. Colorectal Dis 2011; 13(5): 583−7.
32. *Ortega-Deballon P, Radais F, Facy O, d'Athis P, Masson D, Charles PE,* et al. C-reactive protein is an early predictor of septic complications after elective colorectal surgery. World J Surg 2010; 34(4): 808−14.
33. *Vigushin DM, Pepys MB, Hawkins PN.* Metabolic and scintigraphic studies of radioiodinated human C-reactive protein in health and disease. J Clin Invest 1993; 91(4): 1351−7.
34. *Kørner H, Nielsen HJ, Søreide JA, Nedrebø BS, Søreide K, Knapp JC.* Diagnostic accuracy of C-reactive protein for intraabdominal infections after colorectal resections. J Gastrointest Surg 2009; 13(9): 1599−606.
35. *Woeste G, Müller C, Bechstein WO, Wullstein C.* Increased serum levels of C-reactive protein precede anastomotic leakage in colorectal surgery. World J Surg 2010; 34(1): 140−6.
36. *Scepanovic MS, Kovacevic B, Cijan V, Antic A, Petrovic Z, Asceric R,* et al. C-reactive protein as an early predictor for anastomotic leakage in elective abdominal surgery. Tech Coloproctol 2013; 17(5): 541−7.
37. *Søreide K.* Receiver-operating characteristic curve analysis in diagnostic, prognostic and predictive biomarker research. J Clin Pathol 2009; 62(1): 1−5.
38. *Warschkow R, Tarantino I, Torzewski M, Näf F, Lange J, Steffen T.* Diagnostic accuracy of C-reactive protein and white blood cell counts in the early detection of inflammatory complications after open resection of colorectal cancer: a retrospective study of 1,187 patients. Int J Colorectal Dis 2011; 26(11): 1405−13.
39. *Savage FJ, Lacombe DL, Hembry RM, Boulos PB.* Effect of colonic obstruction on the distribution of matrix metalloproteinases during anastomotic healing. Br J Surg 1998; 85(1): 72−5.
40. *de Hingh IH, de Man BM, Lomme RM , van Goor H, Hendriks T.* Colonic anastomotic strength and matrix metalloproteinase activity in an experimental model of bacterial peritonitis. Br J Surg 2003; 90(8): 981− 8.
41. *Stumpf M, Klinge U, Wilms A, Zabrocki R, Rosch R, Junge K,* et al. Changes of the extracellular matrix as a risk factor for anastomotic leakage after large bowel surgery. Surgery 2005; 137(2): 229−34.
42. *Komen N, de Bruin RW, Kleinrensink GJ, Jeekel J, Lange JF.* Anastomotic leakage, the search for a reliable biomarker. A review of the literature. Colorectal Dis 2008; 10(2): 109−17.
43. *Kim KW, Romero R, Park HS, Park CW, Shim SS, Jun JK*, et al. A rapid matrix metalloproteinase-8 bedside test for the detection of intraamniotic inflammation in women with preterm premature rupture of membranes. Am J Obstet Gynecol 2007; 197(3): 292.e1–5.

Received on July 23, 2014.
Revised on August 11, 2014.
Accepted on August 11, 2014.
Online First on March, 2015.

ORIGINAL ARTICLE

UDC: 615.461:616.314-77]:615.9
DOI: 10.2298/VSP140304070K

Artificial saliva effect on toxic substances release from acrylic resins

Uticaj veštačke pljuvačke na oslobađanje toksičnih supstanci iz akrilata za bazu zubne proteze

Milena Kostić*, Nebojša Krunić*, Stevo Najman†, Ljubiša Nikolić‡, Vesna Nikolić‡, Jelena Rajković§, Milica Petrović*, Marko Igić*, Aleksandra Ignjatović‖

***Department of Prosthetic Dentistry, Clinic of Dentistry, †Institute of Biology and Human Genetics, ‖Department of Medical Statistics, Faculty of Medicine, University of Niš, Niš, Serbia; ‡Faculty of Technology, University of Niš, Leskovac, Serbia; §Faculty of Sciences and Mathematics, University of Niš, Niš, Serbia**

Abstract

Background/Aim. Acrylic-based resins are intensively used in dentistry practice as restorative or denture-base materials. The purpose of this study was to analyze the surface structure of denture base resins and the amount of released potentially toxic substances (PTS) immediately upon polymerization and incubation in different types of artificial saliva. **Methods.** Storage of acrylic samples in two models of artificial saliva were performed in a water bath at the temperature of 37 ± 1°C. Analysis of the surface structure of samples was carried out using scanning electronic microscopy analysis immediately after polymerization and after the 30-day incubation. The amounts of PTS *per* day, week and month extracts were measured using high-pressure liquid chromatography. **Results.** Surface design and amount of PTS in acrylic materials were different and depended on the types and duration of polymerization. The surfaces of tested acrylates became flatter after immersing in solutions of artificial saliva. The degree of acrylic materials release was not dependent on the applied model of artificial saliva. **Conclusion.** In order to improve biological features of acrylic resin materials, it was recommended that dentures lined with soft or hard cold-polymerized acrylates should be kept at least 1 to 7 days in water before being given to a patient. So, as to reach high degree of biocompatibility preparation of prosthetic restorations from heat-polymerized acrylate was unnecessary.

Key words:
acrylic resins; saliva, artificial; hazardous substances.

Apstrakt

Uvod/Cilj. Akrilati se u stomatologiji često koriste kao restaurativni materijali ili materijali za izradu baza zubnih proteza. Cilj istraživanja bio je analiza količine oslobođenih potencijalno toksičnih supstanci (PTS) iz akrilatnih materijala neposredno nakon njihove polimerizacije i inkubacije u različitim tipovima veštačke pljuvačke. **Metode.** Uzorci akrilatnih materijala potapani su u dva modela veštačke pljuvačke u vodenom kupatilu temperature 37 ± 1°C. Analiza površinske strukture uzoraka vršena je skenirajućom elektronskom mikroskopijom odmah nakon polimerizacije i posle tridesetodnevne inkubacije. Količina PTS u jednodnevnim, jednonedeljnim i jednomesečnim ekstraktima merena je tečnom hromatografijom pod visokim pritiskom. **Rezultati.** Površinski dizajn i količina PTS bili su različiti kod različitih akrilatnih materijala i zavisili su od vrste i trajanja polimerizacionog postupka. Nakon potapanja u rastvore veštačke pljuvačke površine testiranih akrilata postale su ravnije. Oslobađanje PTS nije zavisilo od primenjenog modela veštačke pljuvačke. **Zaključak.** U cilju poboljšanja bioloških svojstava akrilatnih materijala, preporučuje se da zubne proteze podložene mekim ili čvrstim hladno polimerizovanim akrilatima budu potopljene u vodi 1 do 7 dana pre predaje pacijentu. S obzirom na visok nivo biokompatibilnosti, naknadna obrada proteza od toplo polimerizovanog akrilata nije potrebna.

Ključne reči:
akrilati; pljuvačka, veštačka; toksične supstance.

Introduction

Acrylic-based resins are intensively used in dentistry practice as restorative or denture-base materials [1]. These acrylates are made by polymerization of acrylate related monomers and can be classified depending on the factor that initiates the polymerization reaction (as cold, heat or light polymerization) [2]. These materials are considered as biologi-

Correspondence to: Milena Kostić, Department of Prosthetic Dentistry, Clinic of Dentistry, Blvd. Dr Zoran Djindjic 52, 18 000 Niš, Serbia. Phone: +381 184 226 216. E-mail: kosticmilena76@gmail.com

cally acceptable, which verifies their wide-spread use in medicine and dentistry. However, a great deal of the available reports referring to adverse effect of particular components of acrylic prosthetic materials on human organism both at local (immunological and inflammatory reactions of oral tissues) and systemic level (changes on respiratory and gastrointestinal tract) [3, 4]. Particular components of acrylic materials could diffuse in saliva from prosthetic restorations, and cause the damage of oral tissues [5, 6]. The potential cytotoxicity is influenced by residual monomers as well as other additives such as initiators and stabilizers, mixing liquids, bonded materials, benzoyl peroxide, tertiary amine etc. [7, 8]. The conversion of monomer into polymer is not complete during the polymerization process, and varying amounts of potentially toxic substances (PTS) remain in the polymerized resin. The values of residual monomers remaining in resins is determined by standards [9], considered only as the amount of monomers in the resin but not taking into account their elution characteristics. Many reports of allergic reactions which were associated with acrylic based resins have been attributed to monomer and additives as benzoyl peroxide [10, 11].

Undesirable reaction of oral tissue may occur as the result of toxicity of applied material as well as superficial accumulation of infectious content [12]. In order to be biocompatible, dental restorative material should have such surface design to react with tissue and surrounding agents at the least possible degree [13]. Rough surface of various acrylic materials represents a predilection site for accumulation of plaque, pigments and residual oral tissue [14, 15]. Analysis of the possibility of preparation of acrylic material surface in order to reduce fungal adhesion and microbial plaque in general represents a very significant contribution to the improvement of their biocompatibility [16, 17].

The purpose of the study was to analyze the amount of released PTS and the surface structure of acrylic denture base resins immediately upon polymerization and incubation in two different types of artificial saliva.

Methods

Examined material

To prepare samples two hard and three soft acrylic denture base resins used in prosthetic dentistry for construction and relining of removable dentures were used. The manufacturers and types of cold- and heat-polymerized acrylates used in the study were summarized in Table 1.

The examined material was polymerized according to the manufacturer's instructions. To analyze the influence of artificial saliva on the surface design samples of each acrylic material were prepared in parallelepiped shape, 1 × 2 × 3 mm. In order to determine the dynamics of release of PTS, samples of each test material were made as parallelepiped 10 × 10 × 1 mm (*per* 5 samples in each of the test groups). Preparation of cold-polymerized acrylates was performed at room temperature (18–20°C) for 10–15 minutes without pressure using a condensation silicone mould. Heat polymerization was performed in a water bath (GFS, Germany) within specialized metal flasks for 45 min in boiling water. They were kept in a sterile Petri dish at room temperature, without standard procedure polishing.

Model 1 of artificial saliva was designed according to Preetha and Banarjee [18] (Table 2). Model 2 of artificial saliva represented a modification of model 1 in which 0.20 g α amylase/L deionized water was added.

Table 1

The manufacturers and the used acrylic types of materials

Tested material	Manufacturer	Acrylic type	Content	
			powder	liquid
Bosworth Trusoft	HG Bosworth Company USA	Soft cold polymerized acrylate	Poly (ethyl methacrylate)	Ethyl alcohol, butyl benzyl phthalate
Lang Flexacryl	Lang Dental MFG.Co. USA	Soft cold polymerized acrylate	Poly (ethyl methacrylate)	N-buthyl methacrylate
Lang Immediate	Lang Dental MFG.Co. USA	Soft cold polymerized acrylate	Poly (ethyl methacrylate)	Methyl methacrylate
Triplex Cold	Ivoclar Vivadent, Lichtenstein	Hard cold polymerized acrylate	Poly(methyl methacrylate)	Methyl methacrylate, Ethylene glycol dimethacrylate
Triplex Hot	Ivoclar Vivadent, Lichtenstein	Heat polymerized acrylate	Poly(methyl methacrylate)	Methyl methacrylate, Ethylene glycol dimethacrylate

Table 2

Components of the Model 1 artificial saliva [18]

Components	G components / l deionised water
Xantan gum	0.18
Potassium chloride	1.20
Sodium chloride	0.85
Magnesium chloride	0.05
Calcium chloride	0.13
Di-potassium hydrogen orthophosphate	0.13
Methyl p-hydroxybenzoate	0.35

Incubation of acrylic samples in artificial saliva was performed in a water bath in closed plastic tubes at human body temperature (t = 37 ± 1°C). The ratio of material and artificial saliva was 0.1 g of tested material/1 mL of extraction solution, according to ISO 10993-5: 1992 standard [19].

Scanning electronic microscopy analysis (SEM)

To analyze the influence of artificial saliva on the sample SEM was used. Analysis was used for comparison of surface structure of acrylic materials samples immediately after polymerization cycle (marked as control samples) and after thirty days of immersing in artificial saliva (models 1 and 2), whereby all changes relating to surface appearance, homogeneity and adherence were recorded. The samples were dried and coated with gold layer in ion spray by spattering and analyzed under microscope JSM-5300, JOEL, Japan.

Determination of the amount of PTS

Determination of the presence and amount of PTS was performed in solutions of two different models of artificial saliva after removal of acrylic samples. In order to establish the dynamics of PTS release from the examined samples, extraction periods of one, seven and thirty days were adopted. Quantity of released materials was analyzed by using high-pressure liquid chromatography (HPLC), Agilent 1100 Series (USA), with DAD 1200 detector and analytical column SUPELCO Discovery HS C18 250 × 4.6 mm, 5 μm, Sigma-Aldrich, USA. Methanol [M = 32.04 g/moL, Chromasolv HPLC chromatography grade (purity 99.9%) Sigma-Aldrich GmBH, Steinheim, Germany] was used as an eluent. The mobile phase flow was 1 cm^3/min, and sample injection volume was 20 μL. Since all tested compounds have maximal absorbance around 205 nm, this wave length was selected for calibration curve construction and further sample testing. Determined PTS and reagents used for calibration curves were presented in Table 3.

Calibration curves were made from a solution series of each examined substance in methanol. The initial concentration of tested compound was 1 mg/cm^3, from which, afterwards, a solution series of lower concentrations diluted by methanol were made. From the obtained chromatograms retention time of each compound (R_t) and peak surface area (A) were read. Table 4 shows the R_t values, λ_{max}, concentration range (C) at which peak surface dependence is linear and linear correlation coefficient (R).

Two-way ANOVA for repeated measures was used for statistical analysis of differences in the amounts of PTS in relation to the type of materials and artificial saliva. Data were analyzed in SPSS software, version 16.0.

Results

Figure 1 shows the results of SEM analysis of all the analyzed acrylic materials immediately after the polymerization cycle and 30 days after incubation in two different models of artificial saliva.

Surfaces of samples of soft cold polymerized acrylates analyzed immediately after polymerization showed a granular structure and unequal granular size (10–100 μm) that

Table 3

Potentially toxic substances (PTS) pressure determined in acrylic samples and reagents used for high-pressure liquid chromatography (HPLC) calibration curves

PTS	Used agents	Manufacturer
MMA	$CH_2 = C(CH_3)COOCH_3$, M = 100.12 g/moL, 98,5%	Aldrich, Milwaukee, Wisconsin, USA.
BuMA	$CH_2 = C(CH_3)COOC_4H_9$, M = 142.20 g/moL, 99%	Sigma-Aldrich GmbH, Steinheim, Germany.
EGDM	$CH_2 = C(CH_3)COO(CH_2)_2OCOC(CH_3) = CH_2$, M = 198.22 g/moL, 98%	Fluka Chemie GmbH, Steinheim, Germany.
EMA	$CH_2 = C(CH_3)COOC_2H_5$, M = 114.14 g/moL, 99%	Aldrich, Milwaukee, Wisconsin, USA.
BP	$(C6H5CO)_2O_2$, M = 242.23 g/moL, 99%	Fluka Chemie GmbH, Steinheim, Germany.
dBuFt	$C6H4\text{-}1,2\text{-}[CO_2(CH_2)_3CH_3]_2$, M = 278.34 g/moL, 99%	Aldrich, Milwaukee, Wisconsin, USA.

MMA – methyl methacrylate (monomer); BuMA – buthyl methacrylate (monomer); EGDM – ethylene glycol dimethacrylate (comonomer-cross-linker); EMA – ethyl methacrylate (monomer); BP – benzoyl peroxide (initiator); dBuFt – dibuthyl phthalate (plasticiser).

Table 4

Values of R_t, λ_{max}, concentration range for which linear dependence of peak surface exists and concentration and R for compounds determined by high pressure liquid chromotogrophy (HPLC) method

PTS	Rt (min)	λmax (nm)	Linear correlation for compounds C, (mg/cm^3)	R
MMA	2.637	207	0 to 0.14	0.988
BuMA	2.946	208	0 to 0.10	0.999
EGDM	3.049	208	0 to 0.10	0.995
EMA	2.289	207	0 to 0.14	0.991
BP	3.332	204 and 236	0 to 0.12	0.998
dBuFt	3.514	205 and 225	0 to 0.10	0.996

PTS – potential toxic substances; Rt – retention time of each compound; R – linear correlation coefficient; MMA – methyl methacrylate (monomer); BuMA – buthyl methacrylate (monomer); EGDM – ethylene glycol dimethacrylate (comonomer-cross-linker); EMA – ethyl methacrylate (monomer); BP – benzoyl peroxide (initiator); dBuFt – dibuthyl phthalate (plasticiser).

were noticeable on the material surface (Figures 1a, 1b, 1c and 1d). In contrast to all the other material, heat polymerized acrylic material Triplex Hot, immediately after polymerization, had no granular structure at all (Figure 1e).

During the immersion period in solution of both artificial saliva models, soft cold acrylic materials accumulate salivary components on their surface. After the 30-day immersion in artificial saliva without α amylase, the surface of soft cold-polymerized acrylates became flatter and the appearance of the samples surface remained almost the same after immersion in artificial saliva with enzyme addition (Figures 2a, b, c and d). After immersion of heat polymerized acrylic material in both models of artificial saliva, the surface of this sample was completely flat. The most homogenous surface structure was noticed at heat-polymerized acrylates as compared to all the tested materials (Figure 2e).

The results show that the amount of PTS, regardless of the type of acrylic materials, is mostly released on the first day and continues to decrease during the observation period (Figure 1). However, data clearly suggest that the amount of released PTS is significantly higher immediately after polymerization, compared to the day 7 and 30 after polymerization

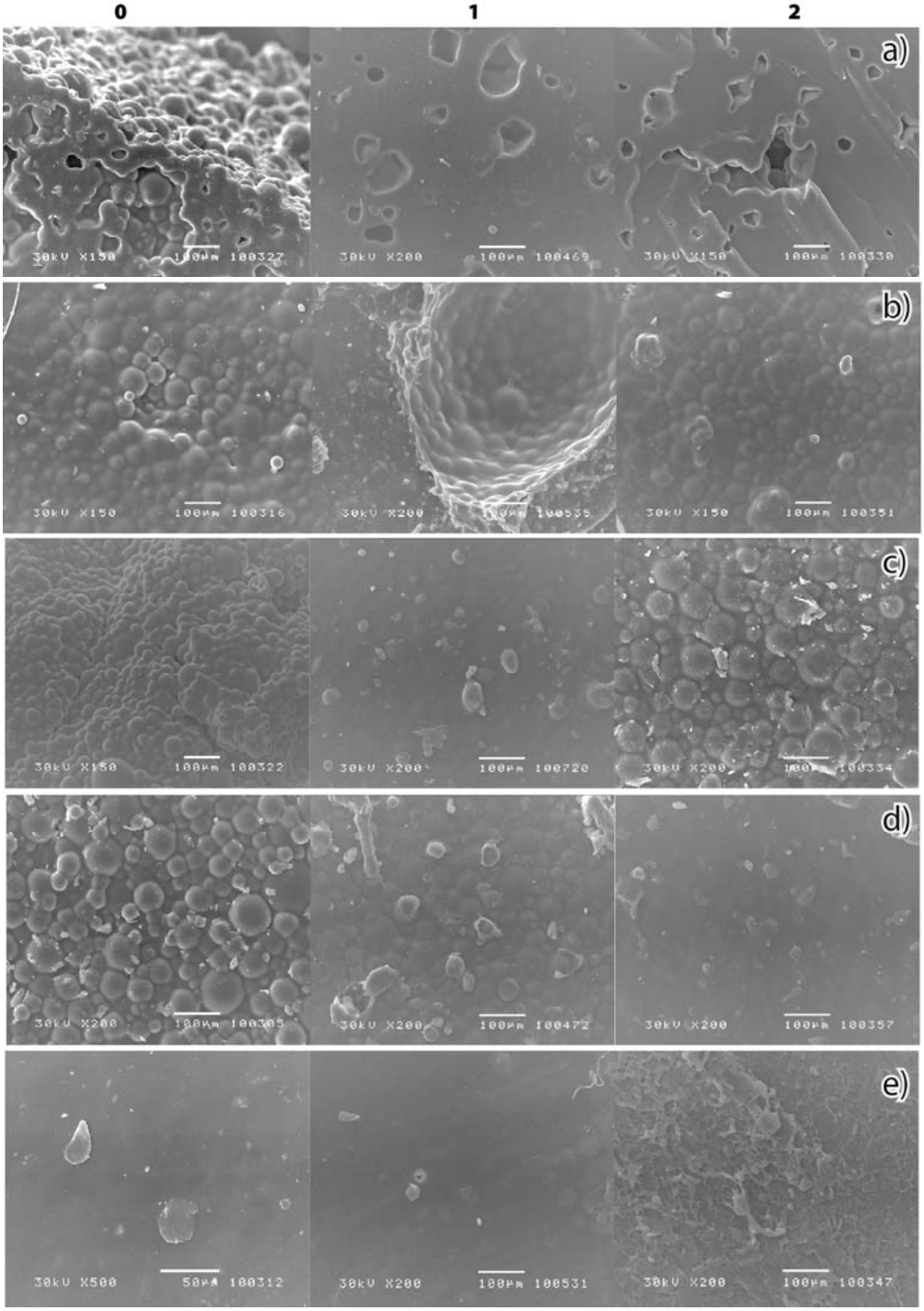

Fig. 1 – Scanning electronic microscopy (SEM) analysis of acrylic materials samples immediately after polymerization cycle (0) and after a thirty-day immersion in two different models of artificial saliva: model 1 (1) and model 2 (2) for different acrylic resins: a) Bosworth Trusoft; b) Lang Flexacryl; c) Lang Immediate; d) Triplex Cold, and e) Triplex Hot.

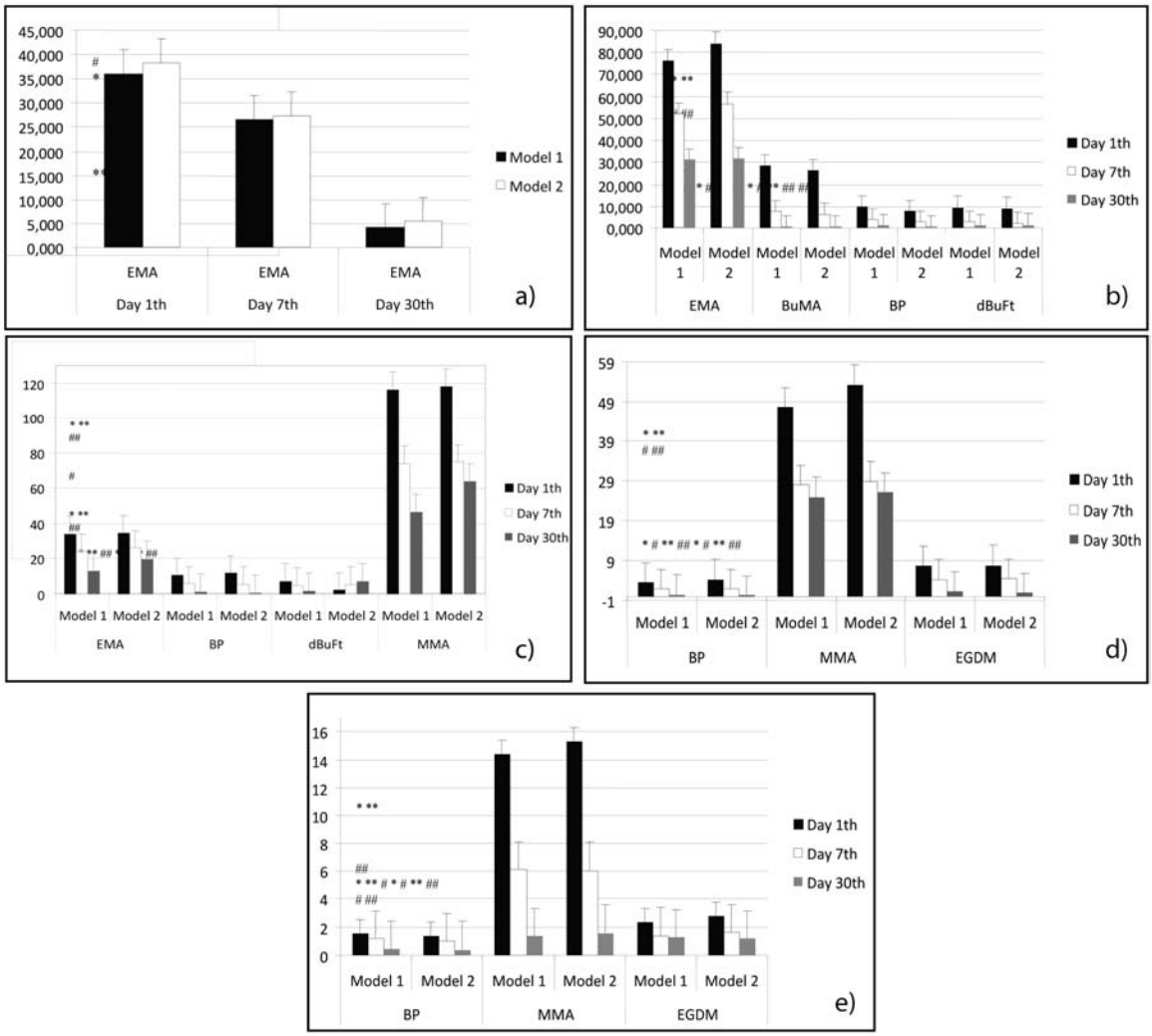

Fig. 2 – Concentrations (mean ± SD, μg/cm^3) of potentially toxic substances given in Table 3 from different acrylic resins: a) Bosworth Trusoft; b) Lang Flexacryl; c) Lang Immediate; d) Triplex Cold; e) Triplex hot at time periods of 1, 7 and 30 days after immersion in two different models of artificial saliva.

***p* < 0.001 – means significant differences detected between the day 1 and the day 7 after immersion in model 1 of artificial saliva without α amylase; #*p* < 0.001 – means significant differences detected between the day 1 and the day 30 after immersion in model 1 of artificial saliva without α amylase; ***p* < 0.001 – means significant differences detected between the day 1 and the day 7 after immersion in model 2 artificial saliva with α amylase; ##*p* < 0.001 – means significant differences detected between the day 1 and the day 30 after immersion in model 2 artificial saliva with α amylase.**

($p < 0.001$). Moreover, when the release of PTS in the model of artificial saliva with the addition of α amylase is tested, it is noticed that there is a tendency of PTS to increase but without making statistically significant differences compared to the model of saliva without this enzyme.

Discussion

It has been assumed that the difference in the amount of PTS and adherence degree depend on the type of material and polymerization conditions, as well as that biocompatibility of acrylic dentures may be increased by adequate postpolymerization treatment [20, 21].

Analysis of the possibility of preparation of acrylic material surface in order to reduce fungal adhesion and microbial plaque in general represents a very significant contribution to the improvement of their biocompatibility. Acrylic restorations in the mouth are coated with salivary pellicle, the layer that is formed by an interaction of material and ingredients of saliva. Precipitation of mucin and proteins of saliva plays the most pivotal role in its formation [16, 17]. Salivary pellicle is removed by hygiene procedures, as well as mechanical cleaning of the surfaces, but in contact with saliva (in the mouth), pellicle is produced again at removable denture. The presence of saliva and salivary pellicle formation in a clinical setting may influence PTS release from acrylic materials [22]. Due to the fact that the quality and composition of natural saliva is different in each individual, its chemical composition is impossible to be reproduced originally. Advantages of artificial saliva use under *in vitro* conditions include standardization of experiment conditions and prevention of sample contamination.

Adverse effect of residual monomer has been well established in numerous studies [23, 24]. It was experimentally established that cold-polymerized acrylates, due to their incom-

plete polymerization, had higher amount of residual monomers, and subsequently, higher release in the oral cavity [25]. Higher level of heat-polymerized acrylates' biocompatibility could be explained by their more complete polymerization and more compact internal structure after polymerization cycle. In fact, heat-polymerized acrylates are prepared at the temperature of boiling water that is close to the point of acrylic glass transition temperature, so, the mobility and conversion of monomer units in polymer structure are significantly higher as confirmed by the previous researches [26, 27]. The obtained results are in accordance with those of Baker et al. [28] who examined the release of methyl methacrylate from heat and cold-polymerized acrylates in the patient's oral cavity.

Two models of artificial saliva were prepared in order to evaluate the influence of artificial saliva composition on released of PTS from denture materials and surface design. The first model was without and the other one was with α amylase, which is one of the components of human saliva for digestion of food in mouth. The utilized models of artificial saliva showed values of viscosity and surface tension similar to those of natural saliva [29]. However, none of the used models had active phospholipids and mucin as the most active surface proteins of natural saliva. Adding of α amylase to model of artificial saliva could have compromised the obtained results due to more intensive coating of materials with salivary pellicle in relation to conditions existing in the oral cavity [29]. There was no significant difference in the amount of toxic substances released from all the examined materials over the time in relation to the type of saliva, which indicates minimal effect of α amylase on reduction of acrylic adherence.

Conclusion

The surfaces of the tested acrylates became flat after immersing in both models of artificial saliva. This research proves that the amount of potentially toxic substances from the samples of acrylic material used for making dentures grows over the time and does not depend on the type of used saliva. Slightest changes in the structure show the sample of heat-polymerized acrylates. In order to improve biological features of acrylic resin materials, the authors suggest that dentures lined with soft or hard cold-polymerized acrylates should be kept at least 1 to 7 days in water before being given to a patient.

Acknowledgement

This study was supported by the Project N0 41017, funded by the Ministry for Education, Science and Technological Development of the Republic of Serbia.

REFERENCES

1. *Ogle RE, Davis EL.* Clinical wear study of three commercially available artificial tooth materials: thirty-six month results. J Prosthet Dent 1998; 79(2): 145−51.
2. *Bettencourt AF, Neves CB, Almeida MS, Pinheiro LM, Oliveira SA, Lopes LP*, et al. Biodegradation of acrylic based resins: A review. Dent Mater 2010; 26(5): e171−80.
3. Ali A, Bates JF, Reynolds AJ, Walker DM. The burning mouth sensation related to the wearing of acrylic dentures: an investigation. Br Dent J 1986; 161(12): 444−7.
4. *van Joost T, van Ulsen J, van Loon LA.* Contact allergy to denture materials in burning mouth syndrome. Contact Dermatitis 1998; 18(2): 97−99.
5. *Moharram MA, Abdel NK, Abdel HN, Abou-Table ZA, Badr NA.* Effect of cross-linking agents on the molecular properties of denture base resins. J Mater Sci 1992; 27(22): 6041−6.
6. *Hongo T, Sato K, A Sato.* Amounts of residual monomer leached from clinically used acrylic resin denture base. J Dent Mater 1994; 13(23): 252−3. (Japanese)
7. *Jorge JH, Giampaolo ET, Machado AL, Vergani CE.* Cytotoxicity of denture base acrylic resins: a literature review. J Prosthet Dent 2003; 90(2): 190−3.
8. *Kostić M, Najman S, Kocić JS, Krunić N, Ajduković Z, Petrović D*, et al. Effect of denture base resin extracts on HeLa cells growth in vitro. Hem Ind 2008; 62(3): 217−22.
9. International Standards Organization. ISO 20795-1: 2008. Dentistry Base Polymers Part 1: Denture Base Polymers. Geneva: ISO; 2008.
10. *Boeckler A, Morton D, Poser S, Dette K.* Release of dibenzoyl peroxide from polymethyl methacrylate denture base resins: An in vitro evaluation. Dent Mater 2008; 24(12): 1602−7.
11. *Babich H, Zuckerbraun HL, Wurzburger BJ, Rubin YL, Borenfreund E, Blau L.* Benzoyl peroxide cytotoxicity evaluated in vitro with the human keratinocyte cell line, RHEK-1. Toxicology 1996; 106(1−3): 187−96.
12. *Schmalz G.* Use of cell cultures for toxicity testing of dental materials: Advantages and limitations. J Dent 1994; 22(Suppl 2): S6−11.
13. *Hanks CT, Wataha JC, Sun Z.* In vitro models of biocompatibility: a review. Dent Mater 1996; 12(3): 186−93.
14. *Zissis AJ, Polyzois GL, Yannikakis SA, Harrison A.* Roughness of denture materials: a comparative study. Int J Prosthodont 2000; 13(2): 136−40.
15. *Radford DR, Sweet SP, Challacombe SJ, Walter JD.* Adherence of Candida albicans to denture-base materials with different surface finishes. J Dent 1998; 26(7): 577−83.
16. *Satyanarayana D, Chatterji PR.* Studies on the enzymatic and fungal degradation of cross-linked gelatin and its graft copolymers. J Polym Environ 1995; 3(3): 177−86.
17. *Moztarzadeh F, Keyanpour-Rad M, Shabani V.* Synthesis of a Photocurable Dental Ionomer Cement Based on the Reaction of Acryloyl Chloride Coupling Compound with Acrylic/Itaconic Acids Copolymer. Iran Polym J 2003; 12(3): 211−6.
18. *Preetha A, Banarjee R.* Comparison of artificial saliva substitutes. Trends Biomater Artif Organs 2005; 18(2): 178−86.
19. International Organisation for Standardization. International Standard ISO 10993-5: Biological Evaluation of Medical Devices - Part 5: Tests for in vitro cytotoxicity, 3rd. Geneva: ISO; 2009.
20. *Pavarina AC, Vergani CE, Machado AL, Giampaolo ET, Teraoka MT.* The effect of disinfectant solutions on the hardness of acrylic resin denture teeth. J Oral Rehabil 2003; 30(7): 749−52.
21. *Mikai M, Koike M, Fujii H.* Quantitative analysis of allergenic ingredients in eluate extracted from used denture base resin. J Oral Rehabil 2006; 33(3): 216−20.
22. *Luckachan GE, Pillai CS.* Biodegradable Polymers- A Review on Recent Trends and Emerging Perspectives. J Polym Environ 2011; 19: 637−76.

23. *Koda T, Tsuchiya H, Yamauchi M, Hoshino Y, Takagi N, Kawano J.* High-performance liquid chromatographic estimation of eluates from denture base polymers. J Dent 1989; 17(2): 84−9.
24. *Kalipçilar B, Karaağaçlioğlu L, Hasanreisoğlu U.* Evaluation of the level of residual monomer in acrylic denture base materials having different polymerization properties. J Oral Rehabil 1991; 18(5): 399−401.
25. *Cimpan MR, Matre R, Cressey LI, Tysnes B, Lie SA, Gjertsen BT*, et al. The effect of heat- and auto-polymerized denture base polymers on clonogenicity, apoptosis, and necrosis in fibroblasts: denture base polymers induce apoptosis and necrosis. Acta Odontol Scand 2000; 58(5): 217−28.
26. *Jorge JH, Giampaolo ET, Vergani CE, Machado AL, Pavarina AC, Carlos IZ.* Biocompatibility of denture base acrylic resins evaluated in culture of L929 cells. Effect of polymerisation cycle and post-polymerisation treatments. Gerodontology 2007; 24(1): 52−7.
27. *Bartolini JA, Murchison DF, Wofford DT, Sarkar NK.* Degree of conversion in denture base materials for varied polymerization techniques. J Oral Rehabil 2000; 27: 488−93.
28. *Baker S, Brooks SC, Walker DM.* The release of residual monomeric methyl methacrylate from acrylic appliances in the human mouth: An assay for monomer in saliva. J Dent Res 1988; 67(10): 1295−9.
29. *Lindh L.* On the adsorption behaviour of saliva and purified salivary proteins at solid/liquid interfaces. Swed Dent J Suppl 2002; 152: 1−57.

Received on March 4, 2014.
Revised on July 10, 2014.
Accepted on September 8, 2014.
Online First August, 2015.

ORIGINAL ARTICLE

UDC: 616.65
DOI: 10.2298/VSP131022069F

The expression and localization of estrogen receptor beta in hyperplastic and neoplastic prostate lesions

Ekspresija i lokalizacija estrogenog receptora beta kod hiperplastičnih i neoplastičnih lezija prostate

Aleksandra Fejsa Levakov*†, Mihaela Mocko Kaćanski*†, Nada Vučković*‡, Mirjana Živojinov*‡, Jelena Amidžić*†, Jelena Ilić Sabo*†

***Pathology and Histology Center, Clinical Center of Vojvodina, Novi Sad, Serbia;**
†Department for Histology and Embryology, ‡Department for Pathology, Faculty of Medicine, University of Novi Sad, Novi Sad, Serbia

Abstract

Background/Aim. Benign acini in benign prostatic hyperplasia (BPH) are lined with pseudostratified cylindrical epithelium with a continuous basal cell layer. Adenocarcinoma of the prostate is the most common cancer in men. High gradus-prostatic intraepithelial neoplasia (HGPIN) lesions precede invasive cancer. Prostate adenocarcinoma (PCa) implies a complete absence of basal cells and stromal invasion by malignant acini. Estrogen receptor (ER) is located in nuclei of acinar basal and secretory cells and partially in stromal cells. The aim of this research was to demonstrate and localize ER in BPH and in PCa of different Gleason scores. Considering literature data for ER-betą expression in different morphologic prostate lesions, it is assumed that there is expression of ER-beta in most moderately differentiated PCa, and that the observed receptor expression is lost with increasing of the Gleason score. **Methods.** Four groups of patients were formed: the control with BPH and three experimental groups with PCa of different grades and scores, according to the Gleason grading system. The patients were male of various ages suspected of PCa, based on clinical and laboratory parameters. The study was conducted in a period 2010–2012. None of the patients received prior hormonal therapy. Sextant byopsies with BPH and PCa were treated for ER-beta (Novocastra). Localization and intensity of ER-betą expression is reported through the score: 0 = zero; 1 = < 1%; 2 = 1–10%; 3 = 11–33%; 4 = 34–66%; 5 – > 66%. Positive fibroblasts and endothelial cells are used for comparison. **Results.** ER-beta expression in acinar epithelial cells was the weakest in well-differentiated adenocarcinoma. A decline of ER-beta expression was noticed in malignant lesions of the prostate *vs* benign ones. Less differentiated adenocarcinomas showed a decrease of ER-beta expression in basal and in the secretory cells. ER-betą expression in basal cells was stronger than in secretory ones in BPH and well-differentiated adenocarcinoma. **Conclusion.** ER-beta expression was most pronounced in BHP samples and declined in malignant prostatic lesions. This finding supports statement on antiproliferative role of ER-beta in prostatic tissue.

Key words:
prostatic neoplasms; adenocarcinoma; estrogen receptor beta.

Apstrakt

Uvod/Cilj. Benigni acinusi kod benigne hiperplazije prostate (BHP) obloženi su pseudostratifikovanim cilindričnim epitelom sa kontinuiranim slojem bazalnih ćelija. Adenokarcinom prostate najčešći je karcinom kod muškaraca. Intraepitelne prostatične neoplazme visokog gradusa (HGPIN) su lezije koje prethode nastanku invazivnog karcinoma (Pca) i podrazumevaju kompletno odsustvo bazalnih ćelija i invaziju strome malignim acinusima. Estrogeni receptor (ER) beta nalazi se u jedrima bazalnih i sekretornih ćelija acinusa i delimično u stromalnim ćelijama. Cilj ovog istraživanja bio je da se prikaže i lokalizuje ER beta u BHP, kao i u PCa sa različitim Gleason skorom. S obzirom na podatke iz literature o ekspresiji ER beta u različitim morfološkim lezijama prostate, pretpostavlja se da je ekspresija ER beta prisutna u većini srednje diferentovanih PCa, i da se ekspresija posmatranog receptora gubi sa povećanjem Gleason scora. **Metode.** Ispitivane su četiri grupe bolesnika: kontrolna grupa sa BHP i tri eksperimentalne grupe sa PCa različitih gradusa i skorova prema Gleason-ovom sistemu. Bolesnici su bili muškarci različite starosti sa sumnjom na PCa, na osnovu kliničkih i laboratorijskih parametara. Studija je sprovedena u periodu 2010–2012. Nijedan od bolesnika nije prethodno

Correspondence to: Aleksandra Fejsa Levakov, Pathology and Histology Center, Clinical Center of Vojvodina 21 000 Novi Sad, Serbia. E-mail: aleksandralevakov@sbb.rs

primio hormonsku terapiju. Sekstant biopsije sa nalazom BHP i PCa bojene su na ER beta (Novocastra). Lokalizacija i intenzitet ER betą ekspresije prikazani su kroz skor: 0 = nula; 1 = < 1%; 2 = 1–10%; 3 = 11–33%; 4 = 34–66%; 5 = > 66%. Pozitivni fibroblasti i endotelne ćelije korišćene su za poređenje. **Rezultati.** Ekspresija ER beta u epitelnim ćelijama acinusa bila je najslabija u dobro diferentovanim adenokarcinomima. Smanjena ekspresije ER beta primećena je kod malignih lezija prostate naspram benignih lezija. Loše diferentovani adenokarcinomi prikazali su smanjenje ekspresije ER beta u bazalnim i sekretornim ćelijama. Kod BHP i dobro diferentovanih adeniokarcinomima bila je veća ekspresija ER betą u bazalnim ćelijama nego u sekretornim. **Zaključak.** Ekspresija Er-beta receptora B najizraženija je u uzorcima tkiva prostate bolesnika sa BHP i smanjuje se kod adenokarcinoma prostate. Ovaj nalaz podupire stanovište o antiproliferativnoj ulozi ER-beta u tkivu prostate.

Ključne reči:
prostata, neoplazme; adenokarcinom; receptor, estrogenski, beta.

Introduction

Benign prostatic hyperplasia (BPH)

Histologically, BPH shows proliferation of epithelial cells of acini and ducts, proliferation of smooth muscle cells and stromal fibroblasts in varying proportions [1]. Hyperplastic acini are lined with pseudostratified cylindrical epithelium with characteristic papillary hyperplasia [1]. Benign glands are surrounded by a continuous layer of basal cells positive for 34 beta E12. In chronic prostatitis, this layer may be discontinuous, and basal cells are progressively lost in prostatic intraepithelial neoplasia (PIN), as dysplasia becomes higher. Periuretheral glandular tissue is responsible for the development of BPH [1] and the true prostate tissue is the origin of prostate adenocarcinoma (PCa). Occult adenocarcinoma is found in 10% of surgical specimens with preoperative diagnosis of BPH.

It is possible that BPH is associated with a disturbed balance of androgen and estrogen in blood [1]. Generally accepted theory of the pathogenesis of BPH is associated with the effect of 5 alfa-dihydrotestosterone (DHT), androgen that controls normal prostate growth and proliferative disorders such as hyperplasia and Pca [1, 2]. DHT is synthesized in stromal cells by the conversion of circulating testosterone in the presence of 5 alfa-reductase. Once synthesized, DHT acts as autocrine agent on stromal cells as a paracrine hormone on the glandular epithelium, leading to its proliferation. In patients with BPH, relationship of circulating testosterone and DHT may be abnormally low. Reduced catabolism of DHT results in imbalance between losing and multiplication of epithelial and stromal cells [1].

Prostate adenocarcinoma

The pathogenesis of PCa referred to genetic and environmental factors [3, 4]. The cause of PCa is still unknown, but endocrine effects are the center of researches. The chemical and physical trauma results in the damage of epithelial cells. Oxidative stress has the underlying causes: endogenous metabolites, inflammation, red meat and animal fat intake and circulating growth factors [1, 3–5]. Chronic inflammation caused by infectious agents of sexually transmitted diseases (STD) or environmental factors (nutrition) in 20% of all cases are the cause of PCa [3]. Most inflammatory lesions of the prostate are associated with focal atrophy of the epithelium [3, 4].

PIN represents the ducts lined with cytologically atypical luminal cells, and reduced in the number of the basal ones. High gradus-prostatic intraepithelial neoplasia (HGPIN) lesions precede invasive cancer [5, 6]. Histological definition of PCa is a complete absence of basal cells and local stromal invasion by malignant acini [4].

Estrogen receptors (ER): biological and tumorigenic role

In men, androgens are generally responsible for proliferation, whereas estrogens have a dual action, both directly and indirectly they affect the proliferation and differentiation of epithelial cells. Estrogens indirectly suppress the release of pituitary luteinizing hormone (LH), decrease testicular androgen synthesis, also decrease systemic androgens and induce apoptosis in prostate epithelium and atrophy [7–11]. At the same time, a local-direct effect of estrogen through ER-alpha in the prostate stroma, stimulates aberrant epithelial differentiation and proliferation of basal layer, developing squamous metaplasia [7, 8]. This proliferation is opposite to proliferation under the androgen influence and can progress to inflammation and cancer [7, 8, 10]. Because of the stromal localization of ER-alpha, the estrogen effect on the epithelium is mediated by paracrine mechanisms [10–16]. Because of the ER-alpha localization in the prostatic epithelium, direct effect of estrogen is possible on the epithelial cells [10, 11, 17].

ER-alpha is required for differentiation and proliferation of epithelial cells, whereas ER-beta has an antiproliferative role [7, 8, 10, 11]. The effect of estrogen through ER-alpha leads to hyperplasia, dysplasia and neoplasia. Antiproliferative activity of estrogen can be explained by activation of epithelial ER-beta over ER-alpha. The loss of the local estrogen effect results in the reduced activation of ER-beta and consequently the increased proliferation and developing glandular hyperplasia [13].

The action of reductase on the testosterone metabolism results in formation of androgens (DHT) and with aromatase results in formation of estrogens. Androgen metabolites such as 5 alpha-androstane-3 beta, 17 beta-diol (3beta adiol) can act as ligands for ER-beta, but less effective than estrogen (E2) [7, 10]. Aromatase is present in the stroma, and ER in the prostatic epithelium. It is assumed that the effect of estrogen through ER-beta involves stromal-epithelial signaling impulses. Androgen acts *via* stromal receptors in induction of epithelial differentiation and proliferation. Lowering androgen

level would reduce proliferation and induce apoptosis of epithelial cells [13].

The amount of 3beta-Adiol in the prostate is 100 times higher than the amount of E2 [7]. As the ER affinity for 3beta-Adiol is 10 times lesser than for E2, its concentration in the prostate makes 3beta-Adiol endogenous ligand for ER. 3beta-Adiol binds to ER-alpha and with even greater affinity for ER-beta, but does not bind to androgen receptors (AR) [12]. DHT is biosynthetic precursor of 3beta-Adiol with antiproliferative role. Thus, the ER-beta is physiological regulator of epithelial growth and differentiation in the prostate [9, 10, 13–15]. Specific effects of estrogen in the tissue depends on the amount of estrogen and ER.

Kuiper et al. [18] found that ER-beta shows the highest affinity for 17 beta-estradiol (E2) > diethylstilbestrol (DES) > estriol (E3) > estrone (E1) > 5alpha-Androstane-3beta, 17 beta-diol (3beta-Adiol) >> testosterone = progesterone = corticosterone. In the absence of other ligands, E2 binds to ER-beta in 100%.

Low levels of circulating estrogens are present throughout life. With againg, circulating estrogen rises due to increase in body fat, which is a peripheral source of estrogen. In addition, the decline of bioavailable testosterone leads to an increase of effector cell (E) target cell (T) ratio and disrupting the balance in favor of estrogen, which can cause reactive growth and consequent neoplastic transformation [7, 10, 16]. The rise of estrogen increases the sensitivity of the prostate to androgens, by increasing the number of AR.

The paradox is that estrogen alone or in combination with androgens induce BPH, dysplasia and PCa [16].

Functional antagonism of ER-beta is reflected in the direct repression of some ER alpha conditional effects, including reduction of fat cell and proliferation in the prostate. ER-beta acts as a major regulator of the estrogen effects, its coexpression with ER-alpha leads to the reduced transcription caused by ER-alpha [8, 15–17]. Although E2 acts on both receptors, ER-alpha stimulates transcription and cell proliferation, and ER-beta inhibits the activity of ER-alpha and suppresses epithelial proliferation and enables the differentiation of the prostatic epithelium [10, 16]. As proliferation and differentiation opposite one another, cellular homeostasis and the overall proliferative response is the result of dynamic balance of ER-alpha and ER-beta [2, 8].

Adverse effects mediated through ER-alpha include unplanned proliferation, inflammation and malignancy. The beneficial effects in prevention of hyperplasia, inflammation and carcinogenesis are played through ER-beta [8] (Figure 1).

ER-beta in prostate pathology

Marked expression of ER-beta is registered in basal cells of NP [2, 9, 10, 11] this subpopulation have different biological characteristics from secretory epithelial cells, especially in their ability to proliferate [9, 10, 13], synthesize steroids and have the crucial role in prostate carcinogenesis. Weaker expression is found in stromal cells [9, 19]. Some authors found no presence of ER-beta in secretory cells [9], but other did [13, 14, 16]. Secretory cells are differentiated cells, androgen-dependent, but without proliferative capacity [13]. Secretory cells that still show positivity for ER-beta or Ki-67 represent incompletely differentiated intermediate cells with retained ability to proliferate throughout life.

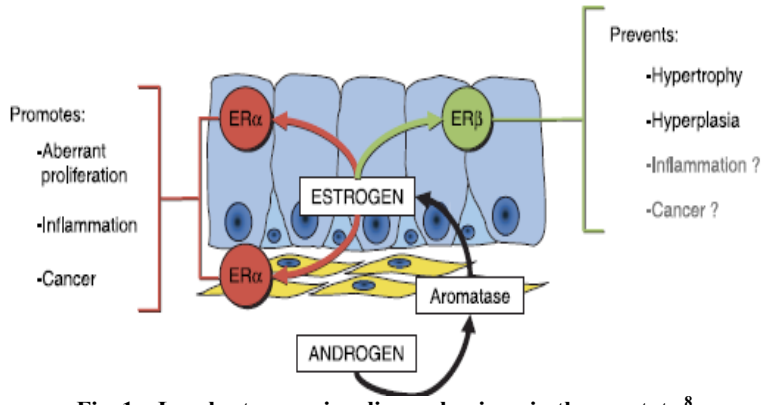

Fig. 1 – Local estrogen signalig mechanisms in the prostate [8].
Testosterone is metabolized to estrogen by aromatase and acts *via* estrogen receptor (ER) alpha or ER-beta. Adverse effects via ER-alphą in stroma and epithelia include aberrant proliferation, inflammation and cancer. In contrast, estrogen also exerts beneficial effects *via* ER-betą in epithelia in preventing hyperplasia and hypertrophy, being antiproliferative and anticarcinogenic.

The controversial results are in the expression of ER-beta in different morphologic lesions of the prostate. ER-beta is strongly present in normal prostate (NP), a progressive loss of expression is registered in hyperplastic epithelium, and even greater loss in invasive carcinoma [2, 10, 13–15, 17]. Pasquali et al. [11] show that the loss of ER-beta in conjunction with unknown molecular events may accelerate cell proliferation and possible carcinogenesis. It was interesting that in a few cases there was no change, or was an increase of ER-beta expression in tumors, compared to NP.

Some of them found ER-beta expression in low-grade prostatic intraepithelial neoplasia (LGPIN), possible as a response to proliferative stimuli in the early stages of dysplasia, and lacking of expression in HGPIN, which may contribute to the initial phase of carcinogenesis [9, 14]. The presence of ER-beta in secretory cells in LGPIN may represent a transi-

ent unsuccessful attempt to stop the growth of these cells. The disappearance of ER-beta positive basal cells in HGPIN can mean the continuous loss of inhibition for proliferation in these precursor lesions [9, 14, 17]. The mechanism of inactivation of ER-beta in PCa remains unknown [2, 14].

Finding all the three receptors (AR, ER-alpha and ER-beta in stroma indicates that the signal transduction of steroid hormones is mediated by paracrine mechanisms to epithelial cells. ER-beta acts as an inhibitor of ER-alpha transcription and leads to a reduction in overall cellular sensitivity to E2. ER-beta and ER-alpha present together in the stromal cells may play a key role in the regulation of paracrine signals to epithelial cells. Estrogens influence over ER- beta placed in the basal cells may directly affect their growth. Loss of ER-beta seen in neoplastic progression may represent receptor function impairment [9].

The following different actions of epithelial ER-beta in the prostate are so far confirmed: pro-differentory, antiproliferative, anti-inflammatory and induction of the antioxidative gene.

The major role of ER-beta is the anti-estrogenic growth inhibition [14, 15]. The result is the arrest in the G2 phase of the cell cycle. Loss of ER-beta leads to uncontrolled cell proliferation [17]. The cells with ER-beta expression undergo apoptosis and may contribute to the reduced proliferation. In cancer cells, ER-beta promotor is methylated, which explains the loss of ER-beta [17]. The ER-beta expression in PCa leads to inhibition of cell proliferation and invasion, and increased apoptosis. The tissues undergoing dysplastic transformation have decline in ER-beta expression that indicates about its 'guardian' role.

Immunohistochemical studies that use only one ER-beta antibody cannot specify which isoform is expressed. There are at least four isoforms of ER-beta mixed in the prostate (485aa, 495aa, 503A). These isoforms have different capacities for binding with estrogen and different effectś [12, 13]. Their existence significantly complicates the understanding of the ER-beta role.

Methods

Four groups of patients were formed: the control with BPH and three experimental groups with PCa of different grades and scores, according to the Gleason grading system: group I – 10 prostate samples with signs of BPH; group II – 8 samples with well-differentiated PCa and Gleason score 2–4; group III – 10 samples with moderately differentiated PCa and Gleason score 5–7; group IV – 10 samples with poorly differentiated PCa and Gleason score 8–10.

A total of 39 specimens were sampled by transrectal ultrasound-guided biopsy. Bioptic samples were fixed in formalin, embedded in paraffin, cutted in 5μ slices and stained with hematoxylin-eosin. We determined histologic grades and Gleason scores in prostates with PCa, and BPH. Also, PSA levels were determined in all the patients.

Immunohistochemical staining for ER-beta was done with lyophilized mouse monoclonal antibody diluted 1 : 50–1 : 100 Novocastra. Staining was performed according to the manufacturer's instructions.

The intensity of ER-beta expression and localization was determnined in the control group with BPH, as well as in experimental groups with different scores of PCa. Counting was done at 40× and 63× magnification. Epithelial and stromal components were separately numbered. Approximately 100 cells on the average, were counted. Tumor cells with any nuclear positivity were specifically examined. ER-beta status was determined on the 2 immuno-slices. The score of six categories was applied, the number of positive cells was expressed in percentage: 0 – zero; 1 – < 1%; 2 – 1–10%; 3 – 11–33%; 4 – 34–66%; 5 – > 66%.

Positive and negative controls were used: external and internal. Epidermis of skin showed positivity for ER-beta. The slices incubated with nonimmune mouse serum instead of primary antibody showed immunoreactivity for ER-beta and represented negative control. Positivity of acinar epithelial cells was also observed in comparison with positively stained fibroblasts and endothelial cells. The results were analyzed in Excel.

Results

The patients were male of various ages (in average (67.34 years) suspected of PCa, based on clinical and laboratory parameters, treated in our institution from 2010 to 2012 (Table 1).

Table 1

Pathological changes and patient's age

Groups of patients	Values										Mean values of GS
BHP		/									
GS	4	7	/	/	/	/	7	/	/	/	6
age (years)	66	72	65	69	68	68	72	61	70	53	
GS 2–4		/							/	/	
GS	4	/	4	4	4	4	4	4	/	/	4
age (years)	74		74	74	61	61	61	61	/	/	
GS 5–7		5									
GS	5	63	7	7	6	7	5	5	5	5	5.9
age (years)	63		72	74	82	69	65	65	63	63	
GS 8–10		9									
GS	9	77	8	9	9	9	8	9	9	9	8.8
age (years)	62	71	59	73	73	60	65	62	77	77	

GS – Gleason score; BHP – benign prostatic hyperplasia.

None of the patients received prior hormonal therapy.

The mean Gleason score was 6.35. In the experimental groups it was 6.17 (Tables 1 and 2). The mean PSA value was 22.39 ng/mL (24.19 ng/mL in the experimental groups) (Table 3). Out of the total of 39 biopsy samples, multiplied with 3 different functional sections, there were 117 observed parameters. The lack of ER-beta expression in any sections was in 9 cases, accounting for 7.69%. The overall positivity was 92.3% (Table 4). Pathological changes and biopsy localization are shown in Table 5.

In the group I (BPH) we found the strongest positivity in basal cells (mean 3.3), than in secretory cells (mean 3.1), and in stromal ones (mean 3.0). The overall positivity in the group I was 90% (Figure 2).

In the experimental groups (PCa) the overall positivity was 92.8% and in 7.2% was negative.

In the group II the positivity was strongest in the stromal cells (mean 2.37), and similar in basal and secretory ones (mean 1.87). The overall positivity in the group II was 87.5% (Figure 3).

In the group III the positivity was strongest in basal cells (mean 3.5), then in stromal cells (mean 3.4) and in

Table 2

Pathological changes and Gleason grades

Group	Gleason grades									
BHP	2 + 2	3 + 4	/	/	/	/	3 + 4	/	/	/
GS 2–4	2 + 2	2 + 2	2 + 2	2 + 2	2 + 2	2 + 2	2 + 2	2 + 2	/	/
GS 5–7	2 + 3	3 + 4	3 + 4	4 + 3	3 + 3	4 + 3	2 + 3	3 + 2	3 + 2	3 + 2
GS 8–10	4 + 5	4 + 5	4 + 4	4 + 5	4 + 5	4 + 5	4 + 4	4 + 5	4 + 5	4 + 5

BHP- benign prostatic hyperplasia; GS – Gleason score.

Table 3

Pathological changes and prostate specific antigen (PSA) levels

Group	PSA levels (ng/mL)										Mean values
BHP	9.78	5.83	11.95	9.20	10.20	10.20	5.83	12.55	6.47	6.64	8.86
GS 2–4	5.76	/	5.76	5.76	7.21	7.21	7.21	7.21	/	/	6.58
GS 5–7	7.91	16.5	16.5	14.42	15.65	1.8	5.67	5.67	7.91	7.91	9.99
GS 8–10	>100	2.4	15.2	66.29	66.29	28	19	>100	>100	>100	>56.01

BHP – benign prostatic hyperplasia; GS – Gleason score; Normal: 0–4, category 1; Gray zone: > 4–10, category 2; Ca suspect: > 10 category, 3.

Table 4

Pathological changes and estrogen receptor (ER) beta expression

Group	ER beta expression									
BHP										
stromal cells	4	4	4	3	4	3	3	2	3	-
basal cells	5	5	5	4	4	3	4	2	1	-
secretory cells	3	5	5	4	4	3	5	1	1	-
GS 2–4										
stromal cells	0	3	4	2	3	2	2	3		
basal cells	0	3	2	1	3	2	2	2		
secretory cells	0	2	3	1	4	1	2	2		
GS 5–7										
stromal cells	3	4	3	3	4	4	4	4	2	3
basal cells	3	4	4	4	5	4	3	4	2	2
secretory cells	3	5	3	5	4	3	4	4	1	1
GS 8–10										
stromal cells	1	4	4	4	3	4	4	1	3	4
basal cells	0	4	5	4	5	3	4	1	3	4
secretory cells	0	4	5	4	4	3	4	0	2	3

Marks for ER-beta positive cells: 0 – zero; 1 – < 1%; 2 – 1–10%; 3 – 11–33%; 4 – 34–66%; 5 – > 66% cells;
BHP- benign prostatic hyperplasia; GS – Gleason score.

Table 5

Pathological changes and biopsy localization

Group	Biopsy localization										Mean
BHP	a.d.	s.l.	a.d.	s.l.	s.d.	a.d.	b.l.	a.l.	a.d.	a.d.	ad. sl
GS 2-4	b.d.	b.l.	b.d.	a.d.	a.d.	a.d.	s.d	b.d.	/	/	bd. ad
GS 5-7	s.l.	s.d.	b.d.	s.b.d.	s.d.	s.l.	b.l.	a.l.	a.l.	a.l.	al. sd
GS 8-10	a.d.	b.l.	s.l.	s.d.	b.d.	a.d.	s.d.	b.l.	d.	l.	bl. sd

a – apex, s – middle, b – base; d – dexter (right), l – left; BHP- benign prostatic hyperplasia; GS – Gleason score.

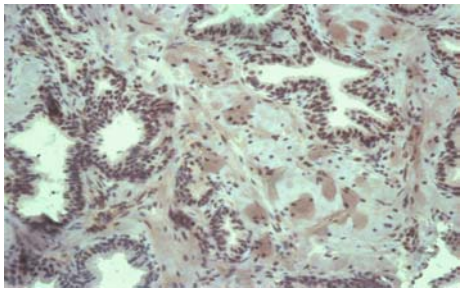

Fig. 2 – Immunohistochemical staining for estrogen receptor (ER) beta in benign prostatic hyperplasia (the control group) showing positivity in stromal cells (mean 4), basal cells (mean 5) and in secretory ones (mean 5) (photomicrograph, ×20) Marks for ER-beta positive cells – 4: 34–66% positive cells; mark 5: > 66% positive cells.

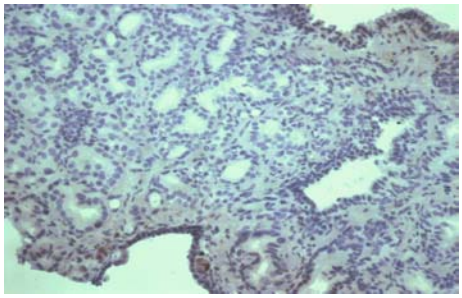

Fig. 3 – Immunohistochemical staining for estrogen receptor (ER) beta in prostate adenocarcinoma (PCa) Gleason score 2–4, showing that stromal, basal and secretory cells were ER-beta negative (photomicrograph ×20).

secretory ones (mean 3.3). The overall positivity in the group III was 100% (Figure 4).

In the group IV the positivity was strongest in basal cells (mean 3.3), then in stromal cells (mean 3.2), and in secretory ones (mean 2.9). The overall positivity in the group IV was 90% (Figure 5).

The strongest basal cell positivity was registered in the group III (mean 3.5), then in the group I and IV (mean 3.3), and weakest in the group II (mean 1.87). The strongest secretory cell positivity was registered in the group III (mean 3.3), then in the group I (mean 3.1), in the group IV (mean 2.9), and the weakest in the group II (mean 1.87). The strongest stromal positivity was registered in the group III (mean 3.4), then in the group IV (mean 3.2), in the group I (mean 3.0) and weakest in the group II (mean 2.37).

Our data showed that expression of ER-beta in epithelial cells of the prostate acini is the weakest in well-differentiated adenocarcinomas (Figure 6).

There was a decline of ER-beta expression in malignant compared to benign prostatic epithelial acini.

Less difernetiated adenocarcinomas showed a decrease in the expression of ER-beta in basal cells and in secretory ones (Figure 7).

The expression of ER-beta in basal cells was stronger, than in secretory ones in BPH (Figure 8) and in moderately differentiated adenocarcinomas (Figure 9).

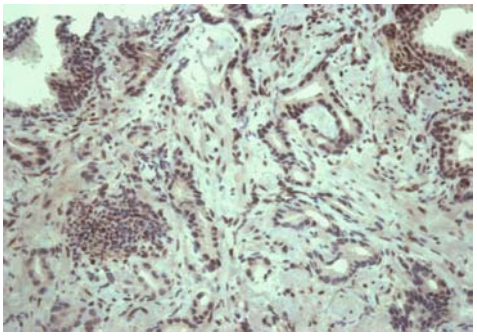

Fig. 4 – Immunohistochemical staining for estrogen receptor (ER) beta, in prostate adenocarcinoma (PCa), Gleason score 5–7, showing ER-beta positivity in stromal cells (mark 3), basal cells (mark 3), and in secretory ones (mark 3) (photomicrograph ×20).
Mark for ER-beta positive cells – 3: 11–33% positive cells.

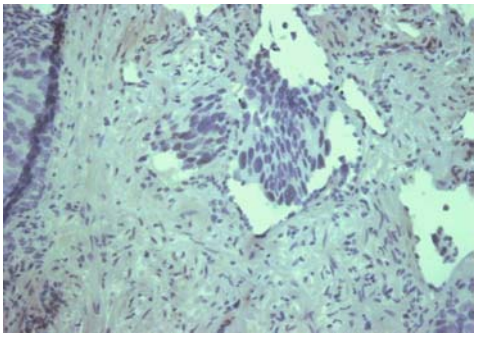

Fig. 5 – Immunohistochemical staining for estrogen receptor (ER) beta, in prostate adenocarcinoma (Pca, Gleason score 8–10) showing ER-beta positivity in stromal cells (mark 1), basal cells (mark 0) and in secretory ones (score 0) (photomicrograph ×20). Marks for ER-beta positive cells – 0 positive cells: zero mark; 1: < 1% positive cells.

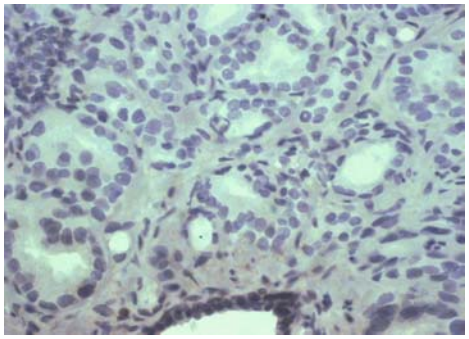

Fig. 6 – Immunohistochemical staining for estrogen receptor (ER) beta, showing ER-beta expression in well-differentiated adenocarcinoma (photomicrograph × 40).

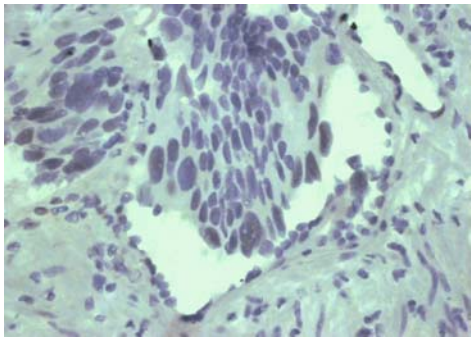

Fig. 7 – Immunohistochemical staining for estrogen receptor (ER) beta, showing ER-beta expression in less-differentiated adenocarcinoma (photomicrograph × 40).

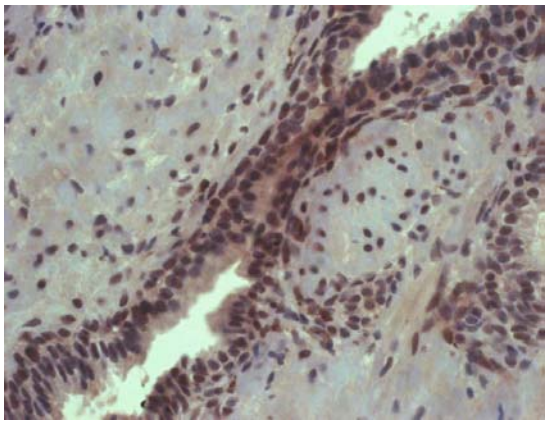

Fig. 8 – Immunohistochemical staining for estrogen receptor (ER) beta, showing ER-beta expression in basal cells was stronger than in secretory ones in benign prostatic hyperplasia (BPH) (photomicrograph ×40).

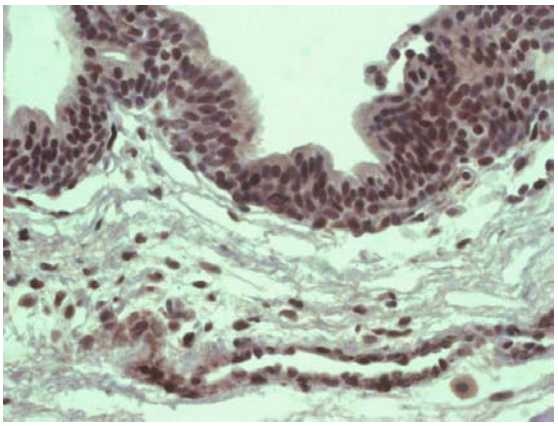

Fig. 9 – Immunohistochemical staining for estrogen receptor (ER) beta, showing ER-beta expression in benign prostatic hyperplasia (BPH), with ER-beta positivity in the stromal cells (mark 3), basal cells (mark 4) and in secretory ones (mark 4) (photomicrograph ×40).
Marks for ER-beta positive cells – 3: 11–33% positive cells; mark 4: 34–66% positive cells.

Discussion

As noted above ER-beta was registered in the nuclei of basal cells of prostatic acini [2, 14, 20] as in stromal cells [21]. Stroma was positive in 20–60% of cases [14]. ER-beta was also located in secretory luminal cells of NP [13, 14]. ER-beta was located in the epithelium of NP, BPH and PCa. [2, 12, 20, 21].

Using antibodies for long isoform of ER-beta. Leav et al. [9] found the positivity in basal cells, mainly. This is in apparent contradiction with the distribution of ER-beta in the secretory cells of the prostate gland in rats. Fixemer et al. [13] used monoclonal antibodies to distinguish long from short isoform of ER-beta and identified positive secretory luminal cells and with lesser intense basal ones [13].

We also found the strongest positivity in basal cells in BPH and moderately differented adenocarcinoma.

The secretory luminal cells have high expression of ER-beta which is lost with transformation into HGPIN [13, 20].

A high ER-beta expression was found in 90% cases of BPH with PSA ≤ 10 ng/ml [2, 9, 10].

The presence of ER-beta in secretory cells of well- to moderately differentiated lesions may represent a transient abortive attempt to prevent their growth. In contrast, disappearance of ER-beta positive basal cells in HGPIN may involve the continuous loss of growth inhibitory functions mediated through ER-beta in these precursor lesions [2, 14]. ER-beta is very intense in BPH [2, 14].

ER-beta localization in secretory luminal cells showed that the differentiated section is the main target of estrogen action in human prostate. Partial loss of ER-beta in HGPIN supports the concept that ER-beta has hemopreventive effects on prostate epithelium [22, 23].

We also found a strong ER-beta expression in BPH.

We noticed the weakest ER-beta expression in well-differentiated PCa.

ER-beta have an important role in proliferation and differentiation of prostatic epithelium [19, 21] and can affect the initial phase of carcinogenesis in the prostate and in androgen independent tumors [13]. Localization of ER-beta in basal cells is related to the role in epithelial proliferation and renewal processes [19]. Estrogen stimulation of cell proliferation leads to the development of cancer [19]. Antiproliferative, anti-invasive and proapoptotic role of ER-beta is associated with the tumor suppressor function [17]. ER-alpha has the proliferative role restricted with the influence of ER-beta [15].

Horvath et al. [14] observed ER-beta in NP and registered positivity in more than 95% of epithelial nuclei and in 35% of stromal cells. In BPH near carcinoma ER-beta positivity fall to 24%, and to 11% in PCa. Progressive loss of ER-beta expression is registered in BPH, and even greater in Pca [14].

We found a progressive lost of ER-beta expression in malignant compared to benign prostate epithelium and a decrease of expression in less differented PCa. This findings are consistent with most of the actual works.

In BHP Horvath et al. [14] found stronger ER-beta expression in epithelial cells than in the stroma.

ER-beta expression was present in stromal and mesenchymal cells in the BPH group (adipocytes, endothelial cells, smooth muscle cells of blood vessels). Secretory luminal cells were more positive than the basal ones [13].

In BHP we found the overall positivity of 90%. Stronger positivity was in basal than in secretory cells and the least in stroma.

PCa expressed ER-beta in 87% of the cases, as in benign epithelium. In 13% of the cases there was a decreased ER-beta expression. There was no correlation between the degree of expression, grade or stage of the disease [13].

In the groups with PCa we found the positivity of 92.8%.

It seems that there is no explanation for the discrepancy between the published results. The lack of specificity of the antibody, or the difference in the primary antibody, or antigen retrival and inadequate tissue processing, or the presence of unknown ER isoforms may affect the results of immunohistochemical staining.

Metastases to lymph nodes and bones expressed ER-beta in 100% of the cases [10]. While the loss of ER-beta may

contribute to the progression of organ localized disease, the appearance of ER-beta re-expression in metastases suggests a possible role in androgen-independent progression [10].

Untreated primary and metastatic tumors retain expression of ER-beta. These tumors use estrogen through ER-beta regulated processes. Partial loss of ER-beta in hormone refractory tumors may represent an androgen-dependent gene expression of ER-beta [13].

Such observations may have clinical implications in cases where tumor cells showed expression of these receptors, potentially responsive to estrogen and survive in conditions of androgen deprivation and also for treatment with estrogen antagonists [24, 25].

Conclusion

ER-beta expression was most pronounced in BHP samples and declined in malignant prostatic lesions. This finding supports statement on antiproliferative role of ER-beta in prostatic tissue.

R E F E R E N C E S

1. *Rosai J.* Rosai and Ackerman's surgical pathology. 9th ed. Philadelphia: Mosby, Elsevier Inc; 2004.
2. *Gabal SM, Habib FM, Helmy DO, Ibrahim MF.* Expression of estrogen receptor-B (ER-B) in bengin and malignant prostatic epithelial cells and its correlation with the clinico-pathological features. J Egypt Natl Canc Inst 2007; 19(4): 239−48.
3. *De Marzo AM, Platz EA, Sutcliffe S, Xu J, Grönberg H, Drake CG,* et al. Inflammation in prostate carcinogenesis. Nat Rev Cancer 2007; 7(4): 256−69.
4. *de Marzo AM, Nelson WG, Isaacs WB, Epstein JI.* Pathological and molecular aspects of prostate cancer. Lancet 2003; 361(9361): 955−64.
5. *Bostwick DG, Qian J.* High-grade prostatic intraepithelial neoplasia. Mod Pathol 2004; 17(3): 360−79.
6. *Montironi R, Mazzucchelli R, Lopez-Beltran A, Cheng L., Scarpelli M.* Mechanisms of Disease: high-grade prostatic intraepithelial neoplasia and other proposed preneoplastic lesions in the prostate. Nature Clin Pract Urol 2007; 4(6): 321−32.
7. *McPherson SJ, Ellem SJ, Simpson ER, Patchev V, Fritzemeier K, Risbridger GP.* Essential role for estrogen receptor beta in stromal-epithelial regulation of prostatic hyperplasia. Endocrinology 2007; 148(2): 566−74.
8. *Risbridger GP, Ellem SJ, McPherson SJ.* Estrogen action on the prostate gland: a critical mix of endocrine and paracrine signaling. J Mol Endocrinol 2007; 39(3): 183−8.
9. *Leav I, Lau KM, Adams JY, McNeal JE, Taplin ME, Wang J,* et al.. Comparative studies of the estrogen receptors beta and alpha and the androgen receptor in normal human prostate glands, dysplasia, and in primary and metastatic carcinoma. Am J Pathol 2001; 159(1): 79−92.
10. *Prins GS, Korach KS.* The role of estrogens and estrogen receptors in normal prostate growth and disease. Steroids 2008; 73(3): 233−44.
11. *Pasquali D, Rossi V, Esposito D, Abbondanza C, Puca GA, Bellastella A,* et al. Loss of estrogen receptor beta expression in malignant human prostate cells in primary cultures and in prostate cancer tissues. J Clin Endocrinol Metab 2001; 86(5): 2051−5.
12. *Weihua Z, Warner M, Gustafsson J.* Estrogen receptor beta in the prostate. Mol Cell Endocrinol 2002; 193(1−2): 1−5.
13. *Fixemer T, Remberger K, Bonkhoff H.* Differential expression of the estrogen receptor beta (ERbeta) in human prostate tissue, premalignant changes, and in primary, metastatic, and recurrent prostatic adenocarcinoma. Prostate 2003; 54(2): 79−87.
14. *Horvath LG, Henshall SM, Lee CS, Head DR, Quinn DI, Makela S,* et al. Frequent loss of estrogen receptor-beta expression in prostate cancer. Cancer Res 2001; 61(14): 5331−5.
15. *Stettner M, Kaulfuss S, Burfeind P, Schweyer S, Strauss A, Ringert R,* et al. The relevance of estrogen receptor-beta expression to the antiproliferative effects observed with histone deacetylase inhibitors and phytoestrogens in prostate cancer treatment. Mol Cancer Ther 2007; 6(10): 2626−33.
16. *Steiner MS, Raghow S.* Antiestrogens and selective estrogen receptor modulators reduce prostate cancer risk. World J Urol 2003; 21(1): 31−6.
17. *Cheng J, Lee EJ, Madison LD, Lazennec G.* Expression of estrogen receptor beta in prostate carcinoma cells inhibits invasion and proliferation and triggers apoptosis. FEBS Lett 2004; 566(1−3): 169−72.
18. *Kuiper GG, Enmark E, Pelto-Huikko M, Nilsson S, Gustafsson JA.* Cloning of a novel receptor expressed in rat prostate and ovary. Proc Natl Acad Sci U S A 1996; 93(12): 5925−30.
19. *Royuela M, de Miguel MP, Bethencourt FR, Sánchez-Chapado M, Fraile B, Arenas MI,* et al. Estrogen receptors alpha and beta in the normal, hyperplastic and carcinomatous human prostate. J Endocrinol 2001; 168(3): 447−54.
20. *Bonkhoff H, Fixemer T, Hunsicker I, Remberger K.* Estrogen receptor expression in prostate cancer and premalignant prostatic lesions. Am J Pathol 1999; 155(2): 641−7.
21. *Signoretti S, Loda M.* Estrogen receptor beta in prostate cancer: brake pedal or accelerator. Am J Pathol 2001; 159(1): 13−6.
22. *Hartman J, Ström A, Gustafsson JÅ.* Current concepts and significance of estrogen receptor β in prostate cancer. Steroids 2012; 77(12): 1262−6.
23. *Asgari M, Morakabati A.* Estrogen receptor beta expression in prostateadenocarcinoma. Diagn Pathol 2011; 6: 61.
24. *McPherson SJ, Hussain S, Balanathan P, Hedwards SL, Niranjan B, Grant M,* Risbridger GP. Estrogen receptor-beta activated apoptosis in benign hyperplasia and cancer of the prostate is androgen independent and TNFalpha mediated. PNAS 2010; 107(7): 3123−8.
25. *Vojinov S, Levakov I, Jeremić D, Zivojinov S, Marusić G.* Hormonal status in patients with advanced prostatic cancer on the therapy with androgen blockade. Vojnosanit Pregl 2011; 68(4): 321−6.

Received on October 22, 2013.
Revised on October 20, 2014.
Accepted on October 22, 2014.
Online First August, 2015.

GENERAL REVIEW

UDC: 616.1-089
DOI: 10.2298/VSP140515079L

Structural features of arterial grafts important for surgical myocardial revascularization: Part I – Histology of the internal thoracic artery

Strukturne karakteristike arterijskih graftova značajnih za hiruršku revaskularizaciju miokarda: Deo I – Histologija unutrašnje torakalne arterije

Milica M. Labudović Borović*, Ivana M. Lalić*, Saša D. Borović†, Ivan V. Zaletel*, Slavica S. Mutavdžin*, Miloš I. Bajčetić*, Jelena V. Kostić‡, Zoran Ž. Trifunović§‖

***Institute of Histology and Embryology "Aleksandar Dj. Kostić", Faculty of Medicine University of Belgrade, Belgrade, Serbia; †Dedinje Cardiovascular Institute, Belgrade, Serbia; ‡Cardiology Clinic, Clinical Center of Serbia, Belgrade, Serbia; §Military Medical Academy, Belgrade, Serbia; ‖Faculty of Medicine of the Military Medical Academy, University of Defence, Belgrade, Serbia**

Key words:
myocardial revascularization; vascular patency; mammary arteries; histology.

Ključne reči:
miokard, revaskularizacija; vaskularni graft, prolaznost; aa. mammariae; histologija.

Introduction

In contemporary heart surgery the following arterial grafts are used: the internal thoracic artery – ITA (*arteria thoracica interna*), the radial artery, the inferior epigastric artery and the right gastroepiploic artery. Favorable features of arterial grafts in surgical revascularization of the myocardium are: uniform size of arterial grafts and diameter which corresponds to the diameter of coronary blood vessels, technical and topographical accessibility, the fact that they do not contain valves, that they are as well adapted to arterial flow and pressure, and, in case of the ITA adaptation to intrathoracic respiratory changes of pressure [1–4]. Arterial graft of the ITA, is one of the most frequently used grafts in surgical revascularization of the myocardium, besides the venous graft of the great saphenous vein, (*vena safena magna*).

Arterial grafts are introduced into surgical practice because of the need to establish efficient system for multiple revascularization of the myocardium, and the peak in their implementation is reached by introducing modern techniques of composite or creative grafts. This contemporary approach implies complete revascularization of myocardium using arterial grafts. At the same time, the left internal thoracic artery is used for revascularization of the left anterior descending coronary artery, while composite graft of the right gastroepiploic artery anastomosed with the radial artery is used for the revascularization of the right coronary artery and the left circumflex artery [5]. The inferior epigastric artery or the right internal thoracic artery can be used instead of the radial artery in this composite fashion.

Indications for using composite arterial grafts are a very small diameter or a high degree of stenosis of target coronary blood vessels, the need for multiple revascularizations with more than three distal anastomosis and avoiding bilateral dissection of internal thoracic artery in diabetic patients [6].

Histology of the internal thoracic artery

Features of the ITA, as almost ideal graft, are determined with its specific histological structure. According to the original definition, it is the only peripheral artery of elastic type in human organism, with well formed internal elastic membrane [7]. However, in modern research it was shown that the internal thoracic artery is an artery of the transitional or mixed type [8] (Figures 1A–H).

The wall of the ITA is composed of three layers: *tunica intima, tunica media* and *tunica adventitia* (Figure 1D). *Tunica intima* has a typical structure and contains endothelium

Correspondence to: Milica Labudović Borović, Institute of Histology and Embryology "Aleksandar Đ. Kostić", Faculty of Medicine, University of Belgrade, 26 Višegradska, 11000 Belgrade, Serbia. Phone: +381 (0)11 3607 149; fax number: +381 (0)11 3612 567. E-mail: sborovic2001@yahoo.com; milica.labudovic-borovic@mfub.bg.ac.rs

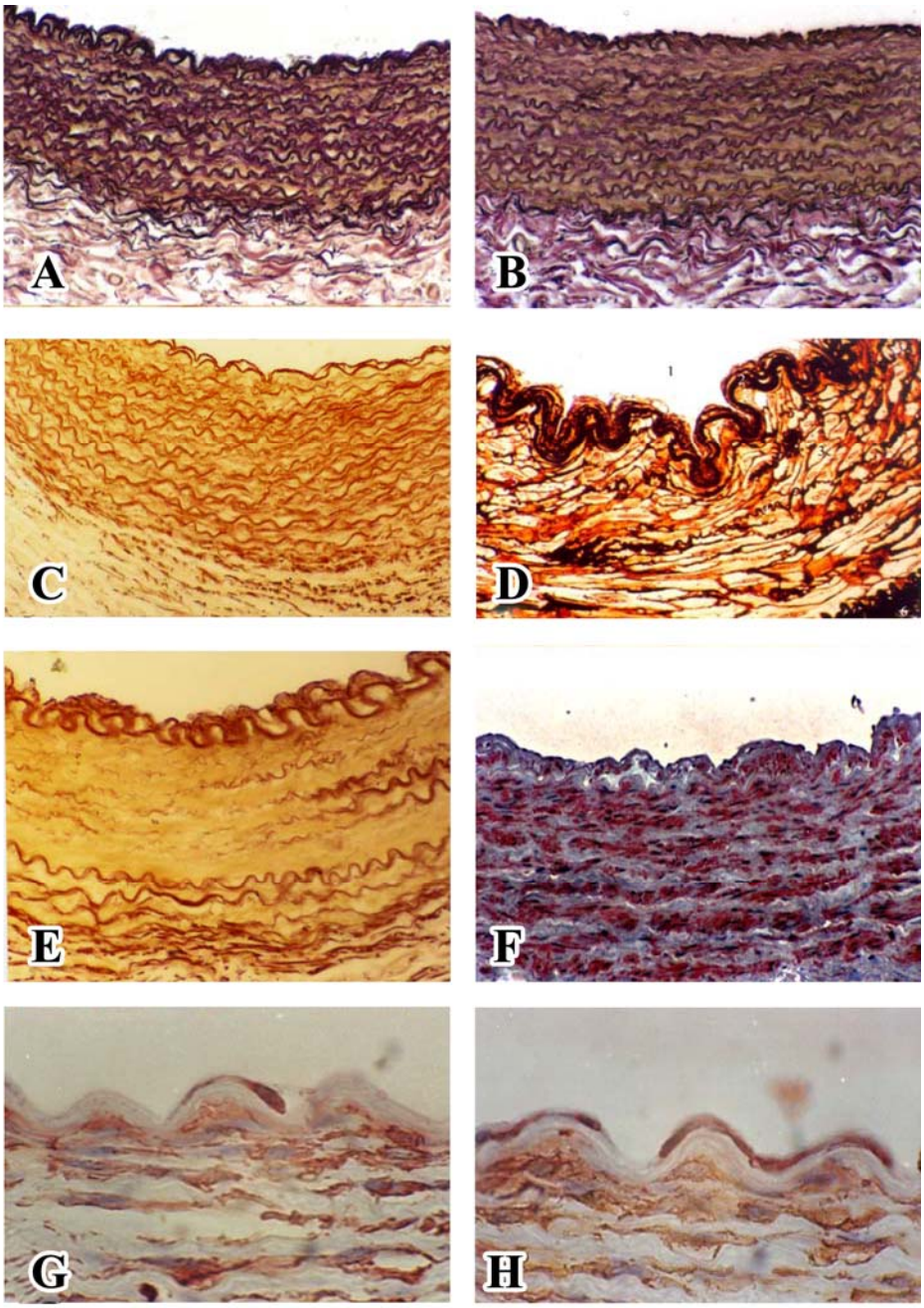

Fig. 1 – The internal thoracic artery: (A, B, C and E) Weigert van Gieson staining for elastic fibers; (D) methenamine silver staining; (F) immunohistochemical staining for alpha smooth muscle (α SMA) (EnVision/AEC); (G and H) immunohistochemical staining for alpha smooth muscle (α SMA) (LSAB+/HRP/DAB) [original magnification: (A) 32×; (B, C, E and F) 64×; (D) 100×; (G and H) 256×]

A and B: artery of mixed (transitional) type, with inner (muscular) layer and outer layer with elastic lamellae; C: segments with elastic phenotype; D: 1. arterial lumen; 2. *tunica intima* and the internal elastic lamina; 3. *tunica media*; 4. elastic lamellae; 5. smooth muscle cells; 6. *tunica adventitia*; E: segments with muscular phenotype and small number of elastic lamellae; F: circular arrangement of smooth muscle cells in the inner layer of the tunica media and spiral arrangement of smooth muscle cells in the outer layer of the tunica media; G and H: smooth muscle cells are present in the subendothelial connective tissue in infant (2 months of age).

and poorly developed layer of subendothelial connective tissue. Thickness of the intima is very small, around 2.5 μm in the thinnest segments, and the mean values of intimal thickness vary between 9 μm, in persons younger than 40 years, and 20 μm, in persons older than 60 years [8, 9].

Molecular, cytological and histological features of the ITA endothelium and the composition of subendothelial connective tissue are important for low level of atherosclerosis. The endothelium of the ITA is an important subject of intensive research. It has been shown that preserving the endothelium is a priority during surgical preparation of the grafts, because the ITA contains a potent system of endogenous nitrate which prevents vasospasm, thrombus formation and occlusion of the graft [10, 11].

Paracrine function of the endothelium is one of the crucial factors responsible for notable differences in the long-term patency of venous and arterial grafts. The level of nitric oxide (NO), which is produced by endothelium of the ITA, is dramatically higher in comparison to low and variable amount of NO secreted by endothelium of the great saphenous vein [12–15]. Generally taken, basal production of NO is higher in arterial than in venous circulation [16, 17], while venous vessels show larger sensitivity to endothelin-1 in comparison to arterial vessels [18].

Intensive release of NO is also typical for vascular endothelium of the ITA branches. Studies have shown that perforating branches of this artery, which provide vascularisation of upper inner quadrant of the breast, have striking ability of endothelium dependent vasodilatation completely induced by nitrogen monoxide (NO or endothelium-derived relaxing factor – EDRF), which is important for perfusion of glandular tissue adequate to changeable physiological requirements during breastfeeding and lactation [19]. This feature, with optimal diameter, makes the ITA an ideal recipient blood vessel for free tissue transfers in thoracic region, especially during breast reconstruction [20].

Reasons for venous grafts insufficiency in comparison to arterial grafts are weaker activity of antioxidant enzyme, superoxide dismutase, larger retention of low-density lipoproteins (LDL) in venous vesseles [21], and as well the fact that several growth factors, such as platelet-derived growth factor (PDGF), stimulate proliferation and migration of smooth muscle cells of the great saphenous vein, but not of the internal thoracic artery [22]. Larger retention of LDL in venous grafts is initiated by larger amount of sulfated glycosaminoglycans in the subendothelial connective tissue of the venous vessels in comparison to arterial vessels. Also, after the implantation of the venous grafts the deposition of sulfated glycosaminoglycans increase, making the venous grafts more permeable and susceptible to lipid retention [21].

The preserved endothelium and its anti-thrombogenic function, as well as the absence of aggregation and activation of platelets due to low level secretion of platelet-activating factor and platelet-activating factor acetylhydrolase, are also designated as causes of delayed atherosclerosis of the internal thoracic artery [23]. The internal thoracic artery endothelium contains more anti-thrombotic molecules as, for example, heparin sulfate and tissue plasminogen activator [24].

Besides, endothelium of the ITA is proved to have fewer fenestrations, lower permeability of intercellular junction and low level of intercellular adhesion molecule-1 (ICAM-1) with lower potential for adhesion, rolling and transmigration of inflammatory cells [24, 25]. This is in concordance with basically lower level of inflammation in the atherosclerotic lesions of the internal thoracic artery [8].

All these factors contribute to low level atherosclerosis and to the superior patency rate of the ITA when used as the coronary artery by-pass graft (CABG).

Low grade atherosclerosis is an unique feature of the ITA. According to many researchers, the ITA rarely develops atherosclerotic lesions. In a comprehensive pathoanatomical study, which included 3,409 specimens of the ITA, 97.5% of them were macroscopically unaltered. Only in six of the arteries, developed atherosclerotic plaques were shown, and 78 arteries have shown atherosclerotic lesions of lower degree [26]. Other similar studies proved that up to 87% of arteries were free of atherosclerosis and that only 3.1% had stenosis on the branching point where the ITA derives from the subclavian artery [27, 28]. According to our research, frequency of atherosclerotic lesions increases with aging. Atherosclerotic lesions type IV occur in 1% of patients younger than 40 years and in 7.6% of patients older than 60 years [9].

However, the ITA is not resistant to the development of intimal hyperplasia with aging [8, 9, 29, 30]. In most of the patients, intimal thickening of the internal thoracic artery develops primarily because of intimal hyperplasia. It is also known that smooth muscle cells in the internal layer (*tunica intima*) of this artery can already be found in the first few years of life [9, 31–33] (Figures 1G–H).

Besides that, it was shown that known risk factors for the development of atherosclerosis: hypercholesterolemia, diabetes mellitus, male gender, smoking and hypertension stimulate intimal hyperplasia and the development of ITA atherosclerosis [8, 9, 34–36].

Specific structural features of the tunica media of the ITA

The *tunica media* of the ITA is composed of two layers: inner, which is made up of several layers of circularly oriented smooth muscle cells, and outer, with a variable number of elastic lamellae and spirally arranged smooth muscle cells in interlamellar units (Figure 1F). Such a structure completely corresponds to the well-known definition of arteries of mixed type and contemporary classification of arteries [37].

In the outer layer of the tunica media, the number of elastic laminae, which are different from internal and external elastic membranes, varies depending on an arterial segment.

van Son et al. [7], who first described histology of the ITA, paid great attention to the appearance of the *tunica media* and the number of elastic lamellae. The first centimeter of the artery after the take off from the subclavian artery (*a. subclavia*) had characteristics of elastic artery with 8–18 elastic lamellae.

In the further course of the artery, four different types of the *tunica media* of the ITA can be distinguished: elastic, which, together with the internal and the external elastic membranes; contains between 8 and 18 well-developed; densely arranged elastic lamellae with moderate number of smooth muscle cells (Figure 1C); elastic-muscular, with five to seven concentric, elastic lamellae and slightly larger number of smooth muscle cells in comparison to the previous type (Figures 1A–B); muscular type, with the domination of smooth muscle cells and three to four poorly formed elastic lamellae, including the internal and the external elastic membrane (Figure 1E); muscular type, which consists almost exclusively of smooth muscle cells with sparse single elastic fibers distributed between muscle cells and without well developed elastic lamellae [7].

However, new studies have shown that, in general, the number of elastic laminae of the ITA progressively decreases from the initial portion to the terminal branches, which is in

accordance with its topographical localization and histological structure of transitional artery, inserted between classically structured elastic artery (subclavian artery) and typical muscle arteries (superior epigastric artery and musculophrenic artery) [29] and represents phenomenon which has been observed in the previous research on the number of elastic lamellae in the aorta and the ITA [7, 38–40]. The number of elastic lamellae in the outer media shows conspicuous individual variations [8, 9, 29].

This kind of morphological finding is particularly significant from the functional point of view. The research shows that transitional arteries, due to their specific structure, are capable of adapting to altered hemodynamic conditions and for vascular remodeling during life, in accordance with the changed functional requirements [41, 42]. Similarly to elastic arteries, the presence of elastic lamellae allows these arteries to maintain a constant blood flow even during diastole by passive contraction. On the other hand, the presence of well-defined muscular layer creates conditions for a wide degree of physiological adaptability of the ITA that is vasospasm in conditions of low flow and an increase in the diameter at increased blood flow, which is extremely important in terms of graft performance. It has been shown that the use of the ITA, even in conditions of low free flow gives good results, because this graft has a high ability to adapt to changing hemodynamic conditions, and if there is no damage to the graft during mobilization, the blood flow can significantly increase following the increased demands of the myocardium [11].

The extracellular matrix of arterial grafts media contains a developed network of collagen type IV. Collagen type IV and laminin stabilize the extracellular matrix of blood vessels, inhibit the activity of matrix metalloproteinases, delay the transformation of vascular smooth muscle cells from contractile to synthetic phenotype as well as their proliferation and migration. These effects of collagen type IV and laminin are opposite to the effects provoked by fibronectin [43–45].

The internal thoracic artery and the positive remodeling

Another important aspect is the fact that the media of the ITA gradually thickens with age and with the development of intimal hyperplasia [8, 9]. Also, this happens during the development of early atherosclerotic lesions types. It was, also, shown that chronic increase in blood flow leads to the increase of the ITA diameter [46, 47]. These facts pointed towards the capability of the ITA for positive remodeling. The ability for positive remodeling probably contributes to the absence of complications after CABG surgery, namely *angina pectoris* and myocardial infarction.

The mean values of the media thickness range between 160 μm and 250 μm [8, 9].

The elastic lamellae features

Between the intima and the media lies a well-developed internal elastic lamina. The thickness of the internal elastic membrane is between 2.0 μm and 2.5 μm, and it is well-formed even at birth and in the first years of life it significantly thickens and contains a small number of fenestrations. This perfectly formed internal elastic membrane represents a specific structure of the ITA and it is especially well-developed in the younger age groups [31]. It was considered that a well formed internal elastic membrane prevents migration of smooth muscle cells from the media to the intima and that it plays a key role in preventing early atherosclerotic changes [31].

However, modern research has shown that perfectly formed internal elastic lamina is not a permanent feature of the ITA. After the age of sixty, there is a sudden decrease in the thickness of the internal elastic membrane, while the number of fenestrations increases significantly from the age of forty, especially in men [29]. This also applies to all elastic lamellas of the ITA, which become thinner with age, and have larger and more numerous fenestrations. Degradation of the elastic skeleton of the internal thoracic artery is particularly well-expressed after the age of sixty. This fact indicates that the process of aging significantly disrupts the integrity of the elastic skeleton of the ITA, and probably makes the artery more vulnerable to the development of intimal hyperplasia and atherosclerosis [29]. Consistent with this finding are conclusions of a study that enclosed 5,601 patients and tested the long-term prognosis of bilateral ITA grafts in patients older than 70 years. There was no clear advantage of bilateral ITA grafting in these patients in comparison to vein grafts or the combination of the ITA and the saphenous vein grafts [48]. Aging limits the superiority of the ITA.

These data are opposite to predominant attitudes from previous studies that claim that parts of the ITA with many elastic lamellae have lower level of hyperplasia than the intima or atherosclerosis, and that elastic lamellae are perfect and continual protection from the smooth muscle cells migration [7]. Nevertheless, among different media patterns or phenotypes there are no differences in the thickness of the intima or the atherosclerosis grade [8]. The benefits from using proximal parts of the ITA came mainly from their functional adaptability caused by characteristics of mixed arteries [8]. Elastic lamellae are not solely factors that delay atherosclerosis or intimal hyperplasia [8].

Between the media and the adventitia there is a well-formed external elastic membrane.

The issue of vascular wall resident progenitor cells in the adventitia of the internal thoracic artery

Tunica adventitia of the ITA contains a wide network of connective tissue composed of longitudinally arranged elastic and collagen fibers. Its thickness is about 100 μm [7]. Thickness of the adventitia in some segments is equal to the thickness of the media, which is also similar to the muscular type arteries, rather than elastic arteries [8, 9]. A particularly important feature is the presence of numerous CD34 immunoreactive cells, which are considered as resident progenitor cells of the vascular wall (vascular wall resident progenitor cells) that are very abundant in the adventitia of the internal thoracic artery [9, 49]. It is believed that these cells have the potential to differentiate to endothelial cells, smooth muscle

cells, and endothelial cells of *vasa vasorum*. Also, the endothelium of the ITA artery contains many CD34 immunoreactive cells. This feature is retained by the endothelium in the aging process, as well as during the development of atherosclerosis, which is opposite to the coronary arteries, the radial artery and the gastroepiploic artery. It is believed that the presence of CD34 immunoreactive cells indicates the regeneration potential, which is continuously maintained, and may explain the low tendency of this artery for the development of atherosclerosis [9].

The wall thickness of the internal thoracic artery and the implication for surgical use

The mean value of the wall thickness of the ITA varies between 240 μm and 360 μm in the different age-related groups with the mean value of 282.79 ± 93.54 μm [8, 9]. This provides nutrition of the wall of the ITA from the lumen of the artery, which was confirmed by immunohistochemical and electron microscopic studies [10]. Specifically, it has been found that the nutritional needs of the artery with a wall thickness of less than 350 μm and with less than 29 lamellar units of media, are provided by the diffusion process from the blood flowing through the artery, and the 29th lamellar layer and 350th μm represent a topographic limit to which it is possible to conduct the process of diffusion. All the other lamellar units of these types of arteries settle their nutritional needs thanks to the presence of *vasa vasorum* [50, 51]. Therefore, the removal of adventitial layer of the artery during graft skeletonization does not impair the ultrastructure of the artery, so integrity of the endothelial cells and their connections and adherences to the basement membrane are preserved, regardless of the aggressiveness of the surgical approach [10]. From the perspective of modern cardiac surgery practice, this histological finding has important implications, because it suggests a certain amount of freedom in the surgical preparation of the graft, as well as the possibility to use the artery as a free, skeletonized or a composite graft without the risk of ischemic damage to the arterial wall [7, 52]. Lymphatic drainage of the wall of the internal thoracic artery is very effective, in contrast to the coronary arteries, which is why this is also considered as a possible cause of delayed development of atherosclerotic changes [7].

Diameter of the internal thoracic artery

The diameter of the internal thoracic artery varies between 1.9 and 2.6 mm [24]. The diameter of the internal thoracic artery is almost ideally suited to the diameter of the left anterior descendening coronary artery. The lack of discrepancy in the caliber of blood vessel combined with a good surgical technique minimizes the occurrence of turbulent flow and thrombosis at the anastomotic site [53].

Gender specific differences

The media of the male patients is significantly larger than the media of female patients and the male gender is an independent predictor factor for the internal elastic membrane disruption during ageing [8]. On the other hand, there is a reduced level of NO and endothelial nitric oxide synthase (eNOS) in the endothelium of the internal thoracic arteries of the post-menopausal women with poor outcome expectance in CABG patients [54].

Left-to-right specific differences

In terms of morphometric parameters there is no difference between the arteries on the left and the right side of the body, a finding that is particularly important from the point of view of numerous studies that determine the efficiency of bilateral internal thoracic artery graft, and the applicability of the right internal thoracic artery grafts within composite graft systems and multiple arterial revascularization systems [8, 55–57].

Angiographic comparision of the left internal thoracic artery (LITA) graft to the nonharvested right ITA in the same patient indicated that the diameters of the LITA were significantly smaller, while the intima thickness, the maximal intimal thickness and the intima-media ratio were significantly larger in the LITA. NO mediated vasodilatation was not different between the left and right arteries [58].

Use in the surgical myocardial revascularization

Due to anatomical features, the most commonly used artery is the left internal thoracic artery, as a direct coronary artery by-pass graft to the left anterior descending, diagonal or marginal branch of the circumflex coronary artery [4, 35]. The right ITA is used as a free graft for anastomosis with the marginal branch of the circumflex coronary artery [56, 59, 60].

A 30-year long surgical practice in the use of this graft, as well as numerous comparative arteriographic, clinical and histopathological studies have clearly demonstrated the superiority of this arterial graft. The monitoring of the patients during the period of 11 to 18 months after coronary artery bypass surgery performed with the ITA graft, determined the rate of graft patency of 89.8% to 100% [61, 62]. During the 10-year postoperative period, this parameter has a value of more than 80% with the development of low level atherosclerotic changes [63, 64]. For example, during the same period, the rate of graft patency of saphenous vein is between 41% and 56% [7, 65, 66]. In addition, in all of the implanted vein grafts, within six months to one year, a diffuse thickening of the intima develops with the accumulation of foam cells along the lumen of the blood vessel, which indicates an unstable morphology of these lesions and a poor prognostic impact on the fate of these grafts [67].

Following a period of 10 years after surgical myocardial revascularization it was found that patients with great saphenous vein graft compared to patients with implanted internal thoracic artery graft have a 1.41 times greater risk of developing late myocardial infarction, 1.25 to 1.27 times greater risk to develop other late cardiac complications and the need for

hospitalization and 2.00 times more likely they will need the reoperation. Finally, the possibility of fatal outcome is 1.61 times higher among patients with venous graft [68].

Contemporary studies proved that the outcome of CABG with ITA is superior to percutaneous coronary interventions (PCI) in terms of outcome, the need for repeated revascularization and mortality rate after 3, 4 and 5 years postoperatively [69, 70] and remains the therapy of choice for multivessel disease [71–75]. Excellent patency rate was observed when the ITA was used in the technique of minimally invasive direct coronary artery bypass grafting (MIDCABG) [71, 72].

Conclusion

The internal thoracic artery is currently the conduit of the first choice in the surgical myocardial revascularization. Its unique histological characteristics and hemodynamic adaptability enable long-term patency and reliable perfusion of ischemic myocardium. The adaptability of the internal thoracic artery comes from the fact that this is the artery of mixed (transitional) type and from the highly active system of endogenous nitrate. The important features from the clinical point of view are low level of atherosclerosis, stable morphology of atherosclerotic lesions and a potential for positive remodeling. The true challenge in future studies should be further research on the capacity for endothelium renewal and the differentiation of vascular wall resident progenitor cells present within the adventitia of the internal thoracic artery.

Acknowledgements

The research activities were supported by the grants No. 175005, 175061, III41002, III45005 and 41022 from the Ministry of Education, Science and Technological Development of the Republic of Serbia.

REFERENCES

1. *Catinella FP, Cunningham JN, Srungaram RK, Baumann FG, Nathan IM, Glassman EA,* et al. The factors influencing early patency of coronary artery bypass vein grafts: correlation of angiographic and ultrastructural findings. J Thorac Cardiovasc Surg 1982; 83(5): 686−700.
2. *Campos EE, Cinderella JA, Farhi ER.* Long-term angiographic follow-up of normal and minimally diseased saphenous vein grafts. J Am Coll Cardiol 1993; 21(5): 1175−80.
3. *Fukui T, Tabata M, Manabe S, Shimokawa T, Takanashi S.* Graft selection and one-year patency rates in patients undergoing coronary artery bypass grafting. Ann Thorac Surg 2010; 89(6): 1901−5.
4. *Fukui T, Tabata M, Taguri M, Manabe S, Morita S, Takanashi S.* Extensive reconstruction of the left anterior descending coronary artery with an internal thoracic artery graft. Ann Thorac Surg 2011; 91(2): 445−51.
5. *Suma H, Takeuchi A, Hirota Y.* Myocardial revascularization with combined arterial grafts utilizing the internal mammary and the gastroepiploic arteries. Ann Thorac Surg 1989; 47(5): 712−5.
6. *Chong CF.* New method of myocardial revascularization with the radial artery. Ann Thorac Surg 2000; 69(1): 318.
7. *van Son JA, Smedts F, de Wilde PC, Pijls NH, Wong-Alcala L, Kubat K,* et al. Histological study of the internal mammary artery with emphasis on its suitability as a coronary artery bypass graft. Ann Thorac Surg 1993; 55(1): 106−13.
8. *Labudović-Borović M, Borović S, Marinković-Erić J, Todorović V, Puškaš N, Kočica M,* et al. A comprehensive morphometric analysis of the internal thoracic artery with emphasis on age, gender and left-to-right specific differences. Histol Histopathol 2013; 28(10): 1299−314.
9. *Labudović-Borović M.* Comparative histological, histochemical and morphometric analysis of arterial grafts in surgical revascularization of the myocardium [thesis]. Belgrade: School of Medicine; 2003. (Serbian)
10. *Gaudino M, Toesca A, Nori SL, Glieca F, Possati G.* Effect of skeletonization of the internal thoracic artery on vessel wall integrity. Ann Thorac Surg 1999; 68(5): 1623−7.
11. *Hata M, Shiono M, Orime Y, Yagi S, Yamamoto T, Okumura H,* et al. Clinical results of coronary artery bypass grafting with use of the internal thoracic artery under low free flow conditions. J Thorac Cardiovasc Surg 2000; 119(1): 125−9.
12. *Angelini GD, Christie MI, Bryan AJ, Lewis MJ.* Surgical preparation impairs release of endothelium-derived relaxing factor from human saphenous vein. Ann Thorac Surg 1989; 48(3): 417−20.
13. *Quist WC, Haudenschild CC, LoGerfo FW.* Qualitative microscopy of implanted vein grafts. Effects of graft integrity on morphologic fate. J Thorac Cardiovasc Surg 1992; 103(4): 671−7.
14. *Deja MA, Wos S, Golba KS, Zurek P, Domaradzki W, Bachowski R,* et al. Intraoperative and laboratory evaluation of skeletonized versus pedicled internal thoracic artery. Ann Thorac Surg 2000; 68(6): 2164−8.
15. *Buyukates M, Kandemir O, Gun BD, Aktunc E, Kurt T.* Immunohistochemical comparison of traditional and modified harvesting of the left internal mammary artery. Tex Heart Inst J 2007; 34(3): 290−5.
16. *Luscher TF, Vanhoutte PM, Raij L.* Antihypertensive treatment normalizes decreased endothelium-dependent relaxations in rats with salt-induced hypertension. Hypertension 1987; 9(Suppl 3): 193.
17. *Luscher TF, Noll G.* The pathogenesis of cardiovascular disease: role of the endothelium as a target and mediator. Atherosclerosis 1995;118(Suppl): S81−90.
18. *Lüscher TF, Yang Z, Tschudi M, von Segesser L, Stulz P, Boulanger C,* et al. Interaction between endothelin-1 and endothelium-derived relaxing factor in human arteries and veins. Circ Res 1990; 66(4): 1088−94.
19. *Pešić S, Grbović L, Jovanović A, Inić M, Radovanović P.* The role of perforating branch of human internal mammary artery endothelium in the vascularisation of mammary gland. Folia Anatomica 1998; 25(Suppl 2): 143.
20. *Ninković M, Anderl H, Hefel L, Schwabegger A, Wechselberger G.* Internal mammary vessels: a reliable recipient system for free flaps in breast reconstruction. Br J Plast Surg 1995; 48(8): 533−9.
21. *Shi Y, Patel S, Davenpeck KL, Niculescu R, Rodriguez E,* et al. Oxidative stress and lipid retention in vascular grafts: comparison between venous and arterial conduits. Circulation 2001; 103(19): 2408−13.
22. *Yang ZH, Stulz P, von Segesser L, Bauer E, Turina M, Lüscher TF.* Different interactions of platelets with arterial and venous coronary bypass vessels. Lancet 1991; 337(8747): 939−43.

23. *Tsoukatos DC, Brochériou I, Moussis V, Panopoulou CP, Christofidou ED, Koussissis S,* et al. Platelet-activating factor acetylhydrolase and transacetylase activities in human aorta and mammary artery. J Lipid Res 2008; 49(10): 2240−9.
24. *Otsuka F, Yahagi K, Sakakura K, Virmani R.* Why is the mammary artery so special and what protects it from atherosclerosis. Ann Cardiothorac Surg 2013; 2(4): 519−26.
25. *Foglieni C, Maisano F, Dreas L, Giazzon A, Ruotolo G, Ferrero E,* Maseri A. Mild inflammatory activation of mammary arteries in patients with acute coronary syndromes. Am J Physiol Heart Circ Physiol 2008;294(6):2831-7. PubMed PMID: 18441195
26. *Nemes A, Sotonyi P, Balogh A, Nagy J.* Use of the internal mammary artery for myocardial revascularization. Acta Chir Acad Sci Hung 1977; 18(2): 123−8.
27. *Sisto T.* Atherosclerosis in internal mammary and related arteries. Scand J Thor Cardiovasc Surg 1990; 24(1): 7−11.
28. *Sisto T, Isola J.* Incidence of atherosclerosis in the internal mammary artery. Ann Thorac Surg 1989; 47(6): 884−6.
29. *Labudović-Borović M, Borović S, Perić M, Vuković P, Marinković J, Todorović V,* et al. The internal thoracic artery as a transitional type of artery: a morphological and morphometric study. Histol Histopathol 2010; 25(5): 561−76.
30. *Živković K, Labudović-Borović M.* Morphological and morphometric characteristics of the inferior epigastric artery. Med Podml 2004; 55(1−2): 23−30. (Serbian)
31. *Sims FH.* The internal mammary artery as a bypass graft. Ann Thorac Surg 1987; 44(1): 2−3.
32. *Sims FH, Chen X, Gavin JB.* The importance of a substantial elastic lamina subjacent to the endothelium in limiting the progression of atherosclerotic changes. Histopathology 1993; 23(4): 307−17.
33. *Labudović-Borović M.* Histological characteristics of grafts used in surgical myocardial revascularization. In: *Perić M*, editor. Proceedings of Ischemic heart disease and revascularization - modern therapy and guidance Symposium. XVII Congress of the cardiology society of Serbia with international participation. Belgrade, 2009 October 18−21; Belgrade: The Ministry of Health of the Republic of Serbia; 2004. p. 54−8. (Serbian)
34. *Loop FD, Spampinato N, Cheanvechai C, Effler DB.* The free internal mammary artery bypass graft. Use of the IMA in the aorta-to-coronary artery position. Ann Thorac Surg 1973; 15(1): 50−5.
35. *Frazier BL, Flemma RJ, Tector AJ, Korns ME.* Atherosclerosis involving the internal mammary artery. Ann Thorac Surg 1974; 18(3): 305−7.
36. *Cizek SM, Bedri S, Talusan P, Silva N, Lee H, Stone JR.* Risk factors for atherosclerosis and the development of preatherosclerotic intimal hyperplasia. Cardiovasc Pathol 2007; 16(6): 344−50.
37. *Fawcett D.* Blood and lymph vascular systems. In: *Fawcett D*, editor. A Textbook of Histology. Philadelphia: WB Saunders Company; 1986. p. 367−406.
38. *Jores L.* Arterien. In: *Henke F, Lubarsch O*, editors. Handbuch der Speziellen Pathologischen Anatomie und Histologie, vol II: Herz und Gefasse, 1st ed. Berlin: Springer; 1924. p. 608−786.
39. *Movat HZ, More RH, Haust MD.* The diffuse intimal thickening of the human aorta with aging. Am J Pathol 1958; 34(6): 1023−31.
40. *Van Son JA, Smedts F, Vincent JG, van Lier HJ, Kubat K.* Comparative anatomic studies of various arterial conduits for myocardial revascularization. J Thorac Cardiovasc Surg 1990; 99(4): 703−7.
41. *Ortiz PP, Díaz P, Daniel-Lamazière JM, Lavallée J, Bonnet J, Torres A,* et al. Morphometry of the human splenic artery: muscular columns, morphofunctional aspects and developmental implications. Histol Histopathol 1998; 13(2): 315−24.
42. *Ortiz PP, Sarrat R, Daret D, Whyte J, Torres A, Lamazière JM.* Elastin variations implicating in vascular smooth muscle cells phenotype in human tortuous arteries. Histol Histopathol 2000; 15(1): 95−100.
43. *Thyberg J.* Phenotypic modulation of smooth muscle cells during formation of neointimal thickenings following vascular injury. Histol Histopathol 1998; 13(3): 871−91.
44. *Helle KB.* Vasostatins. In: *Helle KB, Aunis D*, editors. Chromogranins: Functional and clinical aspects. New York: Kluwer Academic/Plenum Publishers; 2000. p. 225−38.
45. *Rivard A, Andrés V.* Vascular smooth muscle cell proliferation in the pathogenesis of atherosclerotic cardiovascular diseases. Histol Histopathol 2000; 15(2): 557−71.
46. *Bashour TT, Hanna ES, Mason DT.* Myocardial revascularization with internal mammary artery bypass: an emerging treatment of choice. Am Heart J 1986; 111(1): 143−51.
47. *Barner HB.* Remodeling of arterial conduits in coronary grafting. Ann Thorac Surg 2002; 73(4): 1341−5.
48. *Kieser TM, Lewin AM, Graham MM, Martin B, Galbraith DP, Rabi DM*, et el. Outcomes associated with bilateral internal thoracic artery grafting: the importance of age. Ann Thorac Surg 2011; 92(4): 1269−75.
49. *Zengin E, Chalajour F, Gehling UM, Ito WD, Treede H, Lauke H,* et al. Vascular wall resident progenitor cells: a source for postnatal vasculogenesis. Development 2006; 133(8): 1543−51.
50. *Geiringer E.* Intimal vascularization and atherosclerosis. J Pathol Bacteriol 1951; 63(2): 201−11.
51. *Scotland R, Vallance P, Ahluwalia A.* On the regulation of tone in vasa vasorum. Cardiovasc Res 1999; 41(1): 237−45.
52. *Hu X, Zhao Q.* Skeletonized internal thoracic artery harvest improves prognosis in high-risk population after coronary artery bypass surgery for good quality grafts. Ann Thorac Surg 2011; 92(1): 48−58.
53. *Perić M.* Arterial grafts in surgical myocardial revascularization. Beograd: Reprograf; 2002. p. 4−6. (Serbian)
54. *Mannacio V, di Tommaso L, Antignano A, de Amicis V, Stassano P, Pinna GB,* et al. Endothelial nitric oxide synthase expression in postmenopausal women: a sex-specific risk factor in coronary surgery. Ann Thorac Surg 2012; 94(6): 1934−9.
55. *Kinoshita T, Asai T, Murakami Y, Nishimura O, Hiramatsu N, Suzuki T,* et al. Bilateral versus single internal thoracic artery grafting in dialysis patients with multivessel disease. Heart Surg Forum 2010; 13(5): 280−6.
56. *Cho W, Yoo DG, Kim JB, Lee SH, Jung SH, Chung CH,* et al. Left internal thoracic artery composite grafting with the right internal thoracic versus radial artery in coronary artery bypass grafting. J Card Surg 2011; 26(6): 579−85.
57. *Tatoulis J, Buxton BF, Fuller JA.* The right internal thoracic artery: the forgotten conduit--5, 766 patients and 991 angiograms. Ann Thorac Surg 2011; 92(1): 9−15.
58. *Porto I, Gaudino M, de Maria GL, di Vito L, Vergallo R, Bruno P,* et al. Long-term morphofunctional remodeling of internal thoracic artery grafts: a frequency-domain optical coherence tomography study. Circ Cardiovasc Interv 2013; 6(3): 269−76.
59. *Landymore RW, Chapman DM.* Anatomical studies to support the expanded use of the internal mammary artery graft for myocardial revascularization. Ann Thorac Surg 1987; 44(1): 4−6.
60. *Cho KR, Hwang HY, Kim J, Jeong DS, Kim K.* Comparison of right internal thoracic artery and right gastroepiploic artery Y grafts anastomosed to the left internal thoracic artery. Ann Thorac Surg 2010; 90(3): 744−50.
61. *Chenvechai C, Irarrazaval MJ, Loop FD, Effler DB, Rincon G, Sones FM.* Aorta-coronary bypass grafting with the internal mammary artery: clinical experience in 70 patients. J Thorac Cardiovasc Surg 1975; 70(2): 278−81.

62. *Sauvage LR, Wu HD, Kowalsky TE, Davis CC, Smith JC, Rittenhouse EA,* et al. Healing basis and surgical techniques for complete revascularization of the left ventricle using only the internal mammary arteries. Ann Thorac Surg 1986; 42(4): 449−65.
63. *Barner HB, Swartz MT, Mudd JG, Tyras DH*. Late patency of the internal mammary artery as a coronary bypass conduit. Ann Thorac Surg 1982; 34(4): 408−12.
64. *Schwartz D, Factor S, Schwartz J, Petrosian E, Blitz A, Mcloughlin D*, et al. Histological evaluation of the inferior epigastric artery in patients with known atherosclerosis. Eur J Cardiothorac Surg 1992; 6(8): 438−41.
65. *Grondin CM, Campeau L, Lesperance J, Enjalbert M, Bourassa MG*. Comparison of late changes in internal mammary artery and saphenous vein in two consecutive series of patients 10 years after operation. Circulation 1984; 70(Suppl 1): 208−12.
66. Van der Wal A, Becker A, Elbers J, Das P. An immunocytochemical analysis of rapidly progressive atherosclerosis in human vein grafts. Eur J Cardiothorac Surg 1992; 6(9): 469−74.
67. *Kockx MM, de Meyer GR, Bortier H, de Meyere N, Muhring J, Bakker A,* et al. Luminal foam cell accumulation is associated with smooth muscle cell death in the intimal thickening of human saphenous vein grafts. Circulation 1996; 94(6): 1255−62.
68. *Loop FD, Lytle BW, Cosgrove DM, Stewart RW, Goormastic M, Williams GW,* et al. Influence of the internal-mammary-artery graft on 10-year survival and other cardiac events. N Engl J Med 1986; 314(1): 1−6.
69. *Weintraub WS, Grau-Sepulveda MV, Weiss JM, O'Brien SM, Peterson ED, Kolm P*, et al. Comparative effectiveness of revascularization strategies. N Engl J Med 2012; 366(16): 1467−76.
70. *Farkouh ME, Domanski M, Sleeper LA, Siami FS, Dangas G, Mack M*, et al. Strategies for multivessel revascularization in patients with diabetes. N Engl J Med 2012; 367(25): 2375−84.
71. *Holzhey DM, Cornely JP, Rastan AJ, Davierwala P, Mohr FW*. Review of a 13-year single-center experience with minimally invasive direct coronary artery bypass as the primary surgical treatment of coronary artery disease. Heart Surg Forum 2012; 15(2): 61−8.
72. *Katz WE, Zenati M, Mandarino WA, Cohen HA, Gorcsan J*. Assessment of left internal mammary artery graft patency and flow reserve after minimally invasive direct coronary artery bypass. Am J Cardiol 1999; 84(7): 795−801.
73. *Borović S*. Short-term mechanic circulatory support. In: *Perić M*, editor. Surgical Revascularization of the Ischemic Myocardium. Belgrade: Faculty of Medicine, University of Belgrade; 2013. p. 315−29. (Serbian)
74. *Nezić D, Knezević A, Borović S, Cirković M, Milojević P*. Coronary-coronary free internal thoracic artery graft on a single, distal, left anterior descending artery lesion. J Thorac Cardiovasc Surg 2004; 127(5): 1517−8.
75. *Nezić DG, Knezević AM, Cirković MV, Borović SD, Milojević PS*. Arterial coronary-coronary conduit over single, distal left anterior descending coronary artery lesion: 3. 5 years afterward. J Thorac Cardiovasc Surg 2007; 134(1): 238−40.

Received on May 15, 2014.
Accepted on July 28, 2014.
Online First August, 2015.

PRELIMINARY REPORT

UDC: 62::61]::615.835
DOI: 10.2298/VSP140610077S

Opto-magnetic imaging spectroscopy in characterization of the tissues during hyperbaric oxygen therapy

Karakterizacija tkiva tokom hiperbarične oksigenacije primenom optomagnetne imidžing spektroskopije

Mariana Sedlar*, Gorana V. Nikolić†, Aleksandra Dragičević†, Djuro Koruga†

***Centre for Hyperbaric Medicine, Belgrade, Serbia; †Department of Biomedical Engineering, Faculty of Mechanical Engineering, University of Belgrade, Belgrade, Serbia**

Abstract

Background/Aim. Opto-magnetic imaging spectroscopy (OMIS) was used as a novel method to determine tissue molecular conformation changes during hyperbaric oxygen (HBO) therapy. The aim of this study was to examine the usefulness of OMIS for the assessment of HBO therapy effectiveness on the diseased tissue. **Methods.** OMIS is concerned with obtaining paramagnetic/diamagnetic properties of materials, related to the presence of unpaired/paired electrons based on their interaction with visible light. The basic tool is light of wavelength in the range between 400 nm and 700 nm and its interaction with tissue. The study included 22 subjects: 16 angiopathy patients and 6 healthy subjects as the control group. OMIS was used with patients on the 1st, 10th and 20th session and with the control group on the 1st, 10th and 20th day without HBO therapy in between. **Results.** The obtained results showed that healthy skin of all the control group subjects had the same shape curve. In the angiopathy patient group, before the first session OMIS showed tissue disorder and after the last session results resembled more closely the results in healthy tissue. The differences in the tissue state in the angiopathy group before each session were noticeable, showing normalized tissue under the influence of HBO. **Conclusion.** The results show that OMIS could be used as a diagnostic tool for detection of the tissue state before and after the HBO therapy.

Key words:
hyperbaric oxygenation; tissues; spectrum analysis: biomedical engineering; methods; optical imaging.

Apstrakt

Uvod/Cilj. Optomagnetna imidžing spektroskopija (OMIS) je nova metoda primenjena za određivanje molekularnih promena u tkivu tokom hiperbarične oksigenoterapije (HBO). Cilj rada bio je da se ispita efikasnost OMIS u proceni dejstva HBO na obolela tkiva. **Metode.** OMIS se bavi određivanjem paramagnetnih/dijamagnetnih karakteristika materijala, koje su posledica prisustva sparenih i nesparenih elektrona usled interakcije materijala sa vidljivom svetlošću. Osnovni alat je bela svetlost talasne dužine 400–700 nm i njena interakcija sa tkivom. Studija je obuhvatila 22 ispitanika: 16 bolesnika sa angiopatijama različitog porekla i 6 zdravih osoba kao kontrolnu grupu. OMIS je primenjena kod bolesnika tokom prvog, desetog i dvadesetog tretmana, a kod kontrolne grupe prvog, desetog i dvadesetog dana bez HBO terapije, u međuvremenu. **Rezultati.** Dobijeni rezultati pokazuju da je rezultantna kriva kod svih članova kontrolne grupe bila istog oblika. Kod bolesnika sa angiopatijom krive dobijene merenjem pre prvog tretmana prikazivale su neuređenost tkiva, dok je nakon poslednjeg tretmana kriva bila istog oblika kao kod zdravog tkiva. Postojala je uočljiva razlika u stanju tkiva kod bolesnika pre i nakon HBO tretmana. **Zaključak.** Dobijeni rezultati pokazuju da bi OMIS mogla da se primenjuje kao dijagnostičko sredstvo za utvrđivanje stanja tkiva pre i posle HBO terapije.

Ključne reči:
hiperbarička oksigenacija; tkiva; spektar, analize; biomedicinski inženjering; metodi; optičko snimanje.

Introduction

Hyperbaric oxygen (HBO) therapy is breathing 100% oxygen at a pressure higher than atmospheric pressure while in the hyperbaric chamber. It is used to treat patients with different vascular problems, microangiopathy, diabetes mellitus complications, embolism, gangrene, burns, etc [1, 2].

Various optical methods, such as pulse oximetry, near infrared spectroscopy, and fluorescence spectroscopy have been used for measuring hemoglobin oxygen saturation, tissue

Correspondence to: Mariana Sedlar, Department of Biomedical Engineering, Faculty of Mechanical Engineering, University of Belgrade, Belgrade, Serbia. E-mail: mariana.sedlar@gmail.com

oxygenation as well as the glucose level in blood in some diseases [3–5], but due to different limitations in methods and specificities of HBO therapy, their evaluation value is limited [6,7].

In this paper, opto-magnetic imaging spectroscopy (OMIS) is presented as a method used for skin characterization during hyperbaric oxygen therapy. Until now OMIS was used on different types of matter, starting with non-organic compounds such as water [8], biological tissue such as healthy skin [9], contact lenses [10] and live microorganisms such as viruses [11].

The aim of this study was to identify the expected positive effects of HBO therapy on the diseased tissue and to characterize skin properties during the therapy. The results of applied OMIS in the control group are also reported.

Methods

The OMIS method is concerned with obtaining paramagnetic/diamagnetic properties of materials (unpaired/paired electrons) based on their interaction with visible light. The basic tool is the light of wavelength in the range between 400 nm and 700 nm. Since light is composed of coupled electrical and magnetic field perpendicular to each other in propagation wave, if sample is exposed to the white light under the angle of 90˚, reflected unpolarized light will have information about electromagnetic properties of the sample. On the other hand, if the light beam is incident under a particular angle (the Brewster angle) to a sample of the material of interest, the reflected light will be polarized by the sample itself (Figure 1) [12]. The longitudinal wave of the reflected light will dominantly have an electrical component whose properties will depend on the electrical state of the surface. However, the magnetic component of the reflected light will be perpendicular to the electrical one, but as a transverse wave. Since the transverse wave has a small intensity in the longitudinal direction its influence on the sensor will be negligible. Therefore, the electrical properties of a material can be obtained by measuring the reflected light. The difference between reflected non-polarized and polarized lights will give us magnetic properties of the sample.

The digital image is recorded with a standard digital camera, which uses the specially self-constructed extra component placed in front of the objective (Figure 2) [12]. This extra component contains the set of the diodes for illuminating the sample. The NL-B53 device with the Canon digital camera, model IXUS 105, 12.1 Mpix was used. The illumination of the sample was achieved by using white diffused light from the diodes (three light diodes aligned under the angle of 53˚ to vertical axis, and with the mutual angle distance of 120˚ in the horizontal plane). The recording can be conducted over the circle like shaped area with 25 mm in diameter.

This method uses the color system analogous to human eye perception. It consists of red, green, and blue colors (RGB). The algorithm for image processing and chromatic information determination is based on a chromatic diagram called the Maxwell triangle and on an operation of the spec-

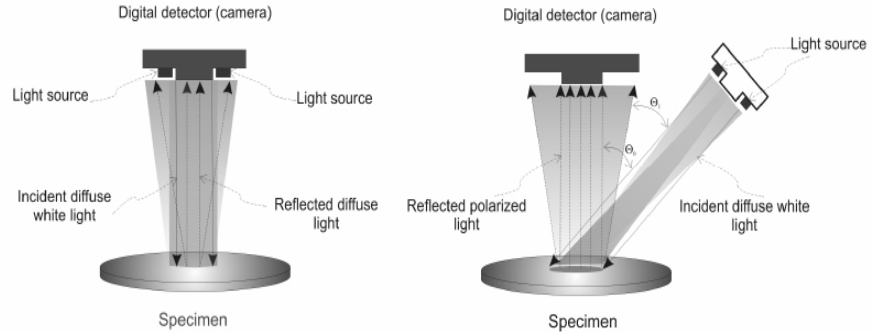

Fig. 1 – The experimental arrangement sketch showing relative positions of light sources for white (a) and reflected polarized light (b). The degree of light polarization is 95.4%, while angular diffusion of the light source (six white light-emittind diodes arranged in a circle) is ± 1:6° (difference between angles θ and θ_1) [12].

Fig. 2 – Basic operational setup (prototype) for opto-magnetic imaging spectroscopy (NanoLab, Faculty of Mechanical Engineering, University of Belgrade) [12].

tral convolution referring to the blue (B) and the red (R) channel. It is marked as (R-B)&(W-P) which indicates the convolution operation of the blue and the red channels (R-B) of "diffusive" (white light-W) and "polarization" (polarized light-P) response (W-P). The result of this operation is the convolution spectrum. The difference of the convolution spectra of the reflected white light and the polarized light of blue and red channels yields the opto-magnetic convolution spectra [12].

Skin represents the largest organ of the human body. It consists of three main parts: epidermis, dermis and hypodermis. The boundary between epidermis and dermis is the basement membrane which presents a barrier for adverse influences from the external environment.

Patients with compromised circulation are candidates for HBO therapy because it is well known that, eventually, angiopathy disarranges the structure and function of the skin with certain consequences [1, 2, 13]. HBO therapy improves regeneration of wounded tissue and promotes healing.

This investigation was performed at the Centre for Hyperbaric Medicine, Belgrade, Serbia in the period from February to March 2012 in a multiplace hyperbaric chamber and included 16 patients with angiopathy of diverse origin and 6 healthy subjects as the control group. All the subjects involved gave written consent to participate in this research. While sitting in the chamber before the regular HBO therapy, OMIS was used on the skin of the leg or arm, depending on the patient diagnosis and on the skin of the arm of the control group subjects. Pictures were taken both with white and polarized light twice each. The same procedure was repeated after 30 min on 222.915 kPa [2.2 absolute atmosphere (ATA)], and the third time immediately at the end of the therapy on 101.325 kPa (1 ATA). Measurements were repeated in the same way on the 10th and 20th session. OMIS was applied with the control group in the same way as angiopathy group but without HBO therapy in between.

Results

The results obtained using the OMIS method of a few randomly chosen subjects from both groups (control and angiopathy) were presented. The differences between these groups were presented as the characteristics of peaks, wavelength differences and intensity given in the tables below each figure.

The diagrams in the Figure 3 show the results in the control group, i.e. healthy people. By taking the pictures with OMIS and processing them [12], the results obtained show that healthy skin of all the control group subjects had the same curve shape.

These values represent dynamic state of healthy tissue. Small variations are expected because each subject is unique (Figure 3). It has to be stressed that curves of all the subjects in the control group had the same shape on the first, 10th and 20th day. Two examples of healthy subjects of the control group are shown in Figure 4.

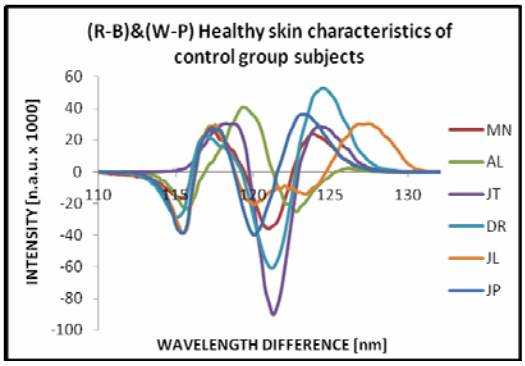

Fig. 3 – Healthy skin opto-magnetic imaging spectrometry spectrum comparison in the control group subjects on the first day. Capital letters indicate initials of the control group subjects.
(R-B) – the blue and the red channels; (W-P) – white light – polarized light response.

a)

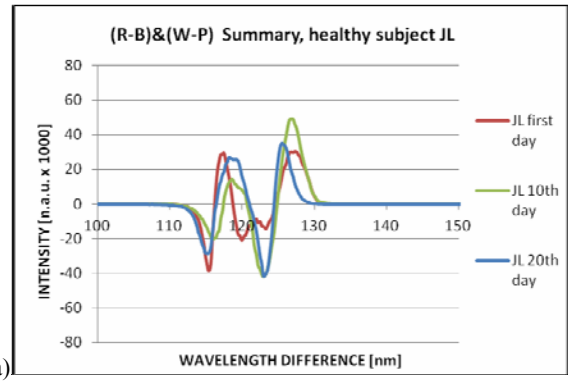

b)

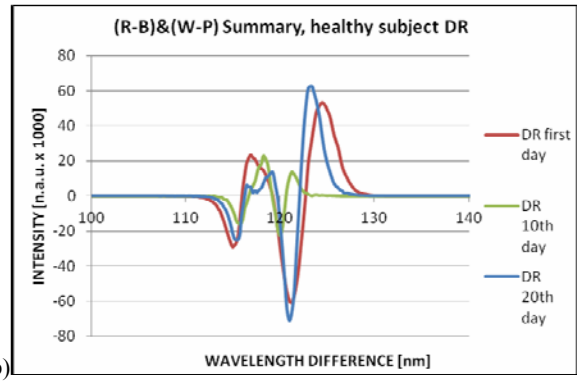

Fig. 4 – Healthy skin opto-magnetic imaging spectrometry spectra comparison on the first, 10th and 20th day: a) of the control group subjects JL (female) and b) DR (male). The same persistency in the curve shape is present in all the control group subjects.
(for abbreviations see under Figure 3).

The values of characteristic peaks are given in Table 1. The negative values represent diamagnetic and positive paramagnetic characteristics. It has to be stressed that diamagnetism indicates stable state of the tissue.

The diagrams in Figure 5 represent the patients with angiopathy. The results in the Figure 5 a (the left figure) show the state of the patients' skin before the first and Figure 5 b (the figure right) after 20th session. After the last session the results obtained show similarity with the control group subjects.

All curves in Figure 5a, (left) start as paramagnetic with one exception indicating the presence of unpaired electrons, which generate tissue disorder. After the last HBO session (Figure 5b, right), the curves within some of the patients again starts as paramagnetic, but all the curves are of narrower shape and higher amplitude.

Wavelength differences and the intensity of the characteristic peaks before the first and after the last therapy are shown in Tables 2 and 3, respectively.

Table 1

Intensities and wavelengths corresponding to characteristic peaks for all the control group subjects

Peaks	DR		JT		AL		JL		MN		JP	
	w [nm]	I [a.u.]*	w [nm]	I [a.u.]	w [nm]	I [a.u.]	w [nm]	I [a.u.]	w [nm]	I [a.u.]	w [nm]	I [a.u.]
Peak 1	114.76	-27.169	117.993	30.131	115.341	-26.576	115.341	-38.47	114.76	-14.283	115.142	-37.246
Peak 2	116.637	21.32	121.224	-90.057	119.22	40.768	117.079	28.63	116.87	23.351	117.079	26.493
Peak 3	120.968	-59.897	123.832	26.49	122.505	-11.402	119.48	-17.528	120.708	-34.856	119.991	-39.842
Peak 4	124.161	51.257	/	/	125.497	0.604	122.249	-11.005	123.343	31.906	122.973	36.665
Peak 5	/	/	/	/	/	/	126.558	29.176	/	/	/	/

***a.u.-arbitrary units [12]; i – intensity; w – wavelength.**

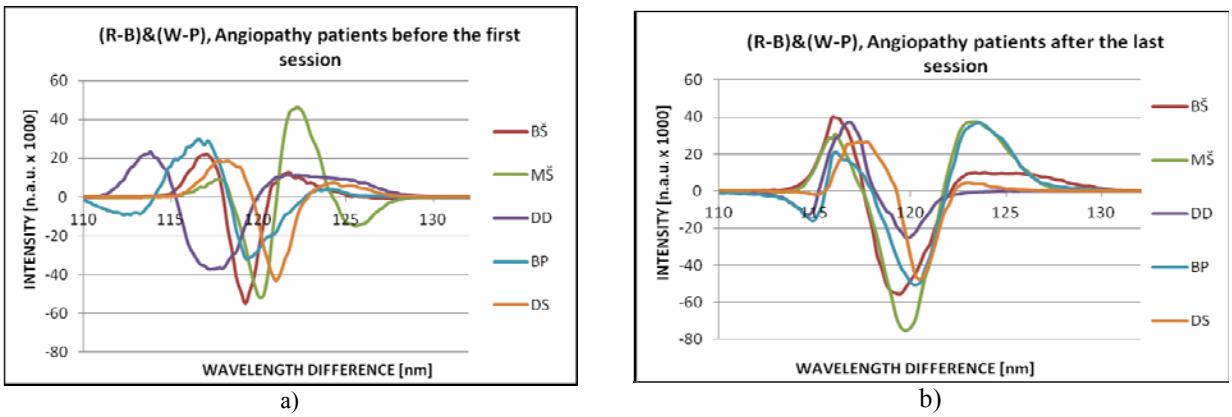

a) b)

Fig. 5 – Comparison of the opto-magnetic imaging spectrometry spectra of the angiopathy patients: a) before the first, and b) after the 20th therapy. (for abbreviations see under Figure 3)

Table 2

Intensities and wavelengths corresponding to characteristic peaks for randomly selected patients with angiopathy before the first therapy

Peaks	MŠ		BŠ		DD		BP		DS	
	w [nm]	I [a.u.]	w [nm]	I [a.u.]	w [nm]	I [a.u.]	w [nm]	I [a.u.]	w [nm]	I [a.u.]
Peak 1	117.33	7.865	116.87	21.999	113.421	21.738	112.461	-8.725	117.737	18.524
Peak 2	119.991	-51.528	119.22	-54.887	117.33	-36.931	116.423	29.326	120.708	-39.044
Peak 3	121.992	45.67	121.224	11.213	120.968	10.09	119.22	-31.797	/	/
Peak 4	125.26	-13.746	/	/	/	/	/	/	/	/

For abbreviations see under Table 1.

Table 3

Intensities and wavelengths corresponding to characteristic peaks for randomly selected patients with angiopathy after the last therapy

Peaks	MŠ		BŠ		DD		BP		DS	
	w [nm]	I [a.u.]	w [nm]	I [a.u.]	w [nm]	I [a.u.]	w [nm]	I [a.u.]	w [nm]	I [a.u.]
Peak 1	115.725	29.000	115.725	35.433	114.189	-9.923	114.571	-13.49	114.571	-1.181
Peak 2	119.48	-73.687	118.967	-54.288	116.423	34.668	116.241	16.241	117.079	26.005
Peak 3	122.973	37.139	122.764	8.257	119.48	-22.107	120.498	-47.428	120.245	-46.19
Peak 4	/	/	128.373	4.086	/	/	123.343	36.673	112.764	4.114

For abbreviations see under Table 1.

After the last therapy, the state of the patients showed an improvement because the differences compared to the control group were diminished.

The diagrams in Figure 6 indicate that OMIS spectra in the angiopathy patients significantly changes during the period of HBO therapy.

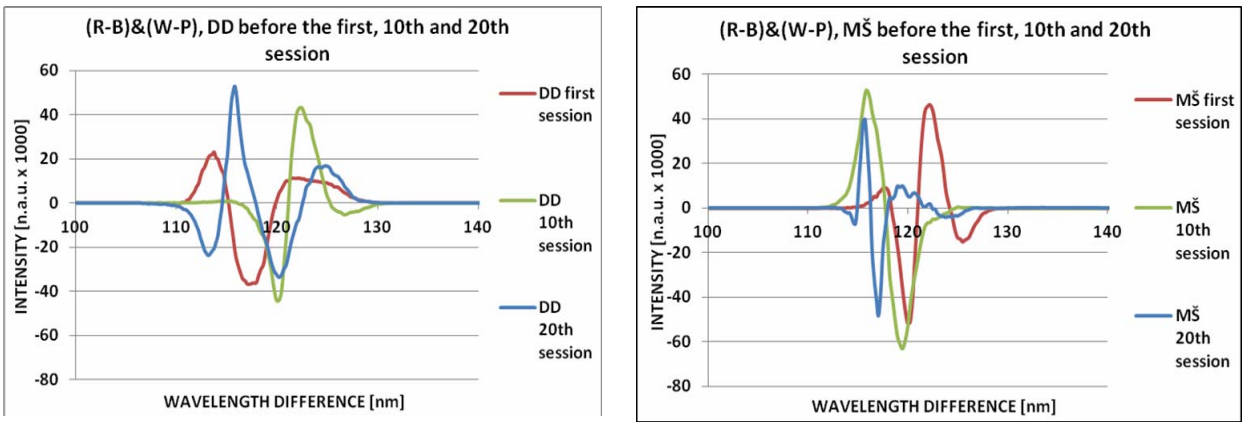

Fig. 6 – Comparison of the opto-magnetic imaging spectrometry spectra of the diseased tissue of two patients with angiopathy on the first, 10th and 20th session.
(for abbreviations see under Figure 3).

Discussion

Small variations of the results of the control group are present which was expected as the skin of the female and male genders differ [9, 14]. The OMIS spectra of healthy skin start as diamagnetic which indicates biophysical stable state of the tissue. After the repeated measurements the shape of the curves for all the control group subjects was not significantly changed (Figure 4) which confirms the stability of healthy tissue. Irregularity in one healthy subject (JT) was noticed as the curve in each measurement started as paramagnetic without proper biophysical explanation. However, the shape of the curve, in general, matched the rest of the curves of other healthy subjects. Further investigation is needed.

The results in Figure 5 within the angiopathy group show shape disorder before the first therapy and after the last therapy. The shape of the curves became more orderly with significantly more resemblance to the healthy tissue results.

The values given in Table 2 show that the first peak of the curves was paramagnetic with one exception (BP) without biophysical explanation according to our knowledge. After the last therapy, some of the subjects had first peaks in the same magnetic state as before the first therapy and in some of them it was changed (Table 3) that needs our further investigation. The result was that all the subjects with the first peak in diamagnetic field belonged to the peripheral neuroangiopathy patients.

Opposite to the results showed in Figure 4, in the angiopathy patients the curve shape before the first, 10th and 20th session was significantly different showing effects of HBO therapy on the tissue normalization (Figure 6).

Conclusion

The obtained results show that opto-magnetic imaging spectrometry can be used as diagnostic tool for detection of the skin state before and after the hyperbaric oxygen therapy. There are the differences between the diagrams and additional biophysical explanation is needed. The study needs to be continued with a larger number of subjects for better understanding of the correlation between opto-magnetic imaging spectrometry, increased level of oxygen and tissue metabolism.

Acknowledgement

This research was supported by the Ministry of Education, Science and Technological Development (Project III41006).

REFERENCES

1. *Thom SR.* Hyperbaric Oxygen: Its Mechanisms and Efficacy. Plast Reconstr Surg 2011; 127(1): 131–41.
2. *Niinikoski JH.* Clinical hyperbaric oxygen therapy, wound perfusion, and transcutaneous oximetry. World J Surg 2004; 28(3): 307–11.
3. *Brown CD, Davis HT, Ediger MN, Fleming CM, Hull EL, Rohrscheib M.* Clinical assessment of near-infrared spectroscopy for noninvasive diabetes screening. Diabetes Technol Ther 2005; 7(3): 456–66.

4. *Mathieu D, Mani R.* A review of the Clinical Significance of Tissue Hypoxia Measurements in Lower Extremity Wound Management. Int J Low Extrem Wound 2007; 6(4): 273−83.
5. *Larsson A, Uusijärvi J, Eksborg S, Lindholm P.* Tissue oxygenation measured with near-infrared spectroscopy during normobaric and hyperbaric oxygen breathing in healthy subjects. Eur J Appl Physiol 2010; 109(4): 757−61.
6. *Stirban A.* Noninvasive skin fluorescence spectroscopy for diabetes screening. J Diabetes Sci Technol 2013; 7(4): 1001−4.
7. *Springett R, Swartz HM.* Measurements of oxygen in vivo: overview and perspectives on methods to measure oxygen within cells and tissues. Antioxid Redox Signal 2007; 9(8): 1295−301.
8. *Koruga Đ, Miljković S, Ribar S, Matija L., Kojić D.* Water Hydrogen Bonds Study by Opto-Magnetic Fingerprint. Acta Phys Polon A 2010; 117(5): 777−81.
9. *Koruga Đ, Bandić J, Janjić G, Lalović C, Munćan J, Dobrosavljević-Vukojević D.* Epidermal layers characterisation by opto-magnetic spectroscopy based on digital image of skin. Acta Phys Polon A 2012; 121(3): 1111−5.
10. *Stamenković D, Kojić D, Matija L, Miljković Z, Babić B.* Physical Properties of Contact Lenses Characterized by Scanning Probe Microscopy and OptoMagnetic Fingerprint. Int J Mod Phys B 2010; 24(6−7): 825−34.
11. *Papić-Obradović M, Kojić D, Matija L.* Opto-Magnetic Method for Epstein - Barr Virus and Cytomegalovirus Detection in Blood Plasma Samples. Acta Phys Polon A 2010; 117(5): 782−4.
12. *Koruga Đ, Tomić A.* System and Method for Analysis of Light-matter Interaction Based on Spectral Convolution. US Patent Pub. No: 2009/0245603, 2009.
13. *Gordillo GM, Sen CK.* Revisiting the essential role of oxygen in wound healing. Am J Surg 2003; 186(3): 259−63.
14. *Ribar S.* A hybrid software system for diagnosing the biophysical properties of the skin based on expert system, neural networks, fuzzy logic and genetic algorithms. Belgrade: Faculty of Mechanical Engineering, University of Belgrade; 2011. (Serbian)

Received on June 10, 2014.
Accepted on July 17, 2014.
Online First August, 2015.

SHORT COMMUNICATION

UDC: 616.6-089
DOI: 10.2298/VSP140426076H

Idiopathic retroperitoneal fibrosis: A report on 15 patients

Idiopatska retroperitonealna fibroza: rezultati lečenja 15 bolesnika

Jovan Hadži-Djokić*, Tomislav Pejčić†, Dragoslav Bašić‡, Ivana Vukomanović§, Zoran Džamić†‖, Miodrag Aćimović†‖, Milan Radovanović†

***Serbian Academy of Sciences and Arts, Belgrade, Serbia; †Urological Clinic, Clinical Center of Serbia, Belgrade, Serbia; ‡Urological Clinic, Clinical Center Niš, Niš, Serbia; §Department of Urology, Medical Center Bežanijska Kosa, Belgrade, Serbia; ‖Faculty of Medicine, University of Belgrade, Belgrade, Serbia**

Abstract

Background/Aim. Retroperitoneal fibrosis (RPF) represents a chronic pathological process characterized by fibrosis which entraps and compresses the ureters and the great blood vessels in the retroperitoneal space. A specific form of RPF is idiopathic RPF, an uncommon collagen vascular disease of unclear etiology. The series of 15 patients which underwent open surgical repair due to idiopathic RPF is presented herein. **Methods.** From 1989 to 2012, 11 male and 4 female patients underwent surgery due to primary RPF. The ureters were entrapped unilaterally (7 patients), or bilaterally (8 patients). Major symptoms included low back pain due to hydronephrosis (9 patients), uremia (4 patients), and urinary tract infection (2 patients). The diagnosis was based on intravenous urography (IVU), retrograde ureteropyelography and computed tomography (CT). **Results.** Surgical procedures included intraperitoneal ureteral displacement (8 patients) and ureteral wrapping with omental flap (6 patients). One patient underwent bilateral ureteral stenotic segments resection and oblique ureterography, followed by wrapping with omental flap. Pathological examination confirmed primary RPF in all patients. The mean operative time was 3.5 h (range 2.5–4.5 h). The average intrahospital stay was 21 days (range 16–26 days). The mean follow up was 32 months (6–46 months). During the follow up, 12 patients had improvement on IVU. **Conclusion.** Early recognition of signs and symptoms of RPF is of the utmost importance for the outcome. Surgical procedures, including ureteral wrapping with omental flap, or intraperitoneal ureteral displacement, usually represent definitive treatment.

Key words:
retroperitoneal fibrosis; diagnosis, differential; urologic surgical procedures.

Apstrakt

Uvod/Cilj: Retroperitonealna fibroza (RPF) predstavlja hronični patološki proces koji karakteriše fibroza koja obuhvata i pritiska ureter i velike krvne sudove u retroperitonealnom prostoru. Specifičan oblik RPF je idiopatska RPF, retka vaskularna kolagena bolesti nejasne etiologije. U ovom radu predstavljena je grupa od 15 bolesnika koji su operisani zbog idiopatske RPF. **Metode.** Od 1989. do 2012. ukupno 11 muškaraca i četiri žene operisani su zbog primarne RPF. Ureteri su bili zahvaćeni jednostrano kod sedam bolesnika ili bilateralno kod osam bolesnika. Glavni simptomi bili su lumbalni bol zbog hidronefroze, uremija i infekcije urinarnog trakta. Dijagnoza je postavljena na osnovu intravenske urografije (IVU), retrogradne ureteropijelografije i kompjuterizovane tomografije (KT). **Rezultati.** Primenjene su sledeće hirurške procedure: intraperiteonalno postavljanje uretera kod osam bolesnika i obmotavanje uretera omentalnim flapom kod šest bolesnika. Kod jednog bolesnika učinjena je bilateralna resekcija stenotičnog segmenta i ureterografija, a potom i obmotavanje uretera omentalnim flapom. Patološki pregled potvrdio je postojanje primarne RPF kod svih bolesnika. Prosečno trajanje operacije bilo je 3,5 sata (od 2,5 do 4,5 sata). Prosečni boravak u bolnici bio je 21 dan (od 16 do 26 dana). Prosečno praćenje iznosilo je 32 meseca (od 6 do 46 meseci). Tokom praćenja, kod 12 bolesnika primenom IVU konstantovano je poboljšanje. **Zaključak.** Rano prepoznavanje znakova i simptoma RPF od najveće je važnosti za ishod lečenja. Hirurški zahvati, uključujući obmotavanje uretera omentalnim flapom ili intraperitonealno postavljanje uretera, obično predstavljaju definitivno lečenje.

Ključne reči:
fibroza, retroperitonealna; dijagnoza, diferencijalna; hirurgija, urološka, procedure.

Correspondence to: Tomislav Pejčić, Urological Clinic, Clinical Center of Serbia, Knez Mihailova 35, 11 000 Belgrade, Serbia.
Phone: +381 11 2121 616. E-mail: tomislav_pejcic@vektor.net

Introduction

Retroperitoneal fibrosis or Ormond's disease is an uncommon collagen vascular disease of unclear etiology. The disease was documented by Albaran in 1905 for the first time and rediscovered by John Kelso Ormond in 1948 [1, 2].

The RPF is a chronic diffuse retroperitoneal inflammatory process that can entrap the retroperitoneal structures, mainly the ureters and the great vessels. Fibrosis may involve the mediastinum, scrotum and the base of mesentery, as well. The symptoms are nonspecific, including flank pain, malaise, anorexia and renal failure. Some patients are asymptomatic and are diagnosed with RPF during the follow-up of the primary disease [3–5]. The RPF is generally idiopathic, often in the presence of inflammatory abdominal aortic aneurysm or syndrome of vasculitis. However, RPF can appear secondary to the use of certain drugs, malignant diseases, infections, radiotherapy and surgery. Some cases are related to gynecological malignancy.

In cases with renal failure, retrograde ureteropyelography may reveal the length of the involved ureter. In addition, computed tomography (CT) urography, or magnetic resonance imaging (MRI) will help to evaluate the extent of fibrotic changes in the retroperitoneum.

The initial treatment of primary RPF consists of ureteral stenting, followed by immunosuppressive therapy. However, the surgical ureterolysis represents definitive treatment for the vast majority of cases. While open ureterolysis still represents traditional option, laparoscopic ureterolysis is widely accepted today. In the centers where it is available, laparoscopic RPF repair offers additional advantages of shorter hospital stay and reduced transfusion requirements [6]. However, some authors think that the limitations of laparoscopic RPF repair are the cases with very long ureteral entrapment and stricture [7].

The aim of this study was to present patients which subjected to the open surgical repair due to idiopathic RPF.

Methods

From January 1989 to December 2012, a total of 15 patients (11 male and 4 female), with a mean age of 56.4 years, (range 28–72 years), underwent open surgery due to RPF. The patients with intrinsic ureteral obstruction, or another cause for extrinsic obstruction, were excluded from this series.

Preoperative assessment included complete laboratory blood and urine analysis, physical examination, digital rectal/or vaginal examination, abdominal ultrasonography, intravenous urography (IVU) and/or CT-urography. The IVU was performed in order to present the renal excretion, ureteral course, and the site of ureteral obstruction. Recently, CT-urography has been more commonly used, as it provides more details, including the assessment of the retroperitoneal scarring process etc. The biopsies of retroperitoneal tissue were done in all the patients. The patients with impaired renal function or a documented allergy to contrast material underwent retrograde ureteropyelography.

Results

Medial unilateral or bilateral ureteral deviation and proximal dilation seen on IVU are typical for the diagnosis of RPF (Figure 1).

Fig. 1 – Bilateral retroperitoneal fibrosis. Medial deviations of both ureters. Percutaneous nephrostomy tubes placed into both kidneys.

A total of 23 renoureteral units were affected: seven patients (2 female and 5 male) had unilateral, while eight patients (2 female and 6 male) had bilateral ureteral entrapment. The most common symptoms and signs were low back pain due to hydronephrosis (9 patients), uremia (4 patients) and urinary tract infection (2 patients).

The mean time from the appearance of the first symptoms to the presentation was 15.8 months.

Severe hydronephrosis or hydronephrosis associated with impaired renal function were the indications for percutaneous nephrostomy (PCN) in nine renoureteral units; PCN tube was retained until the optimization of renal function. A double-J stent was inserted in 14 renoureteral units preoperatively, in order to facilitate the identification of the ureters during the surgery.

In all the patients, the retroperitoneal space was exposed through the midline laparotomy. There were no perioperative complications (Figure 2).

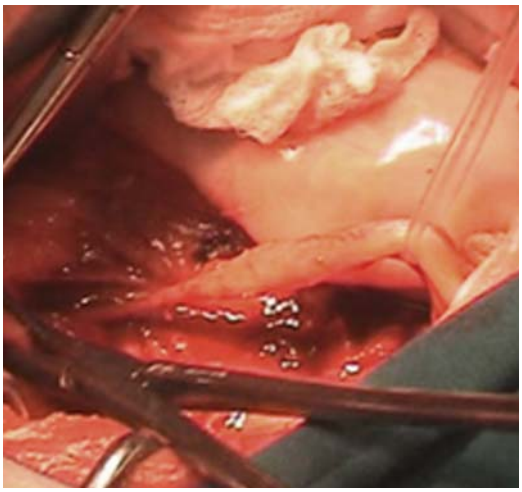

Fig. 2 – The ureter with the stenotic segment deliberated from fibrosis.

After mobilization of the ureters and the dissection of periureteral fibrosis, three different surgical procedures were performed: intraperitoneal ureteral displacement (8 patients), ureteral wrapping with omental flap (6 patients) and bilateral resection of stenotic ureteral segments followed by omental flap wrapping (1 patient) (Figures 3–5).

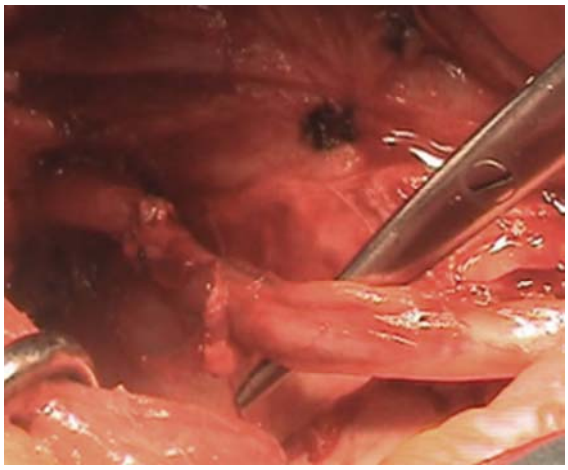

Fig. 3 – Stenotic ureteral segment was removed and the ureter reanastomozed.

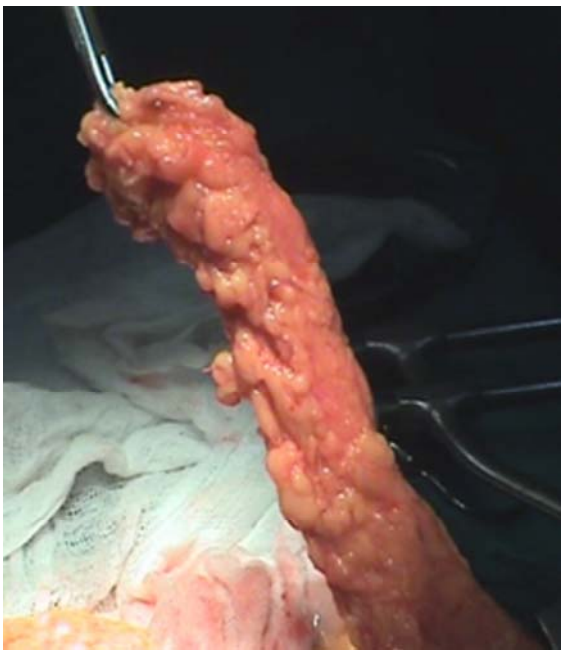

Fig. 4 – Omental flap.

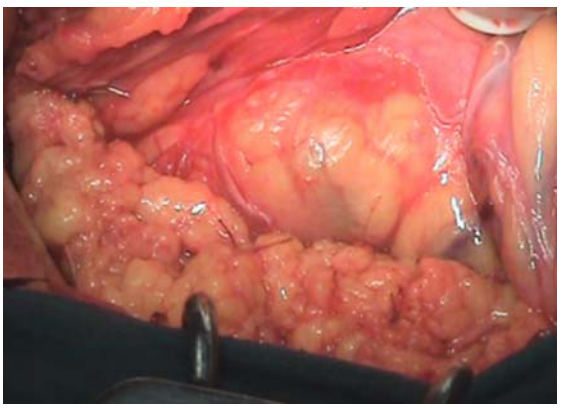

Fig. 5 – The ureter wrapped into the omental flap.

Ureteral stents were removed on the day 21 postoperatively. During the follow-up, serum creatinine measurement, abdominal ultrasonography, IVU and CT-urography were performed.

Pathological examination confirmed primary RPF in all the patients. The mean operative time was 3.5 h (2.5–4.5 h). The average intrahospital stay was 21 days (16–26 days). The mean follow-up was 32 months (6–46 months). During the follow-up, 12 of the patients had improvement on IVU.

Two patients had further deterioration of renal function. One patient had unresolved pelvicalyceal dilation, which required double-J placement.

Discussion

The term retroperitoneal fibrosis denotes the presence of fibroinflammatory tissue in the retroperitoneal space, which surrounds and entraps the great vessels and the ureters.

Primary or idiopathic RPF is probably the result of local inflammatory response to various antigens. The diagnosis of true idiopathic form of RPF is likely in all patients where no potential causative agent may be identified. However, its pathogenesis seems to be related to IgG4 autoimmune mechanisms.

From the other hand, the etiology of secondary forms of RPF is diverse and it can be the consequence of various medications, infections, traumas and malignancies. The RPF secondary to aortic aneurysm is probably the result of inflammatory response induced by leakage of lipids from aneurysm [1, 8]. RPF associated with rheumatoid arthritis or systemic lupus erythematosus probably represents the autoimmune reaction. In addition, these cases usually respond well to steroids and immunosuppressive therapy [9, 10]. Other frequent causes of secondary RPF are previous abdominal or retroperitoneal surgery, retroperitoneal hematoma, and/or extravasation of the urine, and very commonly, radiotherapy. Drugs that potentially cause RPF include methysergide, beta-adrenergic blockers, lysergic acid diethylamide, methyldopa, amphetamines, phenacetin, pergolide, cocaine etc. [1, 11, 12].

The classical clinical signs of RPF are hydronephrosis and medial ureteral deviation seen on IVU or CT-urography. Retrograde ureteropyelography is indicated in patients with impaired renal function; it can be followed by ureteral stenting which facilitates intraoperative identification and handling of the ureters. Percutaneous nephrostomy is indicated in patients with severe hydronephrosis, as a primary treatment before surgery. Preoperative biopsy of retroperitoneal mass is useful to provide information regarding the type of the disease. It is usually performed under the CT guidance, using a true-cut needle, or by fine needle aspiration [13].

Conservative treatment is indicated in patients with RPF associated with some connective tissue disease or with inflammatory abdominal aortic aneurysm. Frequently used medications are methylprednisolon, azathioprine, penicilamine, tamoxifen and various immunosuppressive agents [9, 10, 14]. The last can be used for six months after the surgery, to prevent recurrence [15].

Ureteral stenting or PCN as definitive measures are indicated only in patients with a significant comorbidity.

Surgical management of RPF traditionally included open ureterolysis through the median laparotomy. Rarely, an extensive loss of ureteral length requires various reconstructive procedures, like Boari bladder flap, or even ureteral replacement with the ileum [16, 17].

In the described series, there was no need for ureteral replacement. The most frequent procedure was intraperitoneal ureteral displacement. The procedure starts with ureterolysis, or freeing up the ureters from the fibrous tissue. After that, the ureter can be pulled laterally and completely covered with the folding of the parietal peritoneum. In cases with the abundant omentum, a similar procedure can be performed using the omentum or omental flap. In one patient, there was complicated situation, due to severe fibrosis and stenosis of both ureters. The authors performed bilateral resection of the ureteral segments, oblique end-to-end anastomosis, stenting and the omental flap wrapping.

Recently, more and more RPF repairs have been performed using laparoscopy. Laparoscopic RPF repair is followed by low morbidity; it allows effective ureterolysis and the interposition of omentum or peritoneum. The only possible limitation for laparoscopy is a very long ureteral entrapment and stenosis [18–20].

Conclusion

Retroperitoneal fibrosis represents an uncommon disease of heterogeneous etiology, with the great impact on upper urinary tract. Idiopathic retroperitoneal fibrosis is frequently discovered incidentally, as upper urinary tract obstruction of unknown etiology.

While conservative therapy is rarely successful, surgery still represents the only curative treatment.

REFERENCES

1. *Resnick MI, Kursh ED.* Extrinsic obstruction of the ureter. In: *Walsh PC, Retik AB, Vaughan ED Jr, Wein AJ*, editors. Campbell's Urology. 7th ed. Philadelphia: Saunders; 1998. p. 387−419.
2. *Ormond JK.* Bilateral ureteral obstruction due to envelopment and compression by an inflammatory retroperitoneal process. J Urol 1948; 59(6): 1072−9.
3. *Demko TM, Diamond JR, Groff J.* Obstructive nephropathy as a result of retroperitoneal fibrosis: a review of its pathogenesis and associations. J Am Soc Nephrol 1997; 8(4): 684−8.
4. *Shaunak S, Wilkins A, Pilling JB, Dick DJ.* Pericardial, retroperitoneal, and pleural fibrosis induced by pergolide. J Neurol Neurosurg Psychiatr 1999; 66(1): 79−81.
5. *Palmer LS, Rosenthal SA.* Images in clinical urology. Testicular encasement by retroperitoneal fibrosis: a rare testicular mass. Urology 1999; 53(3): 619−20.
6. *Srinivasan AK, Richstone L, Permpongkosol S, Kavoussi LR.* Comparison of laparoscopic with open approach for ureterolysis in patients with retroperitoneal fibrosis. J Urol 2008; 179(5): 1875−8.
7. *Okumura A, Murakami K, Nozaki T, Fuse H.* Laparoscopic ureterolysis for idiopathic retroperitoneal fibrosis. Int J Urol 2005; 12(12): 1079−81.
8. *Fernández-Codina A, Martínez-Valle F, Castro-Marrero J, Detorres I, Vilardell-Tarrés M, Ordi-Ros J.* Idiopathic retroperitoneal fibrosis: a clinicopathological study in 24 Spanish cases. Clin Rheumatol 2013; 32(6): 889−93.
9. *Liu H, Zhang G, Niu Y, Jiang N, Xiao W.* Retroperitoneal fibrosis: a clinical and outcome analysis of 58 cases and review of literature. Rheumatol Int 2014. (In Press)
10. *Crotty KL, Orihuela E, Warren MM.* Response of renal intrahilar retroperitoneal fibrosis to immunosuppressive therapy. J Endourol 1994; 8(5): 371−3.
11. *Bucci JA, Manoharan A.* Methysergide-induced retroperitoneal fibrosis: successful outcome and two new laboratory features. Mayo Clin Proc 1997; 72(12): 1148−50.
12. *Kunkler RB, Osborn DE, Abbott RJ.* Retroperitoneal fibrosis caused by treatment with pergolide in a patient with Parkinson's disease. Br J Urol 1998; 82(1): 147−9.
13. *Dash RC, Liu K, Sheafor DH, Dodd LG.* Fine-needle aspiration findings in idiopathic retroperitoneal fibrosis. Diagn Cytopathol 1999; 21(1): 22−6.
14. *Harreby M, Bilde T, Helin P, Meyhoff HH, Vinterberg H, Nielsen VA.* Retroperitoneal fibrosis treated with methylprednisolon pulse and disease-modifying antirheumatic drugs. Scand J Urol Nephrol 1994; 28(3): 237−42.
15. *Riedl CR, Zinnbauer B.* Asynchronous bilateral hydronephrosis in retroperitoneal fibrosis with an interval of 44 months. Urologe A 1995; 34(1): 54−8. (German)
16. *Fugita OE, Jarrett TW, Kavoussi P, Kavoussi LR.* Laparoscopic treatment of retroperitoneal fibrosis. J Endourol 2002; 16(8): 571−4.
17. *Kawanishi H, Aoyama T, Sasaki M.* Long-term results of ureteral replacement using ileum: report of four cases. Hinyokika Kiyo 1999; 45(6): 431−4.
18. *Elashry OM, Nakada SY, Wolf JS, Figenshau RS, McDougall EM, Clayman RV.* Ureterolysis for extrinsic ureteral obstruction: a comparison of laparoscopic and open surgical techniques. J Urol 1996; 156(4): 1403−10.
19. *Simone G, Leonardo C, Papalia R, Guaglianone S, Gallucci M.* Laparoscopic ureterolysis and omental wrapping. Urology 2008; 72(4): 853−8.
20. *Fong BC, Porter JR.* Laparoscopic ureterolysis: technical alternatives. J Endourol 2006; 20(10): 820−2.

Received on April 26, 2014.
Revised on October 4, 2014.
Accepted on October 13, 2014.
Online First August, 2015.

CASE REPORTS

UDC: 616.61-006
DOI: 10.2298/VSP140311027M

Acquired cystic disease and renal cell carcinoma in hemodialysis patients – A case report on three patients

Stečena cistična bolest i karcinom bubrega kod bolesnika na hemodijalizi

Mirjana Mijušković*†, Novak Milović†‡, Božidar Kovačević§, Dragan Jovanović*†, Dara Stefanović†‖, Ljiljana Ignjatović*, Brankica Terzić*, Jelena Tadić Pilčević*†, Marijana Petrović*†, Dejan Pilčević*, Katarina Obrenčević¶, Snežana Cerović†§

***Clinic of Nephrology, ‡Clinic of Urology, §Institute of Pathology, ‖Institute of Radiology, ¶Centar for Solid Organ Transplantation, Military Medical Academy, Belgrade, Serbia; †Faculty of Medicine of the Military Medical Academy, University of Defence, Belgrade, Serbia**

Abstract

Introduction. Renal cell carcinoma (RCC) is derived from renal tubular epithelial cells and represents approximately 3.8% of all malignancies in adults. The incidence of renal cell carcinoma has been growing steadily and ranging from 0.6 to 14.7 for every 100,000 inhabitants. Patients with end-stage renal disease and acquired cystic kidney disease are at increased risk of developing RCC while undergoing dialysis treatment or after renal transplantation. **Case report.** We presented 3 patients undergoing hemodialysis, with acquired cystic kidney disease accompanied by the development of RCC. In all the patients tumor was asymptomatic and discovered through ultrasound screening in 2 patients and in 1 of the patients by post-surgery pathohistological analysis of the tissue of the kidney excised using nephrectomy. All the three patients had organ-limited disease at the time of the diagnosis and they did not require additional therapy after surgical treatment. During the follow-up after nephrectomy from 6 months to 7 years, local recurrence or metastasis of RCC were not diagnosed. **Conclusion.** Acquired cystic kidney disease represents a predisposing factor for the development of renal cell carcinoma in dialysis patients and requires regular ultrasound examinations of the abdomen aimed at early diagnosis of malignancies. Prognosis for patients with end-stage renal disease and RCC is mostly good because these tumors are usually of indolent course.

Key words:
renal dialysis; kidney diseases, cystic; hemodyalisis; nephrectomy; treatment outcome.

Apstrakt

Uvod. Karcinom bubrega (*renal cell carcinoma* – RCC) nastaje iz renalnih epitelnih ćelija tubula i čini oko 3,8% svih maligniteta kod odraslih. Incidencija RCC je u stalnom porastu i iznosi 0,6 do 14,7 na 100 000 stanovnika. Bolesnici sa terminalnom bubrežnom insuficijencijom i stečenom cističnom bolešću bubrega su u povećanom riziku od razvoja RCC tokom lečenja dijalizom ili nakon transplantacije bubrega. **Prikaz bolesnika.** U radu su prikazana 3 bolesnika lečena hemodijalizom sa stečenom cističnom bolešću bubrega koja je bila udružena sa razvojem RCC. Kod svih bolesnika tumor je bio asimptomatski i otkriven je ultrazvučnim pregledom kod dva bolesnika, a kod jednog patohistološkom analizom tkiva bubrega odstranjenog nefrektomijom. Kod sva tri bolesnika bolest je bila organ-ograničena u vreme postavljanja dijagnoze i nije zahtevala primenu dodatne terapije nakon hirurškog lečenja. Tokom perioda praćenja od 6 meseci do 7 godina nakon nefrektomije, nije dijagnostikovano postojanje lokalne rekurencije ili metastaza RCC. **Zaključak.** Stečena cistična bolest bubrega predstavlja predisponirajući faktor razvoja RCC kod bolesnika na dijalizi i zahteva redovne ultrazvučne kontrole abdomena u cilju postavljanja rane dijagnoze maligniteta. Prognoza kod bolesnika sa terminalnom bubrežnom insuficijencijom i RCC u najvećoj meri je dobra jer su karcinomi bubrega kod ovih bolesnika, uglavnom, indoletnog toka.

Ključne reči:
bubreg, neoplazme; bubreg, cistični; hemodijaliza; nefrektomija; lečenje, ishod.

Introduction

Renal cell carcinoma (RCC) is derived from renal tubular epithelial cells. This type of cancer represents approximately 3.8% of all malignancies in adults of the general population. The incidence of RCC has been growing steadily for the last 30 years, ranging from 0.6 to 14.7 for every 100,000 inhabitants [1–3]. Treatment of RCC is the current oncologic problem, because, in spite

Correspondence to: Mirjana Mijušković, Clinic of Nephrology, Military Medical Academy, Crnotravska 17, Belgrade, Serbia. Phone.: +381 11 3608 614. E-mail: mirjana.mijuskovic@gmail.com

of modern diagnostic methods and surgical treatment a patient survival with RCC has not significantly improved in the last 15 years. At the time of diagnosis, 30% to 40% of patients either clearly show metastatic disease or it is clinically unrecognizable depending on the stage of the disease. Optimal treatment of kidney cancer is surgery, applying radical or partial nephrectomy for small tumors in order to maintain a functioning renal tissue [3, 4].

Patients with end-stage renal disease (ESRD) and acquired multiple renal cysts are at increased risk of developing RCC during dialysis or after renal transplantation. The prevalence of RCC in this group of patients is 3% to 5%, which corresponds to the rate 100 times higher than sporadic RCC type in the general population [2, 3]. Acquired cystic kidney disease (ACKD) is an independent risk factor for the development of RCC in these patients. ACKD is defined by the presence of multiple renal cysts (three or more per kidney), filled with serous fluid, in a patient with ESRD. Patients with ACKD have 50 times higher risk of developing RCC compared to the general population [4, 5]. To date, the pathogeneses of ACKD and RCC associated with it remain undetermined [5–7]. Several factors are considered to contribute to development of ACKD and RCC in ESRD patients: ischemia, uremic toxins like p-cresol, increased secretion of parathyroid hormone and growth factors, depressed immunity, viral infections, obstruction of renal tubules due to fibrosis and oxalate deposits, and other factors [4–7]. The prevalence of ACKD in dialysis patients is from 30% to 90% and increases with the duration of dialysis. ACKD was reported to be observed in 20% of patients with ESRD in the period before dialysis, rising to 60–80% in patients more than 4 years on dialysis and approximately in 90% of those on dialysis more than 8 years [8].

The association of RCC and ESRD is manifested in specific clinical and pathological characteristics in relation to RCC in the general population. Common clinical symptoms typical for the most forms of sporadic renal cancer, such as hematuria, lumbar pain, infection and elevated temperature, are generally absent in patients with ESRD and RCC. This group of patients are diagnosed with papillary renal cell carcinoma in more than 40% of cases, in contrast to clear cell renal cell carcinoma diagnosed in approximately 70% of the sporadic forms of the tumor [4]. In comparison with the sporadic RCC, these tumors are more frequent in pT1 stage (smaller than 70 mm), low-grade malignancy and rarely with the appearance of distant and regional lymph nodes metastases [9]. The prognosis for patients with ESRD and RCC is mostly good because these tumors are usually of indolent course [10].

The aim of this article was to show clinical and histopathological characteristics in 3 surgically treated patients with ESRD and ACKD associated with RCC. In all the patients malignant disease was asymptomatic. There were no complications related to the surgery, general anesthesia and the cardiovascular system during or immediately after nephrectomy.

The presented patients were still treated according to the protocol of ESRD and controled in accordance with the recommendations of the European Association of Urology Guidelines on Renal Cell Carcinoma [11]. During the clinical follow-up after nephrectomy from 6 months to 7 years, local recurrence or metastatic RCC was not diagnosed.

Case 1

A 35-year-old patient was admitted for a pretransplantation proceeding for potential living related renal transplantation. The main disease which caused end-stage renal disease was systemic lupus erythematosus and lupus nephritis. The patient was treated with hemodialysis for 4 years. We performed regular ultrasound examination of the abdomen and diagnosed the presence of circular, hyperechogenic formation in interpolar part of the right kidney, whose diameter was 23 mm. Both kidneys were reduced in size, the longitudinal diameter of each was about 9 cm, reduced parenchyma, with multiple cysts. The largest diameter of individual cyst was 1.5 cm. Based on ultrasound examination, the patient was suspected to having tumor of the right kidney. Multislice computed tomography (MSCT) of the abdomen was performed and diagnosed the existence of a tumor, 22 × 25 × 30 mm in diameter, with no signs of breaking kidney capsula. The patient underwent a radical right nephrectomy. Histopathological examination showed the existence of tumor whose largest diameter was 20 mm, mostly with hemorrhagic necrosis. Malignancy was diagnosed as: Renal cell carcinoma cysticum et necroticum, Fuhrman grade 2, stage T1Nx (Figure 1). There were a number of renal cysts lined with flattened epithelium, without atypia. Pathology assessment of the non-tumor specimen revealed chronic diffuse and global glomerular and interstitial lesions within the class IV lupus nephritis. The tumor was organ-confined and application of additional therapy was not indicated. Seven years after the operation there was no occurrence of RCC progression.

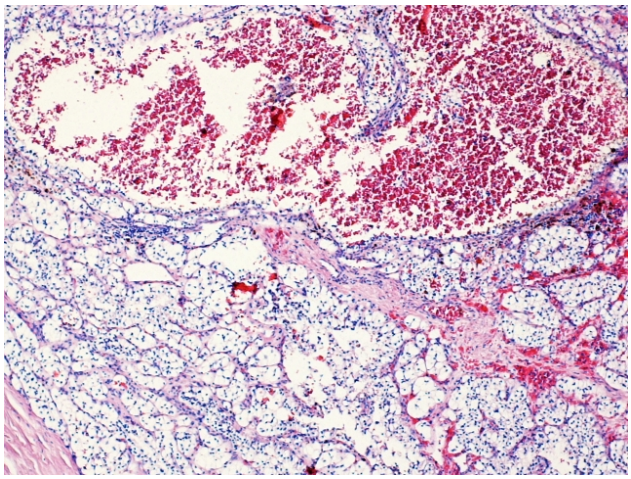

Fig. 1 – Large field of cystic degeneration and hemorrhagic necrosis in clear renal cell carcinoma, Fuhrman grade 2 (Hematoxylin-eosin, ×75).

Case 2

A 76-year-old patient was on chronic hemodialysis for 2 years. The main disease which caused end-stage renal disease was ischaemic nephropathy. Laboratory blood tests were within the range typical for patients undergoing hemodialysis. We performed regular ultrasound examination of the abdomen and incidentally diagnosed the presence of circular formation

in the lower half of the left kidney, dimensions 30 × 35 mm, which was suspected to the presence of tumor. Both kidneys were reduced in size, the right kidney was 8 cm and the left one 9 cm, thinned, echogenic parenchyma, with multiple cysts in both kidneys. The largest diameter of individual cyst was 1 cm. MSCT of the thorax and abdomen was performed showing well-vascularized tumor in the lower pole of the left kidney, measuring 33 × 33 mm, with no signs of local and distant metastases. Radical left nephrectomy along with adrenalectomy and regional lymphadenectomy was performed. Pathology assessment of the nephrectomy specimen revealed Fuhrman grade 2, clear cell renal carcinoma, staged as T1N0, with involvement of tumors vascular space. Due to the localized disease further application of treatment was not indicated.

Case 3

A 58-year-old patient was admitted for nephrectomy of the right dysfunctional kidney. The disease which caused end-stage renal disease was reflux nephropathy. The patient had been on home hemodialysis for 21 years and had recurrent urinary tract infections that required frequent use of antibiotics. That was the reason why the patient had radical left nephrectomy a month before. MSCT of abdomen was performed preoperatively and showed the existence of reduced kidneys size, the right kidney was 9.5 cm and the left one 7.5 cm, markedly thinned parenchyma, with the present small cystic changes. Histopathological examination showed the existence of the atrophic left kidney with cortical cysts. Then, the patient underwent a radical right nephrectomy and the lesion histologically proved to be the subtype of RCC, labeled as acquired cystic disease-associated renal cell carcinoma of nuclear grade Fuhrman 1, stage T1N0 (Figures 2 and 3). Since the disease was organ-confined, urological-oncology data indicated regular controls, with repeated ultrasound and CT examinations, as recommended for the treatment of RCC.

Discussion

Patients with ESRD have an increased risk of developing RCC in their native kidneys and ACKD represents the predisposing factor for its onset [5]. Continuous research on the correlation between RCC and ACKD has been on-going for more than half a century. The first results of this correlation were autopsy findings. A group of authors from Oxford, Dunnill et al. [12], published the autopsy results of 30 patients with ERSD in 1977. Cystic kidney disease, now ACKD, was present in 14 of the patients, of which 6 also had RCC. One autopsy report also showed dissemination of RCC. Thanks to the results of this analysis, ACKD initially obtained a complex definition as macroscopically visible cystic structures which covered at least 25% of the renal parenchyma or more than 3 cysts in the kidney in patients with kidney insufficiency, with negative family medical history regarding cystic kidney disease.

The authors Matson and Cohen [13] drew attention to the significance of the duration of dialysis for the onset of ACKD and its correlation to RCC in 1990. The correlation of RCC and ACKD ranged from 0.3% to 14%, depending on the number of patients involved in studies, but most often they ranged from 3 to 5% [3, 4, 13, 14–16]. Some epidemiological studies show significant differences compared to the presence of RCC in patients on dialysis. The number of patients on dialysis and with newly onset RCC increased by 15 times in Japan in the last three decades, but the correlation of ACKD and RCC is still lower than 6% [14]. Compared to the same group of patients in Europe and North America, this number is 4 to 5 times lower [4].

The results of a great number of studies especially draw attention to the correlation between the duration of dialysis and the onset of RCC [13–16]. In the study of Kojima et al. [14] on 2,624 patients with ESRD, RCC was also diagnosed after 11.2 years of dialysis therapy on the average in 44 (1.68%) of the patients of which ACKD was already present in 36

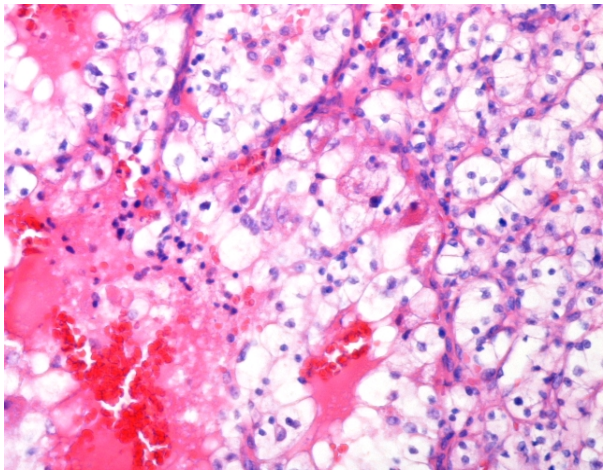

Fig. 2 – Small papillary structures composed of the light of neoplastic cells within the acquired cystic disease-associated renal cell carcinoma, Fuhrman grade 1 (Hematoxylin-eosin, ×75).

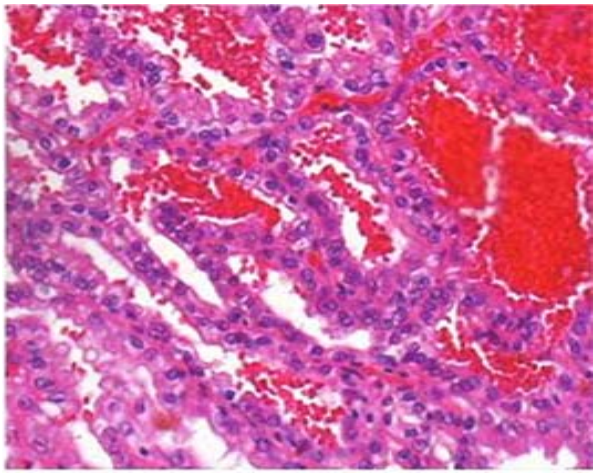

Fig. 3 – Tubular structures within the acquired cystic disease-associated renal cell carcinoma, coated with cubic neoplastic cells and surrounded by hemorrhagic necrosis (Hematoxylin-eosin, ×100).

(81.8%) of them. The results of one of the latest and largest studies which monitored more than 7,000 dialysis patients show that in 22 (0.3%) of them RCC was diagnosed and surgically treated, while at the same time in 18 (82%) patients the acquired cystic kidney disease was already present alongside cancer [15]. Only one of our 3 patients was on a long-term dialysis therapy (21 years), while the other two patients spent significantly less time on hemodialysis (4 and 2 years). All patients were treated with hemodialysis and they had manifested ACKD.

There were no surgery or post-surgery complications in the patients on dialysis with ACKD and RCC in our analysis. Patients on dialysis with RCC are a high-risk group for surgical procedures, especially due to the worsening of cardiologic and respiratory complications which are already present within the basic chronic kidney disease [17].

In dialysis patients, most kidney cancers are detected during ultrasound screening because of ACKD, due to the fact that they are most often asymptomatic [4]. The widespread and modern application of radiologic diagnostic procedures for the detection of presymptomatic tumors in patients with ESRD can be linked to the significant increase of RCC incidence [14–18]. The asymptomatic landscape in relation to RCC was also present in the patients from our study. Kidney tumors were diagnosed in 2 of the patients during routine ultrasound screenings, while in the third patient it was undetected within the kidney cysts. In 2 of the 3 patients, the suspected presence of kidney tumor with ACKD was confirmed by both ultrasound and MSCT examination. On the basis of the conducted radiological examinations, tumorous changes in the right kidney were not suspected in the third patient. Small tumor with cystic degeneration was masked by multiple cysts within ACKD, so the diagnosis of the entity "acquired cystic disease-associated renal cell carcinoma" (ACDAC) was established by the post-surgery pathohistological analysis of the tissue of the removed kidney.

ACDAC represents a more recent pathohistological entity which is often diagnosed in patients with terminal renal insufficiency and with acquired multiple cysts of the kidney. Compared to sporadic RCC, ACDAC has better prognosis due to the fact that it gets detected in its early stages and rarely metastasises [19, 20]. The pathohistological diagnosis of ACDAC is established in 46% of patients with ESRD. The macroscopic appearance of the cystic structure is its most common presentation and it occurs in around 67% of patients [9].

This subtype of kidney cancer manifests microscopic variations of the growth pattern from papillary and cystic to solid and acinar, in part with cribriform areas. Tumorous cells are abundant eosinophil or oncocytic cytoplasms, of prominent nucleoli, at times also with intratumoral deposits of calcium oxalate crystals [9, 19, 20–22]. In the results of previous studies, this type of carcinoma was often diagnosed as clear cell carcinoma with cystic degeneration. According to the latest recommendations of the International Society of Urological Pathology (ISUP), ACDAC has been identified as separate entity [22]. Rare cases of transformation of ACDAC into RCC showing sarcomatoid or rhabdoid differentiation [9, 20, 21] have also been described. The diagnostics of sarcomatoid RCC, as the RCC with the greatest malignant potential are often linked to the duration of dialysis. The results of the study of Sassa et al. [20] in a group of 23 patients with a dialysis period of longer than 20 years show that the sarcomatoid type of RCC was diagnosed in 6 patients. This result shows that dialysis therapy lasting more than 10 years represents a significant risk-factor for the development of a more aggressive type of RCC. In this presentation of the patient 3, with dialysis therapy lasting more than 20 years, the tumor was diagnosed which had the histological features of ACDAC but which was of low malignancy, Fuhrman grade 1, pT1a, L0V0. This patient was subjected to bilateral nephrectomy. In fact, in patients with ACKD bilateral nephrectomy is rarely indicated. Indications for bilateral nephrectomy include ACKD patients with complications of ACKD such as intra- and pericystic bleeding, rupture with retroperitoneal hemorrhage and malignant transformation. Borràs et al. [23] presented the case of spontaneous bilateral cyst rupture with retroperitoneal hemorrhage and hemoperitoneum in the PD patient with ACKD which is an indication for bilateral nephrectomy. Ghasemian et al. [24] presented experience with bilateral laparoscopic radical nephrectomy performed in 10 patients with ACKD and renal lesions suspicious for carcinoma. Our patient had recurrent (an average of 6 episodes *per* year) urinary tract infections in the last 5 years of dialysis treatment, often followed by high temperature and fever. That was the reason for the repeated and prolonged antibiotic administration in this patient and therefore we indicated bilateral nephrectomy.

The duration of kidney disease, less often than the dialysis itself, can be a more significant determining factor in the development of ACKD and RCC [16]. This can explain the development of RCC in our female patient after only 4 years of dialysis therapy; bearing in mind the fact that the patients was treated for systemic erythematous lupus in the previous 21 years with various immunosuppressive drugs (cyclophosphamide, corticosteroids), as well as plasma exchanges. RCC diagnostics is extremely rare in patients with SLE. Hematological neoplasms are often observed in these patients; especially lymphomas and lung carcinoma, as well as hormone-dependant breast and uterus carcinomas [25]. Patients with SLE also demonstrate multiple defects in both humoral and cellular immunity, so the onset of lymphoma can be indirectly linked to the onset of the pathological clone of B lymphocyte [26]. According to the available literature, only two cases of RCC diagnostics in patients with systemic lupus have been published so far [27].

Moderately impaired kidney function may be an independent risk factor for cancer in older men with a graded increase in the risk as glomerular filtration rate (GFR) declines [28]. This group of patients has the higher mortality of liver cancer, kidney cancer and urinary tract cancer [29]. In our patient 2, RCC developed after only 2 years of dialysis therapy, which could be explained by the fact that the patient was 76 years old man at the time of the diagnosis.

The prognosis for dialysis patients with the diagnosed RCC is better than in nonuremic patients with RCC, due to the low incidence rate of metastatic abnormalities [10]. All the three of our patients had organ-limited disease at the time of the diagnosis without any signs of nodal or distant metastases, and they did not require additional therapy after surgical trea-

tment. The patients were regularly examined, and in the follow-up period, which was 6 months in the patient 3, and up to 7 years in the patient 1, no RCC recurrence or dissemination was diagnosed.

Conclusion

This report on the 3 patients on hemodialysis with acquired multiple renal cysts shows that hemodialysis duration of more than 10 years, older age, and duration of treatment of kidney disease that led to end-stage renal disease may be predisposing factors for the development of renal cell carcinoma. The outcome of surgically treated patients on maintenance hemodialysis with the diagnoses of renal cell carcinoma is usually good because acquired cystic kidney disease-associated carcinomas are of low pathological stage.

Acquired cystic kidney disease represents a predisposing factor for the development of renal cell carcinoma in dialysis patients and requires regular ultrasound examinations of the abdomen aimed at the early diagnosis of malignancies.

REFERENCES

1. NCI - National Cancer Institute. SEER Cancer Statistics Review, 1975–2011.
   Available from: http://seer.cancer.gov/statfacts/html/kidrp.html
2. *Goh A, Vathsala A.* Native renal cysts and dialysis duration are risk factors for renal cell carcinoma in renal transplant recipients. Am J Transplant 2011; 11(1): 86−92.
3. *Russo P.* End stage and chronic kidney disease: associations with renal cancer. Front Oncol 2012; 28(2): 1−7.
4. *Schwarz A, Vatandaslar S, Merkel S, Haller H.* Renal cell carcinoma in transplant recipients with acquired cystic kidney disease. Clin J Am Soc Nephrol 2007; 2(4): 750−6.
5. *Truong LD, Krishnan B, Cao JT, Barrios R, Suki WN.* Renal neoplasm in acquired cystic kidney disease. Am J Kidney Dis 1995; 26(1): 1−12.
6. *Faure V, Cerini C, Paul P, Berland Y, Dignat-George F, Brunet P.* The uremic solute p-cresol decreases leukocyte transendothelial migration in vitro. Int Immunol 2006; 18(10): 1453−9.
7. *Stengel B.* Chronic kidney disease and cancer: a troubling connection. J Nephrol 2010; 23(3): 253−62.
8. *Katabathina VS, Kota G, Dasyam AK, Shanbhogue AK, Prasad SR.* Adult renal cystic disease: a genetic, biological, and developmental primer. Radiographics 2010; 30(6): 1509−23.
9. *Bhatnagar R, Alexiev BA.* Renal-cell carcinomas in end-stage kidneys: a clinicopathological study with emphasis on clear-cell papillary renal-cell carcinoma and acquired cystic kidney disease-associated carcinoma. Int J Surg Pathol 2012; 20(1): 19−28.
10. *Neuzillet Y, Tillou X, Mathieu R, Long J, Gigante M, Paparel P,* et al. Renal cell carcinoma (RCC) in patients with end-stage renal disease exhibits many favourable clinical, pathologic, and outcome features compared with RCC in the general population. Eur Urol 2011; 60(2): 366−73.
11. *Ljungberg B, Bensalah K, Bex A, Canfield S, Dabestani S, Hofmann F,* et al. Guidelines on Renal Cell Carcinoma: Europeon Association of Urology 2013 [accessed2013 August 20]. Available from: http://www.uroweb.org/gls/pdf/10 Renal Cell Carcinoma LR.pdf.
12. *Dunnill MS, Millard PR, Oliver D.* Acquired cystic disease of the kidneys: a hazard of long-term intermittent maintenance haemodialysis. J Clin Pathol 1977; 30(9): 868−77.
13. *Matson MA, Cohen EP.* Acquired cystic kidney disease: occurrence, prevalence, and renal cancers. Medicine (Baltimore) 1990; 69(4): 217−26.
14. *Kojima Y, Takahara S, Miyake O, Nonomura N, Morimoto A, Mori H.* Renal cell carcinoma in dialysis patients: a single center experience. Int J Urol 2006; 13(8): 1045−8.
15. *Lee HH, Choi KH, Yang SC, Han WK.* Renal cell carcinoma in kidney transplant recipients and dialysis patients. Korean J Urol 2012; 53(4): 229−33.
16. *Peces R, Martínez-Ara J, Miguel JL, Arrieta J, Costero O, Górriz JL,* et al. Renal cell carcinoma co-existent with other renal disease: clinico-pathological features in pre-dialysis patients and those receiving dialysis or renal transplantation. Nephrol Dial Transplant 2004; 19(11): 2789−96.
17. *Wolters U, Wolf T, Stützer H, Schröder T.* ASA classification and perioperative variables as predictors of postoperative outcome. Br J Anaesth 1996; 77(2): 217−22.
18. *Correas JM, Joly D, Chauveau D, Richard S, Hélénon O.* Renal failure and cystic kidney diseases. J Radiol 2011; 92(4): 308−22.
19. *Kuroda N, Ohe C, Mikami S, Hes O, Michal M, Brunelli M,* et al. Review of acquired cystic disease-associated renal cell carcinoma with focus on pathobiological aspects. Histol Histopathol 2011; 26(9): 1215−8.
20. *Sassa N, Hattori R, Tsuzuki T, Watarai Y, Fukatsu A, Katsuno S,* et al. Renal cell carcinomas in haemodialysis patients: does haemodialysis duration influence pathological cell types and prognosis. Nephrol Dial Transplant 2011; 26(5): 1677−82.
21. *Srigley JR, Delahunt B, Eble JN, Egevad L, Epstein JI, Grignon D,* et al. The International Society of Urological Pathology (ISUP) Vancouver Classification of Renal Neoplasia. Am J Surg Pathol 2013; 37(10): 1469−89.
22. *Bostwick DG, Cheng L.* Urologic Surgical Pathology. 2nd ed. Philadelphia, PA: Mosby Elsevier; 2008.
23. *Borràs M, Valdivielso JM, Egido R, de Vicente VP, Bordalba JR, Fernández E.* Haemoperitoneum caused by bilateral renal cyst rupture in an ACKD peritoneal dialysis patient. Nephrol Dial Transplant 2006; 21(3): 789−91.
24. *Ghasemian S, Pedraza R, Sasaki TA, Light JA, Patel SV.* Bilateral laparoscopic radical nephrectomy for renal tumors in patients with acquired cystic kidney disease. J Laparoendosc Adv Surg Tech A 2005; 15(6): 606−10.
25. Research Update: Cancer in Lupus. (Based on presentation by Dr. Sasha Bernatsky at BC Lupus Society Symposium.) [cited 2005 October 22].
    Available from: <http://www.bclupus.org/resources.html>.
26. *Sultan SM, Ioannou Y, Isenberg DA.* Is there an association of malignancy with systemic lupus erythematosus? An analysis of 276 patients under long-term review. Rheumatology 2000; 39(10): 1147−52.
27. *Gopalakrishnan G, Nampoory NM, Ali JH, Johny KV.* Renal cell carcinoma in a patient with systemic lupus erythematosus: A case report. Med Principles Pract 1996; 5(3): 160−2.
28. *Wong G, Hayen A, Chapman JR, Webster AC, Wang JJ, Mitchell P,* et al. Association of CKD and cancer risk in older people. J Am Soc Nephrol 2009; 20(6): 1341−50.
29. *Weng P, Hung K, Huang H, Chen J, Sung P, Huang K.* Cancer-specific mortality in chronic kidney disease: longitudinal follow-up of a large cohort. Clin J Am Soc Nephrol 2011; 6(5): 1121−8.

Received on March 11, 2014.
Revised on August 28, 2014.
Accepted on September 25, 2014.
Online First April, 2015.

CASE REPORT

UDC: 616.214/.216-006.81
DOI: 10.2298/VSP140414075A

Melanoma of the sinonasal mucosa: A report on the two cases and a review of the literature

Mukozni melanom nosnosinusne sluznice

Aleksandra Aleksić*, Radoslav Gajanin†, Dejan Djurdjević‡, Zorica Novaković*, Dalibor Vranješ*, Slobodan Spremo*, Dmitar Travar*, Nataša Guzina-Golac*, Vesna Tomić-Spirić§

***Department of Ear, Throat and Nose, †Department for Pathology; ‡Department of Maxillofacial Surgery, Clinical Center, Banja Luka, Republic of Srpska, Bosnia and Herzegovina; §Clinic of Allergy and Clinical Immunology, Clinical Center of Serbia, Faculty of Medicine, University of Belgrade, Belgrade, Serbia**

Abstract

Introduction. Primary mucosal melanoma of the sinonasal tract is a rare neoplasm, accounting for less than 1% of all melanomas. It has an aggressive and unpredictable biologic behavior characterized by frequent incidence of local recurrence, local and distant metastasis of the disease. **Case report.** This report summarizes the results of the previous research concerning sinonasal mucosal melanoma, and by the example of the two patients suffering from mucosal melanoma, we described clinical and histopathological features of this rare neoplasm and our experience in its diagnosis and treatment. **Conclusion.** Only histopathological analysis complemented by immunohistochemical analysis contributes to early and accurate diagnosis of the disease.

Key words:
melanoma; nose; paranasal sinuses; diagnosis; neoplasms staging; oral surgical procedures; radiotherapy; treatment outcome; prognosis.

Apstrakt

Uvod. Primarni mukozni melanom nosnosinusnog regiona je retka neoplazma i čini svega 1% svih melanoma. Biološko ponašanje melanoma karakteriše agresivan i nepredvidiv rast, česti lokalni recidivi, lokalne i udaljene metastaze. **Prikaz bolesnika.** Rad sumira rezultate prethodnih studija mukoznog melanoma nosnosinusne sluznice, a kroz prikaz dva bolesnika opisane su kliničke i patohistološke karakteristike ove retke neoplazme i naša iskustva sa dijagnostičkim i terapijskim postupcima. **Zaključak.** Naši rezultati pokazuju da patohistološke i imunohistohemijske analize doprinose postavljanju rane i tačne dijagnoze ovog oboljenja.

Ključne reči:
melanom; nos; paranazalni sinus; dijagnoza; neoplazme, određivanje stadijuma; hirurgija, oralna, procedure; radioterapija; lečenje, ishod; prognoza.

Introduction

Mucosal melanoma is a rare neoplasm accounting for less than 1% of all melanomas. However, head and neck region is the most frequent primary site for mucosal melanomas and consists of 55.4% of all mucosal melanomas. Among head and neck anatomical locations, sinonasal tract is the most common primary site for this malignancy [1–5]. Primary sinonasal mucosal melanoma is a rare entity, which constitutes about 1.5–9% of all malignancies in this site [1, 2]. In an exhaustive review, Manolidis and Donald [5] found 1,000 cases reported in the literature up to 1997.

The etiopathogenesis of this form of melanoma is poorly understood. It is clear, however, that sinonasal mucosal melanoma is derived from melanocytes present in the mucosa of nasal cavity [1, 3, 5]. Approximately 80% of sinonasal melanomas are believed to occur in the nasal cavity, whereas about 20% originate in the sinuses. According to the available literature the most frequent primary site is the lateral wall of the nasal cavity (inferior and middle turbinate), and then nasal septum [2–4]. Epistaxis and unilateral nasal obstruction are the most frequent presenting symptoms, in the most reported series. Pain and deformities in the face region with proptosis, diplopia and epiphora rarely occur (in 9–12% of cases) most frequently in advanced stages of the disease [3–6].

Correspondence to: Aleksandra Aleksić, Department of Ear, Throat and Nose, Clinical Center Banja Luka, Koste Jarića 14b, Banja Luka, Republic of Srpska. Phone: +387 65 535 109. E-mail: alexandraaleksic@gmail.com

One of the difficulties in diagnosing mucosal melanoma relates to its clinical rarity and variable histological presentation. In histopathological sense, especially in case of amelanocit lesions, differential diagnosis includes other epithelial and mesenchymal tumors [6, 7]. One of the key histologic features of melanoma is the identification of intracellular melanin. Hence, crucial for making an accurate diagnosis of mucosal melanoma is immunohistochemical staining analysis for S-100, HMB-45, Melan-A, microphthalmic transcription factor, tyrosinase Mart-1 [6, 7]. In other words, immunohistochemistry is invaluable in making an accurate diagnosis [1, 2, 7].

The staging system for mucosal melanoma has not been well established. Therefore, oncologists use different systems to stage mucosal melanoma [3–5]. Some are considered that the current American Joint Committee on Cancer (AJCC) sinonasal staging system should be the primary staging system for patients with mucosal melanomas of the sinonasal tract [2]. Widely used is Ballantyne's clinical staging system: the lesions confined to the primary site – stage I, regional cervical lymph node involvement – stage II, distant metastasis – stage III [8]. According to Ballantyne's clinical staging system, 76–95% of patients with mucosal melanomas of the sinonasal tract present with stage I disease [1, 2, 5].

In the recent literature there are numerous controversies concerning treatment of mucosal melanoma [1, 2, 9, 10]. In view of this locally aggressive growth pattern, even seemingly early, localized lesions may require radical surgery with planned reconstruction for optimal tumor control. The treatment of choice in mucosal malignant melanoma is radical craniofacial resection followed by radiotherapy, particularly in cases of small or doubtful radically reseced surgical margins [1–6, 9, 10]. Postoperative radiotherapy is usually considered for the majority of patients with sinonasal mucosal melanoma [10–12]. Management of disseminated melanoma includes adjuvant and palliative chemotherapy, in an effort to improve systemic disease control and survival [10–12]. In one pooled analysis from five different case series, patients with nasal mucosal melanoma had a 31% 5-year survival rate, whereas sinus melanoma patients had a 0% 5-year survival rate [1, 5].

We presented two cases suffering from primary mucosal melanoma of the sinonasal region taken from our own experience in diagnosis and treatment of this rare disease. Clinical information retrieved included demographic data, presenting symptoms, results of diagnostic procedures, staging, treatment and outcome. The two patients were retrospectively staged according to the Ballantyne's clinical staging system and to the AJCC staging system for sinonasal tumors [8, 13]. All the available clinical information, such as clinical presentation, radiological data, and intraoperative findings, were used for staging purposes.

Case report

Case 1

A female patient, 82-year-old presented with complaints of persistent unilateral nasal congestion for 6 months. She had also been noticing blood streaks in her mucus for several weeks. Clinical examination revealed a proptosis, nasal deformity and large grayish-black solid mass within the left nasal cavity (Figure 1).

Fig. 1 – Tumor in the left nasal cavity.

A biopsy was obtained and the sample was sent for histopathological analysis. Computed tomography (CT) scan showed an enhancing mass invading the left nasal cavity, left maxillary, ethmoidal and frontal sinus, with destruction of the left medial orbital wall (Figure 2).

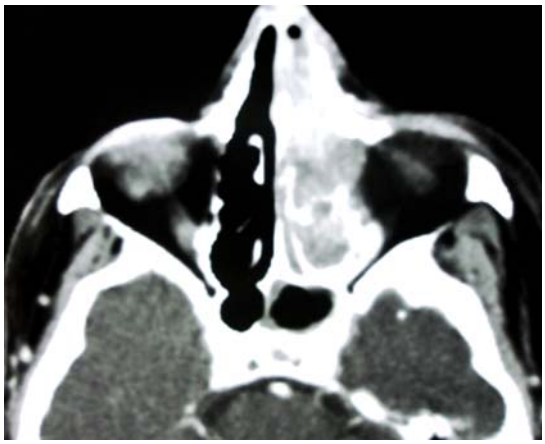

Fig. 2 – Axial computed tomography (CT) image showed an enhancing mass invading the left ethmoid sinus.

CT scan also showed enlarged regional lymph nodes. Histopathological findings were as follows: tumor composed by a cohesive nodule and small nests of tumor cells that have a "pushing" or "expansile" pattern of growth. Tumor cells were of epitheloid type. The cell population was polymorphous, with appearance of cellular enlargement, nuclear enlargement, variation in nuclear size and shape, hyperchromatism, prominent nucleoli, high mitotic count. Immunohistochemistry analysis were : tumor cells positive for CK 7, EMA, S-100, HMB-45 (Figure 3). Antibodies, CK 7 and endomysial antibodies (EMA) were not essential for diagnosis. According to imunohistochemical analysis we confirmed the diagnosis of mucosal melanoma. Meanwhile, a CT scan of thorax showed a distant metastasis in the lung. The findings indicated stage III, T3N2aM1. Taking into consideration the age,

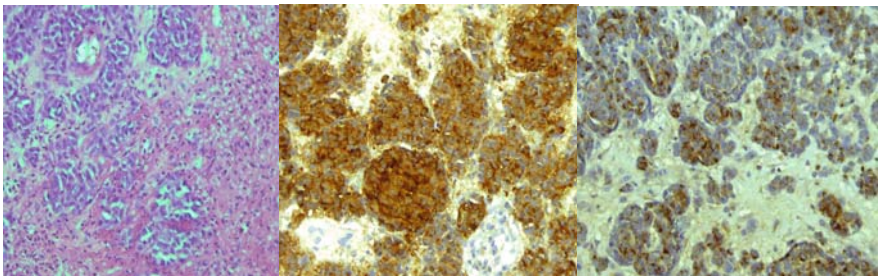

a b c

Fig. 3 – Mucosal melanoma, histopathological findings with imunohistochemical analysis. a) HE, ×200; b) Diffuse cytoplasmic positivity for S-100 (anti- S 100, × 200); c) Diffuse cytoplasmic positivity for HMB-45 (anti-HMB 45, × 200).

advanced stage of the disease (unresectable primary tumor), the presence of regional and distant metastasis, the treatment consisted of radiotherapy. The patient received paliative chemotherapy, but the prognosis was very poor.

Case 2

A 75-year-old male patient presented with complaints of persistent unilateral nasal congestion and nose bleeding for 1 month. Clinical examination revealed a proptosis soft reddish mass on the interior floor of the nasal cavity, partially obstructing the nasal cavity, with adhesion to the nasal septum and inferior turbinate. A biopsy was obtained and the sample was sent for histopathological analysis. CT scan showed a tumor on the floor of the left nasal cavity, with adhesion to the nasal septum and inferior turbinate (Figure 4). Histopathological findings revealed tumor cells of epitheloid type. The cell population was polymorphous with the appearance of cellular enlargement, nuclear enlargement, variation in nuclear size and shape, hyperchromatism, prominent nucleoli, high mitotic count. We performed immunohistochemical analysis and the positive immune response was present at the antibodies S-100 and HMB 45 (Figure 5). According to the clinical examination and immunohistochemical analysis we confirmed

Fig. 4 – Axial computed tomography (CT) image showed tumor in the left nasal cavity, with the adhesion to the nasal septum and inferior turbinate.

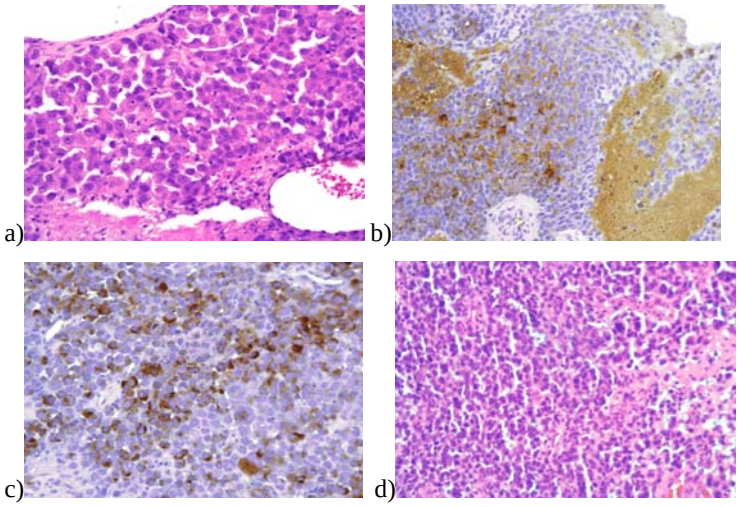

a) b) c) d)

Fig. 5 – Mucosal melanoma, histopathological findings with imunohistochemical analysis. a) HE, ×200; b) Cytoplasmic positivity for S-100 (anti-S 100, ×200); c) Cytoplasmic positivity for HMB-45 (anti-HMB 45, × 200); d) HE, ×200.

the diagnosis of mucosal melanoma of the nasal cavity. The findings indicated stage I, T1N0M0. Taking into consideration the stage of the disease, the patient underwent medial maxillectomy and partial septectomy (Figure 6). The final pathology confirmed the diagnosis of sinonasal melanoma. The patient was followed-up fur ther. At a 3-month follow-up, the patient showed no evidence of local reccurence. Then he was receiving postoperative radiotherapy.

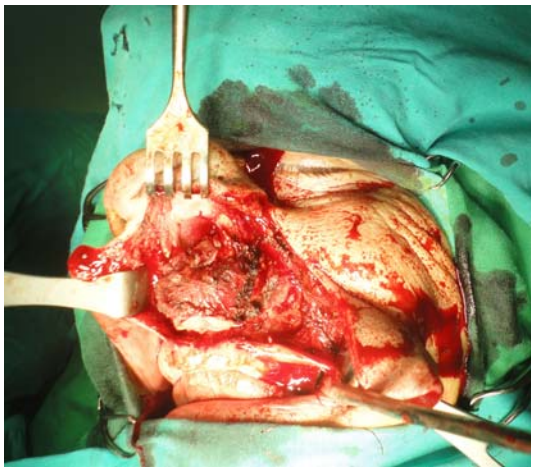

Fig. 6 – Medial maxillectomy and partial septectomy in patient with mucosal melanoma in the nasal cavity.

Discussion

Primary mucosal melanoma of the sinonasal tract has an aggressive and unpredictable biologic behavior characterized by frequent incidence of local recurrence, local and distant metastasis of the disease, despite radical surgical resection [2–7]. Many studies have noted a long time from the appearance of symptoms to evaluation by health care professionals from several weeks to as long as 1–5 months [1–7]. The exact origin is often difficult to ascertain due to anatomic limitations and, for older patients, due to lack of fiberoptic endoscopy and accurate modern anatomic and radiologic diagnostic techniques [1, 2, 5]. Because of its hidden location and rich vascularization, mucosal melanoma is usually diagnosed at a more advanced stage. In a review by Manolidis and Donald [5], 18.7% of patients with malignant mucosal melanoma of the head and neck presented with lymph node metastasis while other reported series showed 26% to 52% [2, 3–10]. The pathologic diagnosis of melanoma hinges on the identification of intracellular melanin [5]. In histopathological sense, especially in case of amelanocit lesions, differential diagnosis includes other epithelial and mesenchymal tumors [6, 7]. Immunohistochemical staining analysis for S-100, HMB-45, Melan-A, microphthalmic transcription factor, tyrosinase Mart-1 are often required to diagnose malignant melanoma [3, 6, 7]. Histopathological features of this neoplasma are as follows: tumor site, specimen, specimen integrity, specimen size, tumor focality, tumor size, maximal tumor thickness, growth phase, histologic type, margins, lymph-vascular invasion, perineural invasion, lymph nodes with metastases [6, 7, 14]. Pathologically, fewer mitoses and the absence of ulceration predict better outcomes and should be reported as part of routine histological profiles of mucosal melanoma [15]. Prasad et al. [14] defined microstaging classification based on histological findings on level I as mucosal melanoma *in situ* (without invasion of the *lamina propria* or with only microinvasion), level II as invasion into the *lamina propria* only, and level III as invasion into deep tissue structures, such as bone, muscle, and cartilage.

There are no randomized trials studying treatment modalities such as surgery, radiotherapy, or chemo and immunotherapy specifically in mucosal melanoma [1–6, 9, 10, 16]. Unfortunately, complete resection achieving melanoma-free margins is often difficult in primary mucosal melanoma of the sinonasal tract because of the close proximity of critical anatomic structures [9, 10, 16]. This likely contributes to the high local recurrence rate, which has been reported to be 50–90% [5, 17]. A study by Dauer et al. [6] which included 61 patients in the period from 1953 to 2003 showed that 50% of patients, despite radical surgical excision, experienced local recurrence. To date, there is no consensus regarding the indications for postoperative radiation therapy, although most authors agree regarding its use in patients with positive and close margins, especially as these have been recently identified as negative prognostic factors [10–12, 16, 17]. In a review of 69 patients with mucosal melanoma, Temam et al. [12] found that the local control rates were 26% with surgery alone and 62% with postoperative radiation therapy, even though the individuals in the radiotherapy group had much more locally advanced tumors. A considerable morbidity in high doses of radiotherapy to the head and neck region, requires new radiographic modalities with better precision [9–12, 16].

Chemotherapy/immunotherapy is usually used with an adjuvant or palliative intention. Combination chemotherapy or biochemotherapy results in higher response rates, in the range of 35–45%, but is associated with significant toxicity and has not been proven to increase overall survival [18]. According to Monolidis and Donald [5] patients with nasal mucosal melanoma have a 31% of 5-year survival rate, whereas sinus melanoma patients fare poorly, with a 0% rate of 5-year survival. One of the prognostic factors is the problem of local recurrence. Of 484 patients in 14 series, 258 (53,3%) patients had local recurrence [1, 2, 15, 19]. Shuman et al. [15] reviewed 52 patients with mucosal melanoma of the head and neck and they demonstrated extremely poor prognosis among patients presenting with advanced primary disease or regional and/or distant metastases.

Conclusion

Primary mucosal melanoma of the sinonasal region is a rare neoplasm with variable clinical and histopathological presentation, invasive growth, frequent local recurrence and poor prognosis despite the implementation of adequate treatment modalities. Immunohistochemical analysis in histopathological diagnosis contributes to early and accurate diagnosis of mucosal melanoma. Most frequent controversies regarding treatment modalities are negative surgical margines, reconstruction of surgical defects and role of radiotherapy. Its location and relatively nonspecific features frequently delay diagnosis, and its rarity avoids an optimal treatment guideline setting.

R E F E R E N C E S

1. *Clifton N, Harrison L, Bradley PJ, Jones NS*. Malignant melanoma of nasal cavity and paranasal sinuses: report of 24 patients and literature review. J Laryngol Otol 2011; 125(5): 479−85.
2. *Moreno MA, Roberts DB, Kupferman ME, DeMonte F, El-Naggar AK, Williams M,* et al. Mucosal melanoma of the nose and paranasal sinuses, a contemporary experience from the M. D. Anderson Cancer Center. Cancer 2010; 116(9): 2215−23.
3. *Wagner M, Morris CG, Werning JW, Mendenhall WM*. Mucosal melanoma of the head and neck. Am J Clin Oncol 2008; 31(1): 43−8.
4. *Seetharamu N, Petrick A, Ott PA, Pavlick AC*. Mucosal Melanomas: A Case-Based Review of the Literature. Oncologist 2010; 15(7): 772−8.
5. *Manolidis S, Donald PJ*. Malignant mucosal melanoma of the head and neck: review of the literature and report of 14 patients. Cancer 1997; 80(8): 1373−86.
6. *Dauer EH, Lewis JE, Rohlinger AL, Weaver AL, Olsen KD*. Sinonasal melanoma: a clinicopathologic review of 61 cases. Otolaryngol Head Neck Surg 2008; 138(3): 347−52.
7. *McLean N, Tighiouart M, Muller S*. Primary mucosal melanoma of the head and neck. Comparison of clinical presentation and histopathologic features of oral and sinonasal melanoma. Oral Oncol 2008; 44(11): 1039−46.
8. *Ballantyne AJ*. Malignant melanoma of the skin of the head and neck. An analysis of 405 cases. Am J Surg 1970; 120(4): 425−31.
9. *Mendenhall WM, Amdur RJ, Hinerman RW, Werning JW, Villaret DB, Mendenhall NP*. Head and neck mucosal melanoma. Am J Clin Oncol 2005; 28(6): 626−30.
10. *Medina JE, Ferlito A, Pellitteri PK, Shaha AR, Khafif A, Devaney KO,* et al. Current management of mucosal melanoma of the head and neck. J Surg Oncol 2003; 83(2): 116−22.
11. *Trotti A, Peters LJ*. Role of radiotherapy in the primary management of mucosal melanoma of the head and neck. Semin Surg Oncol 1993; 9(3): 246−50.
12. *Temam S, Mamelle G, Marandas P, Wibault P, Avril M, Janot F,* et al. Postoperative radiotherapy for primary mucosal melanoma of the head and neck. Cancer 2005; 103(2): 313−9.
13. American Joint Committee on Cancer. In: *Greene FL, Page DL, Fleming ID, Fritz AG, Balch CM, Haller DG,* et al, editors. Nasal cavity and paranasal sinuses. 6th ed. New York: Springer- Verlag; 2002. p. 59−67.
14. *Prasad ML, Patel SG, Huvos AG, Shah JP, Busam KJ*. Primary mucosal melanoma of the head and neck: a proposal for microstaging localized, Stage I (lymph node-negative) tumors. Cancer 2004; 100(8): 1657−64.
15. *Shuman AG, Light E, Olsen SH, Pynnonen MA, Taylor JM, Johnson TM,* et al. Mucosal melanoma of the head and neck: predictors of prognosis. Arch Otolaryngol Head Neck Surg 2011; 137(4): 331−7.
16. *Gavriel H, McArthur G, Sizeland A, Henderson M*. Review: mucosal melanoma of the head and neck. Melanoma Res 2011; 21(4): 257−66.
17. *Lund VJ, Howard DJ, Harding L, Wei WI*. Management options and survival in malignant melanoma of the sinonasal mucosa. Laryngoscope 1999; 109(2 Pt 1): 208−11.
18. *Bartell HL, Bedikian AY, Papadopoulos NE, Dett TK, Ballo MT, Myers JN,* et al. Biochemotherapy in patients with advanced head and neck mucosal melanoma. Head Neck 2008; 30(12): 1592−8.
19. *Thompson LD, Wieneke JA, Miettinen M*. Sinonasal tract and nasopharyngeal melanomas: a clinicopathologic study of 115 cases with a proposed staging system. Am J Surg Pathol 2003; 27(5): 594−611.

Received on April 14, 2014.
Revised on August 4, 2014.
Accepted on August 22, 2014.
Online First August, 2015.

CASE REPORT

UDC: 616.36-003.94-089-06::616.233/.235-007.253
DOI: 10.2298/VSP140311048A

Conservative treatment of bronchobiliary fistula evaluated with magnetic resonance imaging

Konzervativno lečenje bronhobilijarne fistule procenjivano magnetnom rezonancom

Tatjana N. Adžić-Vukičević*†, Ana Z. Blanka*, Aleksandra M. Ilić*†, Snežana V. Raljević*†, Ružica M. Maksimović‡, Srdjan P. Djuranović§

***Clinic for Pulmonology, ‡Centre for Radiology and Magnetic Resonance Imaging, §Clinic for Gastroenterology, Clinical Centre of Serbia, Belgrade, Serbia; †Faculty of Medicine, University of Belgrade, Belgrade, Serbia**

Abstract

Introduction. Bronchobiliary fistula (BBF) is a pathological communication between the bronchial system and the biliary tree that presents with bilioptysis. Many conditions can cause its development. There is still no optimal therapy for BBF. Conservative treatment is rarely indicated, as was published before in a few cases. **Case report.** We presented a 71-year-old Caucasian Serbin woman with BBF secondary to previous laparotomy due to multiple echinococcus liver cysts. The diagnosis was established by the presence of bilirubin and bile acids in sputum and magnetic resonance cholangiopancreatography (MRCP). A repeat MRCP performed after conservative procedure, did not reveal fistulous communication. **Conclusion.** We suggest that in small and less severe fistulas between the biliary and the bronchial tract, conservative treatment may be used successfully, and invasive treatment methods are not needed in all patients.

Key words:
bronchial fistula; biliary fistula; diagnosis; magnetic resonance imaging; drug therapy.

Apstrakt

Uvod. Bronhobilijarna fistula (BBF) predstavlja patološku komunikaciju između bronhijalnog sistema i bilijarnog trakta koja se prezentuje bilioptizijama. Mnoga stanja mogu izazvati njen nastanak. Još uvek ne postoji optimalna terapija za BBF. Konzervativno lečenje je retko indikovano i predhodno je objavljeno samo kod nekoliko bolesnika. **Prikaz bolesnika.** Prikazali smo ženu, staru 71 godinu, sa BBF koja je nastala nakon predhodne laparotomije zbog multiplih ehinokoknih cisti jetre. Dijagnoza je postavljena na osnovu prisustva bilirubina i žučnih kiselina u sputumu i na osnovu holangiopankreatografije primenom magnetne rezonance (MRCP). Ponovljenim MRCP nakon konzervativnog lečenja nije potvrđeno prisustvo fistulozne komunikacije. **Zaključak.** Kod manjih i nekomplikovanih fistula između bilijarnog i bronhijalnog trakta, konzervativno lečenje može biti uspešno. Stoga, invazivne metode lečenja nisu neophodne kod svih bolesnika.

Ključne reči:
fistula, bronhijalna; fistula, bilijarna; dijagnoza; magnetna rezonanca, snimanje; lečenje lekovima.

Introduction

Bronchobiliary fistula (BBF) is defined as the passage of bile in the bronchi and the presence of bile in sputum (bilioptysis). The most common causes are trauma, bile duct obstruction, and liver infections such are hydatid cysts, echinococcosis, or amebic abscess [1]. It can occur, rarely, in the congenital form [2]. Therapeutic options include surgical repair or minimal invasive teatments such are nasobiliary drainage, endoscopic retrograde cholangiopancreatography (ERCP) (endoscopic sphincterotomy and biliary stenting) and percutaneous drainage. Herein, we described a patient with BBF after liver echinococcosis treated conservatively.

Case report

A 71-year-old Caucasian Serbian woman was admitted to our hospital with a 2-month history of bilioptysis. The patient had the history of laparotomy one year previously because of multiple echinococcus liver cysts. Pericystectomy was done with omentoplasty and cholecystectomy. Eight months after the operation an abdominal ultrasound revealed fluid

Correspondence to: Tatjana N. Adžić-Vukičević, Faculty of Medicine, University of Belgrade, Clinic for Pulmonology, Clinical Centre of Serbia, Višegradska 26/20, 11 000 Belgrade, Serbia. Phone/Fax: +381 11 3663 961. E-mail: adzic_tatjana@yahoo.com

collection in the liver. Percutaneus ultrasound-guided drainage was performed with daily drainage of 150–200 mL of green-yellowish content. Intravenous antibiotic therapy was applied in a few days followed with oral therapy. Two months after catheter droppage, the patient noticed green-yellowish sputum similiar to previously drained content. Physical examination revealed fever (38°C), and decreased breath sound over the right basal lung fields. The sputum output range was 50–75 mL/day. Laboratory tests findings showed the elevated sedimentation rate of 70 mm/1h (normal less than 30 mm/h) increased levels of aspartate aminostransferase (AST) 39 U/L (normal < 37 U/L), alkaline phosphatase 370 U/L (normal 40–120 U/L) and gamma glutamyl transferase (GT) 736 U/L (normal < 55 U/L). A chest radiograph showed right pleural effusion (Figure 1). Fiberoptic bronchoscopy was normal. Sputum samples detected the presence of bilirubin and bile acids in concentration of 14 μmol/L (normal serum total bilirubin < 17.1 μmol/L, direct < μmol/L 5, bile acids < 12 μmol/L) (Figure 2), while sputum and blood cultures were negative. ERCP was not successful in selective canulation of common bile duct, so we could not visualize biliary system. Magnetic resonance cholangiopancreatography (MRCP) showed micro fistula between the intrahepatic bile ducts and the right pleural space (Figure 3). The patient was treated with antibiotics (cephalosporin of the third generation with metronidazole) and saline solutions intravenosly in seven days. Bilioptysis disappeared after 5 days and the patient was discharged from the hospital in good clinical condition. Follow-up MRCP performed nine months later did not reveal any fistulous communication (Figure 4). Control chest radiograph made two years after was normal.

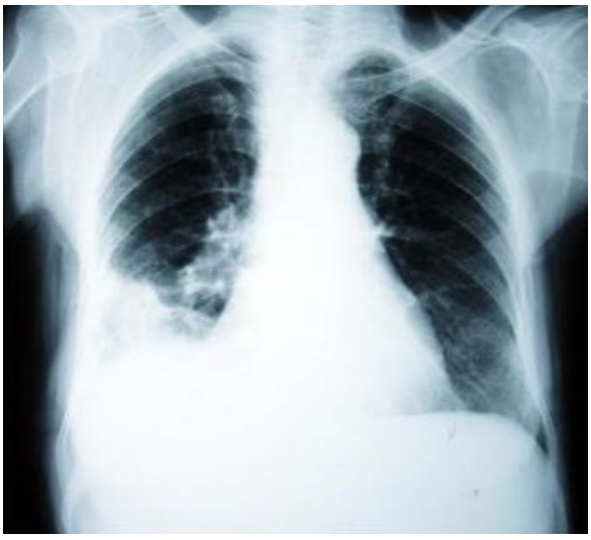

Fig. 1 – Chest radiograph showed right pleural effusion.

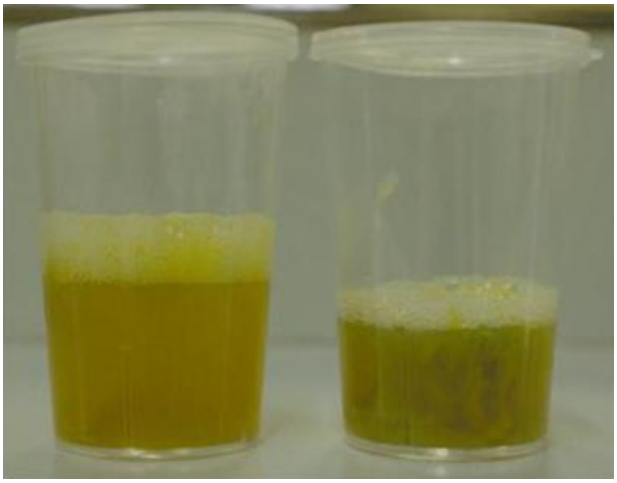

Fig. 2 – Sputum samples.

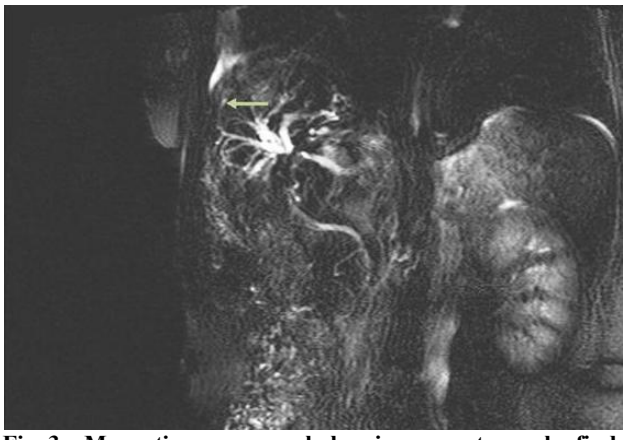

Fig. 3 – Magnetic resonance cholangiopancreatography finding showed a fistula between the intrahepatic bile ducts and the right pleural space.

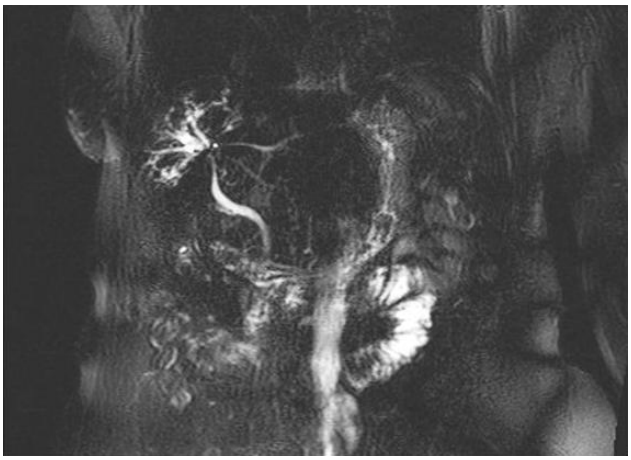

Fig. 4 – Magnetic resonance cholangiopancreatography repeated 9 months later showed no fistulous communication.

Discussion

This case is interesting to clinicians for showing that conservative antibiotic treatment after percutaneus drainage could be successful in the treatment of BBF, alleviating the need for more invasive management.

BBF represents an abnormal communication between the biliary system and bronchial tree. The most common causes for BBF in Western countries are bile duct obstruction due to choledocholithiasis, malignancy, trauma or postoperative complications of hepatobiliary surgery [3–5]. In developing countries, echinococcal cysts, amebiasis, pancreatitis and tuberculosis are the most prevalent causes [6, 7]. BBF can be iatrogenic after radiofrequency ablation for liver metastases or congenital [2, 8] Pathogenesis of BBF includes two mechanisms, biliary obstruction that produces the inflammatory process in the subdiaphragmatic space and rupture towards the bronchial tree [9]. The diag-

nosis of BBF is established by the presence of bile in sputum. Bilioptysis is pathognomonic of BBF. The radiographic finding includes pleural effusion with pneumonic consolidation as in the presented patient. Different diagnostic imaging investigations are useful in visualization of fistula such are percutaneous transhepatc cholangiography ERCP, MRCP, T-tube cholangiography, fistulography, bronchoscopy or bronchography, hepatobiliary iminodiacetic acid scyntigraphy [10, 11]. The main aim of BBF is to reduce the inreased intrabiliary pressure in order to facilitate bile flow to the duodenum. Conservative, minimal invasive and surgical methods are used in the treatment of BBF. Conservative treatment can be used in small, not complicated cases. It includes antibiotic therapy and somatostatin or its analogues. Somatostatin or analogues, reducing the pancreatic and bile secretion, are the most commonly used in the treatment of acute or chronic pancreatitis complicated by the pancreatic-pleural fistula. The use of octreotide in BBF management has been described in the literature [12]. Biliary decompression may be obtained by the following methods of the minimal invasive treatment such as nasobiliary and percutaneous transhepatic drainage [13, 14]. In our patient after liver collection occured, we decided to use ultrasound-guided percutaneus drainage. Percutaneus drainage was successful with daily drainage of 150–200 mL of green-yellowish content. Two months after catheter dropped and a new one was not replaced. Until the presence of biloptysis, the patient did not visit the doctor. On the other hand, in cases of large, persistent fistulas and non-effective non-invasive treatment, surgery is needed. The type of surgical procedure depends on etiology, location and complications of BBF. The following surgical procedures such as drainage of right subphrenic or hepatic abscess, closure of the fistula, resection of hydatid cyst, biliary drainage using T-tube and bilioenteric anastomoses are performed in BBF [3, 5, 8]. In cases of diaphragmatic, pleural, bronchial or pulmonary damage, closure of the diaphragm, pleural drainage, decortication or different pulmonary resections are used [15].

In the presented patient ERCP was performed without successful selective canulation of biliary tree, therefore we decided to treat our patient conservatively. Reduced biliary pressure after bilioptysis associated with antibiotic therapy could facilitate healing and closing of BBF. It is probably, because the described fistula was small. Somatostatin was not used in the presented patient, as was published before [12].

The clinical course of our patient improved. MRCP performed nine months later was without fistulous communication.

Early diagnosis is mandatory because of serious complications such are chemical pneumonitis, pneumonia or necrotizing bronchitis [16].

Conclusion

We suggest that in small and less severe fistulas between the biliary and the bronchial tract, conservative treatment may be used successfully, and invasive treatment methods are not needed in all patients. Accurate therapeutic approach should be a key factor of management.

REFERENCES

1. *Gugenheim J, Ciardullo M, Traynor O, Bismuth H.* Bronchobiliary fistulas in adults. Ann Surg 1988; 207(1): 90−4.
2. *Tommasoni N, Gamba PG, Midrio P, Guglielmi M.* Congenital tracheobiliary fistula. Pediatr Pulmonol 2000; 30(2): 149−52.
3. *Eryigit H, Oztas S, Urek S, Olgac G, Kurutepe M, Kutlu CA.* Management of acquired bronchobiliary fistula: 3 case reports and a literature review. J Cardiothorac Surg 2007; 2: 52.
4. *Baudet JS, Medina A, Moreno A, Navazo L, Avilés J, Soriano A.* Bronchobiliary fistula secondary to ruptured hepatocellular carcinoma into the bile duct. J Hepatol 2004; 41(6): 1066−7.
5. *Liao GQ, Wang H, Zhu GY, Zhu KB, Lv FX, Tai S.* Management of acquired bronchobiliary fistula: A systematic literature review of 68 cases published in 30 years. World J Gastroenterol 2011; 17(33): 3842−9.
6. *Tocchi A, Mazzoni G, Miccini M, Drumo A, Cassini D, Colace L,* et al. Treatment of hydatid bronchobiliary fistulas: 30 years of experience. Liver Int 2007; 27(2): 209−14.
7. *Hansen M, Höier-Madsen K.* A bronchobiliary fistula probably due to exacerbation of chronic pancreatitis. A short review of the literature. Ann Chir Gynaecol 1985; 74(1): 36−9.
8. *Senturk H, Mert A, Ersavasti G, Tabak F, Akdogan M, Ulualp K.* Bronchobiliary fistula due to alveolar hydatid disease: report of three cases. Am J Gastroenterol 1998; 93(11): 2248−53.
9. *Tran T, Hampel H, Qureshi WA, Shaib Y.* Successful endoscopic management of bronchobiliary fistula due to radiofrequency ablation. Dig Dis Sci 2007; 52(11): 3178−80.
10. *Gerazounis M, Athanassiadi K, Metaxas E, Athanassiou M, Kalantzi N.* Bronchobiliary fistulae due to echinococcosis. Eur J Cardiothorac Surg 2002; 22(2): 306−8.
11. *Ragozzino A, De Rosa R, Galdiero R, Maio A, Manes G.* Bronchobiliary fistula evaluated with magnetic resonance imaging. Acta Radiol 2005; 46(5): 452−4.
12. *Ong M, Moozar K, Cohen LB.* Octreotide in bronchobiliary fistula management. Ann Thorac Surg 2004; 78(4): 1512−3.
13. *Aydin U, Yazici P, Tekin F, Ozutemiz O, Coker A.* Minimally invasive treatment of patients with bronchobiliary fistula: a case series. J Med Case Rep 2009; 3(1): 23.
14. *Partrinou V, Dougenis D, Kritikos N, Polydorou A, Vagianos C.* Treatment of postoperative bronchobiliary fistula by nasobiliary drainage. Surg Endosc 2001; 15(7): 758.
15. *Chong CF, Chong VH, Jalihal A, Mathews L.* Bronchobiliary fistula successfully treated surgically. Singapore Med J 2008; 49(8): e208−11.
16. *Singh B, Moodley J, Sheik-Gafoor MH, Dhooma N, Reddi A.* Conservative management of thoracobiliary fistula. Ann Thorac Surg 2002;73(4): 1088−91.

Received on March 11, 2014.
Revised on October 16 , 2014.
Accepted on October 20, 2014.
Online First June, 2015.

INSTRUCTIONS TO THE AUTHORS

Vojnosanitetski pregled (VSP) publishes only papers not published before, nor submitted to any other journals, in the order determined by the Editorial Board. Any attempted plagiarism or self-plagiarism will be punished. When submitting a paper to the VSP electronic editing system, the following should be enclosed: a statement on meeting any technical requirements, a statement signed by all the authors that the paper on the whole and/or partly has not been submitted nor accepted for publication elsewhere, a statement specifying the actual contribution of each author, no conflict of interest statement that makes them responsible for meeting any requirements set. What follows subsequently is the acceptance of a paper for further editing procedure. The VSP reserves all copyrights for the published papers. Accepted are only papers in English. The VSP publishes only papers of the authors subscribed to the VSP for the year of paper submitting for publishing. Subscription is obligatory for each author/coauthor whose paper enters peer review procedure.

On January 1, 2012 the *Vojnosanitetski pregled* turned to the electronic editing system e-Ur: Electronic Journal Editing.

All the users of the system: authors, editors and reviewers have to be registered at:

http://aseestant.ceon.rs/index.php

The VSP publishes: **editorials, original articles**, **short communications**, **reviews/meta-analyses, case reports**, **medical history** (general or military), personal views, invited comments, letters to the editor, reports from scientific meetings, book reviews, and other. Original articles, short communications, meta-analyses and case reports are published with abstracts in both English and Serbian.

General review papers will be accepted by the Editorial Board only if the authors prove themselves as the experts in the fields they write on by citing not less than 5 self-citations.

Papers should be written on IBM-compatible PC, using 12 pt font, and double spacing, with at least 4 cm left margin. **Bold** and *italic* letters should be avoided as reserved for subtitles. Original articles, reviews, meta-analyses and articles from medical history should not exceed 16 pages; current topics 10; case reports 6; short communications 5; letters to the editor and comments 3, and reports on scientific meetings and book reviews 2.

All measurements should be reported in the metric system of the International System of Units (SI), and the standard internationally accepted terms (except for mm Hg and °C).

MS Word for Windows (97, 2000, XP, 2003) is recommended for word processing; other programs are to be used only exceptionally. Illustrations should be made using standard **Windows** programs, **Microsoft Office** (**Excel**, **Word Graph**)**.** The use of colors and shading in graphs should be avoided.

Papers should be prepared in accordance the **Vancouver Convention**.

Papers are reviewed anonymously by at least two editors and/or invited reviewers. Remarks and suggestions are sent to the author for final composition. Galley proofs are sent to the corresponding author for final agreement.

Preparation of manuscript

Parts of the manuscript are: **Title page; Abstract with Key words; Text; Acknowledgements** (to the authors' desire), **References**, **Enclosures**.

1. ***Title page***

a) The title should be concise but informative, while subheadings should be avoided;

b) Full names of the authors signed as follows: ***, †, ‡, §, ‖, ¶, **, ††, ...** .

c) Exact names and places of department(s) and institution(s) of affiliation where the studies were performed, city and the state for any authors, clearly marked by standard footnote signs;

d) Conclusion could be a separate chapter or the last paragraph of the discussion;

e) Data on the corresponding author.

2. ***Abstract and key words***

The second page should carry a structured abstract (250-300 words for original articles and meta-analyses) with the title of the article. In short, clear sentences the authors should write the **Background**/**Aim**, major procedures – **Methods** (choice of subjects or laboratory animals; methods for observation and analysis), the obtained findings – **Results** (concrete data and their statistical significance), and the **Conclusion**. It should emphasize new and important aspects of the study or observations. A structured abstract for case reports (up to 250 words) should contain subtitles **Introduction, Case report, Conclusion**). Below the abstract **Key words** should provide 3–10 key words or short phrases that indicate the topic of the article.

3. ***Text***

The text of the articles includes: **Introduction**, **Methods**, **Results**, and **Discussion**. Long articles may need subheadings within some sections to clarify their content.

Introduction. After the introductory notes, the aim of the article should be stated in brief (the reasons for the study or observation), only significant data from the literature, but not extensive, detailed consideratuion of the subject, nor data or conclusions from the work being reported.

Methods. The selection of study or experimental subjects (patients or experimental animals, including controls) should be clearly described. The methods, apparatus (manufacturer's name and address in parentheses), and procedures should be identified in sufficient detail to allow other workers to reproduce the results. Also, give references to established methods, including statistical methods. Identify precisely all drugs and chemicals used, with generic name(s), dose(s), and route(s) of administration. State the approval of the Ethnics Committee for the tests in humans and animals.

Results should be presented in logical sequence in the text, tables and illustrations. Emphasize or summarize only important observations.

Discussion is to emphasize the new and significant aspects of the study and the conclusions that result from them. Relate the observations to other relevant studies. Link the conclusions with the goals of the study, but avoid unqualified statements and conclusions not completely supported by your data.

References

References should be superscripted and numerated consecutively in the order of their first mentioning within the text. All the authors should be listed, but if there are more than 6 authors, give the first 6 followed by *et al*. Do not use abstracts, secondary publications, oral communications, unpublished papers, official and classified documents. References to papers accepted but not yet published should be cited as "in press". Information from manuscripts not yet accepted should be cited as "unpublished data". Data from the Internet are cited with the date of citation.

Examples of references:

Jurhar-Pavlova M, Petlichkovski A, TrajkovD, Efinska-Mladenovska O, Arsov T, Strezova A, et al. Influence of the elevated ambient temperature on immunoglobulin G and immunoglobulin G subclasses in sera of Wistar rats. Vojnosanit Pregl 2003; 60(6): 657–612.

DiMaio VJ. Forensic Pathology. 2nd ed. Boca Raton: CRC Press; 2001.

Blinder MA. Anemia and Transfusion Therapy. In: Ahya NS, Flood K, Paranjothi S, editors. The Washington Manual of Medical Therapeutics, 30th edition. Boston: Lippincot, Williams and Wilkins; 2001. p. 413-28.

Christensen S, Oppacher F. An analysis of Koza's computational effort statistic for genetic programming. In: *Foster JA, Lutton E, Miller J, Ryan C, Tettamanzi AG,* editors. Genetic programming. EuroGP 2002: Proceedings of the 5th European Conference on Genetic Programming; 2002 Apr 3-5; Kinsdale, Ireland. Berlin: Springer; 2002. p. 182-91.

Abood S. Quality improvement initiative in nursing homes: the ANA acts in an advisory role. Am J Nurs [serial on the Internet]. 2002 Jun [cited 2002 Aug 12]; 102(6): [about 3 p.]. Available from: http://www.nursingworld.org/AJN/2002/june/Wawatch.htm

Tables

Each table should be typed double-spaced 1,5 on a separate sheet, numbered in the order of their first citation in the text in the upper right corner and supplied with a brief title each. Explanatory notes are printed under a table. Each table should be mentioned in the text. If data from another source are used, acknowledge fully.

Illustrations

Any forms of graphic enclosures are considered to bi figures and should be submitted as additional databases in the System of Assistent. Letters, numbers, and symbols should be clear and uniform, of sufficient size that when reduced for publication, each item will still be legible. Each figure should have a label on its back indicating the number of the figure, author's name, and top of the figure (**Figure 1**, **Figure 2** and so on). If a figure has been published, state the original source.

Legends for illustrations are typed on a separate page, with Arabic numbers corresponding to the illustrations. If used to identify parts of the illustrations, the symbols, arrows, numbers, or letters should be identified and explained clearly in the legend. Explain the method of staining in photomicrographs.

Abbreviations and symbols

Use only standard abbreviations. Avoid abbreviations in the title and abstracts. The full term for which an abbreviation stands should precede its first use in the text.

Detailed Instructions are available at the web site:
www.vma.mod.gov.rs/vsp

UPUTSTVO AUTORIMA

Vojnosanitetski pregled (VSP) objavljuje radove koji nisu ranije nigde objavljivani, niti predati za objavljivanje redosledom koji određuje uređivački odbor. Svaki pokušaj plagijarizma ili autoplagijarizma kažnjava se. Prilikom prijave rada u sistem elektronskog uređivanja „Vojnosanitetskog pregleda“ neophodno je priložiti izjavu da su ispunjeni svi postavljeni tehnički zahtevi uključujući i izjavu koju potpisuju svi autori da rad nije ranije ni u celini, niti delimično objavljen niti prihvaćen za štampanje u drugom časopisu. Izjavu o pojedinačnom doprinosu svakog od autora rada potpisanu od svih autora, treba skenirati i poslati uz rad kao dopunsku datoteku. Takođe, autori su obavezni da dostave i potpisanu izjavu o nepostojanju sukoba interesa čime postaju odgovorni za ispunjavanje svih postavljenih uslova. Ovome sledi odluka o prihvatanju za dalji uređivački postupak. Za objavljene radove VSP zadržava autorsko pravo. **Primaju se radovi napisani samo na engleskom jeziku.** VSP objavljuje radove samo autora koji su pretplaćeni na časopis u godini podnošenja rada za objavljivanje. Pretplata je obavezna za svakog autora/koautora čiji rad uđe u postupak recenzije.

Od 1. januara 2012. godine Vojnosanitetski pregled prešao je na e-Ur: Elektronsko uređivanje časopisa.

Svi korisnici sistema: autori, recezenti i urednici moraju biti registrovani jednoznačnom e-mail adresom. Registraciju je moguće izvršiti na:

http://aseestant.ceon.rs/index.php

U VSP-u se objavljuju **uvodnici**, **originalni članci, prethodna** ili **kratka saopštenja**, revijski radovi tipa **opšteg pregleda** (uz uslov da autori navođenjem najmanje 5 autocitata potvrde da su eksperti u oblasti o kojoj pišu), **aktuelne teme, metaanalize**, **kazuistika, seminar praktičnog lekara,** članci iz **istorije medicine**, lični stavovi, naručeni komentari, pisma uredništvu, izveštaji sa naučnih i stručnih skupova, prikazi knjiga i drugi prilozi. Radovi tipa originalnih članaka, prethodnih ili kratkih saopštenja, metaanalize i kazuistike **objavljuju se uz apstrakte na srpskom i engleskom jeziku**.

Rukopis se piše sa proredom 1,5 sa levom marginom od **4 cm**. Koristiti font veličine 12, a načelno izbegavati upotrebu **bold** i *italic* slova, koja su rezervisana za podnaslove. Originalni članci, opšti pregledi i metaanalize i članci iz istorije medicine ne smeju prelaziti 16 stranica (bez priloga); aktuelne teme – deset, seminar praktičnog lekara – osam, kazuistika – šest, prethodna saopštenja – pet, a komentari i pisma uredniku – tri, izveštaji sa skupova i prikazi knjiga – dve stranice.

U celom radu obavezno je korišćenje međunarodnog sistema mera (SI) i standardnih međunarodno prihvaćenih termina (sem mm Hg i °C).

Za obradu teksta koristiti program **Word for Windows** verzije 97, 2000, XP ili 2003. Za izradu grafičkih priloga koristiti standardne grafičke programe za **Windows**, poželjno iz programskog paketa **Microsoft Office** (**Excel, Word Graph**). Kod kompjuterske izrade grafika izbegavati upotrebu boja i senčenja pozadine.

Radovi se pripremaju u skladu sa **Vankuverskim dogovorom**.

Prispeli radovi kao anonimni podležu uređivačkoj obradi i recenziji najmanje dva urednika/recenzenta. Primedbe i sugestije urednika/recenzenata dostavljaju se autoru radi konačnog oblikovanja. Pre objave, rad se upućuje autoru određenom za korespodenciju na konačnu saglasnost.

Priprema rada

Delovi rada su: **naslovna strana, apstrakt sa ključnim rečima, tekst** rada, zahvalnost (po želji), literatura, prilozi.

1. ***Naslovna strana***

a) Poželjno je da naslov bude kratak, jasan i informativan i da odgovara sadržaju, podnaslove izbegavati.

b) Ispisuju se puna imena i prezimena autora sa oznakama redom: *, †, ‡, §, ‖, ¶, **, ††, ...

c) Navode se puni nazivi ustanove i organizacijske jedinice u kojima je rad obavljen mesta i države za svakog autora, koristeći standardne znake za fusnote.

d) Zaključak može da bude posebno poglavlje ili se iznosi u poslednjem pasusu diskusije.

e) Podaci o autoru za korespodenciju.

2. ***Apstrakt i ključne reči***

Na drugoj stranici nalazi se strukturisani apstrakt (250-300 reči za originalne članke i meta-analize) sa naslovom rada. Kratkim rečenicama na srpskom i engleskom jeziku iznosi se **Uvod/Cilj** rada, osnovne procedure – **Metode** (izbor ispitanika ili laboratorijskih životinja; metode posmatranja i analize), glavni nalazi – **Rezultati** (konkretni podaci i njihova statistička značajnost) i glavni **Zaključak**. Naglasiti nove i značajne aspekte studije ili zapažanja. Strukturisani apstrakt za kazuistiku (do 250 reči), sadrži podnaslove **Uvod, Prikaz bolesnika** i **Zaključak**). Ispod apstrakta, „Ključne reči“ sadrže 3–10 ključnih reči ili kratkih izraza koje ukazuju na sadržinu članka.

3. ***Tekst članka***

Tekst sadrži sledeća poglavlja: **uvod**, **metode**, **rezultate** i **diskusiju**. **Uvod.** Posle uvodnih napomena, navesti cilj rada. Ukratko izneti razloge za studiju ili posmatranje. Navesti samo važne podatke iz literature a ne opširna razmatranja o predmetu rada, kao ni podatke ili zaključke iz rada o kome se izveštava.

Metode. Jasno opisati izbor metoda posmatranja ili eksperimentnih metoda (ispitanici ili eksperimentne životinje, uključujući kontrolne). Identifikovati metode, aparaturu (ime i adresa proizvođača u zagradi) i proceduru, dovoljno detaljno da se drugim autorima omogući reprodukcija rezultata. Navesti podatke iz literature za uhodane metode, uključujući i statističke. Tačno identifikovati sve primenjene lekove i hemikalije, uključujući generičko ime, doze i načine davanja. Za ispitivanja na ljudima i životinjama navesti saglasnost nadležnog etičkog komiteta.

Rezultate prikazati logičkim redosledom u tekstu, tabelama i ilustracijama. U tekstu naglasiti ili sumirati samo značajna zapažanja.

U **diskusiji** naglasiti nove i značajne aspekte studije i izvedene zaključke. Posmatranja dovesti u vezu sa drugim relevantnim studijama, u načelu iz poslednje tri godine, a samo izuzetno i starijim. Povezati zaključke sa ciljevima rada, ali izbegavati nesumnjive tvrdnje i one zaključke koje podaci iz rada ne podržavaju u potpunosti.

Literatura

U radu literatura se citira kao superskript, a popisuje rednim brojevima pod kojima se citat pojavljuje u tekstu. Navode se svi autori, ali ako broj prelazi šest, navodi se prvih šest i *et al*. Svi podaci o citiranoj literaturi moraju biti tačni. Literatura se u celini citira na engleskom jeziku, a iza naslova se navodi jezik članka u zagradi. Ne prihvata se citiranje apstrakata, sekundarnih publikacija, usmenih saopštenja, neobjavljenih radova, službenih i poverljivih dokumenata. Radovi koji su prihvaćeni za štampu, ali još nisu objavljeni, navode se uz dodatak „u štampi“. Rukopisi koji su predati, ali još nisu prihvaćeni za štampu, u tekstu se citiraju kao „neobjavljeni podaci“ (u zagradi). Podaci sa *Interneta* citiraju se uz navođenje datuma pristupa tim podacima.

Primeri referenci:

Đurović BM. Endothelial trauma in the surgery of cataract. Vojnosanit Pregl 2004; 61(5): 491–7. (Serbian)

Balint B. From the haemotherapy to the haemomodulation. Beograd: Zavod za udžbenike i nastavna sredstva; 2001. (Serbian)

Mladenović T, Kandolf L, Mijušković ŽP. Lasers in dermatology. In: *Karadaglić Đ,* editor. Dermatology. Beograd: Vojnoizdavački zavod & Verzal Press; 2000. p. 1437–49. (Serbian)

Christensen S, Oppacher F. An analysis of Koza's computational effort statistic for genetic programming. In: *Foster JA, Lutton E, Miller J, Ryan C, Tettamanzi AG,* editors. Genetic programming. EuroGP 2002: Proceedings of the 5th European Conference on Genetic Programming; 2002 Apr 3-5; Kinsdale, Ireland. Berlin: Springer; 2002. p. 182-91.

Abood S. Quality improvement initiative in nursing homes: the ANA acts in an advisory role. Am J Nurs [serial on the Internet]. 2002 Jun [cited 2002 Aug 12]; 102(6): [about 3 p.]. Available from: http://www.nursingworld.org/AJN/2002/june/Wawatch.htm

Tabele

Sve tabele pripremaju se sa proredom 1,5 na posebnom listu. Obeležavaju se arapskim brojevima, redosledom pojavljivanja, u desnom uglu (**Tabela 1**), a svakoj se daje kratak naslov. Objašnjenja se daju u fus-noti, ne u zaglavlju. Svaka tabela mora da se pomene u tekstu. Ako se koriste tuđi podaci, obavezno ih navesti kao i svaki drugi podatak iz literature.

Ilustracije

Slikama se zovu svi oblici grafičkih priloga i predaju se kao dopunske datoteke u sistemu **aseestant**. Slova, brojevi i simboli treba da su jasni i ujednačeni, a dovoljne veličine da prilikom umanjivanja budu čitljivi. Slike treba da budu jasne i obeležene brojevima, onim redom kojim se navode u tekstu (**Sl. 1; Sl. 2** itd.). Ukoliko je slika već negde objavljena, obavezno citirati izvor.

Legende za ilustracije pisati na posebnom listu, koristeći arapske brojeve. Ukoliko se koriste simboli, strelice, brojevi ili slova za objašnjavanje pojedinog dela ilustracije, svaki pojedinačno treba objasniti u legendi. Za fotomikrografije navesti metod bojenja i podatak o uvećanju.

Skraćenice i simboli

Koristiti samo standardne skraćenice, izuzev u naslovu i apstraktu. Pun naziv sa skraćenicom u zagradi treba dati kod prvog pominjanja u tekstu.

Detaljno uputstvo može se dobiti u redakciji ili na sajtu:www.vma.mod.gov.rs/vsp